PACS-2 regulates SIRT1-mediated deacetylation of p53 following DNA damage

By

Katelyn Mae Atkins

A DISSERTATION

Presented to the Department of Cell and Developmental Biology
and the Oregon Health & Science University
School of Medicine
In partial fulfillment of the requirement for the degree of

Doctor of Philosophy
September 2012

School of Medicine
Oregon Health & Science University

CERTIFICATE OF APPROVAL

This is to certify that the Ph.D. dissertation of

Katelyn Mae Atkins

has been approved

Honorable Mentor, Dr. Gary Thomas

Honorable Committee Chair, Dr. Mushui Dai

Honorable Committee Member, Dr. Melissa Wong

Honorable Committee Member, Dr. Soo-Kyung Lee

Honorable Committee Member, Dr. David Jacoby

TABLE OF CONTENTS

LIST OF FIGURES

LIST OF TABLES

LIST OF ABBREVIATIONS

2D	two dimensional
7-AAD	7-aminoactinomycin D
A	adenosine
AceCS1	acetyl coenzyme A (CoA) synthetase
ADP	adenosine diphosphate
ADPKD	autosomal dominant polycystic kidney disease
AIDS	acquired immunodeficiency syndrome
AMP	adenosine monophosphate
AP	adaptor protein
AP-1	adaptor protein-1
AP-2	adaptor protein-2
AP-3	adaptor protein-3
AP-4	adaptor protein-4
AP-5	adaptor protein-5
APC	antigen-presenting cell
APE1	apurinic/apyrimidinic endonuclease 1
APO-1	apoptosis antigen-1
APOBEC3G	cytidine deaminase apolipoprotein B mRNA-editing enzyme catalytic polypeptide-like 3G
AR	androgen receptor
ARF6	adenosine diphosphate (ADP)-ribosylation factor 6
ARNO	ARF6 guanine nucleotide exchange factor
AROS	active regulator of SIRT1
ARR	atrophin-1 related region
ASK1	apoptosis signal-regulating kinase 1
ATM	ataxia telangiectasia mutated
ATP	adenosine triphosphate

ATR	ataxia telangiectasia and Rad3-related protein
BAP31	B-cell receptor-associated protein 31
Bcl-2	B-cell lymphoma-2
Bcl-xL	B-cell lymphoma-extra large
BH	Bcl-2 homology
BiFC	bimolecular fluorescence complementation
BMAL1	brain and muscle Arnt-like protein 1
BrdU	bromodeoxyuridine
C	carboxy
C	cytidine
CA	capsid
cAMP	cyclic adenosine monophosphate
CBP	CREB-binding protein
CCR5	C-C chemokine receptor type 5
CCV	clathrin-coated vesicle
CD209	cluster of differentiation 209
CD28	cluster of differentiation 28
CD3	cluster of differentiation 3
Cd31	cluster of differentiation 31
CD4	cluster of differentiation 4
CD8	cluster of differentiation 8
CD95	cluster of differentiation 95
CDK	cyclin-dependent kinase
ChIP	chromatin immunoprecipitation
Chk1	checkpoint kinase 1
Chk2	checkpoint kinase 2
CI-MPR	cation-independent mannose-6-phosphate receptor
CMV	cytomegalovirus
CoA	coenzyme A

COP	coatomer protein
CREB	cAMP response element binding protein
CtBP	C-terminal binding protein of adenovirus E1A
CTBP1	C-terminal binding protein 1
CTL	cytotoxic T-lymphocte
CTR	C-terminal region
CXCR4	C-X-C chemokine receptor type 4
DAPI	4',6-diamidino-2-phenylindole
DBC1	deleted in breast cancer 1
DC-SIGN	dendritic cell-specific intercellular adhesion molecule-3-grabbing non-integrin
DCAF1	cullin4A-DNA damage-binding protein 1 (DDB1) Cul4 assoicated factor 1
DDB1	cullin4A-DNA damage-binding protein 1
DNA	deoxyribonucleic acid
DNA-PK	DNA-protein kinase
DNase	deoxyribonuclease
Dr5	death receptor-5
Drp1	dynamin-related protein-1
DTT	eithiothreitol
DUB	deubiquitinating enzyme
E2	Ub-conjugating enzyme
EBV	Epstein Barr virus
EDTA	ethylenediaminetetraacetic acid
C. elegans	Caenorhabditis elegans
EndoH	endoglycosidase H
Env	envelope glycoprotein
ER	endoplasmic reticulum
ERGIC	ER-Golgi intermediate compartment

ESCRT	endosomal sorting complex required for transport
FACL-4	fatty acyl-Coenzyme A ligase-4
FBR	furin binding region
FBXO11	F-box only protein 11
FITC	fluorescein isothiocyanate
FOXO	forkhead transcription factor
FSGS	focal segmental glomerulosclerosis
G	guanosine
GGA	Golgi-localized, gamma adaptin ear-containing, ARF-binding
GADD45	growth arrest and DNA damage inducible 45
gB	glycoprotein B
GD-AIF	glioblastoma-derived angiogenesis inhibiting factor
GDP	guanosine diphosphate
GEF	guanine nucleotide exchange factor
GFP	green fluorescent protein
GI	gastrointestinal
gp	glycoprotein
gp120	glycoprotein 120
gp41	glycoprotein 41
GSK3β	glycogen synthase kinase-3β
GTP	guanosine triphosphate
H&E	hematoxylin & eosin
HAART	highly active antiretroviral therapy
HAT	histone acetyltransferase
HCMV	human cytomegalovirus
HDAC	histone deacetylase
HDAC1	histone deacetylase 1
HDAC3	histone deacetylase 3
HHV-5	human herpesvirus-5

HHV-8	human herpesvirus-8
HIC1	hypermethylated in cancer 1
HIF-1α	hypoxia inducible factor-1α
HIV-1	human immunodeficiency virus-1
HIV-2	human immunodeficiency virus-2
HIVAN	HIV-associated nephropathy
HLA	human leukocyte antigen
HSQC	heteronuclear single quantum coherence
IAP	inhibitor of apoptosis
Ig	immunoglobulin
IgA	immunoglobulin A
IgG	immunoglobulin G
IL-2	interleukin-2
IP	immunoprecipitation
IP_3	inositol (1,4,5)-triphosphate
IPTG	isopropylthio-β-galactoside
IR	ionizing radiation
IRS-1	insulin receptor substrate-1
Kb	kilobase
kD	kilodalton
KSHV	Kaposi’s sarcoma associated herpesvirus
LMB	leptomycin B
LMP	lysosomal membrane permeabilization
LSD1	lysine-specific demethylase 1
LXR	liver X receptor
M-CSF	macrophage colony-stimulating factor
MA	matrix
MAM	mitochondria-associated membrane
MAPK	mitogen-activated protein kinase

Mb	megabase
MCMV	murine cytomegalovirus
MDM2	murine double minute 2
MEF2	myocyte enhancer factor 2
mES	mouse embryonic stem
MFI	mean fluorescence intensity
MFI	mean fluorescence intensity
MHC	major histocompatibility complex
MHC-I	major histocompatibility complex class I
MHC-II	major histocompatibility complex class II
miR	microRNA
MIR-1	modulator of immune recognition-1
MIR-2	modulator of immune recognition-2
MMP	mitochondria membrane permeabilization
MOI	multiplicity of infection
MOMP	mitochondria outer membrane permeabilization
MPF	maturation-promoting factor
MPF	mitosis-promoting factor
MR	middle region
mRNA	messenger RNA
MVB	multivesicular body
N	amino
NAD^+	nicotinamide adenine dinucleotide
NC	nucleocapsid
NCID	notch1 intracellular domain
Nef	negative factor
NF-κB	nuclear factor-kappa B
NK	natural killer
NMR	nuclear magnetic resonance

NP-40	Nonidet P-40
NS	not significant
NSCLC	non-small cell lung carcinoma
NTA	nitrilotriacetic acid
ORF66	open reading frame 66
Otubain 1	ovarian tumor (OTU) domain-containing protease
p14ARF	p14 alternate reading frame
p53-AIP1	p53-regulated apoptosis inducing protein 1
PACS	phosphofurin acidic cluster sorting protein
PACS-1	phosphofurin acidic cluster sorting protein-1
PACS-2	phosphofurin acidic cluster sorting protein-2
PAK2	p21-activated kinase 2
PARP	poly (ADP-ribose) polymerase
PBS	phosphate buffered saline
PC6B	proprotein convertase 6B
PCAF	p300/CBP-associated factor
PCNA	proliferating cell nuclear antigen
PCR	polymerase chain reaction
PECAM-1	platelet-endothelial cell adhesion molecule-1
PERP	p53 apoptosis effector related to PMP-22
PGC-1α	PPARγ coactivator 1α
PI3K	phosphatidylinositide 3-kinase
PIG3	p53-inducible gene 3
PIP_3	phosphatidylinositol (3,4,5)-triphosphate
Pirh2	p53-induced RING-H2
PKD1	polycystic kidney disease 1
PKD2	polycystic kidney disease 2
PMP-22	peripheral myelin protein-22
PMSF	phenylmethanesulfonylfluoride

PP2A	protein phosphatase 2A
PPARγ	peroxisome proliferator-activated receptor-γ
PRMT1	protein arginine N-methyltransferase 1
PRMT5	protein arginine N-methyltransferase 5
PSS-1	phosphatidylserine synthase-1
PTEN	phosphatase and tensin homolog
PTP1B	protein phosphatase 1B
Puma	p53-upregulated modulator of apoptosis
qRT-PCR	quantitative reverse transcription PCR
Rb	retinoblastoma
RING	really interesting new gene
RNA	ribonucleic acid
ROS	reactive oxygen species
RPM	revolutions per minute
RRE	Rev Response Elements
SD	standard deviation
SDS	sodium dodecyl sulfate
SDS-PAGE	SDS-polyacrylamide gel electrophoresis
SEM	standard error of the mean
SENP1	sentrin-specific protease 1
SFK	Src family kinase
SH2	Src homology 2
SH3	Src homolgy 3
Sir2	silent information regulator 2
Sir2α	silent information regulator 2α
siRNA	small interfering RNA
SIRT1	Sirtuin 1
SIV	simian immunodeficiency virus
SMAD7	signaling protein mothers against decaoentaplegic homolog 7

Smyd2	SET and MYND domain containing 2
SNARE	soluble N-ethylmaleimide-sensitive fusion protein-attachment protein receptor
SREBP-1c	sterol regulatory element-binding protein-1c
ssRNA	single-stranded RNA ssRNA
STAT3	signal transducer and activator of transcription 3
SUMO	small ubiquitin-like modifier
T-cells	T-lymphocytes
TAFII31	TATA-binding-protein-associated factor II 31
TAFII70	TATA-binding-protein-associated factor II 70
TAP	transporter associated with antigen presentation
TAR	trans-activating response element
TBS	tris buffered saline
TCR	T-cell receptor
TCR	T-cell receptor
TFIID	transcription factor II D
TFIIH	transcription factor II H
TGF-β	transforming growth factor-β
TGN	trans-Golgi network
TNFα	tumor necrosis factor α
TRAIL	TNF α-related apoptosis-inducing ligand
TRPP2	transient receptor potential polycistic 2
TSA	trichostatin A
TSP-1	thrombospondin-1
U	uridine
Ub	ubiquitin
US	United States
US11	unique short region 11
US3	unique short region 3

USP	ubiquitin (Ub)-specific proteases
UTR	untranslated region
V3	third variable loop
VHL	von Hippel-Lindau
Vif	viral infectivity factor
Vpr	viral protein r
Vpu	viral protein u
VV	vaccinia
VZV	varciella zoster virus
WT	wild-type
WBI	whole body irradiation
XPA	xeroderma pigmentosum complementation group A
YFP	yellow fluorescent protein
YY1	yin yang 1
ZAP-70	zeta-chain-associated protein kinase-70

ACKNOWLEDGEMENTS

To my family,
friends,
and all those
who have supported,
motivated,
and inspired me.

Thank you.

ABSTRACT

Following DNA damage, the sequence-specific transcription factor p53 functions as a node for orchestrating biological responses such as cell-cycle arrest, apoptosis, and senescence by promoting the transactivation of various target genes. Importantly, the ability of p53 to orchestrate these diverse processes critically depends on the regulation of p53 by cellular cofactors and modifying enzymes. Notably, p53 acetylation is essential for its transcriptional activation following DNA damage. p53 is deacetylated by Sirtuin 1 (SIRT1), a nicotinamide adenine dinucleotide (NAD^+)-dependent histone deacetylase, thereby repressing p53 transcriptional activation. Therefore, understanding how the SIRT1-p53 axis is regulated during the DNA damage response is essential for gaining insight into the mechanisms controlling p53 activation. Here we demonstrate that the membrane trafficking protein PACS-2 inhibits SIRT1-mediated deacetylation of p53 to modulate the cellular response to DNA damage. We demonstrate that PACS-2 directly interacts with SIRT1 and inhibits SIRT1-mediated deacetylation of p53 *in vivo*. Moreover, PACS-2 deficient cells have a SIRT1-dependent reduction in p53 acetylation and p21 expression, resulting in increased apoptosis and reduced clonogenic survival in a p53- and p21-dependent manner following DNA damage. Based on these observations, I propose that PACS-2 is a critical regulator of the SIRT1-p53-p21 axis to modulate the DNA damage response.

In addition, the studies in this dissertation describe how the identification of PACS-2 as essential for HIV-1 Nef-mediated immune evasion lead to the discovery of a small molecule inhibitor that targets a critical PACS-2-dependent step in HIV-1 Nef action. To evade $CD8^+$ T-cell destruction, HIV-1 Nef assembles a Src family kinase (SFK)-ZAP-70-PI3K complex to trigger MHC-I downregulation. These studies demonstrate that chemical inhibition of the Nef-SFK interaction disrupts formation of the multi-kinase complex and represses Nef-mediated MHC-I downregulation in primary $CD4^+$ T-cells. Moreover, transport studies reveal Nef assembles the multi-kinase complex to trigger downregulation of cell-surface MHC-I early following infection. By three days post-infection, Nef switches to a stoichiometric mode that prevents surface delivery of newly synthesized MHC-I. Together, these studies suggest Nef orchestrates a regulated molecular program to evade immune surveillance and provides new insights into the mechanism of Nef action.

Together, these studies significantly contribute to the understanding of how a membrane trafficking protein can have diverse cellular roles linking viral pathogenesis to DNA damage and tumor suppression pathways. Future studies must systematically determine how PACS-2 coordinates these various functional roles and the cellular and biological contexts for which these regulatory networks are essential. Given the diverse nature of the cellular proteins and processes modulated by PACS-2, the implications of this data are far reaching and suggest that PACS-2 may function in various cellular processes such as gene regulation,

cell growth and survival as well as biological processes such as cancer, viral immunity, aging, and metabolism.

OVERVIEW

The identification and characterization of multifunctional genes has significantly contributed to the understanding of how diverse cellular pathways and networks are intrinsically connected at a multitude of regulatory steps. The central hypothesis of this dissertation is that the phosphofurin acidic cluster sorting protein-2 (PACS-2) is essential for key steps in viral pathogenesis mediated by human immunodeficiency virus-1 (HIV-1) Nef, as well as for regulating p53 acetylation and p21 expression following DNA damage by modulation of the deacetylase activity of Sirtuin 1 (SIRT1). The experiments in this dissertation, 1) describe how the identification of PACS-2 as essential for HIV-1 Nef-mediated immune evasion lead to the discovery of a small molecule inhibitor that targets a critical PACS-2-dependent step in Nef action, and 2) identify PACS-2 as a negative regulator of SIRT1 and as an essential mediator of p53 activation and p21 expression following DNA damage. These studies significantly contribute to the understanding of how a membrane trafficking protein can have diverse cellular roles linking viral pathogenesis to DNA damage and tumor suppression pathways.

This dissertation begins with a general introduction to PACS protein biology (**CHAPTER 1**), including an overview of the eukaryotic endomembrane system and trafficking of itinerant cargo, thus providing the foundation for describing the identification of the PACS proteins. This section will also describe

the known functions of PACS-2 and discuss the various roles for PACS-2 in cellular trafficking, viral pathogenesis, cell death, and cancer. The subsequent chapters of this dissertation are divided into two main components (**PARTS I-II**). The first component (**PART I: CHAPTERS 2-4**) relates to HIV-1 Nef-mediated pathogenesis while the second component (**PART II: CHAPTERS 5-7**) relates to SIRT1-mediated p53 regulation and the DNA damage response. The first component (**PART I**) begins by describing the relevant literature in HIV pathogenesis (**CHAPTER 2**) and will provide essential background pertaining to HIV-1 epidemiology, virology, and disease pathogenesis as well as describe the complex mechanisms HIV-1 Nef employs to coordinate evasion of HIV-1-infected cells from immune surveillance while promoting pathogenicity of the virus. The studies in **CHAPTER 3** describe how the identification of PACS-2 as essential for HIV-1 Nef-mediated immune evasion lead to the discovery of a small molecule inhibitor that targets a critical PACS-2-dependent step in Nef action. This work was published in *Molecular Biology of the Cell* in 2010. The results and implications of these studies are discussed in **CHAPTER 4** and relate to two current models of HIV-1 Nef-mediated immune evasion pathways as well as the broader context of Nef function.

The second component of this dissertation (**PART II: CHAPTERS 5-7**) will introduce the integral role of p53 following DNA damage (**CHAPTER 5**), including its complex regulation via posttranslational modifications and various cofactor recruitment. Specifically, this chapter will describe the activation of p53 and the

function of p53-induced target genes that mediate cell fate processes such as cell cycle arrest and apoptosis. In addition, this chapter will describe how p53 acetylation controls p53 activity following DNA damage, including the role of SIRT1-mediated deacetylation of p53, as well as describe SIRT1 biology and its complex regulation. The studies in **CHAPTER 6** demonstrate a novel role for PACS-2 in regulating how cells respond to DNA damage by modulating p53 activation via inhibition of SIRT1-mediated deacetylation of p53. This data is currently being prepared as a manuscript for publication. The results and implications of these studies are discussed in **CHAPTER 7**. Given the complex nature of SIRT1, p53, p21, and PACS-2, the potential implications of these studies span cellular processes such as gene regulation, chromatin remodeling, cell growth and survival as well as biological processes such as cancer, aging, and metabolism. **CHAPTER 8** summarizes the overall conclusions from the data presented in both components of this dissertation.

Appendices of this thesis include **A**) a published manuscript describing how a hypoxia inducible factor (HIF)-regulated von Hippel-Lindau (VHL)-protein phosphatase 1B (PTP1B)-Src signaling axis identifies a therapeutic target in renal cell carcinoma published in *Science Translational Medicine* in 2011 and **B**) Supplementary and Preliminary data depicting additional cellular roles for PACS-2.

CHAPTER 1. Introduction to PACS proteins

1.1 Membrane traffic in the secretory pathway

1.1.1 The eukaryotic endomembrane system

The endomembrane system is a diverse array of membranes in the cytoplasm of a eukaryotic cell that partition the cell into various compartments or organelles. This complex system includes the nuclear envelope, endoplasmic reticulum (ER), Golgi apparatus, plasma membrane as well as lysosomes, endosomes, secretory granules, vacuoles, and peroxisomes. These organelles are an evolutionarily conserved set of membranes that form a functional and developmental unit through direct connection and/or vesicular transport (Dacks et al., 2007, Dacks et al., 2009, Elias, 2010). The endomembrane system coordinates secretory and endocytic pathways to modify and transport cellular material. Along with these functions, the endomembrane system also provides the organization and machinery necessary to carry out essential homeostatic processes such as the production of proteins and lipids, detoxification of drugs and poisons, protein secretion, uptake of nutrients, turnover of proteins and organelles, as well as the induction of apoptotic pathways (Dacks et al., 2007, Cheng et al., 2010).

The endomembrane system integrates with the secretory pathway via the generation of nascent polypeptides that are packaged into coatamer protein II (COPII) coated vesicles budding from the ER, forming vesicular intermediates that reach the *cis* face of the Golgi complex (Figure 1.1) (Duden, 2003). In the Golgi, newly synthesized peptides are further processed and undergo

modifications such as glycosylation, phosphorylation, and sulfation until they reach their final destination (Mellman et al., 2000). The trafficking of vesicles through the Golgi permits the delivery of newly synthesized proteins to the *trans*-Golgi network (TGN), a major secretory pathway sorting station that directs trafficking of newly synthesized proteins to specific subcellular locations (Gu et al., 2001). Upon exit from the *trans*-Golgi network (TGN), cellular cargo can be sorted to various organelles and may follow a myriad of transport routes (Bonifacino et al., 2004, Cai et al., 2007, Pfeffer, 2007, Stenmark, 2009). Indeed, vesicles may traffic in an anterograde manner to the plasma membrane or in a retrograde fashion originating from the *cis* face of the Golgi back to the ER. Alternatively, these TGN-derived vesicles may fuse with endocytic vesicles derived from the plasma membrane or with late endosomes, the latter of which can undergo fusion with lysosomes to mediate hydrolytic degradation of vesicular contents (Luzio et al., 2007). Moreover, autophagosomes, which are membrane-bound vesicles that sequester cytoplasmic contents, fuse with lysosomes to form autophagolysosomes to mediate the degradation of its contents by lysosomal hydrolases (Tooze et al., 2010).

1.1.2 Sorting signals in the secretory pathway

The trafficking of itinerant proteins is highly dynamic and relies on canonical sorting motifs within the cytosolic domains of these proteins. These motifs are recognized by the cellular sorting machinery and mediate the

subsequent sorting and delivery of various cargo proteins to specific cellular locations (Seaman, 2008). The complex nature of this sorting process reflects the diverse biological functions of these membrane proteins. A well-characterized example is the transferrin receptor, which regulates iron homeostasis by importing transferrin-iron complexes through receptor-mediated endocytosis while constitutively recycling unoccupied receptors from recycling endosomes to the cell surface via early endosomal vesicles (van Dam et al., 2002). Another example are mannose-6-phosphate receptors (MPRs), which bind newly synthesized lysosomal hydrolases in the TGN, sort them to lysosomes, and are then recycled back to the TGN (Griffiths et al., 1988). Similar in this cycling nature is the endoprotease furin, which localizes to the TGN but cycles between the cell surface, immature secretory granules, and endosomes, becoming autocatalytically activated as it transits through the secretory pathway (Molloy et al., 1999). What these itinerant membrane proteins have in common is that they rely primarily on canonical sorting motifs within their cytosolic domains to be appropriately sorted and transported within the secretory pathway. These sorting motifs serve as intracellular “address labels” or “boarding passes” that are read by components of the sorting machinery that will then, in turn, sort and deliver the cargo proteins to their destined compartment (Seaman, 2008, Gu et al., 2001).

Eukaryotic sorting adaptors recognize a vast array of sorting motifs on the cytosolic domains of membrane cargo. Canonical sorting motifs such as the tyrosine-(YXXΦ, where Φ is a bulky hydrophobic residue) and dileucine-based

([DE]XXX[LI]) motifs mediate trafficking in the late secretory pathway by linking cargo to adaptor protein (AP) complexes (Seaman, 2008). These heterotetrameric AP complexes sort cargo into vesicles for transport between various membrane-bound compartments. Currently there are five identified AP complexes that coordinate post-TGN sorting pathways and have distinct localization and function (Hirst et al., 2011, Robinson et al., 2001). AP-1 and AP-2 sort cargo proteins into clathrin-coated vesicles (CCVs), while AP-3, AP-4, and AP-5 are clathrin-independent adaptor molecules ((Hirst et al., 2011) and reviewed in (Boehm et al., 2001, Robinson et al., 2001)). The functions of the AP complexes in post-TGN trafficking are described below and summarized in Figure 1.2. AP-1 is involved in trafficking between tubular endosomes and the TGN and can localize to one or both of these compartments (Robinson et al., 2010). AP-2 is the most well characterized AP complex and directs clathrin-mediated endocytosis (Jackson et al., 2010). Clathrin-independent AP-3 sorts cargo from tubular endosomes to late endosomes and lysosomes, while AP-4 complexes mediate basolateral transport in polarized epithelial cells (Simmen et al., 2002). Lastly, the recently discovered AP-5 associates with late endosomes and is involved in trafficking of the cation independent mannose 6-phosphate receptor (CI-MPR) (Hirst et al., 2011). While the canonical tyrosine- and leucine-based motifs direct trafficking in the late secretory pathway (Seaman, 2008), the -KKXX and FF-motifs mediate sorting steps in the early secretory pathway by linking cargo proteins to coatomer proteins I and II (COPI and COPII),

respectively (McMahon et al., 2004, Zanetti et al., 2012, Lippincott-Schwartz et al., 2006).

Along with canonical sorting motifs, membrane cargo frequently contain additional sorting signals such as stretches of acidic residues, which often contain serine or threonine residues that can be phosphorylated by the acidic-directed protein kinase CK2 and dephosphorylated by isoforms of protein phosphatase 2A (PP2A) (Bonifacino et al., 2003, Gu et al., 2001, Thomas, 2002, Molloy et al., 1999). Importantly, these acidic motifs control the sorting and subcellular distribution of itinerant membrane cargo, such as the endoprotease furin, throughout the secretory pathway (Thomas, 2002). Indeed, the acidic cluster sorting motif in the cytosolic domain of furin contains two serine residues (EECPp$\underline{S}_{773}$Dp$\underline{S}_{775}$EED) that when phosphorylated by CK2 leads to the TGN-localization of furin, as well as controls the recycling of endocytosed furin from early endosomes to the cell surface and facilitates the removal of furin from immature secretory granules in neuroendocrine cells (Jones et al., 1995, Crump et al., 2001, Dittie et al., 1997, Molloy et al., 1998). These discoveries led to the determination that acidic cluster sorting signals mediate trafficking steps used by a diverse array of cargo, such as ion channels, proprotein convertases, various receptors, soluble N-ethylmaleimide-sensitive fusion protein-attachment protein receptors (SNAREs), endosomal sorting complex required for transport (ESCRT) proteins, as well as proteins expressed by herpesviruses and HIV-1 (Youker et al., 2009).

1.1.3 Membrane associated proteins with distinct cytoplasmic and nuclear functions link the endomembrane system with gene regulation pathways

For simplicity, proteins are often functionally categorized as “transcription factors”, “sorting proteins”, or “signaling proteins”, etc. However, while this functional partitioning can be useful, an increasing number of proteins are being identified with various cellular functions in distinct subcellular locations. Indeed, many membrane-associated proteins with well-characterized cytoplasmic trafficking roles have been identified as having distinct nuclear functions, while numerous nuclear proteins have additionally been identified as having membrane-associated functions. These findings support a functional link between the endomembrane system and gene regulation pathways. For instance, the multifunctional protein kinase CK2, which controls various trafficking steps in the TGN/endosomal system and plays a critical role in cell survival (Litchfield, 2003), was identified as undergoing nuclear translocation following ionizing radiation (IR) (Yamane et al., 2005) and hypoxia (Pluemsampant et al., 2008) to exert pro-survival actions and activation of histone deacetylases (HDACs), respectively. Additionally, the well-characterized cytosolic and membrane-associated functions of glycogen synthase kinase-3β (GSK3β) control the phosphorylation and degradation of β-catenin in the canonical Wnt signaling pathway (Ciani et al., 2005, Zeng et al., 2005). However, GSK3β has been additionally identified as localizing to the nucleus to regulate numerous

transcription factors including nuclear factor-kappa B (NF-κB), cyclic adenosine monophosphate (AMP) response element binding protein (CREB), p53, and Myc (Hoeflich et al., 2000, Grimes et al., 2001, Zhou et al., 2004, Jope et al., 2004). Indeed, many well-characterized nuclear proteins have been identified as having membrane-associated functions. For instance, carboxy (C)-terminal binding protein of adenovirus E1A (CtBP) was identified as a transcriptional corepressor but was later implicated in Golgi partitioning, membrane fission during intracellular trafficking, and the organization of ribbon synapses (Corda et al., 2006). In addition, the tumor suppressor p53 can translocate to the cytoplasm where is associates with the integral mitochondria membrane proteins B-cell lymphoma-extra large (Bcl-xL) and B-cell lymphoma-2 (Bcl-2) to mediate mitochondria membrane permeabilization following DNA damage (Green et al., 2009) while histone deacetylase 3 (HDAC3) can localize to the plasma membrane where it is a substrate of the tyrosine kinase Src (Longworth et al., 2006). Together, these findings support a functional link between the endomembrane system and gene regulation pathways.

1.2 The PACS family of sorting proteins

1.2.1 Identification of the PACS proteins

The phosphofurin acidic cluster sorting (PACS) proteins, including PACS-1 and PACS-2, are a family of membrane trafficking proteins expressed in metazoans that have diverse roles in cellular homeostasis and

pathophysiological processes (Youker et al., 2009). The discovery of the PACS proteins was based on a screen of candidate sorting factors that interact with the phosphorylated acidic cluster sorting motif on the cytoplasmic domain of the endoprotease furin (Thomas, 2002, Wan et al., 1998, Youker et al., 2009). Indeed, these studies identified PACS-1 as a “sorting connector” that connects CK2-phosphorylated furin to the heterotetrameric adaptor protein-1 (AP-1), thereby mediating the TGN-localization of furin (Molloy et al., 1999, Jones et al., 1995, Molloy et al., 1994, Wan et al., 1998, Thomas, 2002). Sequence homology of the *PACS-1* gene led to the identification of the *PACS-2* gene (Simmen et al., 2005). The PACS-2 protein also binds to acidic cluster sorting motifs of itinerant proteins (Kottgen et al., 2005, Simmen et al., 2005), but unlike PACS-1, which connects acidic cluster-containing cargo to AP-1 and AP-3 complexes (Crump et al., 2001), PACS-2 connects cargo proteins to COPI coatomer to mediate clathrin-independent, Golgi to ER trafficking in the early secretory pathway (Kottgen et al., 2005). Indeed, a genetic screen performed in Caenorhabditis elegans (C. elegans) determined that the single C. elegans PACS gene product localizes to early endosomes and functions in synaptic transmission (Sieburth et al., 2005). These data are consistent with an evolutionarily conserved trafficking role for the PACS proteins.

1.2.2 PACS-1 and PACS-2 mediate multiple membrane trafficking steps

Itinerant membrane proteins are sorted from early endosomes to various destinations, including recycling to the cell surface, maturation to late endosomes, or sorting to the TGN. In mammalian cells, PACS-1 is required for the TGN-localization of furin, as well as other acidic cluster-containing cargo such as the cation-independent mannose-6-phosphate receptor (CI-MPR), and the viral envelopes from human cytomegalovirus and the feline RD114 retrovirus (described in section 1.2.5) (Wan et al., 1998, Crump et al., 2001, Crump et al., 2003, Bouard et al., 2007). PACS-1 directs additional sorting steps in the late secretory pathway, including the recycling of internalized cargo from the early endosome to the cell surface and the delivery of acidic cluster-containing cargo to the primary cilium (Molloy et al., 1998, Schermer et al., 2005, Crump et al., 2001, Chen et al., 2009, Jenkins et al., 2009). Interestingly, while PACS-2 was initially shown to mediate the ER localization of acidic cluster-containing cargo such as profurin, the ion channel polycystic kidney disease 2 (PKD2) (or polycystin 2), and calnexin (described in section 1.3) (Feliciangeli et al., 2006, Myhill et al., 2008, Kottgen et al., 2005), additional studies revealed PACS-2 also mediates trafficking steps in the TGN/endosomal system (Atkins et al., 2008). Indeed, while PACS-1 and PACS-2 are both required for maintaining the steady-state TGN-localization of the itinerant cellular cargo protein CI-MPR, they have distinct roles in regulating the sorting of an internalized CI-MPR reporter, as knockdown of PACS-2, but not PACS-1, inhibits the transport of endocytosed CI-MPR from early endosomes to the TGN (Atkins et al., 2008). These results

suggest that PACS proteins mediate separate trafficking steps from the early endosome; while PACS-1 mediates recycling of cargo from early endosomes to the cell surface, PACS-2 directs the delivery of cargo from the early endosome to the TGN (Atkins et al., Molloy et al., 1998, Crump et al., 2001, Chen et al., 2009). A summary of PACS-mediated trafficking steps is presented in Figure 1.3. The ability of PACS proteins to coordinate the trafficking of the HIV-1 protein Nef will be described in the following chapter (Chapter 2).

1.2.3 Functional domains of the PACS proteins

The PACS-2 proteins (PACS-1 and PACS-2) share 54% overall sequence homology and are divided into four regions. The atrophin-1 related region (ARR) is an N-terminal region found only in PACS-1 that is enriched in proline/glutamine and serine/alanine stretches and shares homology with the atrophin-1 transcriptional repressor (Wood et al., 2000), however the function of this region is not yet known. Both proteins contain an ~150 amino acid cargo- or furin-binding region (FBR), in which PACS-1 and PACS-2 share >80% sequence homology. The PACS-1 FBR interacts with cargo as well as AP-1, AP-3, and Golgi-localized, gamma adaptin ear-containing, ARF-binding (GGA) complexes, and the protein kinase CK2 (Crump et al., 2001, Scott et al., 2006, Youker et al., 2009). The PACS-2 FBR interacts with cargo as well as COPI coatamer (Kottgen et al., 2005). The middle region (MR) of both PACS-1 and PACS-2 contains an acidic cluster that functions as an autoregulatory domain (Scott et al., 2003). In

the case of PACS-2, the MR also contains an Akt-phosphorylatable serine at position 437 which serves as a 14-3-3 binding site to control the pro-apoptotic action of PACS-2 following death-ligand signaling (described in section 1.3.3) (Aslan et al., 2009). The function of the PACS-1 and PACS-2 C-terminal regions (CTR) is not yet known.

1.2.4 PACS protein biochemistry and cargo protein interactions

Both of the *PACS* genes are ubiquitously expressed, however *PACS-1* is selectively enriched in peripheral lymphocytes while *PACS-2* is enriched in skeletal muscle (Simmen et al., 2005). The binding of PACS FBRs to acidic cluster motifs in cargo such as furin, CI-MPR, and PKD2 is highly dependent on CK2 phosphorylation of specific serine residues within the acidic cluster sites of these proteins (Youker et al., 2009). However, PACS proteins also interact with acidic cluster motifs in cargo that are selectively de-phosphorylated, such as in the case of the ER chaperone calnexin (Myhill et al., 2008). Importantly, some acidic cluster-mediated cargo interactions with PACS proteins are completely independent of phosphorylation status, such as the case with proprotein convertase 6B (PC6B), or are mediated by non-phosphorylatable acidic clusters, as in the case of HIV-1 Nef (Piguet et al., 2000). Interestingly, in the case of Nef, PACS proteins bind a bipartite site in Nef, including the $EEEE_{65}$ acidic cluster as well as a hydrophobic patch (including W_{113}) on an α-helix in the Nef core domain (Dikeakos et al., 2012). Thus, the PACS proteins bind cellular targets using at

least three distinct motifs: acidic cluster sites in which the interaction is dependent on CK2 phosphorylation status; non-phosphorylatable acidic clusters; as well as sites like that in Nef which contain a hydrophobic patch within an α-helical segment (Youker et al., 2009, Dikeakos et al., 2012). These data illustrate the complex nature of PACS protein interactions and the diversity of known cargo proteins.

1.2.5 The role of PACS proteins in viral pathogenesis

Many pathogenic viruses exploit components of the host endomembrane system to increase viral tropism, enhance replication and modulate the host antiviral response. Indeed, viruses including HIV-1, human cytomegalovirus (HCMV, also known as human herpesvirus-5 (HHV-5)), and Kaposi's sarcoma associated herpesvirus (KSHV, also known as human herpesvirus-8 (HHV-8)), use the PACS proteins to module host cell function and enhance viral pathogenesis (Youker et al., 2009).

In the case of HCMV, PACS-1 functions to promote envelopment and assembly of this ubiquitous virus (Crump et al., 2003, Jarvis et al., 2004). Indeed, the seroprevalence of HCMV in the United States (US) is dependent on age, as nearly 60% of individuals 6 years and older are infected with HCMV while >90% of individuals 80+ years old are infected, including 50-80% of US adults (Staras et al., 2006, Staras et al., 2008). Importantly, while HCMV infection generally goes unnoticed in healthy individuals, it has devastating effects on the

immunocompromised, including HIV-infected patients, transplant recipients, and newborn infants (Taylor, 2003). HCMV, like other herpesviruses, uses the host endomembrane system to mediate budding of viral progeny into an assembly compartment formed from the TGN and associated endosomal membranes containing tegument proteins and envelope glycoproteins, such as HCMV glycoprotein B (gB) (Mettenleiter et al., 2006, Sanchez et al., 2000). The cytosolic domain of HCMV gB contains a CK2-phosphorylatable acidic cluster that binds PACS-1 (Crump et al., 2003, Jarvis et al., 2004). Indeed, PACS-1 binds the CK2-phosphorylated gB cytosolic tail to mediate its TGN-localization and promote virus envelopment (Crump et al., 2003, Jarvis et al., 2004). However, this function is not limited to HCMV, as PACS-1 also regulates the envelopment of the feline retrovirus RD114 via an acidic cluster in the cytosolic tail of its envelope glycoprotein to promote virus assembly (Bouard et al., 2007).

KSVH is the causative agent of Kaposi's sarcoma, an acquired immunodeficiency syndrome (AIDS)-related malignancy characterized by highly vascular lesions of the lymphatic endothelium that uniformly contain tumor cells called spindle cells, which are pathognomonic for this disease (Chang et al., 1994, Ganem, 2006). KSVH encodes a ubiquitin ligase K5 which targets cluster of differentiation 31 (CD31), also known as platelet-endothelial cell adhesion molecule-1 (PECAM-1), for degradation, thereby disturbing endothelial contacts and increasing viral spread (Mansouri et al., 2006, Means et al., 2007). K5 contains two acidic clusters in its cytosolic domain that interact with PACS-2 and

are required for downmodulation of CD31 in a PACS-2-dependent manner (Mansouri et al., 2006).

PACS-2 and PACS-1 are also required for the ability of HIV-1 Nef to downregulate cell-surface MHC-I molecules thereby evading immune surveillance (Blagoveshchenskaya et al., 2002, Atkins et al., 2008, Hung et al., 2007). The role of PACS proteins in HIV-1 pathogenesis will be described in the HIV-1 introductory chapter (Chapter 2).

1.3 The multiple roles of PACS-2 in interorganellar communication, membrane traffic, and apoptosis

1.3.1 PACS-2 mediates the ER-localization of polycystin-2

The ER-localized transient receptor potential polycystic 2 (TRPP2) channel (also known as polycystin-2 or polycystic kidney disease 2 (PKD2)) is a calcium-selective ion channel whose function is dependent on its subcellular localization (Cai et al., 1999, Fu et al., 2008, Koulen et al., 2002, Li et al., 2005, Giamarchi et al., 2006). When localized to the ER, PKD2 functions to regulate intracellular calcium concentrations by collaborating with inositol (1,4,5)-triphosphate (IP_3) and ryanodine receptors (Cai et al., 1999, Fu et al., 2008). However, when localized to the primary cilium of the renal tubule, PKD2 coordinates with PKD1 to act as a mechanosensor that monitors fluid flow through the lumen of the renal tubule, modulating signaling pathways that control cell proliferation and tubulogenesis (Nauli et al., 2003). Indeed, mutations in

PKD1 or PKD2 lead to autosomal dominant polycystic kidney disease (ADPKD), an adult-onset hypertensive disorder characterized by large renal cysts that will lead to end-stage renal failure in approximately 50% of patients by the 4^{th}-6^{th} decades of life (Grantham, 2008). Mutations in PKD2 account for approximately 15% of total ADPKD cases (mutations in PKD1 accounting for the rest), and these include mutations that lead to the deletion of the acidic cluster motif in PKD2 (Cai et al., 1999, Sutters et al., 2003, Delmas et al., 2004). Indeed, the cellular distribution of PKD2 between the ER, TGN, and cell surface is controlled by its CK2-phosphorylatable acidic cluster motif in a PACS-1- and PACS-2-dependent manner (Kottgen et al., 2005). While PACS-2 is required for localizing PKD2 to the ER in a COPI-dependent manner, PACS-1 localizes PKD2 to the TGN from endosomes (Kottgen et al., 2005).

1.3.2 PACS-2 regulates ER-Mitochondria communication and ER homeostasis

The ER and mitochondria form close contacts called mitochondria-associated membranes (MAMs) that facilitate communication between these compartments, including lipid biosynthesis and transfer as well as the exchange of calcium ions, which in turn controls ER chaperones, mitochondrial adenosine triphosphate (ATP) production, and apoptosis (Csordas et al., 2006, Berridge, 2002, Franke et al., 1971, Vance, 1990, Achleitner et al., 1999, Gaigg et al., 1995). In addition to mediating the ER-localization of the calcium channel polycystin-2 (PKD2) (Kottgen et al., 2005), PACS-2 also controls MAM

stabilization and/or formation by mediating the tethering of mitochondria to the ER at MAMs, as loss of PACS-2 results in the uncoupling of mitochondria from the ER, leading to the mislocalization of the MAM-associated lipid biosynthesis enzymes fatty acyl-Coenzyme A ligase-4 (FACL-4) and phosphatidylserine synthase-1 (PSS-1), as well as the disruption of histamine-inducible calcium release from the ER (Simmen et al., 2005).

Furthermore, PACS-2 controls the subcellular localization of the ER chaperone calnexin, which distributes between the rough ER, mitochondria, and plasma membrane in a PACS-2-dependent manner (Myhill et al., 2008). Indeed, the ability of PACS-2 to control the subcellular localization of calnexin is dependent on the binding of PACS-2 to the non-phosphorylated CK2 acidic cluster motif within the cytosolic tail of calnexin (Myhill et al., 2008). One manner by which calnexin mediates ER homeostasis is through its association with the ER stress sensor B-cell receptor-associated protein 31 (BAP31), which stimulates dynamin-related protein-1 (Drp1) to fissure mitochondria during ER stress (Breckenridge et al., 2003, Zuppini et al., 2002). Indeed, loss of PACS-2 redistributes calnexin from the ER to the plasma membrane and results in a BAP31-dependent fragmentation of mitochondria (Simmen et al., 2005). These studies determined that PACS-2 acts as a link between ER-mitochondria communication and ER homoeostasis.

1.3.3 PACS-2 controls Bid translocation to mitochondria and is essential for TRAIL-mediated Apoptosis

Cells lacking PACS-2 are resistant to apoptosis induced by staurosporine or by the death ligands tumor necrosis factor α (TNFα) or TNF-related apoptosis-inducing ligand (TRAIL) (Aslan et al., 2009, Simmen et al., 2005). Indeed, PACS-2 is required for TRAIL-induced apoptosis *in vivo* in a mouse model of viral hepatitis, as well as in human tumor cell lines *in vitro* (Aslan et al., 2009). In non-apoptotic cells, PACS-2 mediates cell homoeostasis by coordinating the ER-localization of anti-apoptotic ion channels (PKD2) with ER-mitochondria communication (Kottgen et al., 2005). The ability of PACS-2 to switch between regulating membrane traffic and ER homeostasis to mediating TRAIL-induced apoptosis is controlled by the Akt-phosphorylation of PACS-2 at Ser_{437} (Aslan et al., 2009). Indeed, PACS-2 is bound by anti-apoptotic 14-3-3 proteins in a phospho-Ser_{437}-dependent manner, and this 14-3-3-mediated repression is required for the ability of PACS-2 to mediate ER-localization of PKD2 in non-apoptotic cells (Aslan et al., 2009). In response to TRAIL, PACS-2 is dephosphorylated, releasing PACS-2 from sequestration by 14-3-3 and allowing PACS-2 to promote the translocation of the pro-apoptotic Bcl-2 homology (BH)3-only protein Bid to mitochondria, leading to the subsequent cleavage of Bid on mitochondria, the release of cytochrome c, and the activation of executioner caspases, including caspase-3 (Aslan et al., 2009, Simmen et al., 2005). Indeed, PACS-2 binds full-length Bid in a CK2-phosphorylation dependent manner,

similar to other PACS cargo proteins, to mediate its translocation to mitochondria (Aslan et al., 2009, Simmen et al., 2005).

1.3.4 PACS-2 recruits Bim and Bax to lysosomes to mediate TRAIL-induced lysosomal permeabilization and apoptosis

In liver cancer cells, TRAIL complexes with death receptor-5 (DR5) to recruit proapoptotic Bim and Bax to lysosomes, resulting in lysosomal membrane permeabilization (LMP) and the subsequent release of cathepsin B into the cytosol (Kahraman et al., 2008, Werneburg et al., 2007, Canbay et al., 2003, Johansson et al., 2010). Indeed, LMP occurs upstream of mitochondria membrane permeabilization (MMP) and many cell types require LMP for efficient activation of cell death processes (Guicciardi et al., 2000, Guicciardi et al., 2004, Werneburg et al., 2002, Werneburg et al., 2007, Werneburg et al., 2004, Boya et al., 2003a, Boya et al., 2003b). Accordingly, TRAIL-induced LMP and cathepsin B release mediates subsequent mitochondria membrane permeabilization and the activation of executioner caspases leading to cell death (Kahraman et al., 2008, Werneburg et al., 2007, Canbay et al., 2003, Johansson et al., 2010). As described in the section above, TRAIL signaling leads to the PACS-2-mediated trafficking of Bid to mitochondria, leading to permeabilization of the outer mitochondria membrane (Aslan et al., 2009). Further studies determined that TRAIL requires PACS-2 at additional steps leading to mitochondria permeabilization. Indeed, TRAIL recruits PACS-2 to DR5-positive endosomes,

forming a complex with Bim and Bax on lysosomal membranes. This complex is required for LMP, leading to the release of cathepsin B and the induction of apoptosis (Werneburg et al., 2012).

1.3.5 Dysregulation of the PACS-2 gene

The human *PACS-2* gene is located near the telomere on the long arm of chromosome 14. Interestingly, the 14q32.33 locus containing *PACS-2* is highly susceptible to chromosomal instability in multiple cancers (Anderson et al., 2001, Gallegos Ruiz et al., 2008, Kang et al., 2006, Dijkman et al., 2006, Choi et al., 2010, Bando et al., 1999). Indeed, the 14q32.33 locus is deleted in 44% of non-small cell lung carcinomas (NSCLC) (Gallegos Ruiz et al., 2008) and 68% of primary cutaneous large B-cell lymphomas (Dijkman et al., 2006) and is reported as frequently deleted in recurrent breast cancer (Kang et al., 2006) as well as colorectal cancer (Bando et al., 1999, Bartos et al., 2007). Specifically, the *PACS-2* gene has been reported to be deleted in 15-40% of sporadic colorectal cancer (Anderson et al., 2001), consistent with recent studies from our laboratory showing that PACS-2 protein expression is lost in late stage colorectal cancer (Aslan et al., 2009).

In addition to human cancers, the 14q32.33 locus containing *PACS-2* is susceptible to genetic loss in 14q deletion syndrome. The first case of terminal deletion of chromosome 14 was reported in 1983 (Hreidarsson et al., 1983) and the clinical features of this syndrome include cognitive impairment, microcephaly,

growth retardation, as well as facial dysmorphisms such as epicanthic folds, low-set ears, elongated forehead, micrognathia, smooth philtrum, and thin upper lip (Maurin et al., 2006, Schlade-Bartusiak et al., 2009). Indeed, less than 20 patients with pure 14q32.33 deletions (without a ring chromosome 14, or other chromosomal rearrangements) have been reported (Youngs et al., 2011, Ortigas et al., 1997, Maurin et al., 2006, Schlade-Bartusiak et al., 2009, Holder et al., 2011, Engels et al., 2012). Interestingly, the observation that patients with small 14q32.33 deletions develop similar phenotypes as patients with larger 14q deletions has lead investigators to delineate a proposed critical region that is sufficient for development of this syndrome (Holder et al., 2011, Engels et al., 2012). Indeed, the smallest reported critical regions have been proposed to be as small as 250-305 kb, containing up to seven candidate genes, including *PACS-2* (Holder et al., 2011, Engels et al., 2012). The relative contribution of these genes in mediating the phenotype of 14q32.33 deletion syndrome remains to be determined.

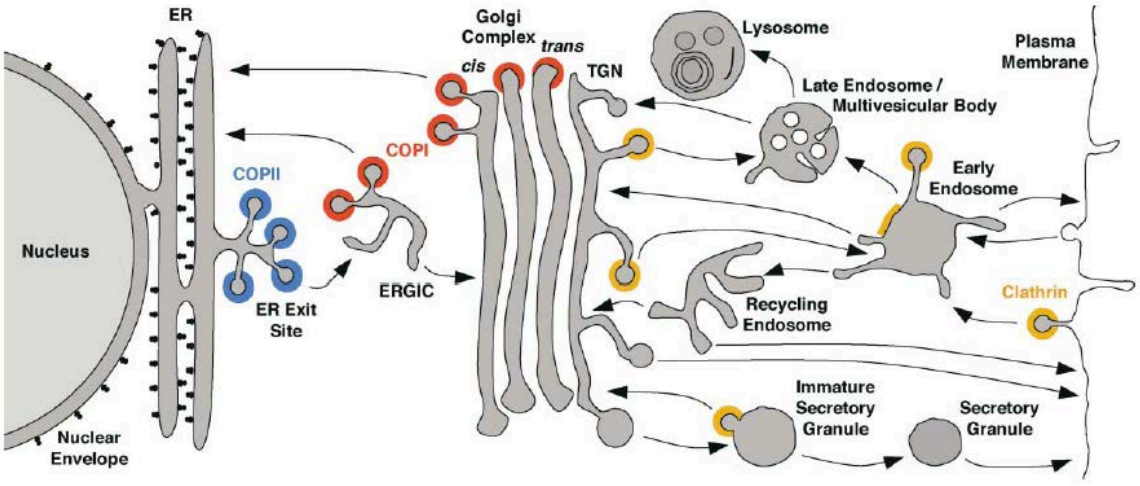

Figure 1.1. A glance at the eukaryotic endomembrane system.

This schematic shows the various compartments of the secretory, lysosomal, and endocytic pathways. Transport steps are denoted by arrows. COPII-mediated trafficking from the ER to the ER-Golgi intermediate compartment (ERGIC) and Golgi is illustrated in blue while COPI-mediated retrieval of cargo from the Golgi is shown in red. Clathrin-mediated steps are shown in orange. Reproduced with permission from (Bonifacino et al., 2004). Copyright 2004 Elsevier.

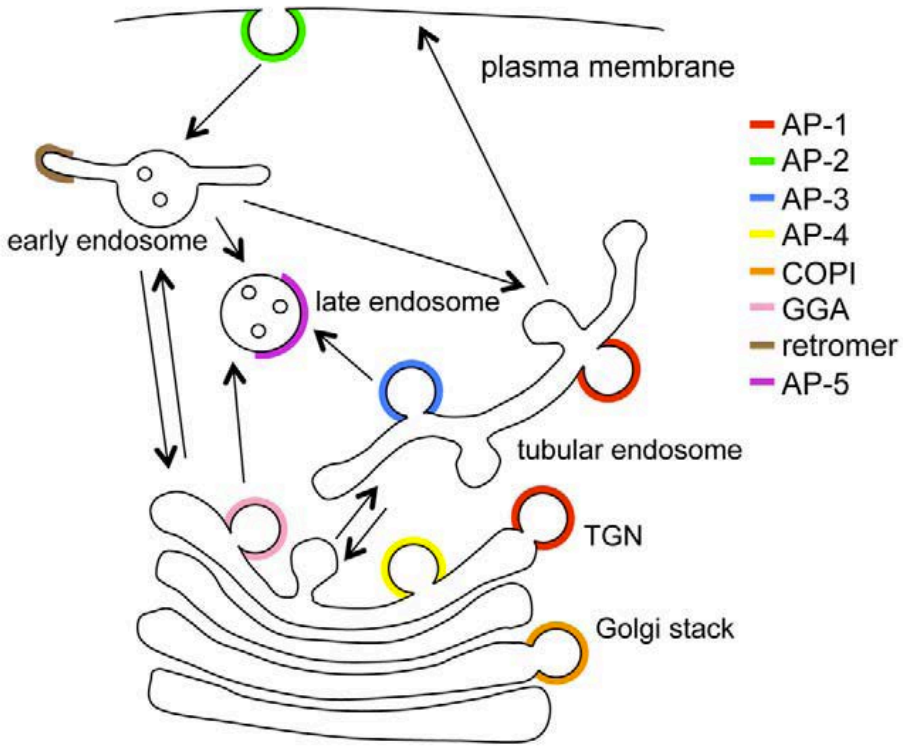

Figure 1.2. Diagram of adaptor protein (AP) complexes in post-TGN trafficking pathways.

AP-1 (red) is localized the tubular endosomes and/or the TGN. AP-2 (green) directs clathrin-dependent endocytosis. AP-3 (blue) traffics cargo from tubular endosomes to late endosomes and lysosomes. AP-4 (yellow) AP-4 mediates basolateral transport in polarized cells. AP-5 (purple) associates with late endosomes. From (Hirst et al., 2011). Copyright 2011 Hirst et al. Open access article distributed under the terms of the Creative Commons Attribution License, which permits unrestricted use, distribution, and reproduction in any medium, provided the original author and source are credited.

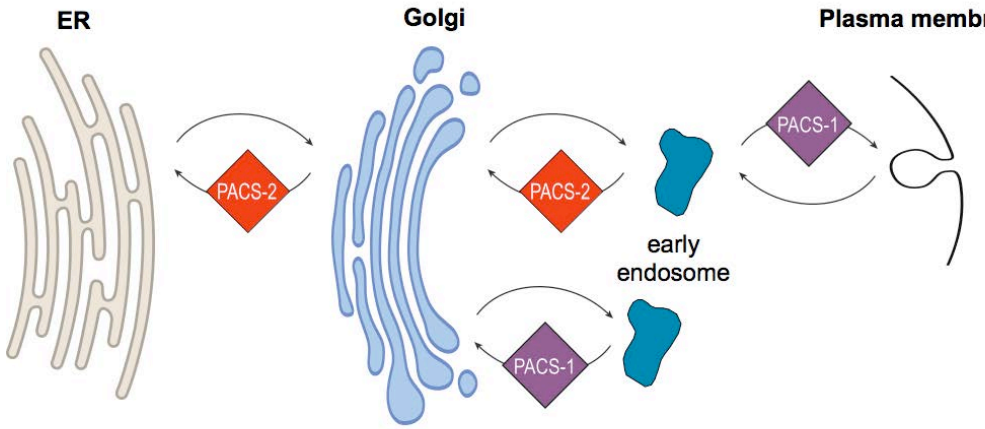

Figure 1.3. PACS-mediated membrane trafficking steps.

PACS-1 is required for the TGN-localization of furin, CI-MPR, and the viral envelopes from human cytomegalovirus and the feline RD114 retrovirus (Wan et al., 1998, Crump et al., 2001, Crump et al., 2003, Bouard et al., 2007). PACS-1 directs the recycling of internalized cargo from the early endosome to the cell surface and the delivery of cargo to the primary cilium (Molloy et al., 1998, Schermer et al., 2005, Crump et al., 2001, Chen et al., 2009, Jenkins et al., 2009). PACS-2 mediates the ER localization of profurin, the ion channel polycystin-2, and calnexin (Feliciangeli et al., 2006, Myhill et al., 2008, Kottgen et al., 2005) as well as directs the delivery of cargo such as CI-MPR and Nef from the early endosome to the TGN (Atkins et al., Molloy et al., 1998, Crump et al., 2001, Chen et al., 2009).

PART I (CHAPTERS 2-4). HIV-1 Nef-mediated pathogenesis

OVERVIEW

This section begins by describing the relevant literature in HIV pathogenesis (**CHAPTER 2**) and will provide essential background pertaining to HIV-1 epidemiology, virology, and disease pathogenesis as well as describe the complex mechanisms HIV-1 Nef employs to coordinate evasion of HIV-1-infected cells from immune surveillance while promoting pathogenicity of the virus. The studies in **CHAPTER 3** describe how the identification of PACS-2 as essential for HIV-1 Nef-mediated immune evasion lead to the discovery of a small molecule inhibitor that targets a critical PACS-2-dependent step in Nef action. The results and implications of these studies are discussed in **CHAPTER 4** and relate to two current models of HIV-1 Nef-mediated immune evasion pathways as well as the broader context of Nef function.

RATIONALE AND HYPOTHESIS

Rationale: To evade $CD8^+$ T-cell destruction, HIV-1 Nef assembles a Src family kinase (SFK)-ZAP-70-PI3K complex to trigger MHC-I downregulation. Two models are currently used to explain the molecular basis of Nef-mediated MHC-I downregulation (described in section 2.5). The first model describes how PACS-2 is required for the Nef-mediated assembly of an SFK-ZAP-70-PI3K complex that accelerates endocytosis of cell surface MHC-I. The second model describes how Nef forms a ternary complex with AP-1 and the cytosolic tail of MHC-I to divert newly synthesized MHC-I to degradative compartments in the endo-lysosomal network. However, the extent to which these models overlap or coexist is unknown. Furthermore, the determination that the Nef-SFK interaction is required for disease progression, including AIDS-like disease in animal models and assembly of the SFK-ZAP-70-PI3K multi-kinase complex, suggests that targeting the Nef-SFK interaction pharmacologically may represent an attractive approach to inhibiting Nef-mediated disease pathogenesis.

Hypothesis: Based on the determination that the small molecule inhibitor 2c disrupts the Nef-SFK interaction, we *hypothesize* that 2c will inhibit MHC-I downregulation in $CD4^+$ T-cells by interfering with formation of the multi-kinase complex. Moreover, due to the overlapping requirement for the membrane adaptor complex AP-1 in both the sequestering of endocytosed MHC-I as well as

in the retention of newly synthesized MHC-I, we further *hypothesize* that the endocytic and retention pathways of MHC-I downregulation may be functionally linked. To test these hypotheses, we have addressed the following experimental goals in Chapter 3:

1. Determine the extent to which 2c disrupts formation of the multi-kinase complex by analyzing Nef-induced SFK activation, ZAP70 phosphorylation, and activation of PI3K.
2. Monitor the extent to which 2c inhibits Nef-mediated downregulation of MHC-I in both Nef-expressing human T-cell lines as well as HIV-1-infected primary $CD4^+$ T-cells.
3. Explore the relationship between the endocytic and retention pathways of MHC-I downregulation using transport assays and chemical probes at various times following infection.

CHAPTER 2. Introduction to HIV-1 pathogenesis

2.1 The clinical implications of HIV-1 infection

2.1.1 HIV epidemiology

It has now been nearly 30 years since the discovery of a novel human retrovirus, later termed human immunodeficiency virus (HIV), as the causative agent of acquired immunodeficiency syndrome (AIDS) (Barre-Sinoussi et al., 1983, Gallo et al., 1984, Popovic et al., 1984, Sarngadharan et al., 1984, Safai et al., 1984, Schupbach et al., 1984). The following three decades studying HIV would provide immense waves of scientific and therapeutic advancements, challenge our political and social views of equality, and reveal a depth of racial, social and economic injustice and discrimination that must absolutely be rectified for this pandemic to conquered. Since the start of the pandemic, HIV has infected approximately 60 million people worldwide and contributed to 25 million deaths (UNAIDS, 2009). For the estimated 33.3 million people living with HIV, including 2.1 million children, the advancements are tangible, the life expectancy living with HIV is now measured in decades with current therapeutic strategies. Indeed, the growth of the global AIDS pandemic appears to have stabilized. Since 1997, the year in which annual new HIV infections was at a global peak, the number of new HIV infections has decreased by 21%. Moreover, since 2004, there are 19% fewer AIDS-related deaths globally and a 24% reduction in mother-to-child transmission (UNAIDS, 2010). Despite these significant advancements, infection rates are still high, curative treatments remain elusive and a prophylactic vaccine is not yet available.

Beyond these numbers is a more troubling picture that depicts significant disparities at racial, gender, social, and economic levels. This is most evident in Sub-Saharan Africa. Indeed, while this region comprises just over 10% of the world's population, it accounts for more than 68% of people living with HIV worldwide, the majority of which are women (AVERT, 2011, UNAIDS, 2010). Moreover, this racial and gender disparity is not limited to developing or impoverished nations. In the US, while African Americans comprise 14% of the total population, they accounted for a staggering 44% of new HIV infections in 2009. Latinos represent 16% of the US Population, yet accounted for 20% of new infections in the same year. If one factors in gender, the numbers become increasingly telling, the estimated rate of new HIV infections among black women was 15 times greater than that of white women, and 6 and a half times greater for black men compared to white men. In their lifetime, 1/16 black men and 1/32 black women will be diagnosed with HIV in the US (CDC, 2011). These statistics clearly illustrate that scientific and therapeutic advancements must be accompanied by a change in societal norms that have enabled racial and ethnic divides to unfairly place the burden of disease upon various groups of individuals.

2.1.2 HIV-1 clinical disease progression

The natural history of HIV-1 infection is characterized by an increase in viral load and a continual depletion of cluster of differentiation 4 $(CD4)^+$ T-lymphocytes (T-cells) until the immune system is irrevocably crippled and the

individual succumbs to opportunistic infections (Figure 2.1) (Hellerstein et al., 1999, Hiby et al., 2004, Mohri et al., 2001, Rowland-Jones, 1999, Wei et al., 1995). The timeline of HIV infection can be divided into three phases: primary infection (or acute phase), latency (or chronic phase), and clinical AIDS. During the primary infection (usually 2-4 weeks post-exposure), individuals often develop influenza or mononucleosis-like symptoms such as fever, lymphadenopathy, malaise, myalgia, phayngitis, and rash lasting a few days to a few weeks (Cooper et al., 1985, Kahn et al., 1998). The acute viremia during this period results in a marked drop in circulating $CD4^+$ T-cells and triggers a robust cytotoxic T-lymphocte (CTL) response, which is critical for killing HIV-infected cells and facilitating a decline in viral load (Gupta, 1993, Pedersen et al., 1990, Vento et al., 1993). While a strong CTL response during the primary infection correlates with slower disease progression (Pantaleo et al., 1997), more severe clinical symptoms correlate with accelerated disease progression (Pedersen et al., 1989). Following seroconversion, the viral load stabilizes and $CD4^+$ T-cell levels recover to a modest degree. The viral load then reaches a steady state referred to as the viral set-point. On average, individuals reach their viral set-point three to five months following infection (Kaufmann et al., 1998). Importantly, the higher the viral set-point, the faster an individual will progress to AIDS (Hughes et al., 1997, Mellors et al., 1995, Mellors et al., 1996).

A strong antiviral immune response triggers a dramatic reduction in viral load following acute HIV infection, this marks the beginning of clinical latency (or

chronic HIV infection), in which there is a near equilibrium between viral replication and the host immune response. The duration of this stage can last from a few weeks to 20 years, depending on host factors, genetic determinants, and availability of treatment. Monitoring $CD4^+$ T-cell levels during this period is critical for determining the appropriate time to initiate antiretroviral therapy. Studies have clearly shown the benefits of initiating antiretroviral therapy when patients are asymptomatic and have not progressed to clinical AIDS (currently defined when $CD4^+$ T-cell counts fall below 200 cells/µL or when the $CD4^+$ T-cell percentage is less than 15%) (Palella et al., 1998, Detels et al., 1998). However, the optimal time to begin therapy has been uncertain (HHS, 2012, Hammer et al., 2008). Importantly, a recent large-scale randomized clinical trial demonstrated that early initiation of antiretroviral therapy (defined as $CD4^+$ T-cell counts > 500 cells/µL) significantly improved survival as compared with deferred therapy (defined as $CD4^+$ T-cell counts between 351-500 cells/µL) (Kitahata et al., 2009). These findings were seminal to the improvement of clinical outcome, as prior guidelines based on accumulating observational data suggested antiretroviral therapy be initiated in asymptomatic patients with a $CD4^+$ T-cell count falls below 350 cells/µL (Egger et al., 1997, May et al., 2007).

Despite the establishment of a viral set-point, most infected individuals will have continual depletion of peripheral $CD4^+$ T-cells (Balotta et al., 1997, Koblin et al., 1999, Lefrere et al., 1997, Moss et al., 1988), ultimately progressing to clinical AIDS. The symptoms of AIDS are the result of conditions that do not normally

develop in an otherwise immune-competent individual. Most of these conditions are infections caused by bacteria, viruses, fungi and parasites as well as an increased risk of developing various cancers such as Kaposi's sarcoma, cervical cancer, and lymphoma. Infected individuals with AIDS often have constitutional symptoms such as fevers, night sweats, chills, weight loss, weakness, and swollen glands (Guss, 1994). Fortunately, implementation of routine prophylaxis and careful testing and monitoring of patients has dramatically increased quality of life and survival following diagnosis of AIDS. In contrast, prior to the advent of antiretroviral therapy, the average survival time following diagnosis of AIDS in the United States was less than one year (Gail et al., 1997).

2.2 HIV Biology

2.2.1 HIV classification

The Baltimore classification system places viruses into one of seven (I-VII) groups depending on their nucleic acid type, strandedness, sense, and method of replication. According to this classification, HIV belongs to the Retroviridae (VI) family due to its ability to reverse transcribe its single-stranded ribonucleic acid (RNA) (ssRNA) genome into a DNA intermediate that is subsequently integrated into host cell DNA. Due to the long incubation period and chronicity of HIV, it is further characterized into the genus lentivirus. There are two types of HIV, HIV-1 and HIV-2, and while they have identical modes of transmission, natural history studies determined that HIV-2 infected individuals have a reduced rate of disease

development (Marlink et al., 1994). Indeed, HIV-2 has a longer latency period, is less frequently transmitted, and is rarely found outside regions of West Africa. HIV-1 is the predominant virus transmitted and accounts for the majority of infections worldwide (McCutchan, 2006). There are currently three major classes of HIV-1: M (main), which accounts for more than 90% of total HIV infections; N (new/neither M or O); and O (outlier). Group M has been further characterized into 9 genetically distinct subtypes, or clades, defined by geographical region and designated by the letters A-D, F-H, J and K (Hu et al., 1996, Spira et al., 2003, McCutchan, 2006). Clade B is the most prevalent among those of western European and American descent and is the subtype to which most experimental drugs are tested and designed (McCutchan, 2006).

2.2.2 The HIV-1 RNA genome

The HIV-1 RNA genome is 9 kilobases in length and encodes 15 proteins from 9 genes (Gallo et al., 1988, Muesing et al., 1985). The HIV-1 RNA transcript undergoes multiple processing steps to produce functional gene products. First, multi-splicing events generate the regulatory proteins for HIV-1 expression, Tat and Rev. Tat binds to the trans-activating response element (TAR) to promote transcription elongation (Kao et al., 1987) while Rev stabilizes viral RNA transcripts, promoting their utilization and nuclear export by binding to Rev Response Elements (RRE) within the viral RNA (Pollard et al., 1998, Nekhai et al., 2006). Early multi-splicing events also generate the accessory proteins

negative factor (Nef), viral protein r (Vpr), viral protein u (Vpu), and viral infectivity factor (Vif), which promote viral fitness and spread (described below).

The second RNA species generated by the HIV-1 genome is a singly spliced RNA that is translated into the envelope glycoprotein (Env). Env is a 160 kilodalton (kD) precursor protein that is proteolytically cleaved into glycoprotein (gp)120 and gp41 by the endoprotease furin or furin-like proteases (Vollenweider et al., 1996). The surface glycoprotein gp120 is anchored to the viral envelope through non-covalent attachment to the transmembrane glycoprotein, gp41, creating the envelope spike. It is the binding of gp120 to its cellular receptor CD4 and a coreceptor, either C-C chemokine receptor type 5 (CCR5) or C-X-C chemokine receptor type 4 (CXCR4), that is responsible for viral entry (Lasky et al., 1987). HIV-1 viruses responsible for primary infection mainly use the coreceptor CCR5 and are called R5 variants (Zhu et al., 1993, van't Wout et al., 1994, Keele et al., 2008, Salazar-Gonzalez et al., 2009). However, CXCR4-using viruses (X4 variants) will evolve from R5 variants during the asymptomatic phase of infection in approximately 50% of patients infected with Clade B HIV-1. The emergence of X4 variants coincides with accelerated progression to AIDS (Schuitemaker et al., 1992, Koot et al., 1993, Richman et al., 1994, Connor et al., 1997) and is due to sequential mutations in the third variable (V3) loop of the envelope spike (Bunnik et al., 2011). This results in a shift in coreceptor usage from CCR5 to CXCR4 during natural HIV-1 infection (Bunnik et al., 2011). Notably, some individuals have a 32-base pair deletion in the *CCR5* gene

(*CCR5-Δ32*) resulting in a nonfunctional receptor, thus preventing entry from HIV-1 R5 variants (Stephens et al., 1998, Dean et al., 1996, Carrington et al., 1997, Carrington et al., 1999, Bamshad et al., 2002). This allele is found in 5-14% of individuals of European descent but is rare among Africans and Asians (Sabeti et al., 2005). The presence of one copy of *CCR5-Δ32* delays the onset of AIDS, while individuals homozygous for this allele exhibit a strong resistance to HIV-1 infection (Dean et al., 1996, Liu et al., 1996, Samson et al., 1996). Moreover, many viruses are known to downregulate, or reduce the surface levels of their entry receptor, to prevent superinfection by viruses using the same receptor (Weiss, 1985). Notably, HIV-1 downmodulates the viral envelope glycoprotein receptor CD4 (Jabbar et al., 1990), thereby preventing CD4 from interfering with viral assembly and release (Lama et al., 1999, Benson et al., 1993) as well as preventing the infected cell from superinfection, which leads to inefficient virus replication due to premature cell death (Michel et al., 2005, Venzke et al., 2006, Wildum et al., 2006).

The third species generated by the HIV-1 genome is an unspliced RNA that enables the translation of the structural polyprotein precursor Gag as well as a GagPol precursor (Briant, 2011). Gag is a 55 kilodalton (kD) protein composed of four major structural domains: p17 matrix (MA), p24 capsid (CA), p7 nucleocapsid (NC), and p6 spaced by two linker peptides (SP1 and SP2) (Freed, 1998). Gag orchestrates the production and release of infectious HIV-1 particles and is necessary and sufficient for assembly of virus-like particles *in vitro* and for

production of virus-like particles *in vivo* (Adamson et al., 2007, Briant, 2011). The GagPol precursor is encapsidated into newly assembled virions that will ultimately produce the viral enzymes protease, integrase, and reverse transcriptase (Briant, 2011, Ganser-Pornillos et al., 2008, Hill et al., 2005).

2.2.3 HIV-1 accessory proteins mediate disease pathogenesis

The hallmark of primate immunodeficiency viruses (human and simian-HIVs and SIVs, respectively) that distinguishes them from other retroviruses is that they encode “accessory” proteins, including viral infectivity factor (Vif), viral protein r (Vpr), viral protein u (Vpu), and negative factor (Nef). While these accessory factors lack intrinsic enzymatic function, they modify the host cellular environment within HIV-1 infected cells to promote viral fitness, replication, dissemination, and transmission (Malim et al., 2008). Viral infectivity factor, or Vif, is a 23 kD protein essential for viral replication. Vif antagonizes the antiretroviral activity of the host restriction factor cytidine deaminase apolipoprotein B messenger RNA (mRNA)-editing enzyme catalytic polypeptide-like 3G (APOBEC3G) (Conticello et al., 2005, Harris et al., 2004, Holmes et al., 2007). Indeed, there is tremendous selective pressure on host cells to block or prevent retroviral replication, evidenced by the evolution of intrinsic restriction factors, such as APOBECs, that inhibit or “restrict” the viral life cycle (Wolf et al., 2008). Specifically, the restriction factor APOBEC3G mutates viral nucleotides by deaminating cytidine (C) to uridine (U) in nascent minus strand reverse

transcripts, these changes are subsequently registered as guanosine (G)-to-adenosine (A) transitions in plus strand sequences (Conticello et al., 2005, Harris et al., 2004, Holmes et al., 2007). In the absence of Vif, this G-to-A hypermutation is sufficient to stop virus spread through the excessive loss of genetic integrity (a form of error catastrophe) (Bogerd et al., 2008, Soros et al., 2007). However, Vif recruits the cullin5-Really Interesting New Gene (RING) finger E3 ubiquitin ligase to target APOBEC3G for proteasomal degradation, thereby eliminating it from HIV-1-infected cells (Mehle et al., 2004, Yu et al., 2003).

Viral protein r, or Vpr, is a 14 kD accessory protein that is incorporated into mature virions, but whose function has been difficult to ascertain. Vpr induces a G_2 mitotic arrest in infected cells and facilitates the infection of macrophages (Malim et al., 2008). Recently, it was determined that Vpr also recruits a cullin-RING ubiquitin ligase, the cullin4A-DNA damage-binding protein 1 (DDB1) complex, through interaction with DDB1 Cul4 assoicated factor 1 (DCAF1) that links it to DDB1 (Belzile et al., 2007, DeHart et al., 2007, Hrecka et al., 2007, Wen et al., 2007). Recent studies show that the cullin4A-DDB1-DCAF1-Vpr complex is necessary for Vpr-induced mitotic arrest (Dehart et al., 2008). Viral protein u, or Vpu, is a 16 kD integral membrane protein that reduces the surface expression of CD4, the primary virus entry receptor, by targeting newly synthesized CD4 molecules in the endoplasmic reticulum (ER) for degradation. As protein degradation is a recurring theme with HIV-1 accessory proteins, Vpu

also recruits a cullin1-Skp1 ubiquitin ligase complex to the cytoplasmic tail of CD4 by interacting with the Skp1-binding receptor protein β-TRCP, triggering its polyubiquitination and proteasomal degradation (Margottin et al., 1998). Lastly, negative factor, or Nef, is a 27 kD, N-myristolated protein associated with the cytoplasmic face of cell membranes and is one of the first viral proteins expressed following infection (described below).

2.3 The immune evasive strategies of HIV-1 Nef

2.3.1 The plethora of ways HIV-1 Nef drives disease progression

While once thought to negatively regulate HIV-1 replication (providing its misleading name, negative factor), the significance of Nef in promoting HIV-1 disease progression was revealed when rhesus macaques infected with simian immunodeficiency virus (SIV) strains lacking functional *Nef* genes displayed a marked reduction in viral loads and a delayed disease progression (Kestler et al., 1991). Following this observation, several studies reported that a subpopulation of HIV-1 infected patients with low viral loads and long-term asymptomatic survival had deletions in the *Nef* gene (Deacon et al., 1995, Kirchhoff et al., 1995, Salvi et al., 1998). These studies identified Nef as indispensable for the establishment of high viral loads and as an accelerator of disease progression. Together with the determination that transgenic expression of Nef alone, without any other HIV component, can independently produce an AIDS-like phenotype in

mice (Hanna et al., 1998), supports the notion that Nef is essential for HIV-1 pathogenesis and may be an attractive therapeutic target.

Nef has a multitude of functions that profoundly influence viral replication, dissemination, and persistence (summarized in Figure 2.2). Nef enhances viral replication and virion infectivity as well as inhibits immunoglobulin (Ig) class switching, thereby profoundly impairing IgG and IgA responses to T-cell-dependent antigens by preventing the production of antibody classes most apt to neutralize and clear the virus (Vermeire et al., 2011, Arhel et al., 2009, Qiao et al., 2006, Xu et al., 2009). Nef modifies the host cellular environment in many ways, including alteration of T-cell activation and maturation (Stevenson, 2003, Stove et al., 2003, Thoulouze et al., 2006), modulation of apoptotic and autophagic pathways (Fackler et al., 2002, Dinkins et al., 2010), as well as disrupts the intracellular trafficking of a multitude of cell surface proteins of helper T-cells and macrophages (the cellular targets of HIV-1 infection) (Roeth et al., 2006). Importantly, Nef accelerates the clathrin-dependent endocytosis of CD4, the primary virus entry receptor. This occurs through the binding of Nef to the cytoplasmic tail of CD4 and the recruitment of the clathrin adaptor protein complex-2 (AP-2) (Chaudhuri et al., 2007). This results in the accelerated internalization of CD4 into clathrin-coated pits, where it is subsequently targeted for lysosomal degradation (Chaudhuri et al., 2007). Other cell surface targets of Nef include: the T-cell receptor (TCR) and cluster of differentiation 3 (CD3) complex (TCR-CD3), a key constituent of the immunological synapse that forms

between antigen-presenting cells (APCs) and T-cells (Thoulouze et al., 2006); the costimulatory T-cell molecule cluster of differentiation 28 (CD28) (Leonard et al., 2011); dendritic cell-specific intercellular adhesion molecule-3-grabbing non-integrin (DC-SIGN, or CD209) (Sol-Foulon et al., 2002); and cluster of differentiation 8 (CD8) β (CD8β) was recently identified as downmodulated by Nef, however the function of this is not yet known (Heigele et al., 2012). Importantly, Nef downmodulates class I major histocompatibility complex (MHC-I) proteins, specifically the human leukocyte antigen (HLA)-A and -B allotypes, from the cell surface of HIV-1 infected cells to evade destruction by cytotoxic T lymphocytes (CTLs) (Roeth et al., 2006). These findings are confirmed in a broader context in SIV-1-infected rhesus macaques, in which Nef-mediated MHC-I downregulation limits CTL-directed killing while contributing to Nef's pathogenic effect (Swigut et al., 2004). Indeed, high viremia and accelerated disease progression correlates with a greater extent of MHC-I downregulation in SIV-1-infected rhesus macaques, suggesting an important role for this immune evasive strategy *in vivo* (Friedrich et al., 2010).

2.3.2 MHC-I biology and its disruption by pathogenic viruses

The ability of cytotoxic T lymphocytes (CTLs) to distinguish peptides presented by MHC-I molecules on the surface of antigen presenting cells (APCs) as "self" or "non-self" is of fundamental importance to proper immune system functioning. In a healthy individual, "self"-derived peptides presented by MHC-I

on the surface of cells fail to elicit any type of CTL response. In contrast, when a virally infected cell presents virus-derived peptides, or “non-self” peptides, on the cell surface, CTLs recognize this foreign signal and subsequently lyse the virally infected cell, effectively preventing further spread of the virus from that cell (Berke, 1995).

Pathogenic viruses use diverse strategies to downregulate MHC-I molecules, thereby evading CTL recognition by their hosts. Human cytomegalovirus (HCMV) escapes immune surveillance by the expression of the immediate early gene unique short region 3 (US3), which retains MHC-I molecules in the ER, followed by unique short region 11 (US11), which degrades MHC-I (Ahn et al., 1996). Similarly, while murine CMV (MCMV) blocks the transport of nascent MHC-I en route to the cell surface through m152 and m06 expression in the early phase of infection, MCMV also mediates the arrest of endocytosed MHC-I in early endosomal populations by inhibiting their recycling and late endosome progression (Tomas et al., 2010). Epstein Barr virus (EBV) similarly encodes the EBV deoxyribonuclease (DNase) BGLF5, which impedes MHC-I transport followed by expression of BILF1, which enhances MHC-I degradation (Zuo et al., 2009). Varciella zoster virus (VZV) encodes the protein kinase open reading frame 66 (ORF66) to sequester MHC-I molecules in a phosphorylation-dependent manner (Eisfeld et al., 2007). The adenovirus E3 protein contains a retention signal that mediates the sequestration of MHC-I molecules in the ER (Paabo et al., 1989). The herpes simplex virus protein IPC47

causes ER retention of MHC-I by inhibiting the transporter associated with antigen presentation (TAP) (Hill et al., 1995, York et al., 1994). The Kaposi's sarcoma-associated herpesvirus or human herpesvirus-8 (HHV-8) expresses the E3 ubiquitin ligases modulator of immune recognition (MIR)-1 and MIR-2, which ubiquitinate lysine residues in the cytoplasmic tail of MHC-I, lead to the rapid endocytosis and degradation of MHC-I (Piguet, 2005, Ishido et al., 2009). Together, these studies illustrate how the downregulation of MHC-I is a common immune evasive strategy mediated by diverse pathogenic viruses.

While it was observed as early as 1989 that HIV-1 downregulates MHC-I (Kerkau et al., 1989, Scheppler et al., 1989), it would be seven more years before it was determined that Nef was responsible for this effect (Schwartz et al., 1996). Subsequent studies then revealed that Nef downregulates MHC-I molecules to evade CTL recognition and killing, thereby allowing HIV-1 infected cells to escape immune surveillance (Collins et al., 1998). The cellular mechanisms by which Nef mediates this effect are described in the sections that follow.

2.3.3 MHC-I alleles and the selective effect of Nef

The human MHC-I locus on chromosome 6 encodes MHC-I molecules that are divided into "classical" and "non-classical" groups. The highly polymorphic classical MHC-I molecules (HLA-A, -B, and -C) present peptides to T-cell receptors (TCRs) of CTLs, while the conserved, non-classical molecules

(HLA-E, -F, and -G) exhibit limited polymorphism and have specialized roles in the immune system, such as inhibition of natural killer (NK) cell activity (Adams et al., 2001). There is evidence that the need to present diverse pathogen-derived antigens to CTLs facilitated the evolution of the HLA-A, -B, and -C loci via pathogen-mediated selection. Indeed, the HLA-A and -B groups are exceptionally polymorphic, with the highest degree of variability found within the peptide-binding region, which is consistent with the evolutionary need to present a diverse array of antigens to CTLs (Hughes et al., 1988, Janeway, 2005). Of the classical MHC-I alleles HLA-C is the most recently evolved, with functional differences among these molecules that may restrict diversity, thus owing to the fewer alleles that have been identified for this group (Adams et al., 2001, Older Aguilar et al., 2010, Blais et al., 2011).

While it is known that MHC-I molecules are necessary to mount a robust CTL response to HIV-1 infection, not all MHC-I alleles are created equally. Indeed, certain MHC-I allotypes are associated with delayed disease progression and effective control of viral replication, such as the over representation of the HLA-B*5701 allele in long-term non-progressing HIV-1 infected patients (Migueles et al., 2003). In addition, recent genome-wide analyses revealed that high HLA-C surface expression may correlate with better control of HIV-1 infection (Pereyra et al., 2010, Fellay et al., 2007, Fellay et al., 2009).

To protect HIV-1 infected cells from the host-mediated adaptive CTL response, HIV-1 Nef directs the removal of MHC-I from the cell surface, thereby

limiting the amount of MHC-I molecules presenting HIV-1-derived viral peptides to CTLs (Collins et al., 1998). However, our immune system has evolved to combat these viral strategies by the ability of natural killer (NK) cells to monitor and recognize cells with low MHC-I surface levels as “infected” or “abnormal” and to target them for destruction (Vivier et al., 2011). Therefore, it is not surprising that while Nef can effectively reduce cell surface MHC-I molecules of HIV-1 infected cells, it does so selectively, discriminately, and to the advantage of viral fitness. Whereas low surface expression of HLA-A and -B molecules can induce NK cell activation, expression of the HLA-C and -E molecules are inhibitory (Natarajan et al., 2002). Indeed, Nef selectively downmodulates the HLA-A and -B molecules to evade CTL recognition, while the NK cell inhibitory molecules HLA-C and -E are resistant to downmodulation by Nef (Cohen et al., 1999, Le Gall et al., 1998, Natarajan et al., 2002). Nef interacts directly with the Y_{320}SQAASS$_{326}$ sequence in the cytoplasmic tail of HLA-A and -B molecules, whereas HLA-C and -E molecules lack this sequence and selectively remain on the cell surface to inhibit NK cell activation (Le Gall et al., 1998, Williams et al., 2002, Cohen et al., 1999). In this manner, HIV-1 is able to evade both CTL and NK cell recognition through the accessory protein Nef. However, It is important to note that while MHC-I downmodulation by Nef is an effective immune evasive strategy, it is neither complete nor solitary, as there is an inevitable generation of anti-HIV CTLs as well as an emergence of HIV escape mutants that are resistant to CTL killing (Leslie et al., 2004, Friedrich et al., 2004). Indeed, as a

consequence of the low fidelity of HIV-1 replication, CTLs select for viral escape variants that are resistant to immune recognition, however this often occurs at a cost to viral fitness (Leslie et al., 2004, Friedrich et al., 2004).

2.3.4 The functional domains of Nef

Nef is a 27 kD, N-myristolated protein associated with the cytoplasmic face of cell membranes. Although Nef is relatively small, containing only 206 amino acids, it is functionally complex, containing overlapping effector domains that interact with a diverse array of cellular proteins to establish a favorable environment for replication and infectivity (Tokarev et al., 2011, Foster et al., 2011, Foster et al., 2008). Nuclear magnetic resonance (NMR) spectroscopy together with X-ray crystallography have identified three structural regions of Nef: an amino (N)-terminal flexible (anchor) region (residues 1-57), a folded core domain (residues 58-149 and 181-206), and a carboxy (C)-terminal flexible loop (residues 150-18) (Lee et al., 1996, Grzesiek et al., 1996a, Arold et al., 1997, Jia et al., 2012). Within the flexible anchor domain, Nef contains a myristoylated glycine residue at position 2 that facilitates association of Nef with the cytoplasmic face of cellular membranes (Geyer et al., 1999). Myristoylation is essential for Nef function, including the ability of Nef to downregulate cell surface CD4 and MHC-I molecules (Geyer et al., 1999, Foster et al., 2011). Indeed, a Nef $G_2 \rightarrow A$ mutant prevents myristoylation and grossly disrupts Nef function, illustrating that Nef predominantly functions at cellular membranes (Geyer et al.,

1999, Geyer et al., 2001). Another residue broadly required for Nef function is D_{123}, which is part of an oligomerization domain (or dimer interface domain) that mediates the formation of Nef homodimers (Arold et al., 2000, Liu et al., 2000, Poe et al., 2009). Similar to the myristoylation mutant, Nef proteins mutated at residue D_{123} are defective for CD4 and MHC-I downregulation, as well as enhancement of viral infectivity (Liu et al., 2000).

Mutations within the various Nef domains have revealed that Nef uses distinct regions for mediating processes that selectively affect MHC-I and CD4 trafficking (Foster et al., 2011). Nef contains a dileucine ($E_{161}xxxLL_{166}$) and a diacidic motif ($DD_{175,176}$), both of which are essential for CD4 downregulation (described below), but are dispensable for MHC-I downregulation. In addition, Nef contains a second diacidic motif ($EE_{155,156}$) that is required for CD4 trafficking to lysosomal compartments for degradation (Geyer et al., 2001, Piguet et al., 1999) as well as a hydrophobic pocket (including $WL_{57,58}$) that binds the cytoplasmic tail of CD4 by NMR spectroscopy (Grzesiek et al., 1997, Grzesiek et al., 1996b).

The ability of Nef to bind the cytoplasmic tail of MHC-I and mediate its downregulation depends on at least four critical sites within the anchor and core domains, including an N-terminal α-helix ($R_{17}ERM_{20}RRAEPA_{26}$) which contains a critical methionine (M_{20}), an acidic cluster ($EEEE_{65}$), an SH3-binding domain that forms a type I polyproline helix ($PQVP_{75}$), and a proline at position 78 (P_{78}) (Akari et al., 2000, Mangasarian et al., 1999, Greenberg et al., 1998, Geyer et al., 2001,

Williams et al., 2005). The functions of these motifs in mediating MHC-I downregulation will be discussed in the sections to follow. Importantly, the significance of these motifs is illustrated by the fact these sequences are conserved in the HIV-1 M group, which accounts for over 90% of HIV-1 infections worldwide (Keele et al., 2006, Agopian et al., 2007).

2.4 Nef uses cellular trafficking pathways to exert its pathogenic function

2.4.1 Nef manipulates host cell trafficking pathways

The ability of Nef to carry out its pathogenic functions is dependent on its ability to manipulate host cell trafficking pathways. The membrane-associated Nef protein acts as an adaptor that links cellular targets (transmembrane proteins) to degradative pathways or reroutes them to alternate trafficking pathways by linking these targets to endosomal coat proteins and to other cellular factors (Tokarev et al., 2011). Notably, Nef downmodulates the viral envelope glycoprotein receptor CD4 (described below), thereby preventing CD4 from interfering with viral assembly and release (Lama et al., 1999, Benson et al., 1993) as well as preventing the infected cell from superinfection, which leads to inefficient virus replication due to premature cell death (Michel et al., 2005, Venzke et al., 2006, Wildum et al., 2006). In addition, Nef mediates viral evasion of acquired cellular immunity by downregulating MHC-I molecules (Arien et al., 2008) (described in section 2.5).

2.4.2 Nef accelerates the endocytosis and degradation of CD4

The ability of Nef to accelerate the internalization of CD4 from the plasma membrane by linking the cytosolic tail of the receptor to the clathrin-associated endocytic machinery is the most well-characterized of Nef's functions (Aiken et al., 1994, Chaudhuri et al., 2007, Doray et al., 2007, Jin et al., 2005, Rhee et al., 1994). Nef binds the cytoplasmic tail of cell surface CD4 and the interface of this interaction, as determined by NMR, is formed by residues in a hydrophobic pocket (including $WL_{57,58}$) on the folded core domain as well as by additional residues in the N-terminal flexible region of Nef (Grzesiek et al., 1996b, Preusser et al., 2001). While these residues are critical for the ability of Nef to interact with CD4, the binding of Nef alone with CD4 is not sufficient to induce internalization of CD4 (Preusser et al., 2001). Indeed, the recruitment of AP-2 is required for Nef to stimulate the increased rate of clathrin-dependent endocytosis of CD4 (Chaudhuri et al., 2007, Lindwasser et al., 2008). The interaction between Nef and AP-2 requires the dileucine ($E_{161}xxxLL_{166}$) and diacidic motifs ($DD_{175,176}$), both of which are essential for CD4 downregulation but are dispensable for MHC-I downregulation (Chaudhuri et al., 2007, Doray et al., 2007, Lindwasser et al., 2008, Mitchell et al., 2008). Indeed, recent studies revealed that Nef, AP-2, and the cytoplasmic tail of CD4 cooperatively form a tripartite complex in which Nef and CD4 fail to interact in the absence of AP-2 (Chaudhuri et al., 2009). These interactions lead to the assembly of clathrin-coated pits surrounding CD4 that eventually form clathrin-coated vesicles for subsequent internalization (Burtey et

al., 2007, Greenberg et al., 1997). Following internalization, Nef suppresses the recycling of CD4 back to the cell surface by facilitating the delivery of CD4 from early endosomes to late endosomes and the multivesicular body (MVB) pathway via the endosomal sorting complex required for transport (ESCRT), and then eventually to lysosomes for degradation, thereby effectively decreasing the total amount of cellular CD4 (Anderson et al., 1994, Giolo et al., 2007, Piguet et al., 1999, Rhee et al., 1994, daSilva et al., 2009, Luo et al., 1996).

2.4.3 Nef-induced MHC-I downregulation requires a multitude of cellular factors

As described in detail in the following section, Nef associates with a plethora of cellular factors to alter the trafficking fate of MHC-I molecules. While the mechanism of Nef-mediated MHC-I downregulation is not as clearly understood as CD4 downregulation, there are interesting parallels in the manner in which Nef recruits coats proteins and other cellular factors to enhance internalization of MHC-I, as well as divert MHC-I from being delivered to the cell surface. The two pathways described in the next section for Nef-mediated downregulation of MHC-I are 1) an increased rate of endocytosis from the plasma membrane (Figure 2.3) and 2) ER-retention via inhibition of MHC-I delivery to the plasma membrane (Figure 2.4). While there are distinct differences in the cellular factors required for mediating these pathways, the studies presented in chapter 3 provide insight into how these pathways may be temporally linked in the context of HIV-1 infection.

2.5 Nef downregulates MHC-I using endocytic and retention pathways

2.5.1 Nef downregulates MHC-I through a PI3K-dependent ARF6 endocytic pathway

In the first reports of Nef-mediated MHC-I downregulation, it was determined that Nef enhances the rate of MHC-I endocytosis in HIV-1 infected cells, resulting in the accumulation of MHC-I in perinuclear and endosomal compartments (Schwartz et al., 1996). Furthermore, these studies revealed that while Nef has no effect on the rate of MHC-I synthesis or trafficking through the ER or cis-Golgi, Nef does induce lysosomal degradation of MHC-I (cited as data not shown in (Schwartz et al., 1996)). In contrast to the Nef-mediated AP-2-dependent downregulation of CD4, Nef-induced endocytosis of MHC-I is clathrin/AP-2-independent, as treatment with a dominant negative dynamin (Le Gall et al., 2000) or an AP-2 dominant negative mutant (μ2-D_{176}→A) (Blagoveshchenskaya et al., 2002) selectively blocks CD4 downregulation while having no effect on Nef-induced MHC-I endocytosis. Furthermore, it was subsequently determined that the domains in Nef required for inducing downregulation of CD4 and MHC-I are genetically separable (Greenberg et al., 1998), suggesting Nef does indeed downmodulate CD4 and MHC-I using distinct mechanisms.

Studies in non-HIV-1-infected cells that show MHC-I colocalizes with the small guanosine triphosphate (GTP)ase, adenosine diphosphate (ADP)-

ribosylation factor 6 (ARF6), a member of the ARF family of GTP-binding proteins (Radhakrishna et al., 1997). ARF6 had been implicated in the endocytosis of transmembrane cargo proteins by connecting vesicles with actin cytoskeletal components, rather than linking cargo to coat proteins such as clathrin or COPI (Chavrier et al., 1999). Indeed, ARF-6-dependent endocytosis and recycling of proteins is controlled by the GTP/GDP bound state of ARF6, as mutants of ARF6 that are either deficient in GTP hydrolysis (ARF6-Q_{67}→L) or in GDP exchange (ARF6-T_{27}→N) act in a dominant-negative fashion (Radhakrishna et al., 1997). Consistent with these findings, Nef-induced endocytosis of MHC-I is selectively inhibited (while CD4 downregulation remains unaffected) when the ARF6 pathway is blocked through either: treatment of cells with aluminum fluoride (AlF_4), a G-protein activator that redistributes ARF6 from endosomal compartments to the plasma membrane, thereby blocking ARF6 function; expression of the dominant-negative, GTP hydrolysis defective ARF6 (Q_{67}→L); or expression of the catalytically inactive, dominant negative ARF6 guanine nucleotide exchange factor (GEF) ARNO (E_{156}→K) (Blagoveshchenskaya et al., 2002). Further analysis revealed that the ability of Nef to induce the ARNO-dependent loading of ARF6 and the subsequent internalization of MHC-I was dependent on the activation of phosphatidylinositide 3-kinase (PI3K) (Blagoveshchenskaya et al., 2002). Indeed, Nef activates PI3K, leading to elevated levels of phosphatidylinositol (3,4,5)-triphosphate (PIP_3) at the cell periphery, which recruits an ARF6 GEF (ARNO), leading to the ARNO-mediated

loading of ARF6 and the subsequent acceleration of MHC-I endocytosis from the cell surface (Blagoveshchenskaya et al., 2002).

2.5.2 Nef-mediated activation of PI3K requires the acidic cluster ($EEEE_{65}$) and polyproline ($PXXP_{75}$) motifs, but not M_{20}

Consistent with previous functional analysis of Nef domains required for MHC-I downregulation (Greenberg et al., 1998), the acidic cluster ($EEEE_{65}$) and polyproline ($PXXP_{75}$) motifs are required for sequential steps leading to the activation of PI3K and stimulation of ARF6-mediated endocytosis of MHC-I (Figure 2.3) (Blagoveshchenskaya et al., 2002, Hung et al., 2007). Interestingly, while Nef M_{20} is essential for downregulation of steady-state levels of MHC-I (Akari et al., 2000, Mangasarian et al., 1999) and the sorting of MHC-I into AP-1 containing compartments (Roeth et al., 2004), this residue is dispensable for the endocytosis of MHC-I (Blagoveshchenskaya et al., 2002). Rather, Nef M_{20} is required for blocking the cell surface retrieval of MHC-I molecules, as Nef M_{20}→A fails to inhibit MHC-I recycling despite its ability to stimulate MHC-I endocytosis (Blagoveshchenskaya et al., 2002). Indeed, the observation that MHC-I is constitutively recycled to the cell surface from a primaquine-sensitive ARF6-regulated endosomal compartment, together with the determination that Nef M_{20}→A can efficiently target MHC-I to the TGN in the presence (but not absence) of primaquine, suggests Nef M_{20} promotes MHC-I downregulation by

impeding cell surface retrieval and diverting MHC-I to the perinuclear region in a primaquine-sensitive manner (Blagoveshchenskaya et al., 2002).

2.5.3 Nef binds PACS-2 to assemble a Src family kinase(SFK)-ZAP-70-PI3K multi-kinase complex to downregulate cell surface MHC-I

The polyproline ($PXXP_{75}$) motif in Nef resides in a type II polyproline helix and fulfills the canonical sequence for a class II Src homolgy 3 (SH3) binding domain (PXXPX(K/R)) (Li, 2005). The Nef polyproline domain recruits and activates a TGN-localized Src family kinase (SFK) to mediate MHC-I downregulation (Hung et al., 2007). Indeed, mutation of the SH3 domain in Nef ($AXXA_{75}$) abrogates the Nef-SFK interaction and subsequent MHC-I downregulation (Hung et al., 2007, Lerner et al., 2002). The Nef-SFK complex then recruits and activates the tyrosine kinase zeta-chain-associated protein kinase-70 (ZAP-70), which then binds the Src homology 2 (SH2) domain of p85, the regulatory subunit of PI3K, thereby activating PI3K and leading to the subsequent downregulation of MHC-I (Figure 2.3) (Hung et al., 2007, Atkins et al., 2008). Indeed, an active SFK bound to $PXXP_{75}$ is required for these steps, as expression of a catalytically inactive SFK mutant (Hck-KE) abrogates the increased recruitment of ZAP-70 and PI3K activation seen with wild-type Hck expression (Hung et al., 2007). Moreover, Nef forms a complex with PI3K and ZAP-70 (or the ZAP-70 homolog Syk in myeloid lineage cells) and inhibition of any of these components pharmacologically or via small interfering RNA (siRNA)

knockdown abolishes Nef-mediated MHC-I downregulation (Hung et al., 2007), confirming the significance of these molecules in this pathway.

While it was determined that the Nef acidic cluster ($EEEE_{65}$) was required for the TGN-localization of Nef (Blagoveshchenskaya et al., 2002), where Nef recruits and activates a TGN-localized SFK to assemble the multi-kinsae complex (Hung et al., 2007), it was unclear the sorting mechanism by which Nef trafficked to the perinuclear region. The acidic-cluster dependent trafficking of Nef was suggestive of a PACS-mediated sorting step (Youker et al., 2009) and indeed, PACS proteins bind Nef directly through a bipartite site on Nef formed by the N-terminal $EEEE_{65}$ acidic cluster and W_{113} in the core domain (Atkins et al., 2008, Dikeakos et al., 2012). Furthermore, siRNA-mediated knockdown of PACS-1 or PACS-2 in primary human $CD4^+$ T-cells blocked Nef-induced downmodulation of HLA-A2 (Atkins et al., 2008), suggesting PACS proteins play an essential role in Nef-mediated MHC-I downregulation. Indeed, subsequent analysis determined that Nef initiates MHC-I downmodulation by interacting with PACS-2, and the Nef/PACS-2 complex is then directed to the TGN where PACS-2 is displaced and Nef binds and activates a TGN-localized SFK (Atkins et al., 2008). The Nef-SFK complex then recruits ZAP-70 to bind the SH2 domain of the p85 regulatory subunit of PI3K, resulting in the activation of PI3K and the generation of PIP_3, which stimulates the guanine nucleotide exchange factor ARNO and the GTP loading of ARF6, thereby accelerating the rate of MHC-I endocytosis (Atkins et al., 2008, Blagoveshchenskaya et al., 2002). Following the

Nef-induced acceleration of endocytosis, MHC-I is sequestered to the paranuclear region in an M_{20}-dependent manner, thereby preventing the recycling of endocytosed MHC-I to the cell surface (Blagoveshchenskaya et al., 2002).

2.5.4 Nef interacts with PACS proteins on endosomes to downregulate MHC-I

While both PACS-2 and PACS-1 are required for MHC-I downregulation, their roles in Nef action are distinct and sequential. Indeed, PACS-2 is required for the ability of Nef to traffic from early endosomes to the perinuclear region, as the expression of Nef in PACS-2 siRNA-depleted or *Pacs2*$^{-/-}$ cells leads to the accumulation of Nef in early endosomal compartments (Atkins et al., 2008). In contrast, PACS-1 is required downstream of PI3K activation, as knockdown of PACS-2, but not PACS-1, prevents assembly of the multi-kinase complex and the subsequent activation of PI3K (Atkins et al., 2008). Moreover, to analyze the subcellular location of Nef-PACS interactions, recent studies from our laboratory utilized bimolecular fluorescence complementation (BiFC); in which cells express reporter constructs composed of PACS-2 fused to the N-terminus of YFP and Nef fused to the C-terminus of YFP, which are individually non-fluorescent, but generate fluorescence upon protein-protein interaction (Dikeakos et al., 2012, Kerppola, 2008). Indeed, these studies demonstrate that PACS-2 interacts with Nef on Rab5-positive early endosomes as well as Rab7-positive late endosomes/ multi-vesicular bodies (MVBs) (Dikeakos et al., 2012), consistent with the role of

PACS-2 in trafficking Nef from the early endosomes to the perinuclear region where it can mediate the assembly of the multi-kinase complex to downregulate MHC-I (Atkins et al., 2008). Furthermore, the ability of PACS-1 to interact with Nef on Rab7-positive late endosomes/MVBs is consistent with a role for PACS-1 downstream of PI3K activation to mediate the sequestration of endocytosed MHC-I molecules as well as with the determination that downregulated MHC-I accumulates in Rab7-positive endosomes (Dikeakos et al., 2012, Schaefer et al., 2008, and Chapter 3).

Mapping studies have further characterized the Nef-PACS interactions by identifying the precise regions on Nef and PACS-1 or PACS-2 required for their interaction (Figure 2.5 and (Dikeakos et al., 2012)). These studies determined that a 15 amino acid fragment within the cargo- or furin-binding region (FBR) of PACS-1 (residues 181-195) or PACS-2 (residues 102-116) are sufficient to interact with a bipartite site on Nef consisting of the $EEEE_{65}$ acidic cluster and W_{113} in the core domain (Dikeakos et al., 2012). Importantly, mutation of a critical residue in the Nef-binding site on PACS-1 or PACS-2 (PACS-1 $N_{188}\rightarrow A$ or PACS-2 $N_{109}\rightarrow A$) repressed Nef-mediated MHC-I downmodulation (Dikeakos et al., 2012). Correspondingly, mutation of the PACS binding site on Nef ($EEEE_{65}\rightarrow AAAA$, $W_{113}\rightarrow A$, or Nef-E4AW_{113}A) disrupted the PACS-dependent trafficking of Nef to the perinuclear region as well as repressed MHC-I downregulation (Dikeakos et al., 2012). Together, these studies illustrate the

molecular basis underlying Nef-PACS interactions and how these interactions contribute to the Nef-induced trafficking events leading to MHC-I downregulation.

2.5.5 Nef recruits AP-1 to the cytoplasmic tail of MHC-I to divert newly synthesized MHC-I to lysosomes for degradation

In addition to the endocytic mechanism for MHC-I downregulation, Nef also forms a ternary complex with the cytoplasmic tail of MHC-I and the adaptor protein AP-1 to divert newly synthesized MHC-I from transit to the cell surface to the endolysosomal network where it is ultimately degraded (Figure 2.4) (Noviello et al., 2008, Singh et al., 2009, Schaefer et al., 2008, Wonderlich et al., 2008). To mediate this effect, Nef binds the cytoplasmic tail of MHC-I early in the secretory pathway (Kasper et al., 2005, Williams et al., 2002, Roeth et al., 2004, Williams et al., 2005) and then the Nef-MHC-I complex recruits AP-1 to redirect MHC-I from the TGN to the endo-lysosomal network (Roeth et al., 2004). Interestingly, despite mechanistic differences in how Nef induces CD4 and MHC-I internalization, recent studies determined that both MHC-I and CD4 are ultimately found in the same endo-lysosomal structures and both are targeted for lysosomal degradation in a β-COP-dependent manner (Schaefer et al., 2008), consistent with the role of COPI in endosomal maturation (Huotari et al., 2011). However, as these experiments rely on the overexpression of MHC-I, examination of the fate of endogenous versus overexpressed MHC-I is warranted. Moreover, the determination that PACS-2 binds β-COP and functions

as a connector for COPI coated vesicles (Simmen et al., 2005), together with the observation that PACS-2 interacts with Nef on Rab5-positive early endosomes as well as Rab7-positive late endosomes (Dikeakos et al., 2012), suggests PACS-2 may function in a β-COP-dependent manner to mediate Nef-dependent trafficking steps.

To mediate the formation of a ternary complex, Nef appears to be functioning as an adaptor or facilitator, as the cytoplasmic tail of MHC-I does not directly bind to AP-1 itself (Noviello et al., 2008, Wonderlich et al., 2008). The ability of the Nef-MHC-I complex to recruit AP-1 requires M_{20} in the N-terminal α-helical domain of Nef as well as Y_{320} in the cytoplasmic tail of MHC-I (Noviello et al., 2008, Wonderlich et al., 2008). Indeed, AP-1 and MHC-I interact via a non-canonical tyrosine-based YXXφ sorting signal (where φ is an amino acid with a bulky hydrophobic side chain) (Bonifacino et al., 2003) in which the cytoplasmic tail of MHC-I contains a Y_{320}SQA instead of a YXXφ sequence and Nef is thought to compensate for the lack of a φ residue to facilitate this interaction (Wonderlich et al., 2008). To date, it is only possible to observe the ternary complex between AP-1, Nef, and the cytoplasmic tail of MHC-I *in vitro* when the MHC-I cytoplasmic tail is fused to the N-terminus of Nef that has been mutated to inactivate the $LL_{164,165}$ dileucine motif (MHCIct-NefLL→AA) (Coleman et al., 2006, Noviello et al., 2008, Wonderlich et al., 2008, Singh et al., 2009). Inactivation of the dileucine motif is necessary because native Nef can directly bind to AP-1 *in vitro* at the canonical (D/E)XXXL(L/I) motif (Bonifacino et al., 2003), thereby precluding

analysis of the *in vivo* ternary complex. While a discrete binding site on Nef required for direct interaction with the cytoplasmic tail of MHC-I has remained elusive, the acidic ($EEEE_{65}$) and polyproline ($PXXP_{75}$) motifs of Nef have been shown to stabilize this interaction (Noviello et al., 2008, Wonderlich et al., 2008). In support of these studies, the recently solved high resolution crystal structure of a ternary complex comprising Nef, the MHC-I cytosolic tail, and the µ1 subunit of AP-1 has shed some light on these complex interactions (Jia et al., 2012). Indeed, this structural analysis revealed cooperativity between various Nef domains to form and stabilize an interaction between the MHC-I cytosolic tail and the µ1 subunit of AP-1. Specifically, the MHC-I cytosolic tail is clamped into a long, narrow binding groove at the Nef-µ1 interface that is secured by regions within the Nef polyproline helix (including $PXXP_{75}$) as well as by electrostatic interactions involving the acidic cluster in the Nef core domain ($EEEE_{65}$) (Jia et al., 2012). These structural analyses provide insight into how Nef functions as a clathrin-associated sorting protein to alter the fate of MHC-I trafficking.

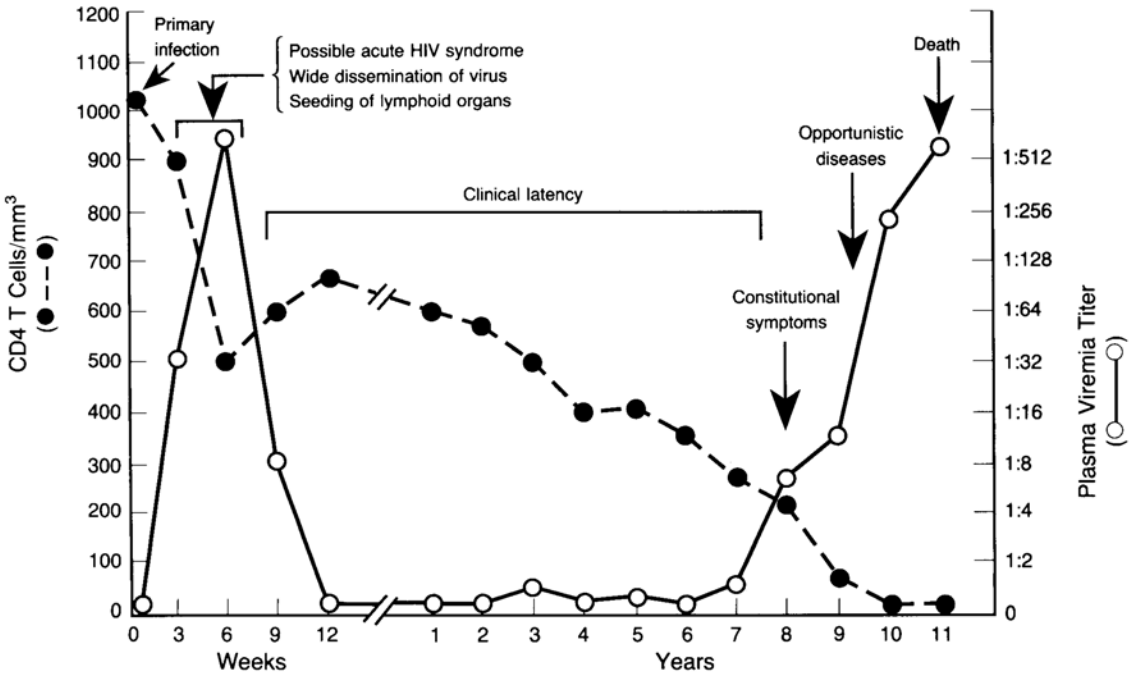

Figure 2.1. Natural history of HIV-1 disease progression.

The timeline of HIV infection can be divided into three phases: primary infection, latency, and clinical AIDS. During the primary infection (usually 2-4 weeks post-exposure), plasma viral titers peak while $CD4^+$ T-cell levels initially decline. A dramatic reduction in viral load following primary HIV infection marks the beginning of clinical latency. As $CD4^+$ T-cell levels continue to decline, the HIV-1 infected individual progresses to AIDS. Reproduced with permission from (Pantaleo *et al.*, 1993), Copyright 1993 Massachusetts Medical Society.

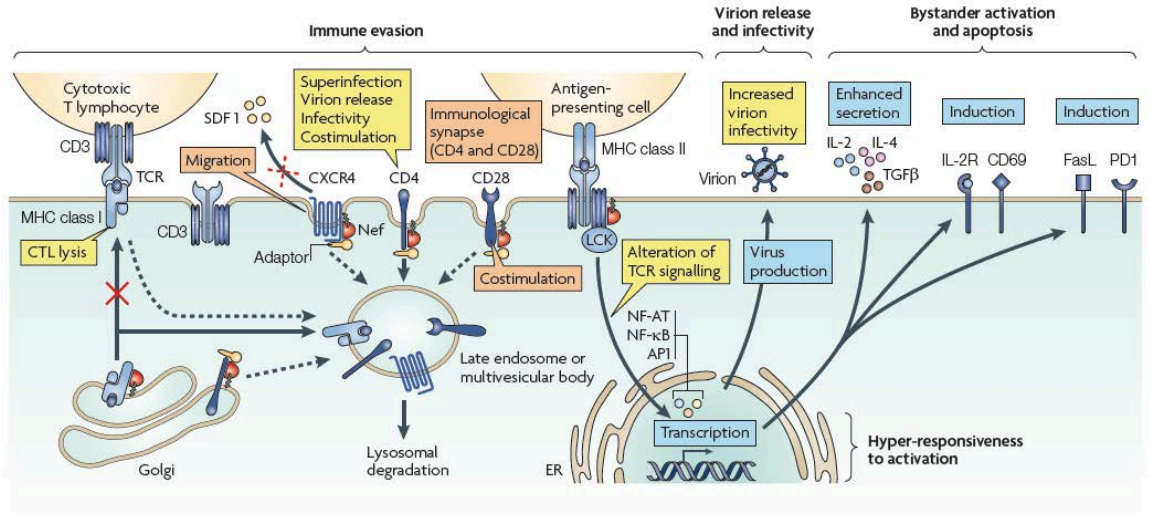

Figure 2.2. Schematic of Nef functions.

HIV-1 Nef downregulates several receptors from the cell surface of $CD4^+$ T-cells to inhibit CTL-mediated lysis, enhance virus release, alter cell migration, and modulate signal transduction by the immunological synapse. Reproduced with permission from (Kirchhoff, 2009), Copyright 2009 Nature Publishing Group.

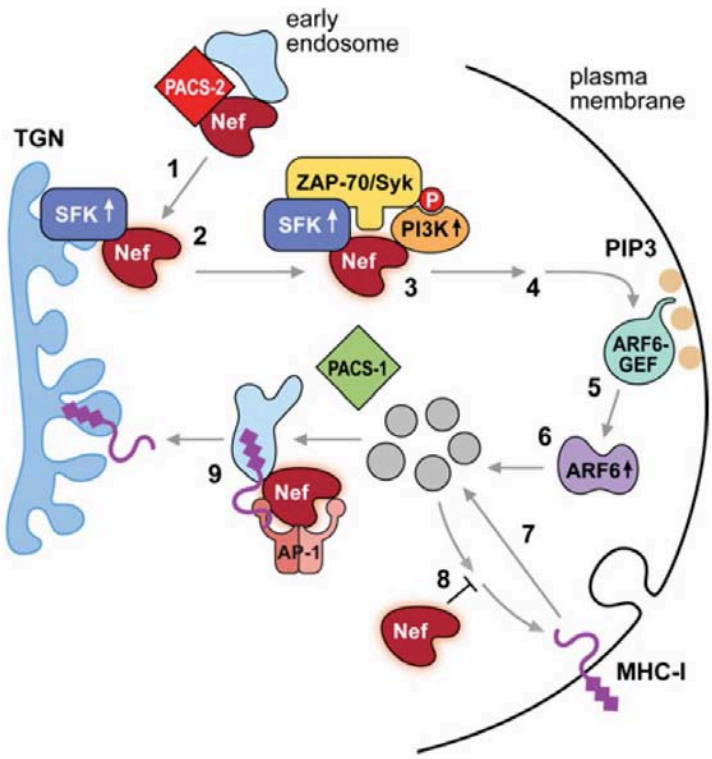

Figure 2.3. Nef assembles a multi-kinase complex to accelerate endocytosis of MHC-I.

1) The Nef $EEEE_{65}$-dependent binding to PACS-2 targets Nef to the perinuclear region. **2)** Nef $PXXP_{75}$ binds and directly activates a TGN-localized SFK. **3)** The Nef-SFK complex recruits and activates ZAP-70/Syk, which then binds and activates class I PI3K. **4)** PI3K generates PIP_3 at the plasma membrane. **5)** An ARF6 guanine-nucleotide-exchange factor (ARF6-GEF) binds PIP_3. **6)** The ARF6-GEF activates ARF6. **7)** ARF6 activation leads to the endocytosis of MCH-I from the plasma membrane to endosomal comparments. **8-9)** Endocytosed MHC-I is sequestered in the perinuclear region in an M_{20}-, AP-1, and PACS-1-dependent manner. Reproduced with permission from (Youker et al., 2009), Copyright 2009 Biochemical Journal.

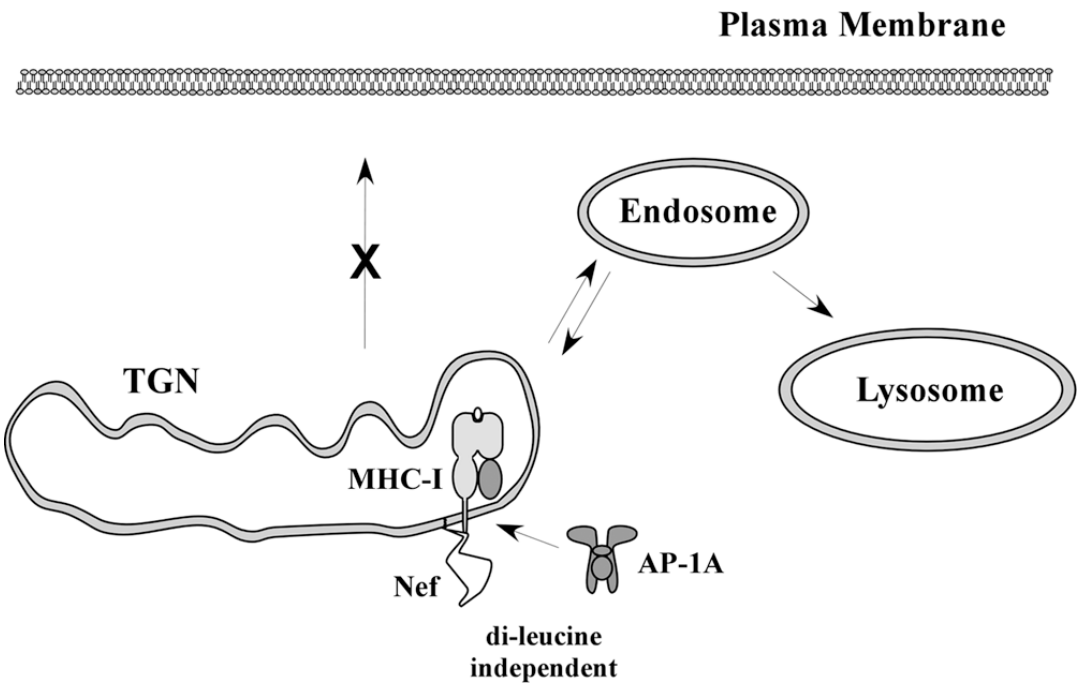

Figure 2.4. Nef reroutes newly synthesized MHC-I to the endolysosomal network.

Nef binds the cytoplasmic tail of MHC-I early in the secretory pathway. The Nef-MHC-I complex then recruits AP-1 to divert newly synthesized MHC-I from transit to the cell surface to the endolysosomal network where it is ultimately degraded. Reproduced with permission from (Roeth et al., 2004). Copyright Roeth et al., 2004, Rockefeller University Press. Originally published in The Journal of Cell Biology. doi: 10.1083/jcb.200407031.

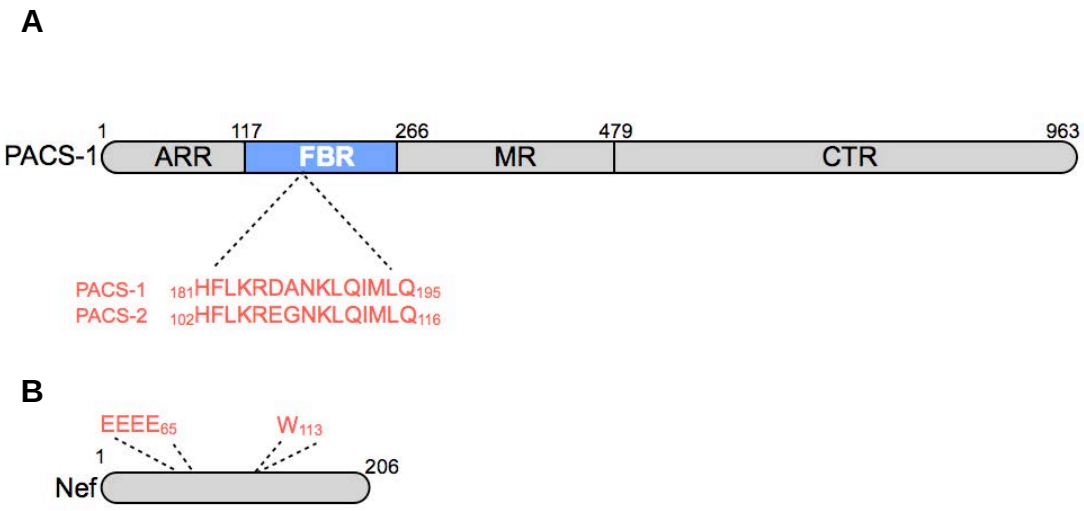

Figure 2.5. Schematic of the PACS-Nef interaction.

(A) Schematic of PACS-1 depicting the ARR, FBR, MR, and CTR. The PACS-1 and PACS-2 FBR residues necessary and sufficient for interaction with Nef are shown below in red. (B) Schematic of Nef depicting the sites required for interacting with PACS-1 and PACS-2, including the acidic cluster $EEEE_{65}$ and W_{113} in the core domain (shown in red).

CHAPTER 3. Small molecule inhibition of HIV-1-induced MHC-I downregulation identifies a temporally regulated switch in Nef action

Small molecule inhibition of HIV-1-induced MHC-I downregulation identifies a temporally regulated switch in Nef action

Jimmy D. Dikeakos[a,g], Katelyn M. Atkins[a,g], Laurel Thomas[a], Lori Emert-Sedlak[b], In-Ja L. Byeon[c], Jinwon Jung[c], Jinwoo Ahn[c], Matthew D. Wortman[d], Ben Kukull[e],Masumichi Saito[f], Hirokazu Koizumi[f], Danielle M. Williamson[a], Masateru Hiyoshi[f], Eric Barklis[e], Masafumi Takiguchi[f], Shinya Suzu[f], Angela M. Gronenborn[c], Thomas E. Smithgall[b], and Gary Thomas[a]

[a]Vollum Institute, Oregon Health & Science University, Portland, OR 97239;

[b]Department of Microbiology and Molecular Genetics, University of Pittsburgh, PA 15260;

[c]Department of Structural Biology, University of Pittsburgh, PA 15260;

[d]Drug Discovery Center, University of Cincinnati, OH 45237;

[e]Department of Molecular Microbiology and Immunology, Oregon Health & Science University, Portland, OR 97239;

[f]Center for AIDS Research, Kumamoto University, Kumamoto, Japan 860-0811;

[g]*These authors contributed equally to this work.*

Author contributions: JDD, KMA and LT collaborated closely to perform most of the experiments. JDD performed the pulse-chase, surface biotinylation and protein binding experiments; KMA performed the co-immunoprecipitation,

western blot and kinase complex assays and the statistical analyses; LT performed the microscopy and flow cytometry experiments; LT and JDD performed the cell toxicity experiments; LES performed the qRT-PCR experiments; ILB, JJ, and MA performed the NMR experiments, LES, KMA and DMA performed the 2c binding experiments, BK and JDD performed the HIV-1 infections; MS, MK, MH and SS supplied 2c; JDD, KMA, MT, MDW, EB, TES and AMG provided critical input into the overall research direction; LT arranged the artwork; G.T. directed the research and wrote the manuscript with input from KMA, JDD, AMG and TES.

Molecular Biology of the Cell 2010 Oct 1; 21(19): 3279-92.

ABSTRACT

HIV-1 Nef triggers downregulation of cell-surface MHC-I by assembling a Src family kinase (SFK)-ZAP-70/Syk-PI3K cascade. Here, we report that chemical disruption of the Nef-SFK interaction with the small molecule inhibitor 2c blocks assembly of the multi-kinase complex and represses HIV-1–mediated MHC-I downregulation in primary $CD4^+$ T-cells. 2c did not interfere with the PACS-2–dependent trafficking of Nef required for the Nef-SFK interaction or the AP-1 and PACS-1–dependent sequestering of internalized MHC-I, suggesting the inhibitor specifically interfered with the Nef-SFK interaction required for triggering MHC-I downregulation. Transport studies revealed Nef directs a highly regulated program to downregulate MHC-I in primary $CD4^+$ T-cells. During the first two days after infection, Nef assembles the 2c-sensitive multi-kinase complex to trigger downregulation of cell-surface MHC-I. By three days post-infection Nef switches to a stoichiometric mode that prevents surface delivery of newly synthesized MHC-I. Pharmacologic inhibition of the multi-kinase cascade prevents the Nef-dependent block in MHC-I transport, suggesting the signaling and stoichiometric modes are causally linked. Together, these studies resolve the seemingly controversial models that describe Nef-induced MHC-I downregulation and provide new insights into the mechanism of Nef action.

INTRODUCTION

After infection by HIV-1, the acute viremia induces an immune response that includes the development of anti-HIV $CD8^+$ cytotoxic T lymphocytes (CTLs) (Gandhi et al., 2002). Though a significant number of the circulating CTL population is directed against HIV-1–infected cells, the virus escapes the adaptive immune response, establishing reservoirs in numerous cell types that can resist highly active antiretroviral therapy (HAART) (Stevenson, 2003). During disease progression, the HIV-1 viral load increases greatly, destroying most of the $CD4^+$ lymphocytes, leaving patients increasingly susceptible to opportunistic infections (Douek et al., 2003).

The adaptive immune response requires members of the class I major histocompatibility complex (MHC-I) to present viral antigens on the surface of infected cells, which destroys the infected cell by the cytolytic, apoptosis-inducing actions of CTLs (Lieberman, 2003). Large DNA viruses, including herpesviruses and poxviruses, possess a large collection of immune evasive genes that are expressed in a coordinated manner to target nearly every step in the biosynthesis, assembly, transport, and cell-surface localization of MHC-I molecules (Yewdell et al., 2002, Peterlin et al., 2003). By contrast, HIV-1 relies on the single 27-kDa N-myristoylated early gene product Nef to downregulate MHC-I (Peterlin et al., 2003). Nef is required for the onset of AIDS and can affect cells in many ways, including alteration of T-cell activation and maturation, subversion of

the apoptotic machinery, and the downregulation of cell-surface molecules, notably CD4 and MHC-I (Fackler et al., 2002). Downregulation of CD4 through the clathrin/AP-2 pathway to lysosomes eliminates interference of the viral receptor with HIV-1 envelopment or release. Downregulation of cell-surface MHC-I molecules encoded by the HLA-A and -B loci to paranuclear TGN/ endosomal compartments mediates the ability of HIV-1 to evade the $CD8^+$ immune surveillance system (Blagoveshchenskaya et al., 2002, Tomiyama et al., 2002, Yang et al., 2002, Peterlin et al., 2003).

Two models—here referred to as the “signaling” and “stoichiometric” downregulation pathways—are currently used to explain the molecular basis of Nef-mediated MHC-I downregulation (see Hung et al., 2007). The “signaling” model describes the sequential roles of three conserved Nef sites in mediating MHC-I downregulation. The pathway is initiated by the $EEEE_{65}$-dependent binding to the sorting protein PACS-2, which targets Nef to the paranuclear region, enabling $PXXP_{75}$ to bind and activate a Golgi region-localized Src family kinase (SFK). This Nef-SFK complex then phosphorylates ZAP-70 (Syk in monocytes and heterologous cells), forming a phosphotyrosine-based docking motif that recruits class I PI3K by ligating the p85 regulatory subunit C-terminal SH2 domain. This multi-kinase complex then triggers internalization of cell-surface MHC-I through a clathrin-independent, ARF6-dependent pathway (Blagoveshchenskaya et al., 2002, Hung et al., 2007, Atkins et al., 2008). After internalization, Nef M_{20}, located within an amphipathic α-helix, mediates the

sequestering of endocytosed MHC-I molecules into paranuclear compartments (Blagoveshchenskaya et al., 2002, Hung et al., 2007, Chaudhry et al., 2008). By contrast, the “stoichiometric” model envisions that Nef mediates MHC-I downregulation by acting solely via a PI3K-independent pathway that diverts newly synthesized MHC-I molecules to degradative compartments by an M_{20}- and AP-1–dependent mechanism (Kasper et al., 2003, Roeth et al., 2004, Kasper et al., 2005). However, an alternative interpretation of the stoichiometric model suggests Nef binds endocytosed MHC-I but the underlying mechanism was not described (Roeth et al., 2004, Noviello et al., 2008). While the stoichiometric model suggests the importance of Nef M_{20} in mediating MHC-I downregulation—a finding consistent with both models—it fails to address the roles of $EEEE_{65}$ and the $PXXP_{75}$ site within the polyproline helix.

The binding of HIV-1 Nef to the SH3 domains of SFKs requires $PXXP_{75}$ and an adjacent hydrophobic pocket, which anchors the SFK on Nef (Lee et al., 1995). The determination that Nef can bind and directly activate a subset of SFKs together with the conservation of the SH3 domain binding site across various Nef alleles (Choi et al., 2004, Trible et al., 2006) suggests the Nef-SFK interaction is required for disease progression, including AIDS-like disease in animal models and assembly of the SFK-ZAP-70/Syk-PI3K multi-kinase complex, which triggers MHC-I downregulation in primary $CD4^+$ T-cells and promonocytic cells (Hanna et al., 1998a, Hung et al., 2007). These findings suggest that targeting the assembly of the multi-kinase complex may represent an attractive

approach to inhibiting AIDS progression. The ability of isoform-specific class I PI3K kinase inhibitors to repress Nef-induced MHC-I downregulation in primary $CD4^+$ T-cells supports this possibility (Hung et al., 2007, Atkins et al., 2008). Alternatively, small molecule inhibitors that disrupt the binding of Nef to one or more of the kinases that form the multi-kinase complex would inhibit Nef action without disrupting the activity of cellular kinases that may be required for host cell function.

Here we report that small molecule disruption of Nef-SFK binding represses MHC-I downregulation in HIV-1–infected primary $CD4^+$ T-cells by interfering with formation of the multi-kinase complex. We further show that Nef-induced MHC-I downregulation in primary $CD4^+$ T-cells is manifest by the sequential action of the signaling mode, which lasts for more than two days after infection, followed by the stoichiometric mode by three days post-infection. Interference with the multi-kinase complex that triggers the signaling mode disrupts the subsequent stoichiometric block in MHC-I transport, suggesting the two modes are causally linked. These studies challenge the current dogma of Nef-mediated MHC-I downregulation (Hansen et al., 2009) and suggest Nef orchestrates a highly regulated molecular program consisting of the sequential use of signaling followed by stoichiometric modes to evade immune surveillance.

RESULTS

3.1 HIV-1 Nef uses a subset of SFKs to trigger MHC-I downregulation

Formation of the SFK-ZAP70/Syk-PI3K multi-kinase complex is initiated by the $PXXP_{75}$-dependent binding of Nef to the SH3 domain of a Golgi region-localized SFK, directly activating the kinase (Hung et al., 2007). Of the seven known SFKs only a subset—Hck, Lyn, and Src—can be directly activated after Nef binding and are found in the Golgi region, suggesting one or more of these kinases mediate MHC-I downdownregulation (Matsuda et al., 2006, Trible et al., 2006, Hiyoshi et al., 2008, Pulvirenti et al., 2008). To test this, H9 $CD4^+$ T-cells treated with siRNAs specific for Hck, Lyn, or Src were infected with recombinant viruses expressing Nef and the extent of MHC-I downregulation was determined (Figure 3.1A, and relative SFK knockdown quantified in Figure 3.2A). Our results demonstrate that Nef-induced MHC-I downregulation was slightly repressed by siRNA knockdown of Hck alone but blocked by knockdown of Hck, Lyn, and Src together. The data suggest that Hck, Lyn, and Src function redundantly in Nef-induced MHC-I downregulation.

3.2 Small molecule inhibition of the Nef-SFK interaction

The determination that Nef assembles a multi-kinase complex to trigger MHC-I downregulation suggests this pathway can be selectively targeted pharmacologically. Indeed, isoform-specific class I PI3K inhibitors repress Nef-

induced MHC-I downregulation in primary $CD4^+$ T-cells (Hung et al., 2007, Atkins et al., 2008). An alternative approach would be to block protein-protein interactions required for complex assembly without affecting cellular enzyme activity directly. The characterized binding of Nef to SFK SH3 domains represents an ideal target for this type of inhibitor (Arold et al., 1997). One candidate compound, 2c (Figure 3.2B), is a derivative of the compound UCS15A that disrupts the PXXP-dependent binding of Sam68 to Src (Oneyama et al., 2003). To test whether 2c disrupts Nef-SFK binding, we treated H9 $CD4^+$ T-cells coexpressing flag-tagged Nef (Nef/f) and Hck with increasing concentrations of 2c. Hck was used because it binds Nef with higher affinity than other SFKs and Nef can assemble Hck into the multi-kinase complex (Hung et al., 2007, Atkins et al., 2008). Coimmunoprecipitation analysis showed 2c repressed the interaction between Nef and Hck in a dose-dependent manner (Figure 3.1B) as well as repressed the interaction with Lyn or Src (Figure 3.2C). Next, we incubated GST-Nef and His_6-Hck with increasing concentrations of 2c and found that 2c disrupted Nef-Hck binding in a dose-dependent manner (Figure 3.1C). To determine whether the ability of 2c to inhibit Nef-SFK binding also blocked Nef-induced SFK activation, we incubated recombinant, purified Nef, and Hck with increasing concentrations of 2c and measured the resulting Nef-induced Hck activity using a FRET-based *in vitro* kinase assay. Under these assay conditions, activation of Hck is dependent upon Nef (Emert-Sedlak et al., 2009). As shown in Figure 3.1D, 25 μM 2c substantially repressed Nef-dependent Hck activity

without affecting Hck in the absence of Nef. High 2c concentrations (≧100 μM), however, directly inhibited Hck activity. These findings suggest 2c has a bimodal effect on Hck activity; at low concentrations 2c disrupts Nef-induced kinase activity, whereas high concentrations of 2c inhibit Hck directly.

The ability of 2c to selectively inhibit Nef-induced Hck activation suggested 2c may bind Nef directly, thereby affecting Hck activity. Accordingly, ^{1}H-^{15}N Heteronuclear Single Quantum Coherence (HSQC) NMR analysis of the interaction of 2c with recombinant Nef in solution revealed 2c induces a number of chemical shift changes in amide resonances of Nef (Figure 3.1E). These include relatively small chemical shift changes (0.025–0.063ppm) at V_{74}, M_{79}, and T_{80} located within the Nef polyproline helix that binds the RT loop of SH3 domains on SFKs (Lee et al., 1995), suggesting 2c may influence the conformation of the polyproline helix. The presence of resonance overlap in the NMR spectra precluded more detailed analysis involving the disordered regions of Nef such as the N-terminal region preceding the polyproline helix and the internal loop consisting of residues E_{149}–K_{178}. More pronounced chemical shift changes (>0.1ppm) were observed for the resonances of Y_{135}, K_{144}, V_{146}, K_{184} (R_{184} in Figure 3.1F [PDB ID:2NEF]), F_{185}, and L_{189} which are clustered on the opposite side of the SH3 domain binding site. Other residues in this region such as V_{148}, A_{190}, F_{191}, M_{194}, and E_{197}, and L_{198} also undergo substantial (>0.06ppm) changes. These chemical shift perturbations caused by the addition of 2c imply that 2c could bind to the cleft formed by the central β-sheet and the C-terminal α-

helices of Nef, which may provide a good binding pocket (Figure 3.1F). Together, these findings suggest 2c may interfere with Nef-induced SFK activation most likely by allosteric inhibition of SFK binding or possibly by directly influencing the binding mode of the polyproline helix to SFKs or both.

3.3 2c represses the ability of HIV-1 to downregulate MHC-I

The 2c concentration range that selectively inhibited Nef-dependent SFK activation showed no measurable cell toxicity up to 60 μM for two days, suggesting 2c could be tested in culture (Figure 3.3A). Accordingly, we treated H9 cells expressing Nef-yellow fluorescent protein (Nef-eYFP) with 2c or the class I PI3K inhibitor PI-103, which specifically blocks Nef-induced MHC-I downregulation (Hung et al., 2007), and measured cell surface MHC-I (Figure 3.4A). In agreement with earlier studies (Hung et al., 2007, Atkins et al., 2008), Nef-eYFP induced an ~two-fold downregulation of MHC-I that was blocked by PI-103. Similarly, 2c partially blocked MHC-I downregulation. Next, we asked whether 2c could interfere with HIV-1–induced MHC-I downregulation in primary $CD4^+$ T-cells. We infected primary $CD4^+$ T-cells with HIV-1^{NL4-3} and treated the cultures with vehicle or 2c. At 8 d post-infection, the cells were analyzed for cell-surface HLA-A2 and CD4 by flow cytometry (Figure 3.4B). We found that 2c partially blocked downregulation of MHC-I but had no effect on downregulation of CD4, which is mediated by a class I PI3K-independent pathway (Hung et al., 2007).

3.4 2c Disrupts formation of the multi-kinase complex

The ability of 2c to disrupt Nef-SFK binding as well as HIV-1–induced MHC-I downregulation suggested this compound would disrupt assembly of the SFK-ZAP-70-PI3K multi-kinase complex. Accordingly, we found that 2c blocked the ability of Nef to recruit class I PI3K activity using an *in vitro* lipid kinase assay (Figure 3.5A). Moreover, this result was not due to cell toxicity or induction of apoptosis (Figures 3.3B-C) nor was it due to nonspecific inhibition of class I PI3K as treatment of the immunoprecipitate with 40 μM 2c had no effect on enzyme activity (Figure 3.5A). The titration analysis of 2c on Nef-induced Hck activation (Figure 3.1D) suggests 40 μM 2c blocked Nef-induced PI3K stimulation by selective inhibition of Nef-induced SFK activation, whereas 100 μM 2c may block Nef-induced PI3K stimulation by additionally inhibiting SFK activation directly. The PI3K activity results were supported by coimmunoprecipitation analysis in which 2c inhibited formation of the multi-kinase complex by disrupting the interaction of Nef with Hck, phospho-ZAP-70 and the class I PI3K p85 regulatory subunit (Figure 3.5B).

The ability of 2c to disrupt Nef-SFK binding did not exclude the possibility that it may affect additional steps in the MHC-I downregulation pathway. We first asked whether 2c interfered with steps upstream of Nef-SFK binding. Accordingly, we found that 2c had no effect on the Nef-PACS-2 interaction (Figure 3.5C) nor the PACS-2–dependent trafficking of Nef-eYFP to the

paranuclear region, which is required for Nef-SFK binding and Nef-induced MHC-I downregulation (Figure 3.5D).

Because Nef M_{20} mediates the interaction with AP-1 (Roeth et al., 2004) and is essential for sequestration of MHC-I molecules after their internalization from the cell surface (Blagoveshchenskaya et al., 2002), we tested whether AP-1 was required in the last stage of this signaling pathway. Accordingly, H9 cells knocked down for AP-1A, PACS-2, or PACS-1 which is required for MHC-I downregulation but not for triggering PI3K stimulation (Piguet et al., 2000, Atkins et al., 2008), were infected with viruses expressing Nef or the Nef_{AXXA}-PI3K* chimera, which rescues the inability of Nef_{AXXA} to downregulate MHC-I by overriding the requirement for assembly of the SFK-ZAP-70-PI3K complex (Figure 3.6 and (Blagoveshchenskaya et al., 2002, Hung et al., 2007). The ability of Nef or Nef_{AXXA}-PI3K* to downregulate MHC-I in cells knocked down for expression of PACS-2, PACS-1, or AP-1A was assessed by antibody uptake to discern the importance of each protein in steps upstream or downstream of PI3K stimulation (Figure 3.7A). Consistent with our determination that Nef requires PACS-2 upstream of PI3K (Atkins et al., 2008), siRNA knockdown of PACS-2 blocked MHC-I uptake by Nef but not by Nef_{AXXA}-PI3K*. By contrast, siRNA knockdown of AP-1A or PACS-1 blocked MHC-I uptake induced by Nef and Nef_{AXXA}PI3K*, demonstrating AP-1 and PACS-1 act downstream of PI3K stimulation.

To test potential effects of 2c on the later stages of this pathway, we asked

whether 2c interfered with the interaction between Nef and PACS-1 or AP-1. We determined that 2c had no effect on the Nef-PACS-1 interaction (Figure 3.7B). Additionally, the interaction of AP-1 with Nef M_{20} and the MHC-I cytosolic domain can be recapitulated using the chimeric protein GST-MHC-I CD-$Nef_{LL/AA}$ to capture AP-1 from cytosol preparations (Noviello et al., 2008). This chimera consists of Nef with an LL_{165}→AA substitution, which blocks the LL_{165}-dependent binding to adaptors, fused to the MHC-I cytosolic domain. We found that 2c did not interfere with the ability of GST-MHC-I CD-NefLL/AA to capture AP-1 (Figure 3.7C, left). Interestingly, we found that GST-MHC-I CD-$Nef_{LL/AA}$ captured PACS-1 but not PACS-2, consistent with our determination that Nef requires PACS-1 subsequent to PI3K stimulation to downregulate MHC-I (Figure 3.7C, right). Moreover, similar to our findings with AP-1, 2c failed to disrupt the interaction of GST-MHC-I CD-$Nef_{LL/AA}$ with PACS-1. To further evaluate whether 2c disrupts MHC-I downregulation downstream of PI3K stimulation, we repeated the antibody uptake experiment (Figure 3.7D). We found that 2c blocked the ability of Nef but not Nef_{AXXA}PI3K* to downregulate MHC-I, indicating 2c specifically acts upstream of PI3K stimulation.

3.5 PTEN-null CEM cells fail to phenocopy Nef action in primary $CD4^+$ or H9 cells

Our results using primary $CD4^+$ T-cells and H9 cells suggest 2c disrupts HIV-1–mediated MHC-I downregulation by interfering with the ability of Nef to assemble the SFK-ZAP-70/Syk-PI3K complex. This signaling pathway explains

the importance of the $EEEE_{65}$ and $PXXP_{75}$ sites, which trigger MHC-I internalization and subsequent M_{20}-mediated sequestering of internalized MHC-I molecules (Blagoveshchenskaya et al., 2002, Hung et al., 2007). However, an alternate model of MHC-I downregulation, which largely relies on CEM T-cells stably expressing MHC-I, envisions a PI3K-independent pathway based largely on the M_{20}-mediated stoichiometric block of newly synthesized MHC-I molecules en route to the cell surface (Kasper and Collins, 2003). We therefore transfected CEM cells with plasmids expressing PTEN alone or together with Nef (Figure 3.8A), and tested whether 2c or PI-103 would repress MHC-I downregulation. Because transfected PTEN can be inhibited by oxidation in leukemic cells, these experiments were conducted in 0.5 mM β-mercaptoethanol (Silva et al., 2008). In contrast to H9 cells or primary $CD4^+$ T-cells, both compounds failed to repress MHC-I downregulation in CEM cells (Figure 3.8B, top), suggesting Nef may downregulate MHC-I in CEM cells by a mechanism different from it uses in H9 or primary $CD4^+$ T-cells. Alternatively, the disparate findings may have resulted from the dysregulated PI3K signaling inherent to CEM cells, which would override the requirement for the multi-kinase complex (Astoul et al., 2001). Indeed, many leukemic cell lines such as CEM and Jurkat lack the tumor suppressor PTEN, which is a lipid phosphatase that attenuates PI3K signaling by dephosphorylating PIP_3. Thus, loss of PTEN results in constitutively elevated levels of PI3K/Akt signaling characteristic of many tumor cell lines. Although acute treatment of CEM or Jurkat cells with PI3K inhibitors prevents new PIP_3 synthesis, the

absence of PTEN results in persistently elevated levels of PIP_3 that mediate PI3K-stimulated pathways even in the presence of PI3K inhibitors, thereby conferring resistance to the effect of multi-kinase complex inhibition (Hung et al., 2007). We therefore expressed PTEN alone or PTEN together with Nef (Figure 3.8A) and determined that PTEN alone had little effect on the cell-surface levels of endogenous MHC-I, which is expected because this enzyme is normally expressed in $CD4^+$ T-cells (Figure 3.8, bottom). Re-expression of PTEN, however, repressed the constitutively elevated PI3K/Akt signaling present in CEM cells as determined by a decrease in active (phosphorylated) Akt (Figure 3.8A), suggesting that PTEN-replete CEM cells may be rescued in their ability to regulate PIP_3 levels and would thus be responsive to treatment with PI3K inhibitors. Accordingly, re-expression of PTEN rescued the ability of PI-103 or 2c to repress MHC-I downregulation in CEM cells, similar to that observed in primary $CD4^+$ T-cells or H9 cells (Figure 3.8B bottom and see Figure 3.4). These results demonstrate that an intact PI3K regulatory network is required to study PI3K-dependent steps in signaling pathways, including Nef-induced MHC-I downregulation.

3.6 Nef downregulates MHC-I by a PI3K-triggered endocytic pathway followed by a transport block

Whereas aberrant phosphoinositide metabolism in CEM cells can explain the confusion underlying the requirement by Nef for the multi-kinase complex to

downregulate MHC-I (Kasper et al., 2003, Schaefer et al., 2008), this defect did not readily explain why some studies found that Nef blocks delivery of newly synthesized MHC-I molecules en route to the cell surface—the stoichiometric model—whereas other studies found Nef relies on its ability to assemble the multi-kinase complex to internalize and sequester MHC-I molecules following their delivery to the cell surface—the signaling model. Although these disparate findings were originally attributed to uncharacterized differences in Golgi-to-cell-surface transport in T-cells versus HeLa cells (Kasper et al., 2003), closer inspection of the experimental paradigm revealed that the signaling model assessed MHC-I transport at 7–44 hours post-infection while the stoichiometric model assessed ER-to-cell surface transport of MHC-I at longer post-infection times (Blagoveshchenskaya et al., 2002, Kasper et al., 2005, Hung et al., 2007). We therefore conducted a time course to measure the ability of Nef to impede cell surface delivery of newly synthesized endogenous MHC-I molecules (Figure 3.9A). Parallel cultures of H9 cells infected for 24, 48, or 72 hours with pseudotyped HIV-1^{NL4-3} that either lack or express Nef were subjected to pulse-chase/surface biotinylation to monitor delivery of MHC-I to the cell surface. At 24 and 48 hoursours post-infection, Nef had no measurable effect on the transport of newly synthesized MHC-I to the cell-surface. By 72 hours post-infection, however, Nef markedly repressed MHC-I transport. To test whether these results were specific to H9 cells or the use of HC10, which recognizes denatured HLA-B and C heavy chains, we repeated the pulse-chase/surface biotinylation in primary

$CD4^+$ T-cells using the conformation dependent antibody, BB7.2, which recognizes HLA-A2. In agreement with our findings in H9 cells, Nef had no appreciable effect on cell-surface delivery of HLA-A2 for the first 48 hoursours post-infection in primary $CD4^+$ T-cells. Again, similar to H9 cells, at 72 hours post-infection Nef markedly repressed HLA-A2 transport to the cell surface (Figure 3.9B).

To determine whether the switch in Nef-induced MHC-I downregulation was coupled with a change in MHC-I stability, H9 cells infected with Nef^- or Nef^+ pseudotyped HIV-1 for 24 or 72 hours were pulse-labeled with [^{35}S]Met/Cys for 15 minutes and chased for up to 20 hours. Immunoprecipitation of endogenous MHC-I with HC10 showed that Nef had no obvious effect on MHC-I stability at 24 or 72 hours post-infection (Figure 3.10). To assess whether Nef altered the rate of MHC-I transport, the immunoprecipitates were subjected to endoglycosidase H (Endo H) digestion, which demonstrated MHC-I molecules became Endo H resistant by 4 hours post-infection irrespective of Nef expression or the time post-infection (Figure 3.9C). These findings suggest Nef does not impede MHC-I transport from early secretory pathway compartments nor does it markedly affect the stability of endogenous MHC-I molecules.

The inability of Nef to block ER-to-cell surface transport of MHC-I molecules for at least 48 hours post-infection suggested that for the first two days Nef may downregulate MHC-I by triggering the multi-kinase–dependent internalization and sequestering of MHC-I molecules from the cell surface. We

tested this possibility using antibody uptake. H9 cells were infected with Nef^- or Nef^+ pseudotyped HIV-1 for 48 or 72 hours and then incubated with anti–MHC-I (W6/32) in the absence or presence of 2c or PI-103. The cells were then fixed, permeabilized, and stained with a secondary antibody to detect internalized MHC-I (W6/32) and with antibody K455 to detect steady-state MHC-I (Figure 3.9D). In agreement with the biotinylation analysis, at 48 hours post-infection Nef induced a marked increase in MHC-I internalization that overlapped with the MHC-I post-fix staining pattern. Treatment of the cells with 2c or PI-103 blocked antibody uptake, suggesting multi-kinase complex formation was required to downregulate MHC-I at these time points. By contrast, at 72 hours post-infection Nef failed to induce W6/32 uptake despite downregulating MHC-I as determined by the K455 post-fix staining pattern. Analysis by flow cytometry revealed that Nef reduced cell surface levels of MHC-I to a similar extent at 48 hours or 72 hours post-infection (Figure 3.9E). Together, these experiments suggest that Nef-induced MHC-I down regulation is manifest for two days by a Nef-assembled PI3K signaling pathway that sequesters MHC-I endocytosed from the cell-surface followed by a switch in Nef action at day three to a stoichiometric mechanism that prevents ER to cell surface transport of newly synthesized MHC-I.

3.7 The signaling mode is required for the switch to the stoichiometric mode

The switch in Nef-induced MHC-I downregulation from a signaling-based pathway to a stoichiometric mechanism did not appear to result from use of

tumor cell lines, differences in antibodies used to immunoprecipitate MHC-I, or levels of Nef expression (see Figure 3.9). We therefore asked whether the conversion of Nef-induced MHC-I downregulation from a signaling- to a stoichiometric-mode depended upon the activity of the multi-kinase complex. To test this possibility, replicate plates of H9 cells were infected with Nef^- or Nef^+ pseudotyped HIV-1 and then treated with 2c or PI-103 at 24 or 48 hours post-infection. At 72 hours post-infection, the level of cell-surface MHC-I was analyzed by flow cytometry, demonstrating that addition of 2c or PI-103 for 24 or 48 hours repressed the ability of Nef to downregulate MHC-I (Figure 3.11). Next, the cells were subjected to the pulse-chase/surface biotinylation assay. In agreement with the results in Figure 3.9 and the flow cytometry results, Nef expressed for 72 hours repressed delivery of newly synthesized MHC-I to the cell surface (Figure 3.12). By contrast, treatment of the infected cells with either 2c or PI-103 for as little as 24 hours before the pulse-chase/surface biotinylation prevented Nef from blocking cell-surface delivery of MHC-I (Figure 3.12A and B, respectively). Together, these results suggest that sustained PI3K signaling driven by the multi-kinase complex is required for Nef-induced MHC-I downregulation to switch from a signaling to a stoichiometric mode.

DISCUSSION

We report that Nef directs a highly regulated program to downregulate MHC-I consisting of the sequential use of the signaling and stoichiometric modes of action. During the first two days after infection, Nef uses the signaling mode to downregulate MHC-I. This mode requires the PACS-2-dependent binding of Nef to a Golgi region-localized SFK that it can directly activate to assemble a multi-kinase complex that triggers downregulation of cell-surface MHC-I in $CD4^+$ T-cells. Using the small molecule inhibitor 2c to disrupt the Nef-SFK interaction, we repressed HIV-1 mediated downregulation of cell-surface HLA-A2 in primary $CD4^+$ T-cells. This 2c-sensitive signaling pathway is present in primary $CD4^+$ T-cells and in H9 cells, which are replete for PTEN and are sensitive to inhibition of the multi-kinase complex. CEM cells, however, lack PTEN and thus fail to phenocopy the MHC-I downregulation pathway used in primary $CD4^+$ T-cells. By three days post-infection, Nef switches to the stoichiometric mode that prevents delivery of newly synthesized MHC-I to the cell surface. Interference with formation of the multi-kinase complex disrupts the temporally controlled block in MHC-I transport, suggesting the Nef-directed signaling and stoichiometric modes are causally linked.

A systematic analysis of the steps underlying MHC-I downregulation suggests 2c selectively blocks Nef action early in the downregulation pathway at the binding of Nef to SFKs, notably Hck, Lyn, or Src (Figures 3.1 and 3.2).

However, the ability of 2c to directly inhibit Hck (or potentially other kinases upstream of class I PI3K), albeit at higher concentrations, may also contribute to the efficacy of 2c. Our NMR studies show that 2c affects the conformation of the N-terminal polyproline helix that binds the RT loop of SH3 domains on SFKs, especially V_{74} (Figure 3.1). Furthermore, the NMR data identify a potential 2c binding pocket, opposite the SH3 domain binding site, in which 2c induces significant changes of the amide resonances surrounding V_{146}, which has been previously identified as essential for Nef-Hck binding (Saksela et al., 1995). Interestingly, 2c induces a change in the resonance at K_{144}, which must be ubiquitylated for Nef to downregulate CD4 (Jin et al., 2008). The lack of effect of 2c on HIV-1–induced CD4 downregulation (Figure 3.4), however, suggests that ubiquitylation of Nef K_{144} is unaffected by 2c. Together, these studies suggest 2c may be a weak competitive inhibitor of Nef-SFK binding or may induce an allosteric change in Nef that indirectly represses binding to SFKs, explaining why micromolar concentrations of 2c are required to inhibit MHC-I downregulation. In support of an allosteric mechanism, Nef alleles from long-term nonprogressors that fail to activate Hck exhibit mutations at a distance from the Hck SH3 docking site on Nef (Trible et al., 2006). The ability of 2c to only partially inhibit MHC-I downregulation in plasmid transfected cells may reflect a lower efficacy of this inhibitor compared with the class I PI3K inhibitor PI-103, which completely inhibits MHC-I downregulation irrespective of the vector used (compare Figure 3.4 and 3.11). However, 2c can completely inhibit Nef-mediated MHC-I

downregulation in pseudovirus-infected cells, suggesting length of treatment, as well as the extent and duration of Nef expression, may influence the efficacy of this compound. The dialdehyde moiety in 2c may also be subject to chemical inactivation by reactive oxygen species characteristic of HIV-1 infection, precluding maximal efficacy of this inhibitor (Figures 3.4 and 3.2 and (Peterhans, 1997)). Nonetheless, the findings reported here, together with the determination that 2c represses the Nef-Hck-dependent downregulation of macrophage colony-stimulating factor (M-CSF) receptor and that diphenylfuropyriminde compounds that selectively block Nef-induced Hck activation also inhibit Nef-dependent HIV-1 replication, suggest that the future generation of potent and selective drug-like molecules that disrupt Nef-SFK binding may represent an attractive approach to the generation of novel HIV-1 therapeutics (Suzu et al., 2005, Hiyoshi et al., 2008, Emert-Sedlak et al., 2009, Hassan et al., 2009).

The signaling mode requires the PACS-2-dependent, Nef-assembled SFK-ZAP-70/Syk-PI3K multi-kinase complex to trigger increased internalization of cell-surface MHC-I molecules through an ARF6-regulated endocytic pathway (Blagoveshchenskaya et al., 2002, Hung et al., 2007, Atkins et al., 2008, Chaudhry et al., 2008). The internalized molecules are then sequestered into paranuclear compartments by a Nef M_{20}-, AP-1–, and PACS-1–dependent process (Figure 3.7 and (Blagoveshchenskaya et al., 2002, Chaudhry et al., 2008). Thus, AP-1 is required for both the signaling and stoichiometric modes of MHC-I downregulation, but whether PACS-1 is also required in the stoichiometric

mode or whether PACS-1 and AP-1 mediate common or separate sorting steps required for sequestering internalized MHC-I molecules into TGN/endosomal compartments remains to be determined. Nonetheless, these findings suggest the PACS proteins mediate distinct steps within the signaling pathway—the trigger phase (PACS-2) and the sequestering phase (PACS-1). By three days post-infection, Nef switches to a stoichiometric mode of downregulation that prevents delivery of newly synthesized MHC-I molecules to the cell surface. The ability of 2c or PI-103 to prevent conversion from the signaling to stoichiometric mode suggests that signaling events directed by one or more of the kinases that form the multi-kinase complex may either result in post-translational modification of MHC-I, or may alter the activity of the membrane trafficking machinery that mediates the switch from the signaling to the stoichiometric mode. The precise mechanism controlling the switch between the signaling and stoichiometric modes warrants further investigation.

The relative contributions of the signaling and stoichiometric modes to Nef-induced MHC-I downregulation have been controversial, and discrepancies may have arisen from different experimental designs, choice of cell lines, and interpretation of negative results. For example, the signaling mode was initially dismissed as a result of differences in the efficiency by which Nef is able to impede cell surface delivery of MHC-I in T-cells versus HeLa cells (Kasper et al., 2003, Kasper et al., 2005). By contrast, we determined using parallel experiments that these differences instead result from the time post-infection at

which MHC-I transport is analyzed. During early times post-infection and continuing for 48 hours, Nef has no effect on the ER to cell surface transport of endogenous MHC-I molecules in HeLa, H9, and primary $CD4^+$ T-cells whereas by 72 hours Nef can block MHC-I transport (Figures 3.9 and 3.12 and (Blagoveshchenskaya et al., 2002, Hung et al., 2007)). This bimodal mechanism of Nef-mediated MHC-I downregulation does not appear to result from differences in Nef expression or in the antibodies used, suggesting the modes of Nef action may be temporally regulated. Second, the failure of PI3K inhibitors to block MHC-I downregulation in PTEN-deficient Jurkat, CEM, or U373 cells together with the confusion regarding regulation of PTEN activity in leukemic cell lines was used to assert that Nef mediates MHC-I downregulation by a PI3K-independent mechanism (Kasper et al., 2003, Larsen et al., 2004, Schaefer et al., 2008). However, reexpression of PTEN in CEM or U373 cells restored sensitivity of Nef-mediated MHC-I downregulation to 2c or PI3K inhibitors, whereas siRNA knockdown of PTEN in H9 T-cells rendered Nef-mediated MHC-I downregulation resistant to PI3K inhibitors (Figure 3.8 and (Hung et al., 2007)). Therefore, the determination that the mechanism of Nef-induced MHC-I downregulation in primary $CD4^+$ T-cells is phenocopied by H9 cells but not CEM cells underscores the importance of choice of cell lines used to model Nef action (Figure 3.8). Thus, the ability of PTEN-deficient CEM and U373 tumor cells to override the requirement for the SFK-ZAP-70/Syk-PI3K multi-kinase complex in triggering Nef action likely explains the confusion in the literature regarding the

importance of Nef sites in MHC-I downregulation (Kasper et al., 2003, Larsen et al., 2004, Casartelli et al., 2006, Noviello et al., 2008, Schaefer et al., 2008). For example, the assertion that the $AXXA_{75}$ mutation nonspecifically disrupts MHC-I downregulation in PTEN-null cells (Swann et al., 2001, Casartelli et al., 2006) conflicts with the ability of Nef_{AXXA}PI3K* to rescue MHC-I downregulation in H9 cells (Figure 3.7) and with the pharamacologic repression of MHC-I downregulation by treatment of primary $CD4^+$ T-cells with PI-103, which inhibits class I PI3K, or with 2c or D1, which block the Nef-SFK interaction ((Betzi et al., 2007, Hung et al., 2007, Hiyoshi et al., 2008, Emert-Sedlak et al., 2009) and Figures 3.1 and 3.4). Reliance on PTEN-deficient cell lines may not only have caused confusion in understanding the mechanism of MHC-I downregulation but may have also contributed to conflicting findings in HIV-1 research ranging from the signaling pathways that reactivate latent HIV-1 to the secretion of HIV-1 Tat (Bosque et al., 2009, Rayne et al., 2010). Third, the failure of a dominant negative dynamin mutant, which interferes with clathrin-dependent endocytosis, to block MHC-I downregulation was used to suggest that Nef does not direct MHC-I endocytosis (Swann et al., 2001). However, MHC-I is internalized by a clathrin/dynamin/AP-2-independent, ARF6-dependent pathway—both basally and in response to Nef (Le Gall et al., 2000, Blagoveshchenskaya et al., 2002, Caplan et al., 2002, Naslavsky et al., 2003, Hung et al., 2007, Chaudhry et al., 2008). Fourth, the ability of GST-MHC-I CD-$Nef_{LL/AA}$ to bind AP-1 µ1 subunit *in vitro* was used to assert that Nef does not require PACS-1 to downregulate MHC-

I *in vivo* (Noviello et al., 2008, Singh et al., 2009). However, GSTMHC-I CD-Nef$_{LL/AA}$ can also interact with PACS-1 (Figure 3.7), contradicting the assumption by Guatelli et al. that this bacterial fusion protein interacts exclusively with AP-1 (Singh et al., 2009). Instead, these protein capture data are consistent with the determination *in vivo* that PACS-1 mediates Nef-induced MHC-I downregulation subsequent to PI3K stimulation (Figure 3.7 and (Atkins et al., 2008); see also (Youker et al., 2009). Lastly, whereas Nef can induce rapid degradation of overexpressed MHC-I (Kasper et al., 2003, Roeth et al., 2004, Kasper et al., 2005, Schaefer et al., 2008), we observed no marked effect on the stability or ER-to-Golgi trafficking of endogenous MHC-I (Figures 3.9-10 and (Blagoveshchenskaya et al., 2002, Hung et al., 2007)). Thus, the extent to which overexpressed HLA-A2.1 is physiologically relevant to the mechanism underlying Nef-induced MHC-I downregulation remains unclear.

The determination that Nef downregulates MHC-I by the sequential use of the signaling mode followed by the stoichiometric mode raises the possibility that HIV-1 may adapt immune evasive strategies specific to the host cell activation state or reservoir type. Because the lifespan of activated CD4$^+$ T-cells infected with HIV-1 is less than two days (Stevenson, 2003), and Nef uses the signaling mode to downregulate MHC-I in CD4$^+$ T-cells for two days before converting to the stoichiometric mode (Figures 3.9 and 3.12), the physiological relevance of the stoichiometric pathway in activated CD4$^+$ T-cells remains uncertain. However, Nef also assembles the multi-kinase complex in cells of monocyte lineages, of

which macrophages produce a low but persistent level of virus that can last the duration of the cell's natural lifespan (Hung et al., 2007, Alexaki et al., 2008). Future studies on the immune evasive program directed by HIV-1 Nef will require membrane trafficking experiments in relevant cell lines to determine the relative contributions of the signaling and stoichiometric modes of Nef action. The physiological significance of Nef's bimodal MHC-I downregulation pathway in viral reservoirs can then be correlated to disease progression. Finally, the ability of 2c and other small molecules to repress multiple actions of Nef suggests the multi-kinase complex may be an attractive approach for HIV-1 therapeutics.

MATERIALS AND METHODS

Cells, Viruses, and Plasmids

293T, A7, BSC-40, HeLa-CD4$^+$, H9 CD4$^+$ T-cells, and CEM T-cells were cultured as described (Hung et al., 2007). Peripheral blood was obtained from healthy HLA-A*0201$^+$ volunteers by leukapheresis or venipuncture using protocols approved by the OHSU Institutional Review Board (protocols IRB00004039 and IRB00002251) or by the International Medical Center of Japan and the Kumamoto University Ethical Committee. Primary human CD4$^+$ T-cells were isolated as described (Hung et al., 2007) and cultured in RPMI 1640 containing 10% FBS and supplemented with IL-2 (50 U/ml; Sigma) and 1 µg/ml PHA (Sigma, St. Louis, MO) before infection. HIV-1^{NL4-3}, vaccinia virus (VV), and vaccinia recombinants expressing FLAG-tagged Nef (Nef/f, C-terminal epitope tag), Nef$_{AXXA}$/f, Nef$_{AXXA}$-PI3K*, Hck, Src, or ZAP-70, and HIV pseudotyped viruses NL4-3ΔG/P-EGFP (titer = 4.5 X 10^7 IFU/ml) and NL4-3ΔG/P-EGFP/ΔNef (titer = 2.1 X 10^7 IFU/ml) were grown and titered by marker expression as described (Blagoveshchenskaya et al., 2002, Hung et al., 2007). Adenoviruses expressing HA-tagged PACS-1 or PACS-2 were described previously (Blagoveshchenskaya et al., 2002, Simmen et al., 2005). Nef-eYFP, Nef$_{AXXA}$-eYFP and pPTEN were previously described (Hung et al., 2007) and pmax green fluorescent protein (GFP) was obtained from Dharmacon (Boulder, CO).

Inhibitors, siRNAs, qRT-PCR, and Kinase Assays

PI-103 (Calbiochem, San Diego, CA) and 2c (2,4-dihydroxy-5-(1-methoxy-2-methylpropyl)benzene-1,3-dialdehyde, (Kyowa Hakko Kirin Co., Tokyo, Japan) were used as indicated. 2c toxicity was determined by MTT (Invitrogen, Carlsbad, CA) according to manufacturer's instructions. Control (nonspecific) siRNA and siRNAs specific for Hck, Lyn, Src, PACS-1, PACS-2, or the μ1A subunit of AP-1 (Smartpool, Dharmacon) were nucleofected (Amaxa, Gaithersburg, MD) into cells according to manufacturer's instructions. RNA was purified from H9 cells nucleofected with siRNAs as indicated in figure legends using the RNeasy kit (Qiagen, Valencia, CA) according to manufacturer's instructions. cDNA was reverse transcribed from RNA using the random decamers from the RETROscript Kit (Ambion, Austin, TX) via manufacturer's instructions. Utilizing commercially available Hck, Lyn, and Src primers (Qiagen) and SYBR green qPCR reagent (SA-Biosciences, Frederick, MD), q-PCR was conducted on a StepOnePlus Real-time PCR system (Applied Biosciences, Foster City, CA). PI3K assays were performed as described (Atkins et al., 2008). *In vitro* Hck kinase assays were performed as described (Emert-Sedlak et al., 2009).

Flow Cytometry and Immunofluorescence Microscopy

For flow cytometry, cells were processed as described (Atkins et al., 2008, Hung et al., 2007) and stained using the following antibodies: anti-MHC-I

(W6/32), anti-HLA-A2 (BB7.2, BD, San Jose, CA), anti-CD4-APC (Biolegend, San Diego, CA), or anti-p24-FITC (Virostat, Portland, ME) as indicated in legends. PE-conjugated donkey anti-mouse IgG (Jackson IR, West Grove, PA) was used to stain MHC-I– and HLA-A2–positive cells. Isotype-matched antibodies (Serotec, Raleigh, NC) were used as negative controls. Samples were processed on a FACSCalibur (BD) as described (Atkins et al., 2008) and data analyzed using FCS express (De Novo Software, Los Angeles, CA). For immunofluorescence microscopy, cells were processed as indicated in legends and processed for immunofluorescence as described (Atkins et al., 2008). Confocal images were captured as described (Atkins et al., 2008) and colocalization of Nef-eYFP with Golgin-97 was quantified morphometrically using Imaris 7.0. A mask for each field of cells was generated based on the fluorescent signal of Golgin-97 and the percent colocalization of Golgin-97 with Nef-eYFP was determined and presented as the mean ± SD from at least 20 cells per condition.

Immunoprecipitation, Western Blot, and Antibody Uptake

Cells infected with the indicated VV recombinants were harvested as described (Atkins et al., 2008). Where indicated, cells were treated with the corresponding concentration of 2c before harvest. Flag-tagged Nef constructs were immunoprecipitated with mAb M2-agarose (Sigma), and associated proteins were detected by Western blot. The following antibodies were obtained

as indicated: mAb HA.11 (Covance, San Diego, CA); anti-Hck, anti-Lyn (Santa Cruz, Santa Cruz, CA); anti-p85, anti-Src, anti-ZAP-70 (Upstate, Bedford, MA); anti-phospho292ZAP-70 (BD); anti-Akt, anti-pAkt, anti-His6, anti-PTEN, anti-cleaved caspase-3 (Cell Signaling, Danvers, MA); anti-actin (Chemicon, Bedford, MA); anti-Nef #2949 (obtained through NIH AIDS Research and Reference Reagent Program), anti-MHC-I K455 (provided by K. Früh, OHSU), W6/32 and HC10 (provided by D. Johnson, OHSU); anti-AP-1 μ1A subunit (provided by L. Traub, University of Pittsburgh), AP-γ1 (Sigma), anti-PACS-1 (703), anti-PACS-2 (Atkins et al., 2008). Antibody uptake using mAb W6/32 was performed as described (Blagoveshchenskaya et al., 2002).

NMR Spectroscopy

The cDNA encoding consensus nef (obtained from the NIH AIDS Research and Reference Reagent Program) was His6-tagged, inserted into pET21 vector (EMD chemicals, San Diego, CA), and protein was expressed in Rosetta 2 (DE3) E. coli, cultured in modified minimal medium using $^{15}NH_4Cl$ as the sole nitrogen source, and induced with 0.4 mM isopropylthio-β-galactoside (IPTG) at 18°C for 16 hours. Soluble forms of His_6-tagged Nef proteins were purified over a Ni^{+2}-nitrilotriacetic acid (NTA) column (GE Healthcare, Uppsala, Sweden) and subsequent gel-filtration on a Superdex200 26/60 column (GE Healthcare) equilibrated with 25 mM sodium phosphate buffer (pH 7.5), 150 mM NaCl, 1 mM DTT, and 0.02% sodium azide. Two-dimensional (2D) ^{1}H-^{15}N

heteronuclear single quantum coherence (HSQC) experiments (Geoffrey Bodenhausen, 1980) were performed at 27°C on a Bruker Avance 700 MHz spectrometer equipped with a 5-mm, triple resonance, and z-axis gradient cryoprobe. The ^{1}H-^{15}N HSQC spectrum of free Nef was obtained using a 80-_Muniform 15N-labeled Nef sample in 10 mM HEPES, 10 mM DTT, 100 mM NaCl, and 5% (vol/vol) D2O (pH 8.0). A series of 1H-15N HSQC spectra were acquired to monitor chemical shift changes upon addition of aliquots of a 10 mM 2c stock solution, dissolved in DMSO, to the Nef sample. The Nef:2c molar ratios of the solutions were 1:0, 1:0.6, 1:1.75, 6.25, and 12.5. A control series of ^{1}H-^{15}N HSQC spectra were also obtained after adding the same amounts of DMSO without 2c to the free Nef sample. In this series, in contrast to the titration with the 2c solution, minimal spectral changes occurred (data not shown), confirming that the changes after addition of 2c were indeed caused by this organic molecule and not the solvent.

Transport Assay and Endo H Treatment

H9 cells were infected with Nef^{-} or Nef^{+} pseudotyped HIV-1^{NL4-3} viruses for 24, 48, or 72 hours. After infection, cells were subjected to pulse-chase/surface biotinylation as described (Blagoveshchenskaya et al., 2002). Briefly, to IP with HC10, cells were lysed in m-RIPA [1% Nonidet P-40 (NP-40), 1% sodium deoxycholate, 150 mM NaCl, 50 mM Tris-HCl (pH 8.0)] and then heated for 1 hour at 55°C to denature MHC-I proteins. To IP with BB7.2, cells were lysed in

PBS (pH 7.2) containing 1% NP-40. Bound MHC-I proteins were eluted from protein A sepharose beads (Sigma) by boiling in tris buffered saline (TBS), 5% sodium dodecyl sulfate (SDS), 2% NP-40, and 2% sodium deoxycholate. One-third of the eluate was used to assess total MHC-I while the rest was incubated with streptavidin agarose (Pierce, Rockford, IL) to capture biotinylated MHC-I. For Endo H treatment, MHC-I was eluted by boiling in 10 mM Tris-HCl (pH 7.4) containing 1% SDS, precipitated with acetone and resuspended in glycoprotein denaturation buffer (NEB, Ipswich, MA) and digested with 10 units of Endoglycosidase H for 1 hour at 37°C. Samples were separated by sodium dodecyl sulfate-polyacrylamide gel electrophoresis (SDS-PAGE) and processed using Amplify (GE Healthcare). Quantification was performed using NIH Image J.

Protein Interaction Assays

Plasmids expressing GST, GST-MHC-I CDNef$_{LL/AA}$ (provided by J. Guatelli, UCSD), His$_6$-Hck or GST-Nef (strain NL4-3), were transformed in BL21 E. coli and cultures were induced with 1 mM IPTG (Calbiochem) for 4 hours at 37°C. Bacterial pellets were resuspended in lysis buffer [50 mM Tris (pH 7.6), 1.5 mM ethylenediaminetetraacetic acid (EDTA), 100 mM NaCl, 0.5% Triton X-100, 0.1 mM eithiothreitol (DTT), 10 mM MgCl2] containing protease inhibitors (0.5 mM phenylmethanesulfonylfluoride (PMSF) and 0.1 M each of aprotinin, E-64, and leupeptin), lysed using a French Press (Aminco, Rockville, MD) and incubated with GST-sepharose (GE Healthcare). For the interaction with GST-

MHC-I CDNef$_{LL/AA}$, A7 cells were lysed in 50 mM Tris-HCl (pH 8.0), 1% Triton X-100, 5 mM EDTA, 150 mM NaCl, 10 mM MgCl2 with protease inhibitors (0.5 mM PMSF and 0.1 M each of aprotinin, E-64, and leupeptin). A7 lysates were added to GST-Sepharose bound to the proteins of interest overnight at 4°C. The resin was incubated or not with 20 μM 2c for one hour, washed three times in lysis buffer and once in 50 mM Tris (pH 8.0), and resuspended in SDS-PAGE sample buffer. For the His$_6$-Hck interaction with GST-Nef, the proteins were mixed at a 2:1 ratio (Hck:Nef) for 30 minutes at 4°C in binding buffer [0.1% NP-40, 0.1 mM EDTA, 20 mM Tris (pH 7.9), 150 mM NaCl] containing the indicated concentrations of 2c. After incubation, GST-Sepharose was added and subsequently washed three times in binding buffer and resuspended in SDS-PAGE sample buffer.

ACKNOWLEDGMENTS

The authors thank K. Früh, A. Hill, and R. Papoian for helpful discussions and critically reading the manuscript, N. Morris, H. Krishnamurthy, A. Ghering, and A. Weinberg for advice, M. Delk for NMR instrumental support, and J. Guatelli, D. Johnson, J. Douglas, L. Traub, and the National Institutes of Health (NIH) AIDS Research and Reference Reagent Program for reagents. This work was supported by CIHR fellowship HFE-87760 (to J.D.D.), NRSA T32 GM71338 (to K.M.A.), Ruth L. Kirschstein NRSA AI14149 (to L.E.S.), by the Global COE program Global Education and Research Center Aiming at the control of AIDS (to M.T. and S.S.), The Pittsburgh Center for HIV Protein Interactions via NIH grant P50GM082251 (to A.M.G.), CA81398 and AI57083 (to T.E.S.), GM060170 and AI071798 (to E.B.), and GM82251 and DK37274 (to G.T.).

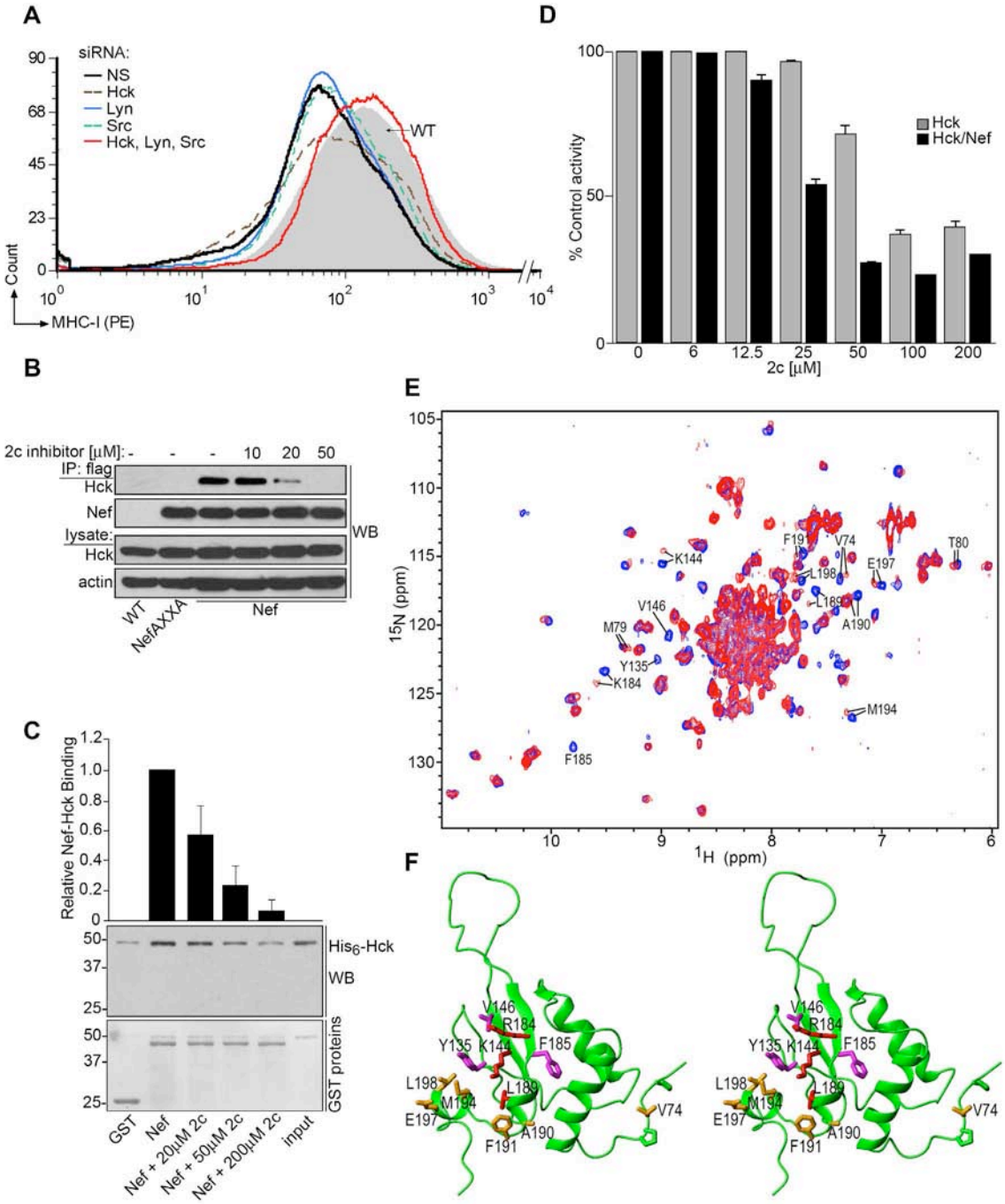

Figure 3.1. 2c interferes with Nef-SFK binding.

(A) H9 CD4+ T-cells were nucleofected (Amaxa) on days 1 and 3 with pmaxGFP and nonspecific siRNA or siRNAs that target Hck, Lyn, or Src alone or in

combination. On day 4 cells were infected with vaccinia (VV):WT (gray filled) or VV:Nef (lines, unfilled) (multiplicity of infection (moi) = 10, 8 h), and analyzed by flow cytometry using mAb W6/32 as described in experimental procedures. Mean fluorescence intensity (MFI): NS siRNA (WT = 167, Nef = 99.5); Nef + Hck siRNA = 120; + Lyn siRNA = 103; + Src siRNA = 117; + Hck, Lyn, Src = 169. (B) H9 cells were coinfected with VV:WT, VV:Nef/f or NefAXXA/f (moi = 10, 8 h) and VV:Hck (moi = 2, 8 h) and treated with 10, 20, or 50 μM 2c for 4hoursbefore harvest. Nef/f proteins were immunoprecipitated, and coprecipitating Hck was detected by western blot. (C) GST-Nef was incubated with His_6-Hck and treated with increasing concentrations of 2c. GST-Nef was captured, and bound His_6-Hck was quantified using NIH Image J. Accordingly, nonspecific binding of GST to His_6-Hck was subtracted and values were normalized to the binding of GST-Nef to His_6-Hck in the absence of 2c. Each condition was assayed in triplicate, and results are presented as the mean ± SD. (D) Hck alone (gray bars) or Hck plus Nef (black bars) were treated with increasing concentrations of 2c. The resulting Hck enzyme activity was measured using a fluorometric assay and expressed relative to 100% control activity. Each condition was assayed in quadruplicate and results are presented as the mean ± SD. (E) Superposition of ^{1}H-^{15}N HSQC spectra of Nef in the absence (blue) and presence (red) of 2c. The ^{1}H-^{15}N HSQC spectra were recorded on 80 μM uniform ^{15}N-labeled Nef samples at 27°C in the absence (blue) and presence (red) of 1 mM 2c (1:12.5 M ratio of Nef to 2c). All assignable amide resonances (J. Jung, I.-J.L. Byeon, J. Ahn, and A.M.

Gronenborn, unpublished data) that exhibit chemical shift changes >0.06 ppm are labeled with residue name and number. The resonances of Y_{135}, V_{146}, and F_{185} are labeled only on the free Nef spectrum because the identification of the bound resonances was not straightforward either due to very large shift changes or severe line broadening beyond detection. The resonances of M_{79} ($\Delta\delta$ = 0.041ppm) and T_{80} ($\Delta\delta$ = 0.025ppm), which are located immediately after the $P_{72}XXP_{75}$ motif, are also labeled. Concentrations of 2c as low as 48 μM, representing a 1:0.6 M ratio of Nef to 2c, revealed chemical shift changes between ^{15}N-Nef and 2c. (F) Structural mapping of the chemical shift changes in the ^{1}H-^{15}N HSQC spectrum of Nef induced by 2c onto the Nef NMR structure (PDB ID: 2NEF, see (Grzesiek et al., 1997)). The ^{1}H-^{15}N-combined chemical shift changes were calculated using $\sqrt{\Delta\delta_{HN}{}^{2} + (\Delta\delta_{N} \times 0.1)^{2}}$, with $\Delta\delta_{HN}$ and $\Delta\delta_{N}$ the ^{1}HN and ^{15}N chemical shift differences, respectively, between the free and 2c-bound Nef protein spectrum. On a stereoview of the structure in ribbon representation, sidechains of residues whose amide resonances exhibit significant changes are shown in stick representation and color coded according to the size of the change: orange; 0.06–0.1 ppm, and red; >0.1 ppm. Residues whose ^{1}H-^{15}N HSQC amide resonances are only detectable/assignable in free Nef are colored in magenta and the sidechains of the two prolines in the $P_{72}XXP_{75}$ region are shown in green.

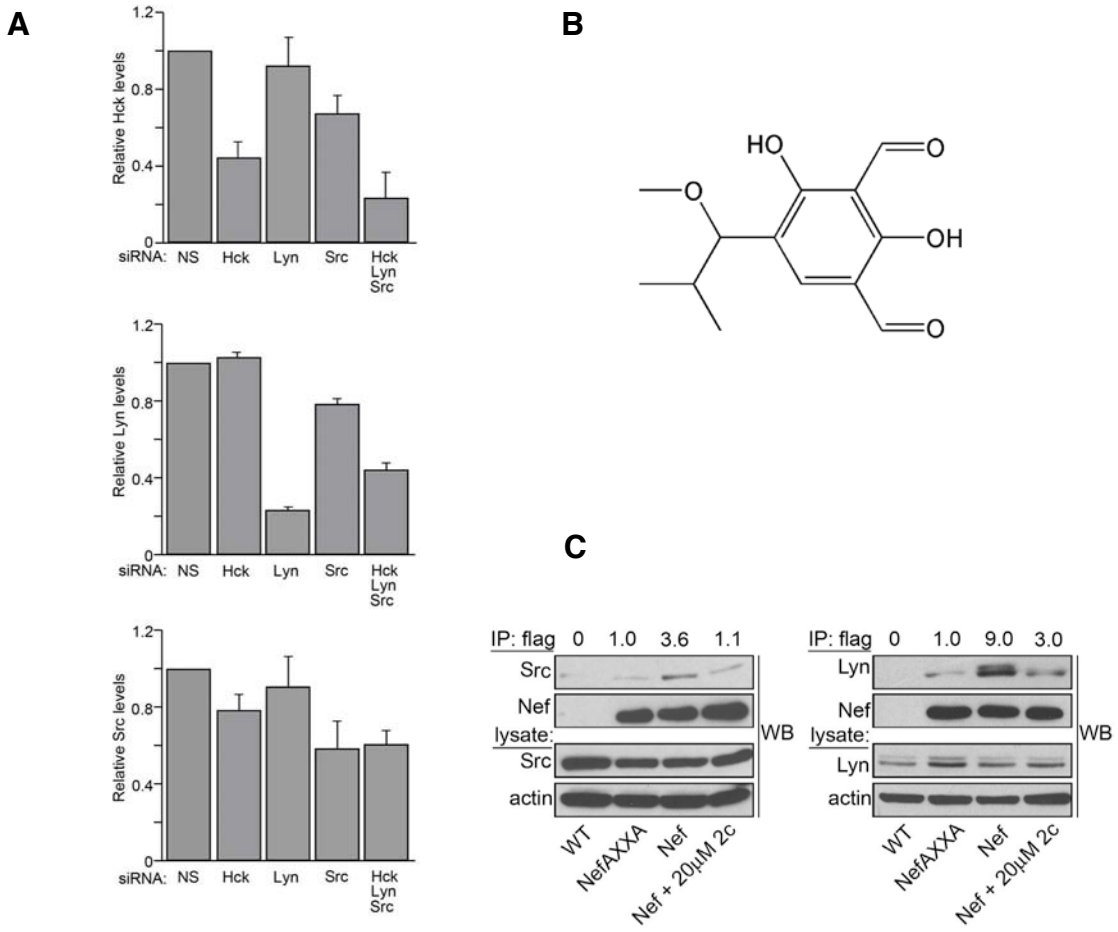

Figure 3.2. The interaction between Nef and SKFs is sensitive to 2c.

(A) H9 CD4$^+$ T-cells were nucleofected (Amaxa) on days 1 and 3 with pmaxGFP and nonspecific siRNA or siRNAs that target Hck, Lyn, or Src alone or in combination. On day 4 cells were infected with VV:WT (gray filled) or VV:Nef (lines, unfilled) (moi = 10, 8 h), and analyzed by qRT-PCR for relative SFK knockdown as described in experimental procedures. (B) Chemical structure of compound 2c (2,4-dihydroxy-5-(1-methoxy-2 methylpropyl)benzene-1,3-dialdehyde. (C) Left: H9 cells were co-infected with VV:WT or VV:Nef/f (moi = 6,

8hr) and VV:Src (moi = 4, 8hr) and treated or not with 20 μM 2c for 4 hours prior to harvest. Nef/f was immunoprecipitated and co-precipitating Src was detected by western blot. Right: H9 cells were infected with VV:WT or VV:Nef/f (moi = 10, 8hr) and treated or not with 20μM 2c for 4 hours prior to harvest. Nef/f was immunoprecipitated and co-precipitating Lyn was detected by western blot. The amount of associated SFK was quantified with Image J and presented numerically as the fold-change.

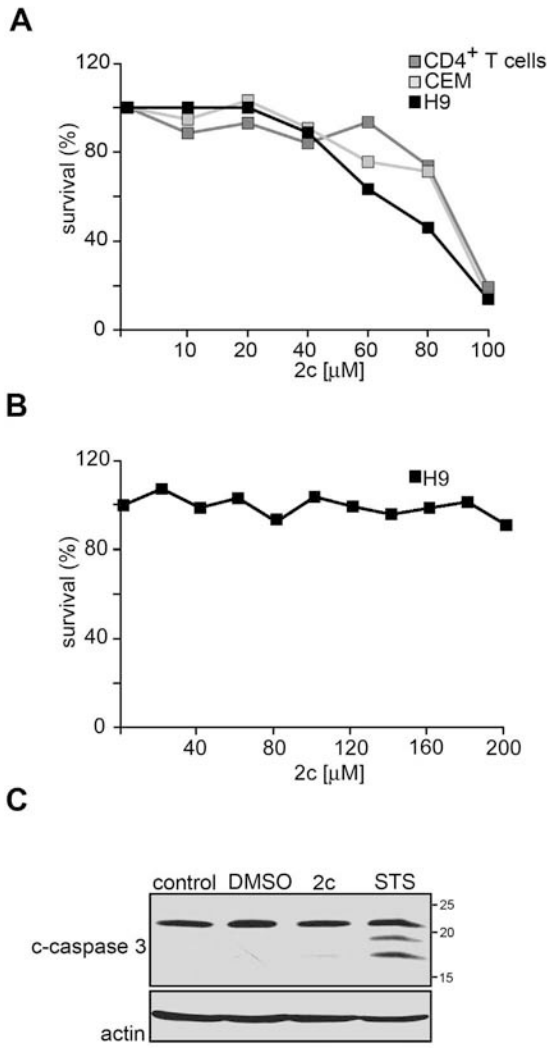

Figure 3.3. Analysis of compound 2c cytotoxicity.

(A) Parallel cultures of primary CD4+ T-cells, H9 cells or CEM cells were cultured in Phenol Red-free RPMI in the absence (0) or presence of 10, 20, 40, 60, 80 or 100 µM 2c. After 48 hours, cell viability was measured by MTT (Invitrogen) according to the manufacturer's instructions. MTT assay readings were normalized to 100% survival. (B) H9 cells were cultured in the absence (0) or

presence of 40, 80, 120, 160, or 200 μM 2c for 4 hours and cell viability was measured by MTT as described above. (C) H9 cells were treated or not with DMSO, 100 μM 2c, or 1.2 μM STS (staurosporine, positive control) for 4 hours and cleaved caspase-3 was detected by western blot.

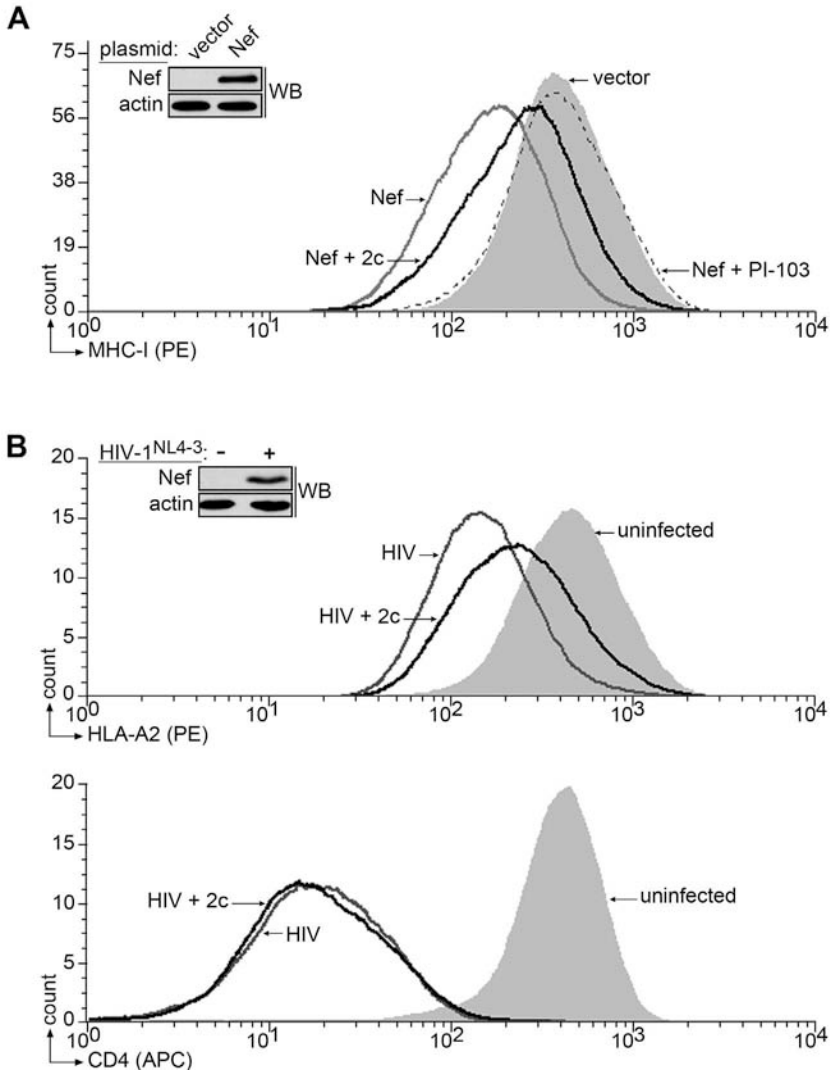

Figure 3.4. 2c represses HIV-1-induced downregulation of MHC-I but not CD4.

(A) H9 cells expressing eYFP (vector) or Nef-eYFP (Nef) for 24 hours were treated or not with 20 µM 2c (Nef + 2c) or 5 µM of the class I PI3K inhibitor, PI-103 (Nef + PI-103) for another 16 hours. At 40 hours, cultures were analyzed by flow cytometry using W6/32. MFI: vector = 479, Nef = 208, Nef + 2c = 312,

Nef + PI-103 = 444. Inset: western blot showing expression of Nef-eYFP and actin. (B) Parallel cultures of primary $CD4^+$ T cells were infected with $HIV\text{-}1^{NL4\text{-}3}$ and treated or not with 20 μM 2c at days 5 and 7 post-infection. At 8 days post-infection the cells were stained with p24-FITC, BB7.2, and CD4-APC and then analyzed for downregulation of HLA-A2 (top) and CD4 (bottom) by flow cytometry as described in Methods. MHC-I MFI: uninfected = 518, HIV = 193, HIV + 2c = 301. CD4 MFI: uninfected = 413, HIV = 25.1, HIV + 2c = 25.2. Inset: western blot showing expression of Nef and actin.

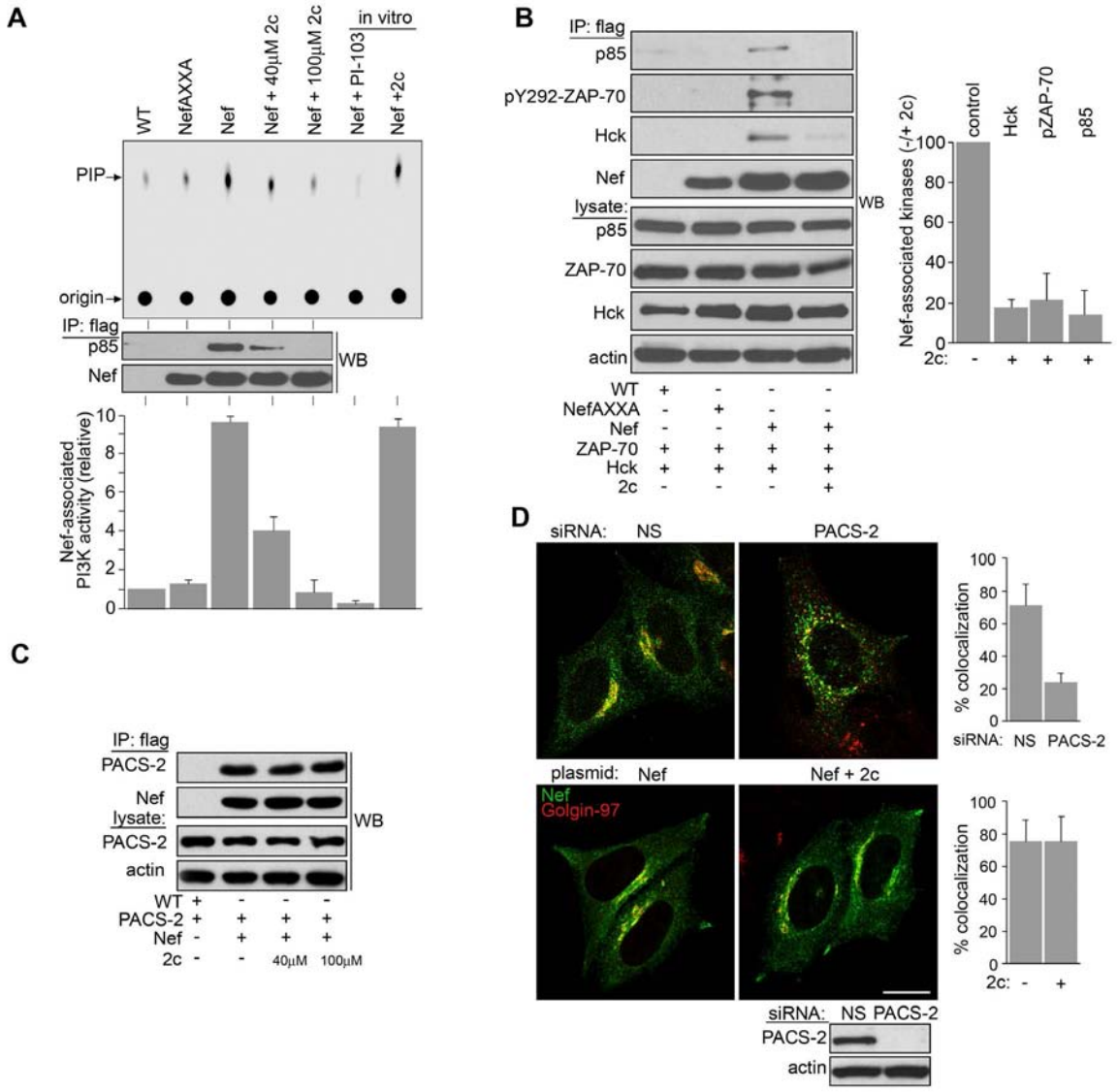

Figure 3.5. 2c blocks the ability of Nef to assemble the multi-kinase complex.

(A) H9 cells were infected with VV:WT, VV:Nef$_{AXXA}$/f or VV:Nef/f (moi = 10, 8 hours) and treated with 40 or 100 μM 2c for 4 hours (which showed no toxicity in this time, Figures 3.3B-C). Nef/f was immunoprecipitated and Nef-associated class I PI3K p85 regulatory subunit was detected by western blot and associated

PI3K activity was measured using an *in vitro* lipid kinase assay as described in Methods. As controls, 40 μM 2c and 1 μM PI-103 were incubated with the eluted fraction for 10 min prior to kinase assay (*in vitro* samples). Each assay was measured in triplicate and results are presented as the mean ± S.D. (B) Left: H9 cells were co-infected with VV:WT, VV:Nef_{AXXA}/f or VV:Nef/f (moi = 6, 8hr) and VV:ZAP70 (moi = 4, 8 hours). Nef/f was immunoprecipitated and co-precipitating Hck, phospho-ZAP-70 and p85 were detected by western blot. Right: The amount of each Nef-associated kinase was quantified with Image J and presented numerically as the relative amount of Nef-associated kinase +/- 20 μM 2c. Error bars represent the mean ± S.D. from 3 independent experiments. (C) H9 cells were co-infected with VV:Nef/f (moi = 6, 8hr) and VV:PACS-2 (moi = 4, 8hr) and treated with 40 or 100 μM 2c for 4 hours prior to harvest. Nef/f was immunoprecipitated and co-precipitating PACS-2 was detected by western blot. (D) Upper: HeLa cells expressing Nef-eYFP together with a control siRNA (NS) or PACS-2 siRNA (western blot of siRNA knockdown shown at bottom). Lower: HeLa cells expressing Nef-eYFP were treated with 20 μM 2c for 16 hours. Cells were stained with anti-Golgin 97 (red) and visualized by confocal microscopy (scale bar, 10 μm). Morphometric analysis was performed as described in Methods. Error bars are presented as the mean ± S.D. from at least 20 cells per condition and 3 independent experiments.

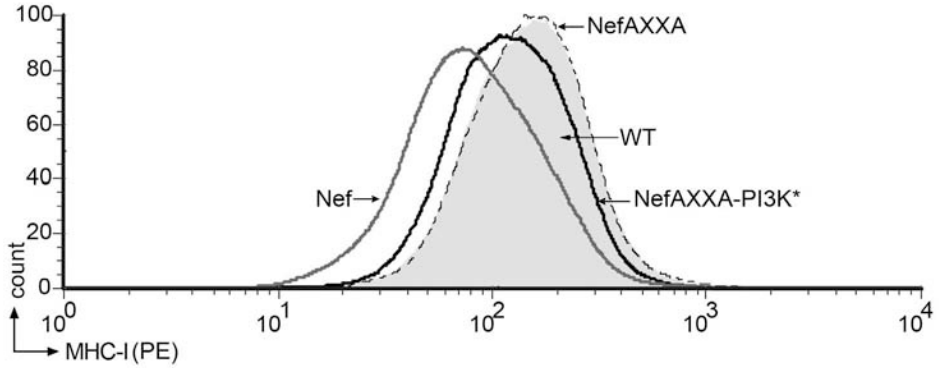

Figure 3.6. The Nef_{AXXA}-PI3K* chimera can override the requirement for assembly of the SFK-ZAP-70-PI3K complex.

H9 cells were infected with VV:WT, Nef_{AXXA}/f, VV:Nef/f, or Nef_{AXXA}-PI3K* (moi = 10, 8 hours) and analyzed for downregulation of MHC-I as described in Methods. MFI: WT = 174, Nef_{AXXA} = 179, Nef = 103, Nef_{AXXA}-PI3K* = 144).

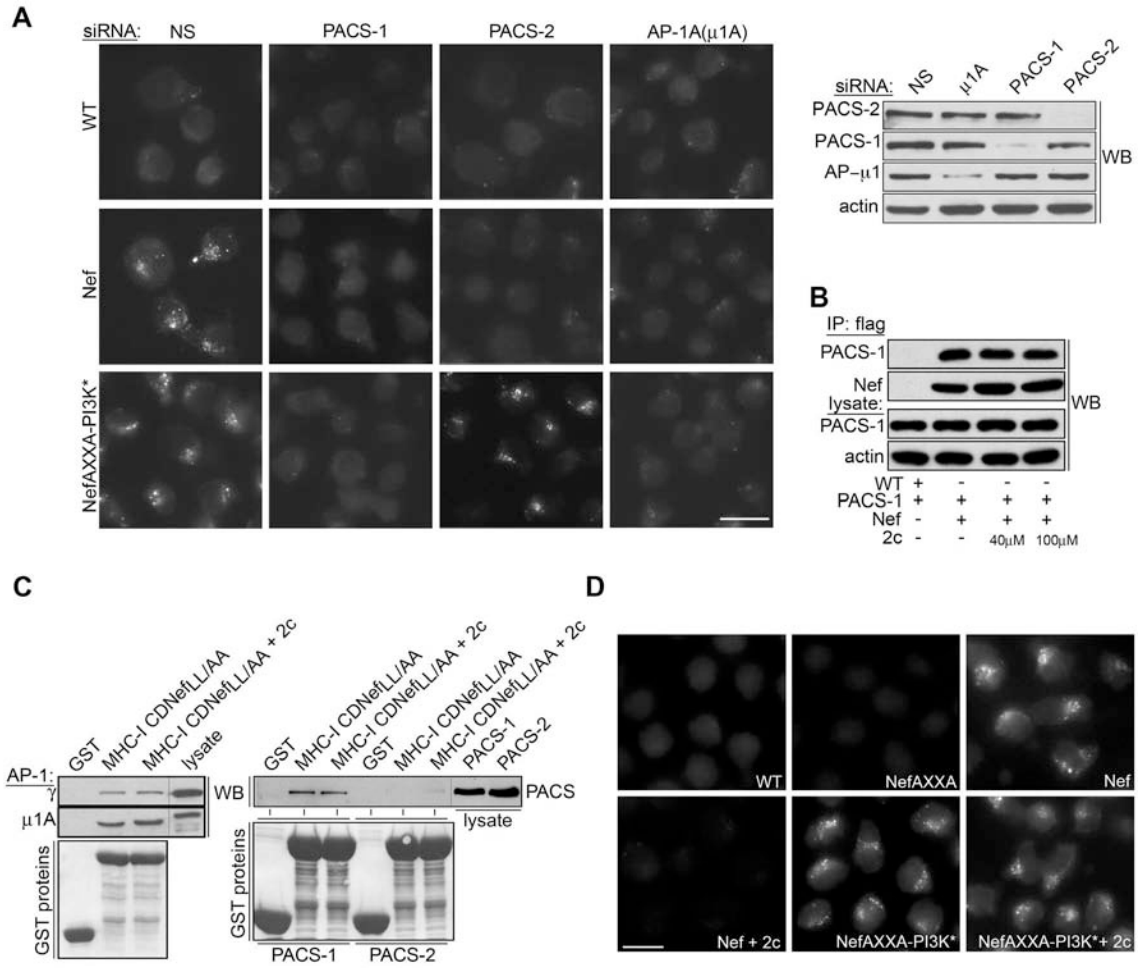

Figure 3.7. PACS-1 and AP-1 are required downstream of the 2c-sensitive multi-kinase complex.

(A) Left: H9 cells were nucleofected with pmaxGFP together with a control siRNA (NS) or siRNAs specific for PACS-1, PACS-2 or μ1A. After 48 hours, cells were infected with VV:WT, VV:Nef or VV:Nef_{AXXA}-P13K* (moi = 10, 5 hours). Cells were incubated with W6/32 (3 μg/ml) for 30 min, chased for an additional 30 min then incubated with 0.5% acetic acid (pH 3.0) in 0.5M NaCl to remove surface antibody, fixed, and processed for immunofluorescence microscopy. Scale bar,

10 µm. Right: A portion of the cells from left were analyzed by western blot for extent of siRNA knockdown (B) H9 cells were co-infected with VV:Nef/f (moi = 6, 8hr) and VV:PACS-1 (moi = 4, 8hr) and treated with 40 or 100 µM 2c for 4 hours prior to harvest. Nef/f was immunoprecipitated and co-precipitating PACS-1 was analyzed by western blot. (C) Left: GST-MHC-I CDNef$_{LL/AA}$ or GST was mixed with A7 cell lysate, treated with 20 µM 2c and captured g or 1µA subunits of AP-1 detected by western blot. Right: Lysates from A7 cells expressing HA-tagged PACS-1 or PACS-2 were incubated with GST-MHC-I CDNef$_{LL/AA}$ or GST, treated with 20 µM 2c and bound PACS proteins detected by western blot. (D) H9 cells were treated or not with 20µM 2c for 18 hours and then infected with VV:WT, VV:Nef, VV:Nef$_{AXXA}$ or VV:Nef$_{AXXA}$-P13K* (moi = 10, 5 hours). Cells were incubated with W6/32 (3 µg/ml) for 30 min and then chased for an additional 30 min and processed for immunofluorescence microscopy as described in the legend to panel A. Scale bar, 10 µm.

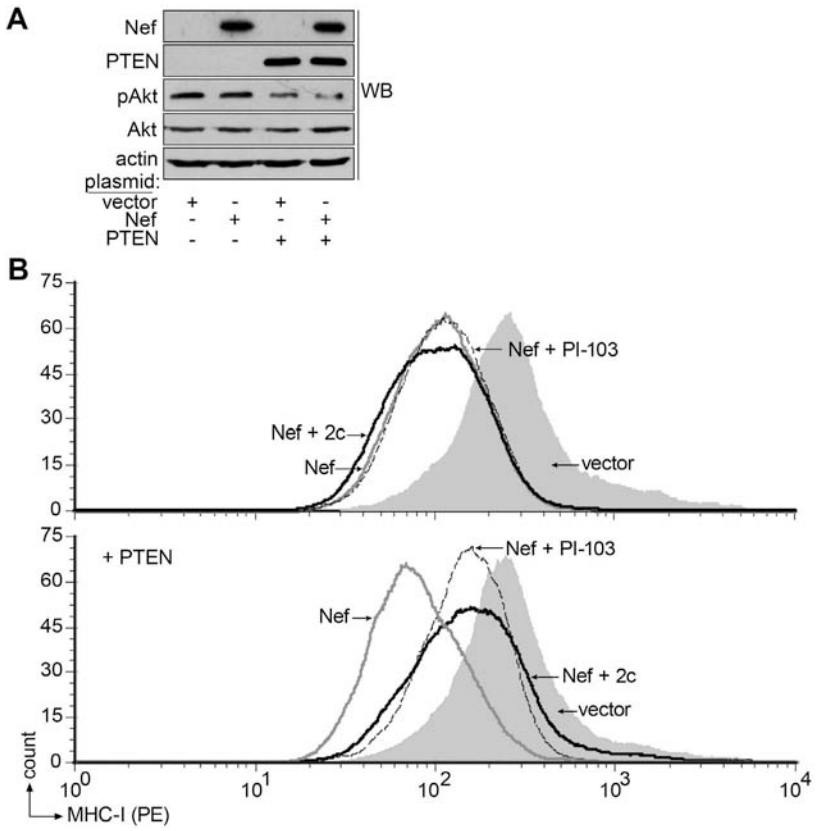

Figure 3.8. CEM cells do not model primary CD4⁺ T-cells in Nef action.

(A) Western blot analysis of PI3K-dysregulated CEM cells rescued or not for PTEN. (B) Top: CEM cells expressing eYFP (vector) or Nef-eYFP (Nef) were treated or not with 20 μM 2c (Nef + 2c) for 16 hours prior to analysis or 1 μM PI-103 (Nef + PI-103) for 3 hours prior to analysis in media containing 0.5 mM β-mercaptoethanol. Cells were analyzed by flow cytometry using W6/32 as described in Methods. MFI: vector = 425, Nef = 125, Nef + 2c = 123, Nef + PI-103 = 128. Bottom: CEM cells expressing PTEN with either eYFP (vector) or Nef-eYFP (Nef) were processed as described above. MFI: vector = 384, Nef = 94.6, Nef + 2c = 232, Nef + PI-103 = 162.

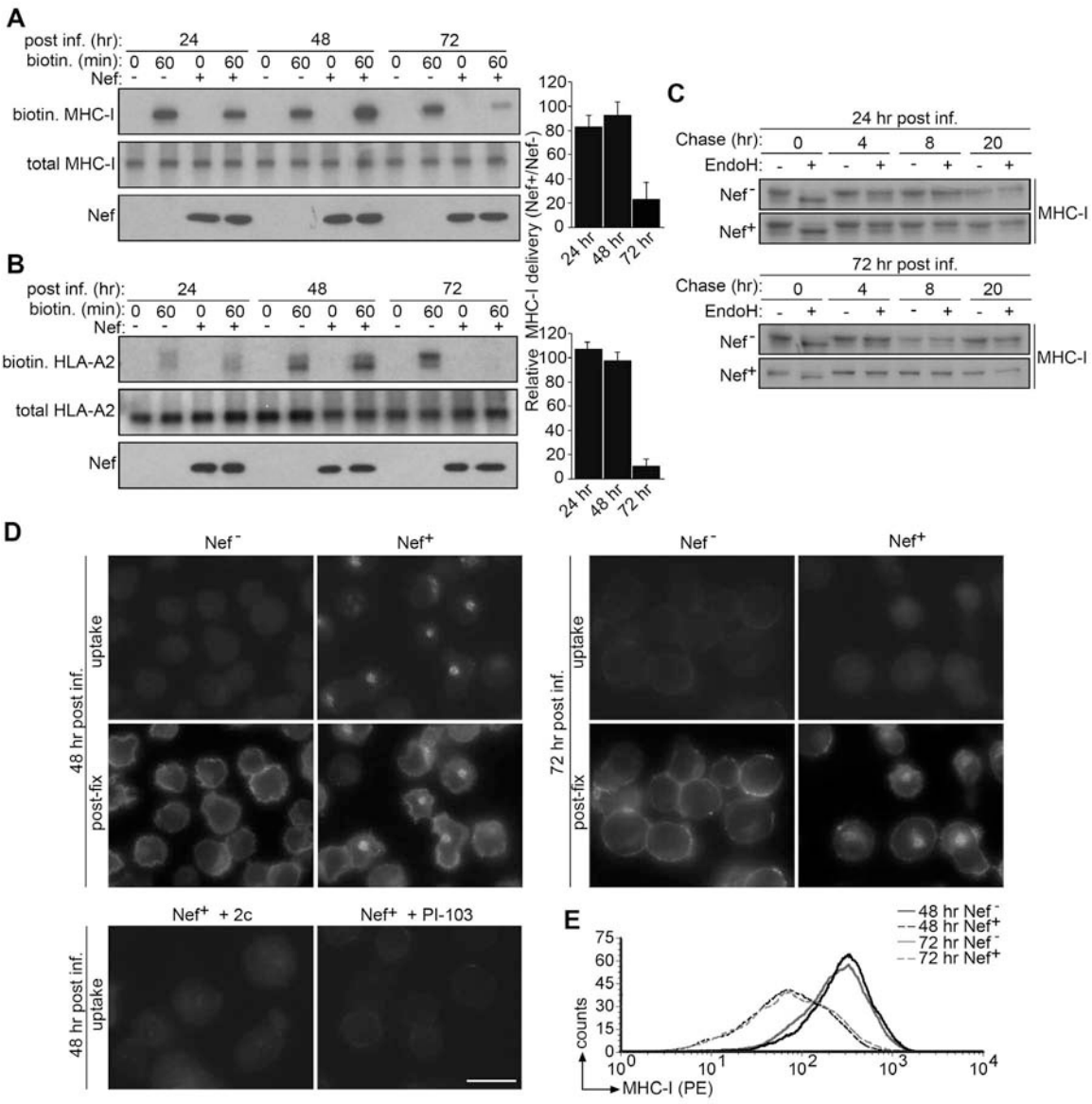

Figure 3.9. Nef-induced MHC-I downregulation switches from a signaling to a stoichiometric mechanism.

(A) H9 cells infected with Nef$^-$ or Nef$^+$ pseudotyped HIV-1^{NL4-3} viruses (moi = 2.3) for 24, 48 or 72 hours and subjected to pulse-chase/surface biotinylation using HC10 associated MHC-I and quantified as described in Methods. Error bars

represent the mean ± S.D. from 3 independent experiments. Cell viability was greater than 95% at each time point as measured by trypan blue exclusion and greater than 90% of the cells were infected with each virus as determined by GFP staining. (B) Primary $CD4^+$ T cells were processed and quantified as in panel A except using BB7.2 to IP native MHC-I. (C) H9 cells were infected with Nef^- or Nef^+ pseudotyped HIV-1^{NL4-3} viruses for 24 or 72 hours, MHC-I was immunoprecipitated with mAb HC10 as in A and then digested or not with Endo H as described in Methods. (D) H9 cells were infected with Nef^- or Nef^+ pseudotyped HIV-1^{NL4-3} viruses for 48 or 72 hours and then treated or not with PI-103 (5 μM) or 2c (20 μM) for 16 hours. Cells were incubated with W6/32 (3 μg/ml) for 30 min and then chased and processed for immunofluorescence microscopy as described in the legend to Figure 3.7A. Post-fix: Total MHC-I was detected post-fixation by staining the cells with K455. Scale bar, 10 μm. (E) H9 cells were infected with Nef^- or Nef^+ pseudotyped HIV-1^{NL4-3} viruses for 48 or 72 hours and analyzed for downregulation of MHC-I as described in Methods. MFI: 48 hours Nef^- = 341, 48 hours Nef^+ = 110, 72 hours Nef^- = 302, 72 hours Nef^+ = 125.

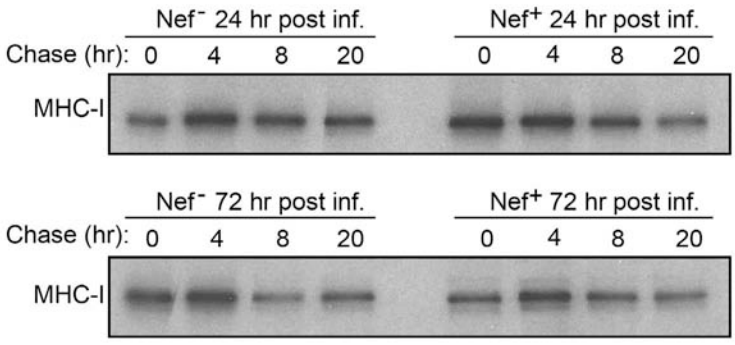

Figure 3.10. Nef does not markedly increase degradation of endogenous MHC-I.

H9 cells were infected with Nef^{-} or Nef^{+} pseudotyped HIV-1^{NL4-3} viruses for 24 hours (top) or 72 hours (bottom) and then pulse-labeled for 15 min with [^{35}S]Met/ Cys and chased in complete media for 0, 4, 8 or 20 hours. Cells were lysed and MHC-I was immunoprecipitated with HC10 and analyzed by fluorography as described in Methods.

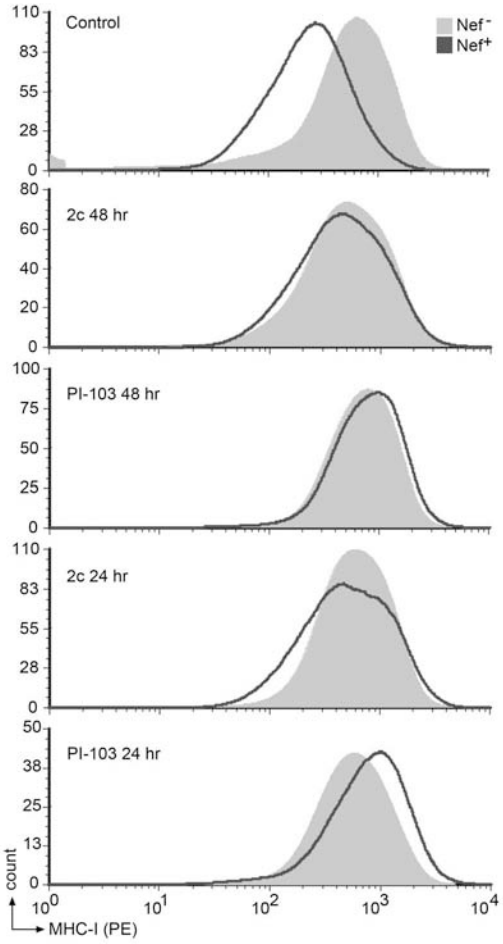

Figure 3.11. Multi-kinase complex inhibition at various time points during the signaling mode blocks MHC-I downregulation.

H9 cells were infected with Nef^{-} or Nef^{+} pseudotyped HIV-1^{NL4-3} for a total of 72 hours and either left untreated (control) or pre-treated with 20 µM 2c or 5 µM PI-103 for 48 hours (2c 48 hr, PI-103 48 hr) or 24 hours (2c 24 hr, PI-103 24 hr) prior to MHC-I downregulation analysis at 72 hours post-infection. MFI: control (Nef^{-} = 685, Nef^{+} = 306), 2c 48 hr (Nef^{-} = 632, Nef^{+} = 631), PI-103 (Nef^{-} = 825, Nef^{+} = 935), 2c 24 hr (Nef^{-} = 723, Nef^{+} = 717), PI-103 (Nef^{-} = 700, Nef^{+} = 954).

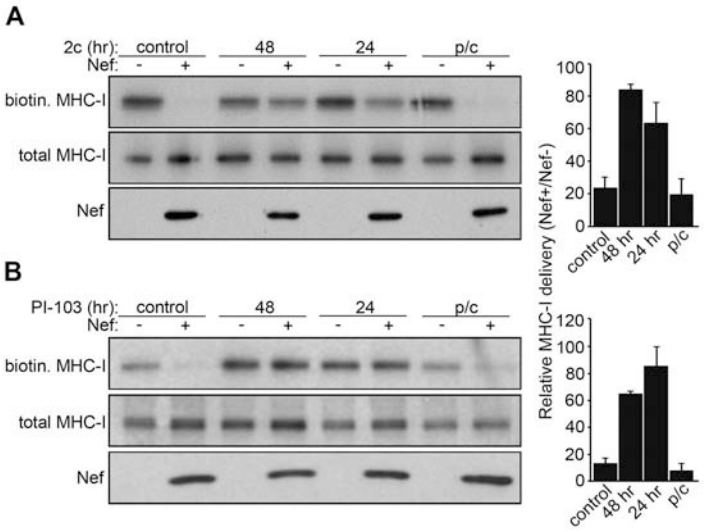

Figure 3.12. The PI3K signaling pathway is required for stoichiometric inhibition of MHC-I.

(A) H9 cells were infected with Nef^- or Nef^+ pseudotyped HIV-1^{NL4-3} viruses for a total of 72 hours and either left untreated (control) or pre-treated with 20 μM 2c for 48 hours (2c 48 hr) or 24 hours (2c 24 hr) prior to analysis at 72 hours post-infection. The cells were then subjected to pulse-chase/surface biotinylation as described in Methods. The amount of HC10 associated MHC-I delivered to the cell surface was quantified as described in Methods. Error bars are presented as the mean ± S.D. from 3 independent experiments. (B) H9 cells were infected as above and left untreated (control) or pre-treated with 5 μM PI-103 for 48 hours (PI-103 48 hr) or 24 hours (PI-103 24 hr) prior to analysis at 72 hours post-infection and then processed as in panel A. The amount of MHC-I delivered to the cell surface was quantified as described in Methods. Error bars are presented as the mean ± S.D. from 3 independent experiments. (p/c), cells treated with 20 μM 2c (A) or 10 μM PI-103 (B) during the pulse-chase only.

CHAPTER 4. DISCUSSION

CHAPTER 4. DISCUSSION

4.1 Summary

The results presented in Part I of this dissertation provide evidence that Nef directs a regulated program to downregulate MHC-I consisting of the sequential use of the signaling and stoichiometric modes of action. During the first two days after infection, Nef uses the signaling mode to downregulate MHC-I. This mode requires the PACS-2-dependent binding of Nef to a TGN-localized SFK that Nef can directly activate to assemble a multi-kinase complex that triggers downregulation of cell-surface MHC-I in $CD4^+$ T-cells. Indeed, chemical disruption of the Nef-SFK interaction with the small molecule inhibitor 2c blocks assembly of the multi-kinase complex and represses HIV-1–mediated MHC-I downregulation in primary $CD4^+$ T-cells. 2c did not interfere with the PACS-2–dependent trafficking of Nef required for the Nef-SFK interaction or the AP-1 and PACS-1–dependent sequestering of internalized MHC-I, suggesting the inhibitor specifically interfered with the Nef-SFK interaction required for assembling the multi-kinase complex and triggering MHC-I downregulation. By three days post-infection, Nef switches to the stoichiometric mode that prevents delivery of newly synthesized MHC-I to the cell surface. Pharmacologic inhibition of the multi-kinase cascade disrupts the temporally controlled block in MHC-I transport during the stoichiometric mode, suggesting the Nef-directed signaling and stoichiometric modes are causally linked.

4.2 Controversies in MHC-I downregulation

There has been divergence regarding the relative significance of the signaling and stoichiometric modes in Nef-mediated MHC-I downregulation. These contradictions have stemmed from different experimental paradigms, including analysis of endogenous versus overexpression of HLA-A2 as well as the length of infection; choice of cell lines, such as those that may or may not be sensitive to PI3K stimulation or inhibition; as well as the interpretation of negative results (Chapter 3 and Kasper et al., 2005).

Early experiments suggested that endocytosis was not a key determinant of Nef-induced MHC-I downregulation due to the differences in efficiency by which Nef blocks transport of MHC-I in T-cells versus HeLa cells, suggesting that T-cells are more active at supporting Nef-mediated HLA-A2 downregulation that HeLa cells (Kasper et al., 2003, Kasper et al., 2005). However, the studies in Chapter 3 demonstrate that, in fact, these discrepancies result from the time post-infection at which MHC-I transport is analyzed. Indeed, during early times post-infection and up to 48 hours, Nef has no effect on the ER to cell surface delivery of endogenous MHC-I molecules in H9 and primary $CD4^+$ T-cells. However, by 72 hours, Nef switches to a stoichiometric mode of downregulation that prevents delivery of newly synthesized MHC-I molecules to the cell surface. The ability of the Nef-SFK inhibitor 2c or the PI3K inhibitor PI-103 to prevent conversion from the signaling to stoichiometric mode suggests the modes of Nef

action are temporally regulated. However, the precise mechanism controlling the switch between the signaling and stoichiometric modes warrants further investigation. Therefore, in future studies it will be important to elucidate the mechanism directing the switch between the signaling and stoichiometric modes. In addition, it will be important to understand if the degree of replication or Nef expression correlates with the temporal nature of the switch, by analyzing whether the switch occurs at earlier or later times in different cell types or following infection from different HIV isolates that may support a greater or lesser degree of viral replication and/or Nef expression.

Previous studies have suggested that Nef-mediated MHC-I downregulation occurs in a PI3K-independent manner, as these studies demonstrate a failure of PI3K inhibitors to block MHC-I downregulation in various cell lines lacking the PIP_3 phosphatase PTEN, including Jurkat, CEM, or U373 cells (Kasper et al., 2003, Larsen et al., 2004, Schaefer et al., 2008). Indeed, dysregulation of the tumor suppressor PTEN is not uncommon in various cancers, therefore caution should be used when analyzing PI3K-dependent pathways in cell lines lacking the PIP_3 phosphatase PTEN, as the inordinately high levels of PIP_3 confer constitutive activation of PI3K signaling, thereby confounding interpretation of these results. Indeed, we demonstrate that re-expression of PTEN in CEM or U373 cells restores sensitivity of Nef-mediated MHC-I downregulation to PI3K inhibition (Chapter 3 and (Hung et al., 2007)). While conversely, siRNA knockdown of PTEN renders MHC-I downregulation in

H9 T-cells resistant to PI3K inhibition (Chapter 3 and (Hung et al., 2007)). Moreover, the determination that the signaling mechanism of Nef-induced MHC-I downregulation observed in primary $CD4^+$ T-cells is phenocopied by H9 cells but not CEM cells illustrates that choice of cell line is critical for analyzing Nef action. Therefore, the ability of PTEN-deficient CEM and U373 tumor cells to override the requirement for the multi-kinase complex via constitutive activation of PI3K explains the contradictory data in the literature regarding the relative significance of the Nef-SFK interaction and the activation of PI3K (Kasper et al., 2003, Larsen et al., 2004, Casartelli et al., 2006, Noviello et al., 2008, Schaefer et al., 2008).

The signaling mode requires the PACS-2-dependent, Nef-assembled SFK-ZAP-70-PI3K multi-kinase complex to trigger downregulation of cell-surface MHC-I molecules (Atkins et al., 2008, Hung et al., 2007). The internalized molecules are then sequestered into perinuclear compartments by a Nef M_{20}-, AP-1–, and PACS-1–dependent process (Chapter 3 and (Blagoveshchenskaya et al., 2002, Chaudhry et al., 2008). Thus, while both PACS-2 and PACS-1 are required for MHC-I downregulation, their roles in Nef action are distinct and sequential. Indeed, PACS-2 is required for the ability of Nef to traffic from early endosomes to the perinuclear region, while PACS-1 is required downstream of PI3K activation to mediate the sequestration of MHC-I (Chapter 3 and (Atkins et al., 2008)). However, recent studies suggested Nef does not require PACS-1 to downregulate MHC-I due to the ability of a chimeric protein consisting of the cytosolic tail of MHC-I fused to Nef (GST-MHC-I CD-$Nef_{LL/AA}$) to directly bind the

membrane adaptor AP-1 μ1 subunit *in vitro* (Noviello et al., 2008, Singh et al., 2009). However, our studies in Chapter 3 demonstrate that GSTMHC-I CD-Nef$_{LL/AA}$ can also interact with PACS-1, consistent with the determination that PACS-1 mediates Nef-induced MHC-I downregulation subsequent to PI3K stimulation (Chapter 3 and (Atkins et al., 2008)). Moreover, the ability of PACS-1 to interact with Nef on Rab7-positive late endosomes/MVBs is consistent with a role for PACS-1 downstream of PI3K activation to mediate the sequestration of endocytosed MHC-I molecules as well as with the determination that downregulated MHC-I accumulates in Rab7-positive endosomes (Dikeakos et al., 2012, Schaefer et al., 2008, and Chapter 3). However, whether PACS-1 and AP-1 mediate common or separate sorting steps required for sequestering internalized MHC-I molecules in TGN/endosomal compartments has yet to be determined. Therefore, in future studies it will be important to understand the mechanism of Nef-induced MHC-I sequestration and to what extent PACS-1 and AP-1 coordinate or independently function to mediate this process.

Various studies demonstrate that Nef can induce rapid degradation of overexpressed MHC-I (Kasper et al., 2003, Roeth et al., 2004, Kasper et al., 2005, Schaefer et al., 2008). Indeed, recent studies determined that overexpressed MHC-I is targeted for lysosomal degradation in a β-COP-dependent manner (Schaefer et al., 2008), consistent with the role of COPI in endosomal maturation (Huotari et al., 2011). However, these experiments rely on the overexpression of MHC-I rather than analysis of endogenous MHC-I. Indeed,

we observe no marked effect on the stability or ER-to-Golgi trafficking of endogenous MHC-I (Chapter 3). Moreover, the determination that PACS-2 binds β-COP and functions as a connector for COPI coated vesicles (Simmen et al., 2005), together with the observation that PACS-2 interacts with Nef on Rab5-positive early endosomes as well as Rab7-positive late endosomes (Dikeakos et al., 2012), suggests PACS-2 may function in a β-COP-dependent manner to mediate Nef-dependent trafficking steps. Therefore, in future studies it will be important to investigate whether PACS-2 functions in a β-COP-dependent manner to mediate Nef-dependent trafficking steps in the endo-lysosomal network.

Together, the studies in Chapter 3 use cellular, biochemical, biophysical, and pharmacologic methods to clarify the divergence surrounding the signaling versus the stoichiometric mode. Moreover, these studies reveal Nef orchestrates a controlled program to downregulate MHC-I by the sequential use of the signaling followed by the stoichiometric mode and that these modes are temporally linked.

4.3 Diverse viral strategies to mediate MHC-I downregulation

Many pathogenic viruses express a variety of immune evasive proteins that can modulate nearly every step in the biosynthesis, assembly, transport and cell-surface localization of MHC-I molecules (Peterlin et al., 2003, Yewdell et al., 2002). Perhaps the most well-characterized of these proteins are expressed by

the herpesvirus and poxvirus families. For instance, human cytomegalovirus (HCMV) expresses the immediate early gene US3, which leads to the retention of newly synthesized MHC-I molecules in the ER, followed by the expression of US11, which induces degradation of MHC-I (Ahn et al., 1996). Epstein Barr virus (EBV) similarly coordinates a regulated immune evasive program initiated by BGLF5, which like HCMV US3, impedes MHC-I transport, while the subsequent expression of BILF1 leads to the degradation of MHC-I, similar to HCMV US11 (Zuo et al., 2009, Ahn et al., 1996). Interestingly, the determination that HIV-1 uses just a single gene product, Nef, to sequentially downregulate MHC-I by the signaling mode followed by the stoichiometric mode illustrates a novel viral strategy for coordinating immune evasion. While these studies illustrate the unique functions of Nef in mediating MHC-I downregulation by the sequential action of the signaling mode followed by the stoichiometric mode, it remains unclear how Nef mediates this switch. Therefore, it will be important for future studies to more precisely elucidate the mechanism of how Nef switches from the signaling to the stoichiometric mode to have a greater understanding of the biological context in which this regulation is critical.

4.4 The role of Nef-mediated MHC-I downregulation in cellular reservoirs

Nef can promote immune evasion and escape from the CTL response during both the early viremic phase and the late persistent phase of HIV-1 infection (Collins et al., 1998, Lewis et al., 2008). Therefore, the determination that Nef

downregulates MHC-I by the sequential use of the signaling mode followed by the stoichiometric mode raises the possibility that HIV-1 may adapt immune evasive strategies specific to the host cell activation state or reservoir type. This is consistent with the determination that HIV-1 can exist in multiple forms with differing rates of viral turnover or production, such as free virions in plasma, or as integrated provirus in activated $CD4^+$ T-cells and macrophages, as well as latent forms in resting $CD4^+$ T-cells (Finzi et al., 1998). Indeed, in resting $CD4^+$ T-cells HIV-1 can exist in one of two latent forms: a labile, unintegrated cytoplasmic form (Zack et al., 1990) or a stable, integrated nuclear form (Chun et al., 1995). Indeed, while activated $CD4^+$ T-cells produce the majority of infectious virus particles, accumulating evidence suggests $CD4^+$ T-cells can persistently produce low levels of virus after reverting to a quiescent state, particularly in viremic patients (Gondois-Rey et al., 2001, Chun et al., 2003). Interestingly, while resting or memory $CD4^+$ T-cells are quiescent and long-lived, the lifespan of activated $CD4^+$ T-cells infected with HIV-1 is less than two days (Stevenson, 2003). Due to this shortened lifespan, and the determination that the signaling mode is present early following infection of $CD4^+$ T-cells before switching to the stoichiometric mode, the relative contribution of each pathway during this period is not clear.

Along with resting $CD4^+$ T-cells, macrophages are also capable of harboring latent viral reservoirs (Stevenson, 2003, Alexaki et al., 2008). Indeed, macrophages are known to produce a low, but persistent levels of virus through the duration of the cell's lifespan, often days to months (Alexaki et al., 2008). It is

thought that the limited expression of viral proteins may contribute to establishment of cellular HIV-1 reservoirs by allowing them to escape immune surveillance (Alexaki et al., 2008). Specifically, macrophages expressing HIV-1 Nef have been shown to promote latent infection by facilitating the infection of resting $CD4^+$ T-cells (Swingler et al., 2003). Therefore, the determination that Nef can assemble the multi-kinase complex in both lymphocyte and monocyte lineages (Hung et al., 2007, Atkins et al., 2008) suggests this pathway may function in multiple cell types or cellular reservoirs. Indeed, it is possible that in macrophages the early signaling mode of MHC-I downregulation converts to a stoichiometric mode that does not require persistent activation of these signaling molecules. Future studies of the immune evasive program directed by Nef will require membrane trafficking experiments in relevant cell populations harboring viral reservoirs to determine the relative contributions of the signaling and stoichiometric modes of Nef action. Future studies should therefore determine whether the signaling and stoichiometric modes of MHC-I downregulation occur only in activated $CD4^+$ T-cells or monocyte-macrophage cells, or whether these pathways exist in longer-lived HIV-1 reservoir populations such as resting $CD4^+$ T-cells. Moreover, it will be important for future studies to investigate whether conversion from the signaling to the stoichiometric pathway occurs in monocytes-macrophages or whether the signaling mode remains functional. Together, these studies are essential for understanding the physiological conditions in which the respective MHC-I downregulation pathways exist.

4.5 Implications of the signaling mode on antigen presentation

The ability of viral peptide-loaded MHC-I molecules to properly activate $CD8^+$ T-cells through the formation of an immunological synapse requires a number of key factors, including: an optimal half-life (dwell-time) of the interaction between peptide-loaded MHC-I and the cognate T-cell receptor (TCR) (Kalergis et al., 2001, Riquelme et al., 2009), epitope density on the antigen-presenting cell (APC) (Gonzalez et al., 2005), as well as appropriate costimulatory molecules such as CD80 and CD28 (Huppa et al., 2003). Indeed, the half-life (dwell-time) of the interaction between peptide-loaded MHC-I and a TCR sufficient to elicit T-cell activation must be within an optimal range (Kalergis et al., 2001), with shortened or lengthened dwell time significantly impairing CTL activation and response (Riquelme et al., 2009). These findings raise the possibility that the accelerated endocytosis of MHC-I induced by Nef during the signaling mode results in a premature dissociation of peptide-loaded MHC-I from the TCR, thereby reducing dwell time and resulting in inadequate $CD8^+$ T-cell activation and a failed CTL response. Nef can additionally impair the formation and function of the immunological synapse by downregulating the costimulatory molecule, CD28 (Bell et al., 2001, Swigut et al., 2001), and by dampening signal transducton via the downmodulation of CD4 (Garcia et al., 1991). Collectively, these findings suggest the ability of Nef to transform the cell surface landscape of HIV-1 infected cells greatly contributes to the pathogenic roles of Nef. Therefore, in

future studies it will be important to quantify the antigen presenting properties and kinetics during HIV-1 infection.

4.6 Nef PXXP$_{75}$ as a pharmacologic target

Despite continued efforts, the development of an HIV-1 vaccine remains elusive and current HIV-1 therapeutics rely principally on the few HIV-1 proteins that possess intrinsic enzymatic activity, including reverse transcriptase, integrase and protease (HHS, 2012, Hammer et al., 2008). While current therapeutic strategies have dramatically decreased morbidity and mortality in HIV-1 infected patients, their therapeutic efficacy is compromised by the low fidelity of HIV-1 replication, leading to the emergence of drug-resistant mutants (Moutouh et al., 1996, Tamalet et al., 2000). While the lack of intrinsic enzyme activity of HIV-1 accessory proteins initially caused them to be overlooked as candidate therapeutic targets, studies from us and others suggest the ability of Nef to directly bind and activate cellular kinases may represent an attractive approach to inhibiting Nef-driven pathogenesis (Choi et al., 2004, Trible et al., 2006, Hung et al., 2007). Indeed, the determination that the Nef-SFK interaction is required for assembly of the multi-kinase complex that initiates downregulation of MHC-I, together with the determination that the extent of MHC-I downregulation in SIV-1-infected rhesus macaques correlates with high viremia and accelerated disease progression (Friedrich et al., 2010), suggests

pharmacologic inhibition of the Nef-SFK interaction may represent an attractive therapeutic approach.

The importance of Nef-mediated pathogenesis was confirmed *in vivo* in an AIDS-like mouse model in which Nef is expressed as a transgene in $CD4^+$ T-cells, macrophages, and dendritic cells from the CD4 gene promoter (Hanna et al., 1998b). These mice develop a severe AIDS-like disease characterized by wasting, premature death, atrophy of lymphoid organs and preferential loss of $CD4^+$ T-cells as well as multi-organ disease including interstitial pneumonitis, interstitial nephritis (Hanna et al., 1998a, Hanna et al., 1998b) and depressed cardiac function (Kay et al., 2002). Importantly, the determination that transgenic mice expressing a mutated Nef deficient in SFK binding (Nef $AXXA_{75}$) are completely protected from the AIDS-like phenotype induced by wild-type Nef (Hanna et al., 2001), suggests an intact $PXXP_{75}$ domain is critical for Nef-induced pathogenesis. Moreover, while transgenic mice expressing wild-type Nef on an Hck-null background still develop disease, they have a significantly prolonged latency of disease progression (Hanna et al., 2001), suggesting Hck is not the sole mediator of Nef action. This is consistent with our studies in Chapter 3 demonstrating that while knockdown of Hck partially represses MHC-I downregulation, combined knockdown of Hck, Lyn, and Src completely blocks MHC-I downregulation, suggesting multiple SFKs can function redundantly in Nef action. Moreover, the ability of Nef to traffic to the perinuclear region where it interacts with SFKs requires PACS-2, as the Nef-SFK interaction and subsequent

assembly of the multi-kinase complex and downregulation of MHC-I is blocked in PACS-2 siRNA-depleted or *Pacs2*$^{-/-}$ cells (Atkins et al., 2008). Together, these studies suggest that the PACS-2-dependent priming of Nef $PXXP_{75}$-mediated functions, as well as the cellular binding proteins that mediate these effects, are essential for the ability of Nef to drive disease.

Along with the requirement for the Nef-SFK interaction in Nef-induced MHC-I downregulation, the ability of Nef to selectively enhance the intrinsic infectivity of progeny viruses is also dependent on Nef-SFK interactions (Chutiwitoonchai et al., 2011). Indeed, Chutiwitoonchai and colleagues have shown that cells expressing Nef $AXXA_{75}$ are deficient in Nef-mediated enhancement of viral infectivity and that blocking the Nef-SFK interaction with the small molecule 2c also reduces Nef-mediated infectivity enhancement (Chutiwitoonchai et al., 2011). These studies, together with the determination that 2c also represses the Nef-Hck-dependent downregulation of macrophage colony-stimulating factor (M-CSF) receptor (Suzu et al., 2005, Hiyoshi et al., 2008, Hassan et al., 2009) and that diphenylfuropyriminde compounds capable of blocking Nef-SFK complex formation inhibit Nef-dependent HIV-1 replication in promonocytic cells (Emert-Sedlak et al., 2009), suggest the generation of small molecules that disrupt Nef-SFK binding represent an attractive approach to inhibiting Nef function.

Nef also promotes viral fitness and optimizes the environment for HIV-1 replication by rerouting kinase-active pools of the SFK family member and TCR

signaling mediator Lck from the plasma membrane to the TGN in a $PXXP_{75}$-dependent manner (Pan et al., 2012). This effectively prevents the recruitment of active Lck to the immunological synapse after TCR engagement and limits TCR-mediated signal transduction from the plasma membrane (Pan et al., 2012). However, the significance of this mislocalization is not simply the removal of Lck from the cell surface, but rather, Nef induces the Lck-dependent activation of TGN-associated Ras-Erk signaling to promote the production of the T-cell survival factor interleukin-2 (IL-2), thereby prolonging the life cycle of HIV-1 and facilitating viral spread (Pan et al., 2012).

The effects of Nef-induced pathogenesis are not limited to cells of the immune system. Indeed, direct infection of glomerular visceral epithelial cells (podocytes) by HIV-1 can lead to HIV-associated nephropathy (HIVAN) in genetically susceptible individuals (Bruggeman et al., 2000, Marras et al., 2002). HIVAN is one of the leading causes of end-stage renal disease in HIV-1 infected patients, who frequently present with heavy proteinuria, chronic renal failure, and pathologic findings of collapsing focal segmental glomerulosclerosis (FSGS) and microcystic dilation of tubules (D'Agati et al., 1998). Podocytes, the specialized filtration cells of the glomerulus, while normally quiescent and highly differentiated, undergo dedifferentiation and resume proliferation in both human and mouse kidneys with HIVAN (Barisoni et al., 2000a, Barisoni et al., 1999, Barisoni et al., 2000b). Indeed, transgenic mice studies determined Nef was responsible for mediating the pathology of HIVAN (Hanna et al., 1998b), and that

this phenotype was reversed in the transgenic Nef $AXXA_{75}$ mice (Hanna et al., 2001), suggesting Nef requires an intact $PXXP_{75}$ site to mediate the dysfunction of glomerular podocytes. Moreover, subsequent studies determined that Nef mediates podocyte proliferation and dedifferentiation via the $PXXP_{75}$-mediated interaction with Src, resulting in Src-dependent activation of signal transducer and activator of transcription 3 (STAT3) and Ras-cRaf-mitogen-activated protein kinase (MAPK1,2) signaling pathways (He et al., 2004). Therefore, along with the immune modulatory Nef-SFK-dependent functions, Nef also mediates end-organ pathology, which may additionally be sensitive to therapeutic inhibition of the Nef-SFK interaction.

While Nef-SFK interactions control a myriad of Nef functions, the Nef $PXXP_{75}$ site also interacts with additional host cellular proteins to modulate cell motility, immunological and virological synapse formation, as well as the intercellular transfer of viral proteins and virus (Rudnicka et al., 2009, Haller et al., 2008, Mukerji et al., 2012). Notably, Nef interacts with and activates p21-activated kinase 2 (PAK2), a protein that regulates T-cell signaling and actin cytoskeletal dynamics, in a $PXXP_{75}$-dependent manner to stimulate the formation of long-range tunneling nanotubes and virological synapses (Rudnicka et al., 2009, Haller et al., 2008, Mukerji et al., 2012). A recent proteomic analysis demonstrates that Nef $PXXP_{75}$ is critical for interacting with PAK2 and recruiting the exocyst complex of proteins, which mediate the tethering of vesicles at the plasma membrane, as well as regulate polarized exocytosis and nanotube

formation (Mukerji et al., 2012). Nef $PXXP_{75}$ interacts with PAK2 and recruits the exocyst complex to induce the formation of tunneling nanotubes that function as a virological synapse, or junction, through which viral proteins and virus can be efficiently transferred from cell-to-cell (Mukerji et al., 2012). Nef also mediates the destruction of healthy bystander cells, including $CD4^+$ and $CD8^+$ T-cells, through the $PXXP_{75}$-dependent secretion of exosomes containing Nef and the death ligand FasL (Muratori et al., 2009, Lenassi et al., 2010) as well as the increased expression of FasL on the surface of Nef-expressing cells (Muthumani et al., 2005). These studies provide insight into the mechanisms Nef uses to increase virus and viral protein dissemination within the infected host, respectively. While the precise membrane composition of the various conduits or vesicles used for intercellular transfer is not fully understood, the universal requirement for the Nef $PXXP_{75}$ site in each of these pathways suggests a common mechanism may exist to mediate these effects. Indeed, the determination that the Nef $PXXP_{75}$ site is required for interacting with various host cell kinases, including SFKs and PAK2, to mediate a myriad of functions such as immune evasion, viral replication, intercellular communication, and virological synapse formation, further supports the hypothesis that pharmacologic disruption of Nef $PXXP_{75}$ interactions, such as Nef-SFK or Nef-PAK2, may be a viable therapeutic target.

4.7 Implications of PACS-2-dependent Nef trafficking

The ability of Nef $PXXP_{75}$ to bind and activate a subset of TGN-localized SFKs to mediate various downstream pathogenic effects is dependent on its trafficking from early endosomes to the perinuclear region. Indeed, the trafficking of Nef from peripheral early endosomes to the perinuclear region requires a PACS-2-dependent sorting step, as the expression of Nef in PACS-2 siRNA-depleted or *Pacs2*$^{-/-}$ cells leads to the accumulation of Nef in early endosomal compartments (Atkins et al., 2008). This observation is consistent with recent studies from our laboratory demonstrating that PACS-2 interacts with Nef on Rab5-positive early endosomes as well as Rab7-positive late endosomes/multi-vesicular bodies (MVBs) using bimolecular fluorescence complementation (BiFC); in which cells express reporter constructs composed of PACS-2 fused to the N-terminus of YFP and Nef fused to the C-terminus of YFP, which are individually non-fluorescent, but generate fluorescence upon protein-protein interaction (Dikeakos et al., 2012, Kerppola, 2008). Moreover, the ability of Nef to traffic to the perinuclear region enables it to bind and activate a TGN-localized SFK, thereby triggering the assembly of the multi-kinase complex and the downregulation of MHC-I (Hung et al., 2007, Atkins et al., 2008). Importantly, the interaction of Nef with PACS-2 or SFKs is mutually exclusive, consistent with the absence of PACS-2 in the multi-kinase complex (Atkins et al., 2008). Together, these studies illustrate the essential requirement for PACS-2 upstream of the Nef-SFK complex and suggest that disruption of the Nef-PACS-2 interaction may be an effective strategy to prevent downstream Nef-SFK-, or potentially other Nef

$PXXP_{75}$-dependent events. Therefore, in future studies it will be essential to solve a high resolution crystal structure of Nef with PACS-2, as the identification of how this interaction is mediated in three-dimensional space will facilitate the development of small molecule compounds that may target these points of contact to disrupt the Nef-PACS-2 interaction. In support of this approach, recent mapping studies have identified the precise regions on Nef and PACS-2 required for their interaction; including a bipartite site on Nef consisting of the $EEEE_{65}$ acidic cluster and W_{113} in the core domain that interacts with a minimal sequence within the PACS-2 FBR (residues 102-116) (Dikeakos et al., 2012). Indeed, mutation of critical residues within either of these sites on Nef or PACS blocks MHC-I downregulation (Dikeakos et al., 2012), supporting the essential nature of this interaction for Nef function and the viability of its inhibition as a therapeutic target.

4.8 Conclusion to PART I

The results presented in Part I of this dissertation provide evidence that Nef directs a regulated program to downregulate MHC-I consisting of the sequential use of the signaling and stoichiometric modes of action. During the first two days after infection, Nef uses the signaling mode to downregulate MHC-I. This mode requires the PACS-2-dependent binding of Nef to a TGN-localized SFK that Nef can directly activate to assemble a multi-kinase complex that triggers downregulation of cell-surface MHC-I in $CD4^+$ T-cells. Indeed, chemical

disruption of the Nef-SFK interaction with the small molecule inhibitor 2c blocks assembly of the multi-kinase complex and represses HIV-1–mediated MHC-I downregulation in primary $CD4^+$ T-cells. 2c did not interfere with the PACS-2–dependent trafficking of Nef required for the Nef-SFK interaction or the AP-1 and PACS-1–dependent sequestering of internalized MHC-I, suggesting the inhibitor specifically interfered with the Nef-SFK interaction required for assembling the multi-kinase complex and triggering MHC-I downregulation. By three days post-infection, Nef switches to the stoichiometric mode that prevents delivery of newly synthesized MHC-I to the cell surface. Pharmacologic inhibition of the multi-kinase cascade disrupts the temporally controlled block in MHC-I transport during the stoichiometric mode, suggesting the Nef-directed signaling and stoichiometric modes are causally linked.

PART II (CHAPTERS 5-7). Regulation of the p53-SIRT1 axis following DNA damage

OVERVIEW

This section will introduce the integral role of p53 following DNA damage (**CHAPTER 5**), including its complex regulation via posttranslational modifications and various cofactor recruitment. Specifically, this chapter will describe the activation of p53 and the role of p53-induced target genes that mediate cell fate processes such as cell cycle arrest and apoptosis. In addition, this chapter will describe how p53 acetylation controls p53 activity following DNA damage, including the role of SIRT1-mediated deacetylation of p53, as well as describe SIRT1 biology and its complex regulation. The studies in **CHAPTER 6** demonstrate a novel role for PACS-2 in regulating how cells respond to DNA damage by modulating p53 activation via inhibition of SIRT1-mediated deacetylation of p53. The results and implications of these studies are discussed in **CHAPTER 7**. Given the diverse and complex nature of p53, SIRT1, and PACS-2, the potential implications of these studies span cellular processes such as gene regulation, chromatin remodeling, cell growth and survival as well as biological processes such as cancer, aging, and metabolism.

RATIONALE AND HYPOTHESIS

Rationale: Following DNA damage, the sequence-specific transcription factor p53 functions as a node for orchestrating biological responses such as cell-cycle arrest, apoptosis, and senescence by promoting the transactivation of various target genes. Importantly, the ability of p53 to orchestrate these diverse processes critically depends on the regulation of p53 by cellular cofactors and modifying enzymes. Notably, p53 acetylation is essential for its transcriptional activation following DNA damage. p53 is deacetylated by Sirtuin 1 (SIRT1), a nicotinamide adenine dinucleotide (NAD^+)-dependent histone deacetylase, thereby repressing p53 transcriptional activation. Therefore, understanding how the SIRT1-p53 axis is regulated during the DNA damage response is essential for gaining insight into the mechanisms controlling p53 activation.

Hypothesis: Based on the determination that the membrane trafficking protein PACS-2 directly interacts with SIRT1 and that PACS-2 deficient cells have reduced acetylation of p53 and p21 expression, as well as increased apoptosis following DNA damage, I *hypothesize* that PACS-2 regulates the response to DNA damage by inhibiting SIRT1-mediated deacetylation of p53, thereby modulating p53 transcriptional activation. To test this hypothesis, I have addressed the following experimental goals in Chapter 6:

1. Determine whether the increased apoptosis in PACS-2 deficient cells correlates with reduced long-term survival or altered cell cycle control following DNA damage.
2. Determine whether PACS-2 inhibits SIRT1-mediated deacetylation of p53 and the extent to which reduced p53 acetylation following loss of PACS-2 is SIRT1-dependent.
3. Examine whether the reduced p21 expression seen with PACS-2 loss is SIRT1-dependent.
4. Explore the subcellular localization of PACS-2 and whether PACS-2 interacts with SIRT1 in the nucleus.

CHAPTER 5. Introduction to p53, SIRT1, and the DNA damage response

5.1 The tumor suppressor p53

5.1.1 The guardian of the genome

It has been over 30 years since the discovery of p53 (Lane et al., 1979, Linzer et al., 1979, DeLeo et al., 1979) and more than 20 years since p53 was identified as a tumor suppressor (Baker et al., 1989, Finlay et al., 1989). A seminal article by Vogelstein and colleagues in 1989 reported that the *TP53* gene encoding p53 is frequently mutated in colorectal carcinomas (Baker et al., 1989). Following this discovery, subsequent studies revealed that *TP53* may in fact be the most frequent target of genetic alternations in human cancer (Levine et al., 1991, Hollstein et al., 1991, Oren, 1991, Weinberg, 1991, Caron de Fromentel et al., 1992). Mutations that disrupt p53 function or its regulatory network have been found in more than half of all human cancers and germline mutations in p53 lead to the autosomal dominant Li-Fraumini syndrome, in which individuals are predisposed to a wide range of malignancies at an unusually early age (Hainaut et al., 2000, Vogelstein et al., 2000). These findings lead to p53 being termed the "guardian of the genome" (Lane, 1992) and the "cellular gatekeeper" (Levine, 1997), as p53 functions to relay an array of stress-inducing signals, such as DNA damage, oncogene activation, and hypoxia, to coordinate various cellular responses. Following such signals, p53 functions as a node that orchestrates diverse biological responses, such as cell-cycle arrest, apoptosis, senescence, DNA repair, cell metabolism, or autophagy (Green et al., 2009, Yee et al., 2005, Riley et al., 2008). Importantly, these tumor suppressor functions of p53 are

context-dependent and modulated by a variety of factors, including cell and tissue type, microenvironment, metabolic state, and oncogenic alterations acquired during tumor progression (Zilfou et al., 2009). To coordinate and fine-tune responses to various stress signals, p53 functions as a sequence-specific transcription factor, binding specific DNA sequences to mediate the activation and/or repression of a vast array of target genes (Brooks et al., 2003, Laptenko et al., 2006). Indeed, the majority of the tumor suppressive properties of p53 have been attributed to its transcription factor capabilities. This level of regulation requires an exquisitely complicated network, as evidenced by the droves of cofactors associated with p53 as well as the multitude of posttranslational modifications of p53 during homeostatic and stress-induced processes. Indeed, more than 36 amino acids within p53 are posttranslationally modified by phosphorylation, ubiquitination, acetylation, methylation, sumoylation, neddylation, O-glycosylation, and ADP-ribosylation (Figure 5.1) (Kruse et al., 2008), illustrating the complex and intricate network of p53 regulation.

5.1.2 The functional domains of p53

The 393 amino acid p53 protein can be functionally and structurally divided into several domains. There are two identified acidic N-terminal transactivation domains (residues 1-42, 43-73) (Fields et al., 1990, Venot et al., 1999) that have been shown to interact with components of the basal transcription machinery such as transcription factor II D (TFIID), transcription factor II H (TFIIH), TATA-

binding-protein-associated factor II 31 (TAFII31), and TATA-binding-protein-associated factor II 70 (TAFII70) (Xiao et al., 1994, Lu et al., 1995, Thut et al., 1995, Farmer et al., 1996, Di Lello et al., 2006). Importantly, the murine double minute 2 (MDM2) oncoprotein and negative regulator of p53 also binds the N-terminal domain of p53, thereby inhibiting its transcriptional activity (Oliner et al., 1993). p53 contains a highly conserved, globular hydrophobic central DNA binding core domain (residues 102-292) which mediates its sequence-specific DNA binding activity (Wang et al., 1993) as well as harbors the majority of mutation hot-spots identified in human tumors (Pavletich et al., 1993). An oligomerization or tetramerization domain is located between residues 324-355 and mediates the binding of p53 to DNA as a tetramer (Friedman et al., 1993, Wang et al., 1994, McLure et al., 1998). The tetramerization of p53 is mediated by the C-terminus (Pavletich et al., 1993, Wang et al., 1993) via the formation of a symmetric dimer of dimers composed of four geometrically equivalent subunits (Clore et al., 1994, Clore et al., 1995a, Clore et al., 1995b, Lee et al., 1994, Jeffrey et al., 1995). Lastly, p53 contains a basic C-terminal regulatory domain (residues 363-393) which has been shown to bind DNA nonspecifically as well as negatively regulate specific DNA binding via the central core domain (Anderson et al., 1997). Indeed, the N-terminal transactivation domain and the C-terminal regulatory domains harbor the majority of residues that are posttranslationally modified and that contribute to p53 function (Appella et al., 2001).

5.2 p53 coordinates multiple cell fate processes following DNA damage

5.2.1 Overview of p53 effector functions

p53 has been implicated in a multitude of anti-proliferative and tumor suppressive processes such as cell-cycle arrest, apoptosis, senescence, differentiation, DNA repair, angiogenesis, metabolism, and autophagy, each of which contribute to its tumor suppressive capabilities depending on the cellular context (Yee et al., 2005, Vousden et al., 2009). Indeed, the genes modulated and pathways initiated by p53 following stress signals are often dependent on the nature of the stimulus, the frequency or magnitude of the insult, as well as the cell type and tissue microenvironment (Zilfou et al., 2009).

The ability of p53 to transcriptionally regulate a vast array of target genes is essential for mediating various cellular processes following stress signals. For instance, to initiate growth arrest, p53 upregulates the Cip/Kip family cyclin-dependent kinase inhibitor p21; 14-3-3σ, a negative regulator of the cell cycle; the M-phase inducing Cdc25C phosphatase; as well as the growth arrest and DNA damage inducible (GADD) family member GADD45 (el-Deiry et al., 1993, Hermeking et al., 1997). To modulate DNA repair processes following DNA damage, p53 induces the expression of p21, GADD45, as well as the p48 xeroderma pigmentosum protein (Smith et al., 1994, Li et al., 1994a, Pan et al., 1995, Hwang et al., 1999). Interestingly, while a more limited number of genes are targeted by p53 to modulate cell-cycle and DNA repair processes, the induction of p53-mediated apoptosis is associated with a growing number of

identified p53 targets, including, but not limited to, B-cell lymphoma-2 (Bcl-2) family members such as the Bcl-2 homology (BH)3-only proteins p53-upregulated modulator of apoptosis (PUMA) and NOXA, as well as the multi-BH domain-containing proapoptotic effector Bax; the p53-regulated apoptosis inducing protein 1 (p53-AIP1); the p53 apoptosis effector related to peripheral myelin protein-22 (PMP-22) (PERP); the p53-inducible gene 3 (PIG3); as well as the death ligand receptors FasR (also known as apoptosis antigen-1 (APO-1) or cluster of differentiation 95 (CD95)) and KILLER/DR5 (Miyashita et al., 1995, Owen-Schaub et al., 1995, Polyak et al., 1997, Wu et al., 1997, Oda et al., 2000a, Oda et al., 2000b, Nakano et al., 2001, Riley et al., 2008). A more detailed description of p53-induced apoptosis is provided in section 5.2.3.

Importantly, p53 creates an auto-regulatory feedback loop by inducing the expression of its own negative regulators, such as MDM2, p53-induced RING-H2 (Pirh2), COP1, and cyclin G (Juven et al., 1993, Okamoto et al., 1994, Haupt et al., 1997, Okamoto et al., 2002, Leng et al., 2003, Dornan et al., 2004). Indeed, while modulation of immediate processes such as growth arrest, DNA repair, and apoptosis are essential following DNA damage, p53 can additionally coordinate long-term cellular changes such as the inhibition of angiogenesis by the transcriptional upregulation of thrombospondin-1 (TSP-1), glioblastoma-derived angiogenesis inhibiting factor (GD-AIF), and hypoxia inducible factor-1α (HIF-1α) (Dameron et al., 1994, Van Meir et al., 1994, Fukushima et al., 1998, Ravi et al., 2000).

While the preceding paragraphs are not a comprehensive list of p53 function and target gene modulation, they serve to briefly illustrate the diversity of p53 regulation. The following sections will describe in more detail some of the most well-characterized p53 functions relevant to this dissertation, including regulation of cell-cycle checkpoints and the induction of apoptosis, as well as the functions of p53 target genes that mediate these processes. Additional pathways mediated by p53, while intriguing and relevant to p53 biology and the diversity of its functions, are outside the scope of this dissertation and have been summarized in great detail elsewhere (Vousden et al., 2009, Reinhardt et al., 2012, Ryan, 2011, Maddocks et al., 2011).

5.2.2 Cell cycle arrest

The fidelity of cell division is ensured by the presence of cell-cycle checkpoints. Following various cellular stresses, activation of these checkpoints will arrest cells from continuing through cell division, thereby preventing the replication of damaged DNA, preserving chromosomal integrity, and ensuring that each daughter cell receives a complete and faithful copy of the genome (Giono et al., 2006).

Progression through the cell cycle is regulated by a group of cyclin-dependent kinases (CDKs), which are activated upon binding to their regulatory subunits, the cyclins (Morgan, 1995). Of the 13 and 25 loci encoding CDKs and cyclins, respectively, only a subset of CDK-cyclin complexes are critical for

promoting cell cycle progression. These include the mitotic CDK (CDK1), three interphase CDKs (CDK2, CDK4, and CDK6), as well as 10 cyclins belonging to four classes (A-, B-, D-, and E-type cyclins) (Malumbres et al., 2005, Malumbres et al., 2001). Progression through cell cycle is driven by a series of sequential phosphorylation events mediated by active cyclin/CDK complexes (Malumbres et al., 2009). According to the classic model of cell cycle progression (Figure 5.2), growth signals induce the expression of D-type cyclins that bind and activate CDK4/6 during G_1, leading to phosphorylation and partial inactivation of the retinoblastoma (Rb) protein family members Rb, p107, and p130. This leads to reduced inhibition of the transcription factor E2F, allowing expression of the E-type cyclins, which bind and activate CDK2. The pocket proteins are then further phosphorylated and completely inactivated by CDK2-cyclin E complexes, allowing E2F-mediated transcription to drive the G_1/S transition. Finally, A-type cyclins activate CDK2 and CDK1 to drive the S/M transition while B-type cyclins activate CDK1 to proceed though mitosis (Malumbres et al., 2009).

The broad and potent role of cyclin/CDK complexes across the cell cycle is evidenced by the fact that they are the main targets of endogenous cell cycle inhibitors as well as effectors of the G_1/S checkpoint (Sherr, 1994). CDKs are inhibited by two classes of CDK inhibitors, the INK4 family, including $p16^{INK4a}$, $p18^{INK4c}$, and $p19^{INK4d}$, and the Cip/Kip family, including $p57^{Kip2}$, $p27^{Kip1}$, and $p21^{Cip1/Waf1}$ (hereafter, p21). While the INK4 family specifically targets CDK4/6, the Cip/Kip family targets multiple CDKs across the cell cycle (Sherr et al., 1995,

Sherr et al., 1999). Indeed, p21 is a broad spectrum cell cycle inhibitor, targeting multiple cyclin-CDK complexes including cyclin D-CDK4/6, cyclin E-CDK2, cyclin A-CDK2, and cyclin B-CDK1 complexes (Harper et al., 1993, Gu et al., 1993, Xiong et al., 1993, Harper et al., 1995) as well as blocks proliferating cell nuclear antigen (PCNA)-dependent DNA polymerase activity during S-phase (Li et al., 1994a, Waga et al., 1994).

The function of the G_1/S checkpoint is to prevent cells harboring DNA damage from transitioning into S-phase, thereby replicating the damaged DNA. This process is largely dependent on p53 (Giono et al., 2006), as both DNA damage as well as the ectopic expression of p53 mediates arrest of cells at the G_1/S checkpoint (Kastan et al., 1991, Lin et al., 1992). Following DNA damage, p53 induces G_1 arrest primarily via the transactivation of the CDK inhibitor p21 (el-Deiry et al., 1993, Deng et al., 1995, Brugarolas et al., 1995). Indeed, in cells lacking p53, expression of p21 alone is sufficient to induce G_1 growth arrest (Rousseau et al., 1999). Conversely, G_1 arrest is abrogated following DNA damage in mouse embryonic fibroblasts and human cancer cells from which p21 has been genetically deleted (Brugarolas et al., 1995, Deng et al., 1995, Waldman et al., 1995). Together, these studies illustrate the essential role for p21 in mediating G_1 arrest following DNA damage. However, since the initial discovery of p21 as a cell-cycle inhibitor and p53 effector (el-Deiry et al., 1993, Harper et al., 1993, Gu et al., 1993, Xiong et al., 1993, Noda et al., 1994, Dulic et al., 1994), p21 has been implicated in a multitude of cellular processes including

apoptosis, differentiation and senescence, DNA repair, aging, reprogramming of induced pluripotent stem cells (Coqueret, 2003, Garner et al., 2008, Gartel et al., 2002, Li et al., 2009a) as well as tumor suppression and tumor formation (el-Deiry et al., 1993, Efeyan et al., 2007, Barboza et al., 2006, Martin-Caballero et al., 2001, Roninson, 2002, Gartel, 2006, Abbas et al., 2009).

While initially described as a critical mediator of the G_1/S checkpoint, the role for p53 in growth arrest following DNA damage extends to additional checkpoints as well. The S-phase checkpoint prevents cell division before the cell has completed replicating its genome and can be activated by multiple mechanisms, including stalled replication forks resulting from nucleotide depletion or polymerase inhibition as well as by damaged DNA detected outside the replicon (Bartek et al., 2004). p53 has been implicated as functioning within the S-phase checkpoint to ensure that cells do not enter mitosis with unreplicated DNA (Taylor et al., 1999). Further studies demonstrate p53 is also required for the maintenance of S-phase arrest induced by the downregulation of Cdc7 kinase, a protein involved in the firing of replication origins (Montagnoli et al., 2004).

Following S-phase, the G_2/M progression is driven by the cyclin B1/CDK1 complex termed the maturation-promoting factor (MPF, or mitosis-promoting factor). The inactive MPF complex is sequestered in the cytoplasm of cells and upon entry into mitosis is translocated to the nucleus and activated by the Cdc25 phosphatase (Nurse, 1990). Following DNA damage, activation of the G_2/M

checkpoint is mediated primarily through factors that inhibit the cyclin B1/CDK1 (or MPF) complex (Nyberg et al., 2002). Similar to G_1 arrest, the p53-mediated expression of p21 is involved in the maintenance of the G_2/M checkpoint via the inhibition of cyclin B1/CDK1 complex activity (Stewart et al., 1995, Bunz et al., 1998). While there is no defect in the ability of p53- or p21-null cells to activate or initiate the G_2 checkpoint, they are unable to sustain this arrest, eventually escaping G_2 and entering mitosis (Bunz et al., 1998). This functional analysis is consistent with early studies demonstrating that expression of *p21* mRNA in cycling cells is bimodal, peaking in G_1, decreasing during S-phase, and peaking again in G_2 (Li et al., 1994b). Moreover, p21 induces a pause before the onset of mitosis, as nuclear localization of p21 in late G_2 correlates with delayed entry into mitosis in wild-type cells, but not in p53- or p21-null cells (Dulic et al., 1998). Furthermore, following DNA damage, p53- and p21-null cells display a premature mitotic entry that is often followed by a failure to undergo cytokinesis, resulting in abnormal DNA content and an increased susceptibly to aberrant mitoses, leading to mitotic catastrophe and cell death (Bunz et al., 1998).

5.2.3 Apoptosis

The phenomena of p53-dependent apoptosis was first observed following the reintroduction of p53 into a p53-null myeloid leukemia cell line and the resultant apoptosis that ensued (Yonish-Rouach et al., 1991). This observation was followed by seminal studies analyzing apoptosis in wild-type and p53-null

mouse thymocytes which showed that p53 was required for radiation-induced apoptosis, but not cell death induced by several other stimuli (Clarke et al., 1993, Lowe et al., 1993b). Subsequent studies determined that p53-dependent apoptosis was also induced by certain DNA damaging cancer therapeutic agents as well as by the expression of oncogenes (Lowe et al., 1993a). The central role for p53 in modulating apoptotic responses following DNA damage is evidenced by the evolutionary conservation of p53 structure and function in both drosophila (Brodsky et al., 2000, Jin et al., 2000, Ollmann et al., 2000) and C. Elegans (Frantz, 2001, Schumacher et al., 2001), where the respective p53 orthologs are critical components of DNA damage surveillance. Indeed, these early studies established a crucial role for p53 in controlling apoptosis following DNA damage and therefore, implicated p53 in the prevention of transformation and controlling the efficacy of cancer therapeutic agents.

As mentioned above, there are many more p53 target genes implicated in DNA damage-induced apoptosis than other p53 effector functions such as cell cycle arrest or DNA repair. Moreover, p53-induced apoptosis involves the coordination of both transcription-dependent and transcription-independent functions of p53 (Zilfou et al., 2009). As a sequence-specific DNA binding protein, p53 transactivates multiple classes of proteins that regulate apoptosis and cell survival. Early studies revealed an intuitive link between p53 transactivation function and apoptosis when it was determined that p53 transactivates multiple pro-apoptotic members of the Bcl-2 family, including the multidomain-containing

Bax (Miyashita et al., 1995) as well as the BH3-only members Puma (Nakano et al., 2001), Noxa (Oda et al., 2000a), and Bid (Sax et al., 2002). Indeed, cells maintain a critical balance between pro- and anti-apoptotic Bcl-2 proteins to ensure that appropriate responses to survival and death cues are enacted (Youle et al., 2008). In this manner, p53 functions to increase the ratio of pro- to anti-apoptotic Bcl-2 proteins following DNA damage, thereby facilitating mitochondria outer membrane permeabilization (MOMP) and the release of apoptotic factors to the cytosol (Youle et al., 2008, Wei et al., 2001). While additional genes are known to be induced by p53 to mediate apoptosis following DNA damage, such as PIG3, KILLER/DR5, CD95 (FasR), p53-AIP1, and PERP (Riley et al., 2008), PUMA is the only p53 target gene whose genetic loss produces a similar apoptotic defect to p53 loss in irradiated thymocytes *in vivo* (Jeffers et al., 2003).

Along with these transcription-dependent functions, p53‘s pro-apoptotic actions extend beyond the nucleus as evidenced by the pivotal role of cytoplasmic p53 in coordinating mitochondrial apoptosis (Green et al., 2009). In response to DNA damage such as ionizing radiation, p53 rapidly translocates to the mitochondria where it can interact with the Bcl-2 members Bcl-2, Bcl-xL, and Bak to induce MOMP, thereby releasing pro-apoptotic factors into the cytosol. In this manner, p53 is suggested to act like a BH3-only protein, either as a direct activator of Bax or Bak or as a derepressor by neutralizing the inhibitory functions of the anti-apoptotic Bcl-2 members Bcl-2 and Bcl-xL (Chipuk et al., 2004, Green et al., 2009, Mihara et al., 2003, Vaseva et al., 2009).

Importantly, recent studies determined that transcription-dependent and transcription-independent functions of p53 are linked via the transactivation and expression of PUMA (Chipuk et al., 2005). In this model, stress-induced cytosolic p53 is initially sequestered by anti-apoptotic Bcl-xL. This transient restraint is overcome by the p53-induced transactivation of PUMA, which translocates to mitochondria where it binds Bcl-xL, thus liberating p53 to induce Bax activation and subsequent MOMP (Chipuk et al., 2005, Chipuk et al., 2004, Ming et al., 2006). These studies suggest that PUMA couples the nuclear and cytoplasmic pro-apoptotic functions of p53 (Chipuk et al., 2005) and illustrates the complex nature of the p53 network.

5.3 p53 activation and regulation

5.3.1 The classical model of p53 stabilization and activation

A comprehensive illustration of p53 activation is essential for understanding the exquisite complexity of the transcriptional profiles and biological responses following DNA damage. However, it is essential to understand the traditional views of p53 activation before we can delve into these additional layers of intricacy, to provide framework for understanding data which is aligned (or maligned) along these logic threads. The classical model of p53 activation following cellular stress is described in three basic steps: stabilization of p53, sequence-specific DNA binding, followed by transactivation of target genes (Figure 5.3) (Yee et al., 2005). Stabilization of p53 is primarily mediated via the

inhibition of its interaction with the E3 ubiquitin ligase MDM2, a negative regulator and itself a p53 target gene that catalyzes the ubiquitin-dependent proteasomal degradation of p53 (Haupt et al., 1997, Honda et al., 1997, Kubbutat et al., 1997, Brooks et al., 2006, Michael et al., 2003). In this process, the rapid N-terminal phosphorylation of p53 is traditionally viewed as the first event in the stabilization of p53 following DNA damage, such as from ionizing radiation or chemotherapeutic agents. This DNA damage-induced phosphorylation of the p53 N-terminus can be catalyzed by a broad range of kinases, including ataxia telangiectasia mutated (ATM), ataxia telangiectasia and Rad3-related protein (ATR), DNA-protein kinase (DNA-PK), and checkpoint kinases 1 and 2 (Chk1/ Chk2) (Appella et al., 2001). The N-terminal phosphorylation of p53 at Ser_{15} (mouse Ser_{18}) and Ser_{20} (mouse Ser_{23}) is generally thought to stabilize p53 by preventing or disrupting the interaction between p53 and MDM2 (Appella et al., 2001, Shieh et al., 2000, Shieh et al., 1997). Additionally, the stabilization of p53 also is known to occur in response to oncogene activation, which leads to inhibition of the p53-MDM2 interaction primarily via upregulation of the p14 alternate reading frame (p14ARF) tumor suppressor, which binds to the p53-MDM2 complex to inhibit MDM2-mediated p53 ubiquitination and degradation (Lowe et al., 2003, Sherr, 2006).

Following stabilization of p53, the second step in the classical model of p53 activation is the sequence-specific binding of p53 to DNA (el-Deiry et al., 1992). Indeed, a seminal discovery to the initial understanding of p53 function was the

observation that p53 is a sequence-specific DNA binding protein (Bargonetti et al., 1991, Kern et al., 1991). In this manner, tetrameric p53 binds DNA in a sequence-specific manner to a DNA consensus sequence consisting of either two inverted pentameric sequences containing 5'-PuPuPu-C(A/T) (T/A)GPyPyPy-3' (Pu and Py represent purines and pyrimidines, respectively) or a palindromic site with four five-base pair inverted repeats with a similar sequence (el-Deiry et al., 1992, Funk et al., 1992, Kern et al., 1991, Cho et al., 1994, Wang et al., 1995, Waterman et al., 1995). The importance of p53 binding to promoter regions of target genes in a sequence-specific manner is illustrated by the fact that the DNA binding domain of p53 is a "hot spot" for mutation in human cancer, as the overwhelming majority of p53 mutations occur within this region (Hainaut et al., 2000). This selective pressure illustrates that the sequence-specific DNA binding ability of p53 is critical for its anti-tumor effects.

In the classical model, p53 becomes posttranslationally modified following cellular stress, thereby facilitating p53 to bind promoter response elements in a sequence-specific manner via its conserved hydrophobic central core domain, while the basic C-terminal regulatory domain acts as a negative modulator that must be modified to allow this sequence-specific DNA binding (Appella et al., 2001). Indeed, the C-terminus of p53 undergoes significant posttranslational modifications, including phosphorylation, ubiquitination, methylation, sumoylation, and neddylation, which can modulate the ability of p53 to bind DNA (Appella et al., 2001, Brooks et al., 2003).

Following stabilization of p53 and sequence-specific DNA binding, the third step in the classical model of p53 activation is the transactivation or repression of target genes. This model suggests that p53 mediates transcriptional activation or repression of target genes simply by interacting with components of the basal transcription machinery, including general transcription factors such as TFIID, TFIIH, TAFII31, and TAFII70 (Xiao et al., 1994, Lu et al., 1995, Thut et al., 1995, Farmer et al., 1996) as well as components of SRB/mediator complexes (Thut et al., 1995, Gu et al., 1999). As described in the following section, this simplified model under-appreciates the complexity of p53 activation, the redundancy of pathways, and the additional necessary steps of p53 activation that are context- and stress-dependent.

5.3.2 The multiple layers of regulation surrounding p53 stabilization

A continuing study of p53 activation reveals increasing complexity in the number and extent of p53 posttranslational modifications. In addition, *in vivo* functional analysis of these sites from recent knockin mice studies suggests significant redundancy, indeed challenging current dogma regarding some of the classical regulatory events in p53 activation (Iwakuma et al., 2007, Marine et al., 2006, Wahl, 2006). While the classical model suggests the rapid N-terminal phosphorylation of p53 at Ser_{15} (mouse Ser_{18}) and Ser_{20} (mouse Ser_{23}) is crucial for p53 activation by disrupting the interaction between p53 and MDM2, thereby reducing p53 ubiquitination and degradation (Appella et al., 2001, Shieh et al.,

2000, Shieh et al., 1997), mouse knockin studies with individual mutations of these residues challenge the importance of modification of these individual sites in the stabilization of p53 *in vivo*. Indeed, knockin studies with a Ser_{18}→Ala ($S_{18}A$) point mutation results in no difference compared to wild-type mice in the extent of stress-induced p53 stabilization nor the extent of DNA binding to p53-dependent promoters (Chao et al., 2003, Sluss et al., 2004). Similar results were also observed with Ser_{23}→Ala ($S_{23}A$) point mutant mice (MacPherson et al., 2004, Wu et al., 2002). While more severe defects in p53 stabilization and function were seen with $S_{18}A/S_{23}A$ double mutant mice, these defects were still limited to specific tissues and primarily affected DNA damage-induced apoptosis rather than other p53 effector functions such as cell cycle arrest (Chao et al., 2006). These studies suggest that the dramatic results seen in the *in vitro* studies are only partially recapitulated *in vivo*, and therefore, that the physiologic requirement of p53 phosphorylation is context-dependent and may not be a universal prerequisite for p53 stabilization. This is consistent with studies showing that p53 activation can indeed occur in a phosphorylation-independent manner (Ashcroft et al., 1999, Ashcroft et al., 2000, Blattner et al., 1999, Wu et al., 2002).

Recently, more appreciation has been given to the notion that p53 activation *in vivo* requires not just the stabilization and activation of p53, but the release of p53 from active repression, termed “antirepression” (Kruse et al., 2009, Zilfou et al., 2009). This neglected step is based on observations that p53 has intrinsic

potency that is actively repressed by its negative regulators MDM2 and its homologue MDMX (also known as Mdm4) (Montes de Oca Luna et al., 1995, de Rozieres et al., 2000, Parant et al., 2001). Like MDM2, MDMX is a critical negative regulator of p53, however it lacks intrinsic E3-ligase activity for p53 (Marine et al., 2005). Indeed, both *Mdm2*- and *MdmX*-deficient mice display embryonic lethality which is rescued by the inactivation of p53 (Jones et al., 1995, Montes de Oca Luna et al., 1995, Parant et al., 2001, Migliorini et al., 2002) suggesting both of these proteins are required in a non-redundant manner to repress p53 activity. Moreover, inactivation of MDM2 induces p53-mediated apoptosis (de Rozieres et al., 2000) and mice containing a knockin p53 mutant that is able to bind DNA and transactivate some p53 targets, yet is defective in MDM2 binding, p53 L_{25}→Q,W_{26}→S (p53QS), is embryonic lethal (Johnson et al., 2005). Together, these studies support the observation that negative regulators suppress an active p53 and that antirepression of p53 is critical for its own activity.

Multiple layers of regulation exist on MDM2-mediated p53 stability. Notably, as described above, the tumor suppressor p14ARF, which interferes with the p53-MDM2 interaction thereby stabilizing p53 (Lowe et al., 2003). In addition, the transcription factor yin yang 1 (YY1) promotes ubiquitination of p53 by enhancing association between p53 and MDM2 (Sui et al., 2004). Conversely, the ribosomal proteins L5, L11, and L23 bind to and inhibit MDM2, leading to p53 activation upon ribosomal stress (Dai et al., 2004, Lohrum et al., 2003, Zhang et al., 2003).

Additional regulation exists in the determination that p53 ubiquitination can be reversed by deubiquitinating enzymes (DUBs), of which several ubiquitin (Ub)-specific proteases (USPs) have been shown to regulate the MDM2-p53 axis. USP7 (also known as HAUSP) deubiquitinates p53, leading to p53 stabilization and activation (Li et al., 2002a) while additionally deubiquitinates MDM2 and MDMX (Cummins et al., 2004, Li et al., 2004). In addition, USP10 specifically deubiquitinates p53, but not MDM2 and MDMX (Yuan et al., 2010), while USP29 deubiquitinates p53 (Liu et al., 2011a) and USP2 deubiquitinates MDM2 (Stevenson et al., 2007) and MDMX (Allende-Vega et al., 2010) but not p53. Recently, an enzyme from an additional class of DUBs was shown to suppress p53 independent of its catalytic activity, namely, the ovarian tumor (OTU) domain-containing protease Otubain 1, which suppresses MDM2-mediated p53 ubiquitination by inhibiting the activity of the MDM2 cognate Ub-conjugating enzyme (E2) UbcH5 (Sun et al., 2012). Together, these studies illustrate how the model of p53 stabilization has shifted from a previous focus on simply the phosphorylation of p53 to a greater understanding of the extent to which de-repression of MDM2 and MDMX is required for efficient p53 stabilization and activation.

5.3.3 p53 is bound to DNA in unstressed cells

Along with sequence-specific DNA binding by p53, recent studies have shown that the C-terminal regulatory domain mediates structure-specific p53

DNA binding and that a significant portion of p53 is bound to DNA in unstressed cells via the C-terminal domain (Liu et al., 2004). Indeed, an unbiased global chromatin immunoprecipitation analysis revealed that the C-terminal region enhances non-sequence-specific binding of p53 to genomic DNA and that, surprisingly, only 5% of genomic DNA fragments bound to p53 contain p53 consensus sites (Liu et al., 2004). This is consistent with studies combining chromatin immunoprecipitation with high-density oligonucleotide microarrays demonstrating that only 2% of binding events between p53 and genomic DNA contain p53 consensus sites (Cawley et al., 2004). Additional studies determined that not only is p53 nonspecifically bound to DNA in unstressed cells via its C-terminal region, but that p53 can specifically bind consensus sequences within the promoters of its target genes such as p21 (Kaeser et al., 2002, Szak et al., 2001). Consistent with this determination, analysis of transcription initiation components associated with p53 target gene promoters in unstressed cells revealed that basal levels of p53 are required for assembly of a paused RNA polymerase II initiation complex on the p21 promoter (Espinosa et al., 2003). Together, these studies demonstrate that p53 can ubiquitously bind genomic DNA via its C-terminal region as well as bind the promoters of certain target genes in unstressed cells.

While the traditional view holds that p53 requires stress-induced activation to bind DNA (Hupp et al., 1992), this assertion has been challenged by studies using larger DNA fragments as targets (Cain et al., 2000, Kim et al., 1999).

Indeed, these studies demonstrate that the binding of p53 to DNA is dependent on additional factors such as DNA structure and topology, including conformational alterations within p53 responsive sites. While there is no question that p53 DNA binding is crucial for its function, recent studies illustrate the complex nature of this process. Together, these findings challenge the classical model that sequence-specific DNA binding follows the stress-induced stabilization of p53 and suggest that p53 has ubiquitous DNA binding activity. However, whether the p53 molecules bound to DNA in unstressed cells are transcriptionally active or are inactive due to repression by MDM2 or MDMX remains uncertain.

5.4 Promoter-specific activation by p53

5.4.1 The barcode hypothesis

Initially it was proposed that promoter selectivity was driven by promoter affinity and the levels of p53 induced following stress (Vousden, 2000). This model was based on studies suggesting cell-cycle arrest genes are regulated through high affinity promoters, while apoptosis-related genes were conversely regulated via low affinity promoters and require additional factors for activation (Inga et al., 2002). In this setting, low levels of stress or DNA damage would result in the activation of genes with high-affinity promoters, such as cell-cycle arrest genes, but when p53 levels are high, apoptotic genes with low affinity promoters can be activated (Chen et al., 1996, Weinberg et al., 2005, Inga et al.,

2002).

While this model takes into account the affinity of p53 for various response elements within the promoters of target genes, it does not address the role of posttranslational modifications of p53 or recruitment of cofactors that may, in turn, influence the ability of p53 to bind promoter sequences. Indeed, where this classical model falls short is in the understanding or appreciation of the complexity of achieving promoter specificity. While a thorough understanding of p53 promoter selection is in its infancy, it is now known to be influenced by numerous factors, including posttranslational modifications of p53 that can facilitate recruitment of p53 binding proteins that may function as activators or repressors (Kruse et al., 2009). In this manner, p53 is at the hub of a stress response network, and the manner in which it responds to specific stimuli is determined by the dynamic contribution from protein cofactors and modifying enzymes. Recruitment of these factors results in various posttranslational modifications of p53 such as phosphorylation, acetylation, ubiquitination, methylation, sumoylation, and nedylation, each of which represent a bar from a “barcode”, and different combinations of bars form different barcodes which enable p53 to activate specific promoters and mediate different cellular responses (Figure 5.4) (Murray-Zmijewski et al., 2008, Kruse et al., 2009, Toledo et al., 2006).

5.4.2 Overview of p53 acetylation

A critical component of p53 transcriptional regulation is the function of histone acetyltransferases (HATs) (Brooks et al., 2003). Histones are highly alkaline nuclear proteins that package DNA into structural units called nucleosomes and are the principal protein component of chromatin. Histones were the first identified proteins discovered to have acetyl groups covalently attached to lysine residues and since this seminal discovery, histone acetylation has been established as an essential element of transcriptional regulation (Jenuwein et al., 2001). Indeed, the complexity of histone acetylation in transcriptional regulation is analogous to p53 regulation, as histone-specific modifications have been colloquially referred to as the 'histone code' (Strahl et al., 2000). Subsequent studies determined that non-histone proteins were also acetylated and that non-histone protein acetylation is an essential regulatory step controlling diverse cellular processes such protein folding, cellular metabolism, and transcription (Kim et al., 2006, Choudhary et al., 2009, Wang et al., 2010b, Zhao et al., 2010). Indeed, p53 was the first non-histone protein identified as functionally regulated by acetylation and deacetylation (Gu et al., 1997, Luo et al., 2000, Luo et al., 2001, Vaziri et al., 2001). Later work determined that acetylation of p53 is a crucial regulatory element controlling promoter-specific activation of p53 target genes following stress stimuli (Berger, 2010, Kruse et al., 2009).

There are 13 sites of acetylation on human p53 that have been identified thus far (Figure 5.5), these include three lysine residues within the DNA-binding

domain (K_{120}, K_{164}, K_{292}), one lysine in a linker region between the DNA binding domain and tetramerization domain (K_{305}), one in the tetramerization domain (K_{320}), as well as eight lysines in the C-terminal region (K_{351}, K_{357}, K_{370}, K_{372}, K_{373}, K_{381}, K_{382}, and K_{386}) (Meek et al., 2009, Kruse et al., 2009, Brooks et al., 2011). Importantly, many of these lysines residues targeted for acetylation can also be ubiquitinated (as well as methylated or neddylated), and these modifications are mutually exclusive events that mediate different p53 responses (described in section 5.4.5) (Meek et al., 2009).

The acetylation of p53 is predominantly mediated by the histone acetyltransferase cyclic adenosine monophosphate (cAMP) response element-binding (CREB)-binding protein (CBP)/p300 (Gu et al., 1997, Liu et al., 1999, Sakaguchi et al., 1998, Iyer et al., 2004). CBP/p300 interacts with p53 and is recruited to the promoter regions of p53 target genes. The CBP/p300 interaction enhances both histone and p53 acetylation, resulting in a more accessible chromatin conformation and a more active p53 protein, respectively (Chan et al., 2001, Goodman et al., 2000). Specifically, CBP/p300 acetylates all eight of the C-terminal lysines in p53 (K_{370}, K_{372}, K_{373}, K_{381}, K_{382}, and K_{386}), two residues in the DNA-binding domain (K_{164} and K_{292}), as well as K_{305} (Gu et al., 1997, Sakaguchi et al., 1998, Liu et al., 1999, Wang et al., 2003, Tang et al., 2008, Brooks et al., 2011). However, p53 acetylation is not limited to that mediated by CBP/p300, as p53 can recruit additional transcriptional coactivators to modulate acetylation, including the p300/CBP-associated factor (PCAF), which acetylates p53 at K_{320}

(Sakaguchi et al., 1998, Liu et al., 1999), as well as Tip60/hMOF, a MYST family HAT unrelated to CBP/p300 that acetylates K_{120} (Sykes et al., 2006, Tang et al., 2006, Li et al., 2009b).

Since acetylation and ubiquitination are mutually exclusive events, p53 acetylation following DNA damage has been proposed to mediate the stabilization and activation of p53, in part because acetylated residues cannot be ubiquitinated by MDM2 (Sakaguchi et al., 1998, Ito et al., 2001, Li et al., 2002b). This is consistent with studies showing that p53 acetylation is increased following DNA damage and the level of stress-induced p53 acetylation correlates well with p53 activation and stabilization (Luo et al., 2001, Luo et al., 2000, Vaziri et al., 2001, Knights et al., 2006, Ito et al., 2001).

5.4.3 p53 acetylation mutants reveal complex phenotypes

Multiple studies have sought to investigate the roles played by p53 acetylation sites *in vitro* by overexpression studies as well as *in vivo* using knockin mice in which lysine to arginine substitutions were made at the indicated sites. Indeed, mice substituted at six C-terminal lysines (p53-6KR) show impaired gene expression in a promoter-specific manner following DNA damage in both embryonic stems cells and thymocytes, but not in embryonic fibroblasts (Feng et al., 2005). While this is consistent with a role for p53 acetylation in p53-dependent transactivation following DNA damage, these data also reveal that there is cell-type specificity, as the most dramatic differences were observed in

embryonic stem cells, intermediate differences seen in thymocytes, while no significant changes in gene expression were observed in embryonic fibroblasts (Feng et al., 2005). In a similar study, embryonic fibroblasts generated from p53-7KR knockin mice (in which seven C-terminal lysines were substituted to arginine) did not show significant differences in p53-induced growth arrest or apoptosis (Krummel et al., 2005). Interestingly, both the 6KR and 7KR mice develop normally and show no increased susceptibility to spontaneous tumor formation (Feng et al., 2005, Krummel et al., 2005). Together, these studies show that the importance of C-terminal p53 acetylation is context-dependent. While there are some transcriptional defects in a cell-type- and promoter-specific manner, these mice lack an overt defect or phenotype expected based on the results obtained from *in vitro* studies, suggesting p53 acetylation is more complicated than previously expected.

Indeed, subsequent studies determined that p53 acetylation was not limited to the C-terminal region and in fact, the DNA binding domain contains additional functional acetylation sites at K_{120} and K_{164} (Sykes et al., 2006, Tang et al., 2006). These studies determined that the Tip60/hMOF-mediated acetylation of K_{120} is essential for p53-mediated apoptosis, but dispensable for cell-cycle arrest, as transactivation of the pro-apoptotic genes PUMA and Bax were impaired with a K_{120}→R mutant, but there was no obvious effect on the expression of p21 and MDM2 (Sykes et al., 2006, Tang et al., 2006). Consistent with these studies, knockin mice in which K_{117} (K_{120} in humans) is substituted with an arginine, are

abolished for p53-mediated apoptosis, yet cell-cycle arrest and senescence pathways remain unaffected (Li et al., 2012). Additionally, K_{164} was identified as a novel CBP/p300-mediated acetylation site located within the DNA binding domain (Tang et al., 2008). Interestingly, both K_{120} and K_{164} are highly conserved residues that are frequently mutated in human cancers (Hainaut et al., 2000) and simultaneous substitution of both of these lysines with arginines in knockin mice completely abolishes p53-mediated cell-cycle arrest, apoptosis, and senescence *in vivo* (Li et al., 2012). However, while p53-null mice rapidly develop spontaneous thymic lymphomas (Donehower et al., 1992, Jacks et al., 1994, Lozano, 2010), neither p53-K_{117}→R mice nor p53-3KR mice, in which all DNA-binding domain lysines are simultaneously substituted with arginines (including mouse K_{117}, K_{161}, and K_{162} (K_{120}, K_{164}, and Q_{165} in human)), are susceptible to early onset tumorigenesis (Li et al., 2012). This is consistent with the studies in C-terminal acetylation deficient mice (Feng et al., 2005, Krummel et al., 2005). Together, these results demonstrate that tumor suppression can be mediated by an acetylation-deficient p53 protein that lacks the ability to induce cell-cycle arrest, apoptosis, and senescence, suggesting that other aspects of p53 function are crucial for its tumor suppressive functions (Li et al., 2012).

A recent study performed a comprehensive mutational analysis of the major sites of p53 acetylation (Tang et al., 2008). Consistent with the knockin mice studies (Feng et al., 2005, Krummel et al., 2005), substitution of individual lysines or groups of lysines had only subtle effects on the p53-mediated expression of

target genes when expressed at physiological levels in cultured cells. Indeed, these studies demonstrated that mutational loss of acetylation at K_{120}, K_{164}, or the 6KR sites can be compensated by acetylation at others sites, resulting in p53 activation and the subsequent p53-mediated transcription of p21 following DNA damage. However, simultaneous loss of acetylation at all eight major acetylation sites (p53-8KR) completely abolished p53-mediated expression of p21 and growth suppression following DNA damage. Moreover, p53-mediated expression of both cell-cycle and apoptotic genes was completely abrogated in the p53-8KR mutant, suggesting p53 acetylation is indispensable for p53 activation and effector function (Tang et al., 2008).

Importantly, while loss of acetylation in the p53-8KR mutant abolishes p53-mediated transactivation of cell-cycle arrest and apoptosis genes, this action is promoter-specific, as p53-8KR can still function as a DNA-binding transcription factor that can fully mediate the expression of MDM2 (Tang et al., 2008). These promoter-specific effects suggest that while acetylation of p53 plays an essential role in p53 effector function, it does not affect the p53-MDM2 negative feedback loop (Tang et al., 2008, Kruse et al., 2009, Li et al., 2012). Importantly, these studies suggest that there is a degree of redundancy between acetylation sites that allows compensation by remaining sites when one or more is mutated.

5.4.4 Acetylation mediates anti-repression and promoter-specific activation by p53

A current model of p53 activation proposed by Kruse and colleagues suggests that p53 is bound to promoters of p53 target genes, but is prevented from interacting with the transcriptional machinery via its association with the negative regulators MDM2 and MDMX (Kruse et al., 2009, Zilfou et al., 2009, Meek et al., 2009). Following DNA damage, p53 is acetylated by the HATs CBP/p300, PCAF, and Tip60/hMOF, and the acetylation of p53 subsequently disrupts its interaction with MDM2 and MDMX (Tang et al., 2008, Kruse et al., 2009). Consistent with this determination, the interaction of wild-type p53 with MDM2 and MDMX on the *p21* or *PIG3* promoters can be competitively disrupted by increased expression of the HATs CBP/p300 or Tip60, however the interaction between MDM2 and MDMX with the acetylation deficient p53 mutant (8KR) cannot be disrupted by HAT expression (Tang et al., 2008). This release of MDM2 or MDMX from promoter-bound p53 following acetylation is termed ‘antirepression’, and is proposed to be a necessary step for p53 activation (Tang et al., 2008, Kruse et al., 2009, Zilfou et al., 2009).

These studies suggest that distinct mechanisms induce different classes of genes following DNA damage and that p53 can activate at least three classes of target genes to mediate various effector functions depending on the nature of the stress and cell-type affected (Kruse et al., 2009, Zilfou et al., 2009). The first class of p53 target genes induced are negative regulators of p53, such as MDM2, which prevent deleterious effects on cell viability by attenuating p53 activation. Expression of these genes is mediated in an acetylation-independent

manner and does not require recruitment of coactivators such as CBP/p300 or Tip60/hMOF (Tang et al., 2006, Tang et al., 2008). The second class of p53 target genes induced include those involved in growth arrest, in particular p21, and this step absolutely requires recruitment of coactivators such as CBP/p300 or Tip60/hMOF (Sykes et al., 2006, Tang et al., 2006, Tang et al., 2008). Interestingly, while there is a complete loss of p21 induction when all major acetylation sites are mutated, demonstrating the requirement for p53 acetylation in p21 expression (Tang et al., 2008), this effect can be reversed by partial acetylation of p53 suggesting p21 induction is redundantly regulated via the acetylation of p53 at multiple sites (Tang et al., 2006, Tang et al., 2008). The third class of p53 target genes are those involved in the induction of apoptosis, such as PUMA, Bax, and NOXA. Given the irreversible nature of the apoptotic response, the requirement for transcription of this class of genes is more stringent than the previous and requires the recruitment of coactivators, specific modifications (e.g. p53 K_{120} acetylation), and complete removal of MDM2- and MDMX-mediated repression from target gene promoters (Sykes et al., 2006, Tang et al., 2006, Tang et al., 2008, Li et al., 2009b).

Based on these proposed mechanisms, a refined three-step model for promoter-specific p53 activation was proposed (Figure 5.6) (Kruse et al., 2009). In this model, the first step is the stabilization of p53 following DNA damage, which primarily occurs through inhibition of MDM2-mediated ubiquitination and degradation of p53. The second step is the release of p53 from MDM2- and

MdmX-mediated inhibition, termed “antirepression”. This process requires acetylation of p53 and results in the transactivation of select p53 target genes, such as p21 or other growth arrest genes. The third step is the recruitment and interaction of numerous cofactors with p53 to facilitate the formation of regulatory complexes and various posttranslational modifications, resulting in full activation of target gene expression (Kruse et al., 2009).

5.4.5 Additional modifications fine-tune the p53 stress response

Acetylation and ubiquitination are not the only modifications competing for lysine residues on p53. Indeed, various methyltransferases have been shown to methylate p53’s C-terminal lysines to modulate p53 function. For instance, while Set7/9-mediated monomethylation of K_{372} promotes p53-mediated transactivation of p21 (Chuikov et al., 2004), monomethylation of K_{370} and K_{382} by SET and MYND domain containing 2 (Smyd2) and Set8/PR-Set7, respectively, represses p53 function (Huang et al., 2006, Shi et al., 2007). Moreover, dimethylation of K_{370} and K_{382} creates a binding site for the DNA repair protein p53-binding protein 1 (53BP1), which regulates p53 promoter specificity following DNA damage (Iwabuchi et al., 1994). Furthermore, the levels of p53 dimethylation increase following DNA damage, thereby facilitating the p53-53BP1 interaction. However, the binding of p53BP1 to dimethylated sites is disrupted by the demethylase activity of lysine-specific demethylase 1 (LSD1), which specifically demethylates p53 K_{370} (Huang et al., 2007). The role for methylation in p53 regulation is

supported by additional studies demonstrating that both p53 (Jansson et al., 2008) and nearby histones (An et al., 2004) are arginine methylated following DNA damage. Specifically, protein arginine N-methyltransferase 1 (PRMT1)-mediated methylation of p53 and histones regulates the expression of p53 targets genes (An et al., 2004), while protein arginine N-methyltransferase 5 (PRMT5)-mediated methylation alters target gene specificity of p53 (Jansson et al., 2008).

Additional competition at C-terminal lysines is mediated by the small ubiquitin-like modifier (SUMO) (Melchior et al., 2002) and the small ubiquitin-like protein Nedd8 (Xirodimas et al., 2004, Abida et al., 2007). The role of p53 sumoylation at K_{386} is incompletely understood, with some studies suggesting that p53 sumoylation promotes p53 transcriptional activity (Melchior et al., 2002), while others report that sumoylation promotes p53 nuclear export (Carter et al., 2007). The C-terminal neddylation of p53 has been demonstrated to repress p53 transactivation function via MDM2-mediated neddylation of K_{370}, K_{372}, and K_{373} (Xirodimas et al., 2004) and F-box only protein 11 (FBXO11)-mediated neddylation of K_{320} and K_{321} (Abida et al., 2007). So while acetylation, ubiquitination, methylation, sumoylation, and neddylation all compete for p53's C-terminal lysines, it is unclear to what extent methylation, sumoylation, and neddylation are required for p53 activation *in vivo*.

5.4.6 Deacetylation represses p53 transcriptional activation

Additional regulation of p53 transcriptional activation exists in the determination that p53 can be deacetylated by distinct histone deacetylase (HDAC) complexes containing HDAC1 (Luo et al., 2000) or the class III HDAC silent information regulator 2α (Sir2α)/SIRT1 (Luo et al., 2001, Vaziri et al., 2001), thereby mitigating the acetylation-dependent activation of p53 transcription. This type of regulation is analogous to the reversal of p53 ubiquitination by deubiquitinating enzymes to modulate the MDM2-p53 axis (described in section 5.3.2). Initially, p53 deacetylation was observed to be mediated by the p53 target protein in the deacetylase complex (PID)/HDAC1 complex, which deacetylates p53 following stress signals to repress p53 transcriptional activity (Luo et al., 2000). However, these studies observed that p53 acetylation remained unstable even in the presence of trichostatin A (TSA), which inhibits class I and II HDAC activity, suggesting there may yet be additional factors regulating p53 acetylation (Luo et al., 2000). Indeed, the determination that class III HDAC (SIRT1) deacetylase activity was resistant to TSA-mediated inhibition (Imai et al., 2000) suggested SIRT1 may additionally target p53. Subsequent work determined that p53 is indeed a SIRT1 substrate (Luo et al., 2001, Vaziri et al., 2001) and that SIRT1 binds the lysine-rich C-terminal region of p53 (Langley et al., 2002) to induce p53 deacetylation and thereby regulate p53 transcriptional activities and function (Luo et al., 2001, Vaziri et al., 2001, Langley et al., 2002). The role of SIRT1-mediated deacetylation of p53 is an essential component of this dissertation and will be further described in section 5.5.3.

5.5 The diverse biology of SIRT1

5.5.1 The identification and function of SIRT1

There are seven members of the evolutionarily conserved silent information regulator (SIRT or Sirtuin) family of nicotinamide adenine dinucleotide (NAD^+)-dependent protein deacetylases and adenosine diphosphate (ADP)-ribosylases that differ in their subcellular localization, substrate specificities, and functions (Horio et al., 2011, Cen et al., 2011, Haigis et al., 2010). Initial studies observed that while SIRT1, SIRT6, and SIRT7 are predominantly nuclear, SIRT2 is cytoplasmic and SIRT3, SIRT4, and SIRT5 are localized to the mitochondria (Michishita et al., 2005). Sirtuins catalyze the hydrolysis of NAD^+ to mediate the transfer of an acetyl group to the 2'-OH position of ADP-ribose to form 2'-O-acetyl-ADP-ribose, nicotinamide, and a deacetylated protein (Tanner et al., 2000, Yang et al., 2006). To note, while all seven Sirtuins are classified as protein deacetylases based on structural homology, little or no lysine deacetylase activity has been observed with SIRT4 or SIRT6 and the primary enzymatic activity of SIRT4-7 is ADP ribosylation (Mahlknecht et al., 2009, Pan et al., 2011).

Human SIRT1 is the first identified and most widely studied member of the Sirtuin family (Tanner et al., 2000, Tanno et al., 2007). SIRT1 is the mammalian ortholog to the yeast Sir2 (silent information regulator 2), which regulates aging and lifespan in several lower organisms (Lin et al., 2000, Tissenbaum et al., 2001, Wood et al., 2004). Early reports in yeast determined that Sir2 associates

with heterochromatin and functions to silence transcription at silent mating loci (Rine et al., 1987), telomeres (Gottschling et al., 1990), and ribosomal DNA (Bryk et al., 1997, Smith et al., 1997) as well as suppresses recombination in ribosomal DNA (Gottlieb et al., 1989) and enhances replicative lifespan (Kaeberlein et al., 1999). Interestingly, it was discovered that yeast cells lacking Sir2 had reduced replicative lifespan, while those containing an extra copy of Sir2 had significantly increased lifespan compared to wild-type cells (Kaeberlein et al., 1999). Key studies determined that overexpression of Sir2 promotes global histone deacetylation (Braunstein et al., 1996, Braunstein et al., 1993), suggesting Sir2 may have a novel role in histone deacetylation. Indeed, this lead to the seminal discovery that Sir2/SIRT1 is an NAD^+-dependent histone deacetylase, which deacetylates lysine 26 in histone 1 (H1), lysines 9 and 14 in histone 3 (H3) and lysine 16 in the N-terminal tail of histone 4 (H4) (Imai et al., 2000, Vaquero et al., 2004). Importantly, mutational studies suggest these particular residues are acetylated in active chromatin and hypoacetylated in silenced chromatin (Thompson et al., 1994, Braunstein et al., 1996), consistent with the role of Sir2/ SIRT1 in transcriptional silencing. In addition, yeast show an age-associated increase in H4K16 acetylation and concomitant decrease in Sir2 protein that leads to reduced chromatin silencing (Dang et al., 2009). Together, these studies were instrumental in the investigations into the role of SIRT1 in aging, cancer, and metabolism.

5.5.2 The non-histone deacetylase functions of SIRT1

Along with the deacetylation of histones H1, H3, and H4, SIRT1 also deacetylates many non-histone proteins, suggesting the function of SIRT1 is not limited to epigenetic silencing. Indeed, one of the first non-histone substrates of SIRT1 identified was the tumor suppressor p53 (Luo et al., 2001, Vaziri et al., 2001). As described in the following section (5.5.3), SIRT1-mediated deacetylation of p53 represses p53-mediated transcriptional activities in response to DNA damage and oxidative stress (Luo et al., 2001, Vaziri et al., 2001, Langley et al., 2002).

Along with p53, SIRT1 deacetylates a diverse array of other non-histone proteins that have broad biological functions. In particular, SIRT1 deacetylates many proteins involved in energy and metabolism, including: coactivator peroxisome proliferator-activated receptor-γ (PPARγ) coactivator 1α (PGC-1α), a nuclear coactivator controlling genes involved in gluconeogenesis (Rodgers et al., 2005); the nuclear hormone receptors PPARγ (Picard et al., 2004, Moynihan et al., 2005, Banks et al., 2008, Han et al., 2010) and the liver X receptor (LXR) (Li et al., 2007), which regulate fatty acid/glucose metabolism and reverse cholesterol transport, respectively; the transcription factor sterol regulatory element-binding protein-1c (SREBP-1c), which controls hepatic lipogenesis (Ponugoti et al., 2010); as well as the metabolic enzyme acetyl coenzyme A (CoA) synthetase (AceCS1) (Hallows et al., 2006, North et al., 2007).

A number of SIRT1 substrates have been identified that function in cell

proliferation, cell growth, differentiation, and survival, such as: the androgen receptor (AR) in prostate cancer cells (Fu et al., 2006); the p53 family member p73, a putative tumor suppressor involved in cell-cycle and apoptosis (Dai et al., 2007); the forkhead transcription factors (FOXO), which regulate genes involved in cell growth, proliferation, differentiation, and longevity (Brunet et al., 2004, Motta et al., 2004, van der Horst et al., 2004, Xiong et al., 2011); the cell-cycle transcription factor E2F1 (Wang et al., 2006); phosphatase and tensin homolog (PTEN), a tumor suppressor regulating PI3K/AKT (Ikenoue et al., 2008); the cell migration protein cortactin (Zhang et al., 2009); β-catenin, a component of the Wnt signaling pathway (Firestein et al., 2008); the RelA/p65 subunit of the inflammation and immune regulator NF-κB (Yeung et al., 2004, Schug et al., 2010); and hypoxia-inducible factors HIF-1α, HIF-2α (Dioum et al., 2009, Lim et al., 2010, Leiser et al., 2010).

SIRT1 plays an additional role in the deacetylation of proteins critical in development, such as: Notch1 intracellular domain (NCID) (Guarani et al., 2011); the transcription factor myocyte enhancer factor 2 (MEF2) (Zhao et al., 2005); the muscle differentiator MyoD (Fulco et al., 2003); and the transforming growth factor (TGF)-β-induced signaling protein mothers against decapentaplegic homolog 7 (SMAD7) (Kume et al., 2007). Interestingly, SIRT1 was identified as regulating proteins involved in circadian rhythm and neurodegeneration, including: the circadian rhythm/clock proteins brain and muscle Arnt-like protein 1 (BMAL1) and Per2 (Nakahata et al., 2008, Asher et al., 2008); the neuroprotector

insulin receptor substrate-1 (IRS-1) (Li et al., 2008); and the neurodegeneration related protein Tau (Min et al., 2010).

Importantly, SIRT1 plays a role in DNA repair processes and chromatin remodeling by deacetylating proteins such as: the DNA repair protein Ku70 (Jeong et al., 2007); the nucleotide excision repair protein xeroderma pigmentosum complementation group A (XPA) (Fan et al., 2010); the base excision repair protein apurinic/apyrimidinic endonuclease 1 (APE1) (Yamamori et al., 2010); the acetyltransferases PCAF (Pediconi et al., 2009), Tip60 (Wang et al., 2010a), and p300 (Bouras et al., 2005); as well as the histone methyltransferase SUV39H1 (Vaquero et al., 2007).

Given the tremendous number of substrates and the biologic complexity of these potential targets, SIRT1 has been associated with diverse normal and abnormal processes such as aging, neural plasticity, memory, metabolism, inflammation, immunity, neurodegeneration, and cancer (Haigis et al., 2010, Saunders et al., 2007). Indeed, SIRT1 activity has broad biological implications, that while intriguing and relevant to the diversity of SIRT1 functions, are outside the scope of this dissertation and have been well described elsewhere (Horio et al., 2011, Haigis et al., 2010, Stunkel et al., 2011). Therefore, the following section (5.5.3) will focus on SIRT1-mediated deacetylation of p53.

5.5.3 SIRT1-mediated deacetylation of p53

SIRT1 was identified as a p53 deacetylase that negatively regulates p53

transcriptional activation (Luo et al., 2001, Vaziri et al., 2001, Langley et al., 2002). Elegant cell culture studies demonstrate that overexpression of SIRT1 strongly represses p53 transcriptional activity and p53-dependent apoptosis following DNA damage and oxidative stress (Luo et al., 2001, Vaziri et al., 2001). Conversely, expression of a catalytically inactive SIRT1 mutant, in which a highly conserved histidine residue in the catalytic core is mutated to tyrosine (SIRT1-$H_{363}Y$), effectively abolishes SIRT1 deacetylase activity and consequently, increases p53 acetylation levels (Luo et al., 2001, Vaziri et al., 2001). Moreover, this dominant negative SIRT1 was able to increase the expression levels of the p53 targets p21 and Bax, as well as sensitize cells to apoptosis following ionizing radiation, chemotherapeutic treatment, and oxidative stress, consistent with the positive regulatory effects of acetylation on p53 activity (Luo et al., 2001). The role of SIRT1 in p53 regulation was confirmed *in vivo* in subsequent studies that analyzed p53 acetylation and apoptosis following ionizing radiation in SIRT1-deficient mice (Cheng et al., 2003). These studies observed that p53 is hyperacetylated in SIRT1-deficient mice and cells from these mice are sensitized to radiation-induced apoptosis (Cheng et al., 2003).

Following the determination that SIRT1-mediated deacetylation of p53 regulates transcription-dependent apoptosis, subsequent studies observed that SIRT1 additionally plays a role in p53 transcription-independent apoptosis (Han et al., 2008). These studies show that oxidative stress induced by increased intracellular reactive oxygen species (ROS) results in the translocation of p53 to

mitochondria and induction of apoptosis in wild-type mouse embryonic stem (mES) cells. However, in SIRT1-null mES cells, p53 fails to translocate to mitochondria and instead localizes to the nucleus. These findings suggest SIRT1 facilitates p53-mediated mitochondria apoptosis by deacetylating p53, thereby blocking its nuclear translocation following oxidative stress (Han et al., 2008). However, whether this function of SIRT1 is specific to mES cells or extends to additional cell types following DNA damage remains unclear.

5.6 Regulation of SIRT1

5.6.1 Transcriptional and posttranscriptional control of SIRT1 expression

The role of SIRT1 deacetylase activity in diverse cellular processes is underscored by the multiple layers of regulation that exist on SIRT1 expression and function. Indeed, several mechanisms modulate SIRT1 expression at the transcriptional and posttranscriptional levels (Liu et al., 2009, Zschoernig et al., 2008). The induction of SIRT1 transcription is tightly controlled by at least two negative feedback loops. In one of these regulatory loops, the cell cycle regulator E2F1 directly binds the SIRT1 promoter and induces SIRT1 transcription following DNA damage (Wang et al., 2006). Reciprocally, E2F1 is also a substrate of SIRT1 and deacetylation of E2F1 inhibits its transcriptional activities (including SIRT1) (Wang et al., 2006). Thus, the E2F1-SIRT1 negative feedback loop illustrates an additional layer of complexity governing cell survival pathways following DNA damage.

There exists another well known SIRT1 substrate that functions in a negative feedback loop to control SIRT1 expression. Indeed, while SIRT1-mediated deacetylation of p53 attenuates p53-dependent transcriptional activities (Luo et al., 2001, Vaziri et al., 2001), p53 can also bind the SIRT1 promoter to directly repress SIRT1 transcription (Nemoto et al., 2004). Consistent with this finding, p53-null mice and tumor cells lines have increased levels of SIRT1 in a tissue- and cell type-specific manner, respectively (Ford et al., 2005, Nemoto et al., 2004). Transcription of SIRT1 is also repressed by the tumor suppressor hypermethylated in cancer 1 (HIC1), which forms a transcription corepression complex with C-terminal binding protein 1 (CTBP1) that binds enhancer elements upstream of the SIRT1 promoter to inhibit SIRT1 transcription (Chen et al., 2005).

Regulation of SIRT1 expression is not limited to the control of transcription, as additional mechanisms exist to regulate the stability of *SIRT1* mRNA. Indeed, the oncogenic RNA binding protein HuR binds the 3'-untranslated region (UTR) of *SIRT1* mRNA, stabilizing the transcript and thus increasing *SIRT1* mRNA expression (Abdelmohsen et al., 2007). Moreover, ATM-mediated signaling following DNA damage leads to the phosphorylation and activation of the tumor suppressor cell cycle checkpoint kinase 2 (Chk2), which phosphorylates HuR, disrupting HuR-mediated stabilization of *SIRT1* mRNA, thereby reducing SIRT1 expression and promoting p53-mediated responses following DNA damage (Abdelmohsen et al., 2007).

Recently, the tumor suppressive microRNA (miR)-34a was shown to bind the 3'-UTR of *SIRT1* mRNA, repressing SIRT1 expression and leading to the hyperacetylation of p53 (Yamakuchi et al., 2008). Interestingly, miR-34a is also a p53 target (Chang et al., 2007, Tazawa et al., 2007, He et al., 2007, Tarasov et al., 2007, Raver-Shapira et al., 2007), suggesting the existence of a positive feedback loop between miR-34a and p53 and further underscoring the complexity of networks that regulate the SIRT1-p53 pathway.

5.6.2 Modulation of SIRT1 deacetylase activity by protein-protein interactions

This diversity of substrates, together with the lack of a defined consensus sequence (Blander et al., 2005), suggests SIRT1 substrate specificity may be mediated by potential SIRT1 chaperones or binding partners that form regulatory complexes with SIRT1. In support of this notion, SIRT1 deacetylase activity can be modulated by direct interaction with other cellular proteins, including active regulator of SIRT1 (AROS) (Kim et al., 2007), the neuronal specific protein necdin (Hasegawa et al., 2008), the tumor suppressor deleted in breast cancer 1 (DBC1) (Kim et al., 2008, Zhao et al., 2008), the nuclear desumoylase sentrin-specific protease 1 (SENP1) (Yang et al., 2007), as well as the methyltransferase Set7/9 (Figure 5.7) (Liu et al., 2011b).

AROS was the first identified endogenous, direct regulator of SIRT1 (Kim et al., 2007). Specifically, AROS directly binds the N-terminus of SIRT1, enhancing SIRT1 deacetylase activity and reducing p53 acetylation, thereby attenuating

p53-dependent transcriptional activation following DNA damage (Kim et al., 2007). A second positive regulator of SIRT1, necdin, was identified shortly thereafter (Hasegawa et al., 2008). Necdin is a maternally imprinted gene that promotes cell differentiation and survival and is primarily localized in post-mitotic neurons (Jay et al., 1997). Necdin forms a complex with SIRT1 and p53 to enhance SIRT1-mediated deacetylation of p53 and attenuate p53-induced apoptosis following DNA damage (Hasegawa et al., 2008).

While AROS and necdin positively modulate SIRT1 deacetylase activity (Kim et al., 2007, Hasegawa et al., 2008), DBC1, which is homozygously deleted in some breast cancers, was identified as a native inhibitor of SIRT1 deacetylase activity by direct binding to the catalytic domain of SIRT1 (Kim et al., 2008, Zhao et al., 2008). Indeed, knockdown of DBC1 increases SIRT1-mediated p53 deacetylation, thereby reducing p53-mediated transcriptional activity. However, these effects can be abrogated via concomitant knockdown of SIRT1, suggesting DBC1 promotes p53 transcriptional activity in a SIRT1-dependent manner (Zhao et al., 2008). SIRT1 is additionally inhibited by SENP1-mediated desumoylation, in which SENP1 binds and desumoylates K_{734} in the C-terminus of SIRT1, reducing SIRT1 deacetylase activity and increasing p53 acetylation and activation following cellular stress signals (Yang et al., 2007). Recently, the methyltransferase Set7/9, which is also known to increase p53 transcriptional activation by monomethylating p53 K_{372} (Chuikov et al., 2004) (and described in section 5.4.5), was identified as a negative regulator of SIRT1-mediated

deacetylation of p53 (Liu et al., 2011b). Interestingly, these studies demonstrate that while Set7/9 can methylate SIRT1, the resulting methylation is dispensable for SIRT1-mediated deacetylation of p53. Rather, the physical interaction between Set7/9 and the N-terminus of SIRT1 induces the dissociation of SIRT1 from p53, thereby increasing p53 acetylation following DNA damage (Liu et al., 2011b).

Together, these proteins have provided insight into the complex regulation of SIRT1 and the SIRT1-p53 axis, however a complete picture of this regulation remains to be determined.

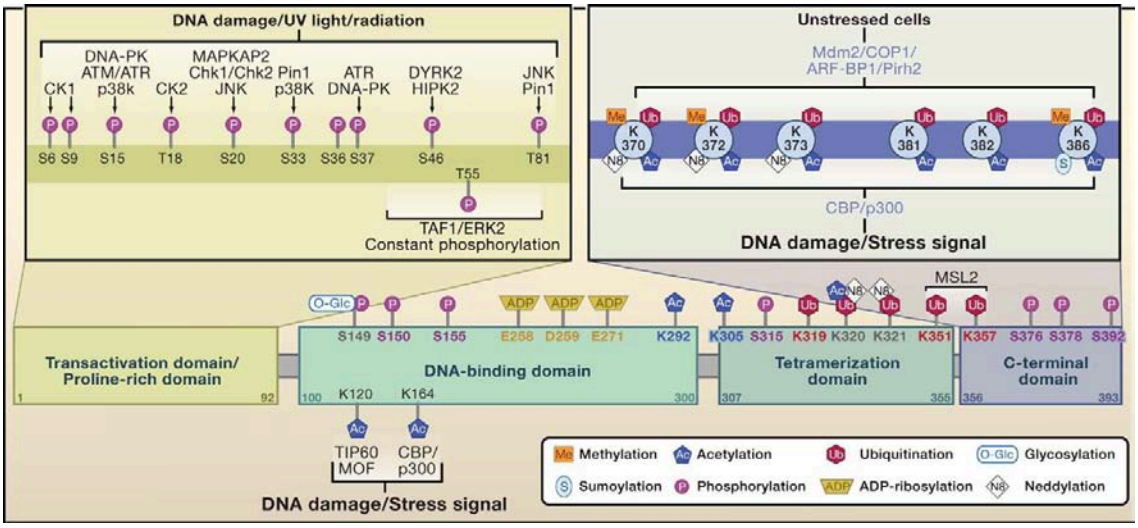

Figure 5.1. Overview of p53 posttranslational modifications.

Schematic of the principal functional domains of p53 are shown together with the major sites of p53 that undergo phosphorylation (P), acetylation (Ac), ubiquitination (Ub), neddylation (N8), sumoylation (S), methylation (Me), O-glycosylation (Glc), and ADP-ribosylation (ADP). Reproduced with permission from (Kruse et al., 2009). Copyright 2009 Elsevier.

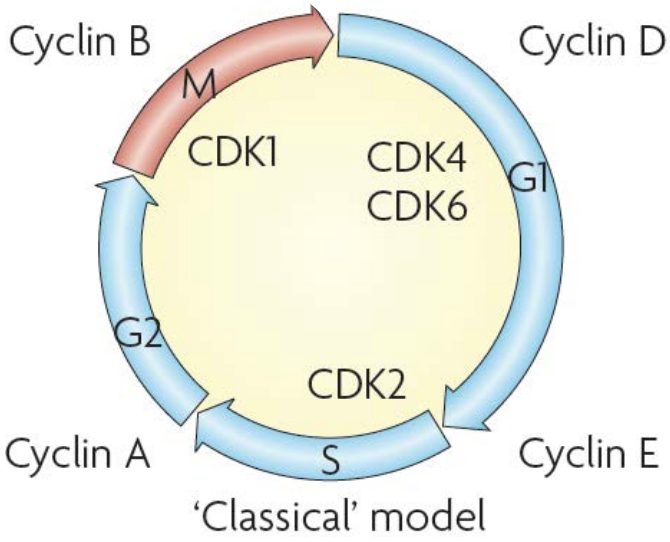

Figure 5.2. Overview of the cell cycle.

In the classical model, growth signals induce the expression of D-type cyclins that bind and activate CDK4/6 during G_1, leading to phosphorylation and partial inactivation of the retinoblastoma (Rb) protein family members Rb, p107, and p130. This leads to reduced inhibition of the transcription factor E2F, allowing expression of the E-type cyclins, which bind and activate CDK2. The pocket proteins are then further phosphorylated and completely inactivated by CDK2-cyclin E complexes, allowing E2F-mediated transcription to drive the G_1/S transition. Finally, A-type cyclins activate CDK2 and CDK1 to drive the S/M transition while B-type cyclins activate CDK1 to proceed though mitosis. Reproduced with permission from (Malumbres et al., 2009). Copyright 2009 Nature Publishing Group.

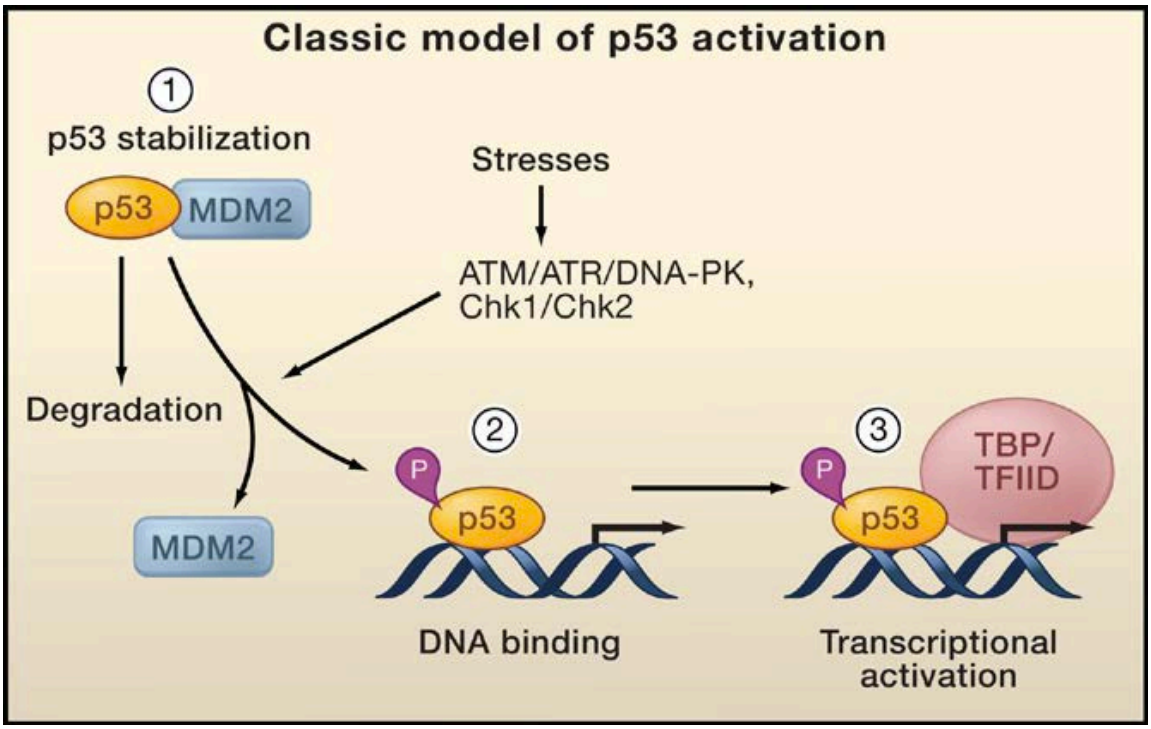

Figure 5.3. The classical model of p53 activation.

The classical model of p53 activation following cellular stress is described in three basic steps, **1)** stabilization of p53 mediated by phosphorylation (P), **2)** sequence-specific DNA binding, followed by **3)** association with the general transcriptional machinery and the subsequent transactivation of target genes. Reproduced with permission from (Kruse et al., 2009). Copyright 2009 Elsevier.

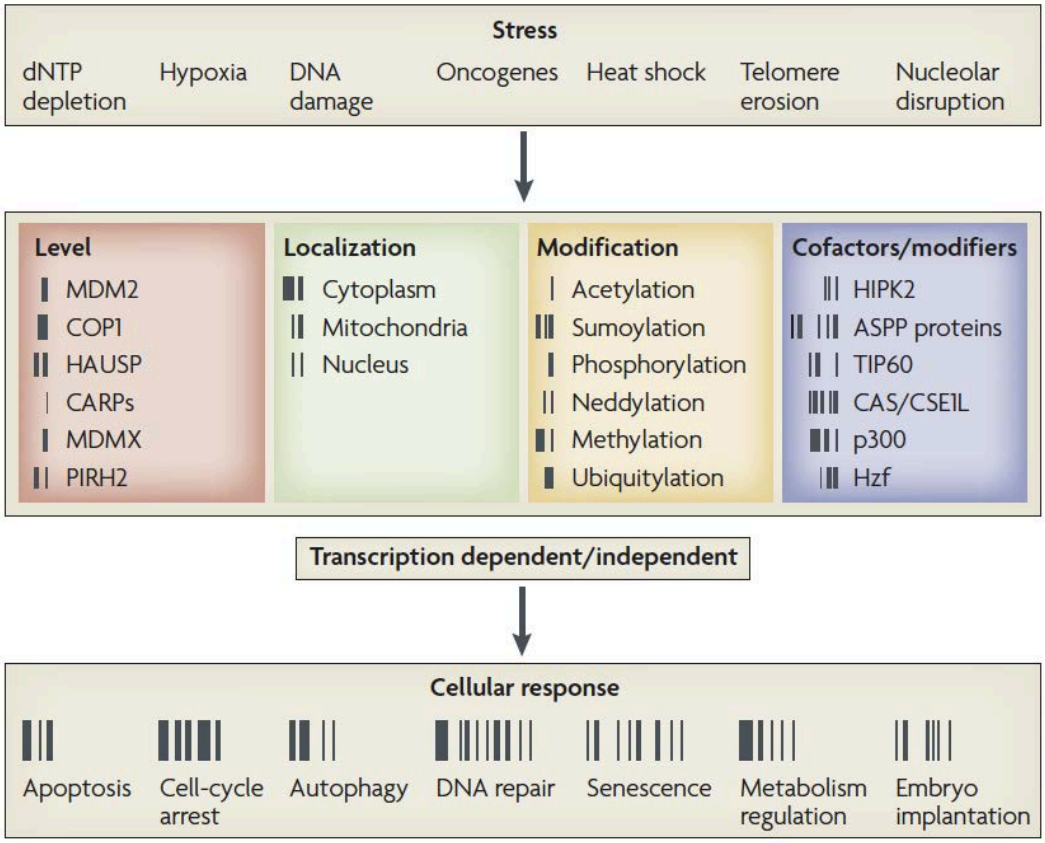

Figure 5.4. The p53 barcode hypothesis.

In this model, p53 is at the hub of a stress response network, and the manner in which it responds to specific stimuli is determined by combinations of various cofactors and modifying enzymes. Recruitment of these cellular facors results in various posttranslational modifications, each of which represent a bar from a "barcode", and different combinations of bars form different barcodes which enable p53 to activate specific promoters and mediate different cellular responses. Reproduced with permission from (Murray-Zmijewski et al., 2008). Copyright 2008 Nature Publishing Group.

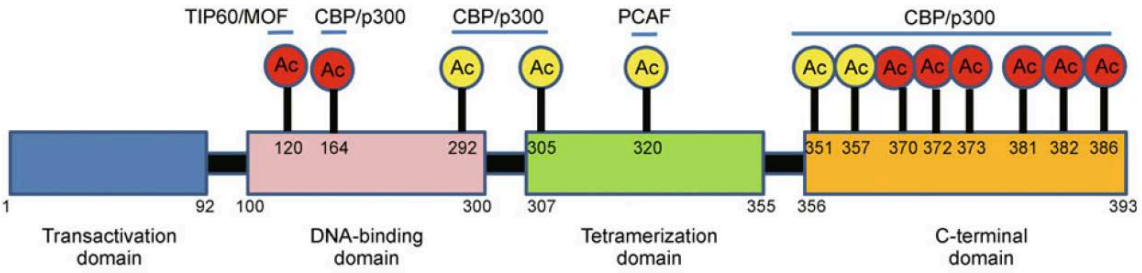

Figure 5.5. Diagram of identified p53 acetylation sites.

The eight acetylation sites that are indispensable for p53 activation are shown in red. The corresponding acetyltransferases are indicated. Reproduced with permission from (Brooks et al., 2011). Copyright 2011 Higher Education Press and Springer-Verlag Heidelberg.

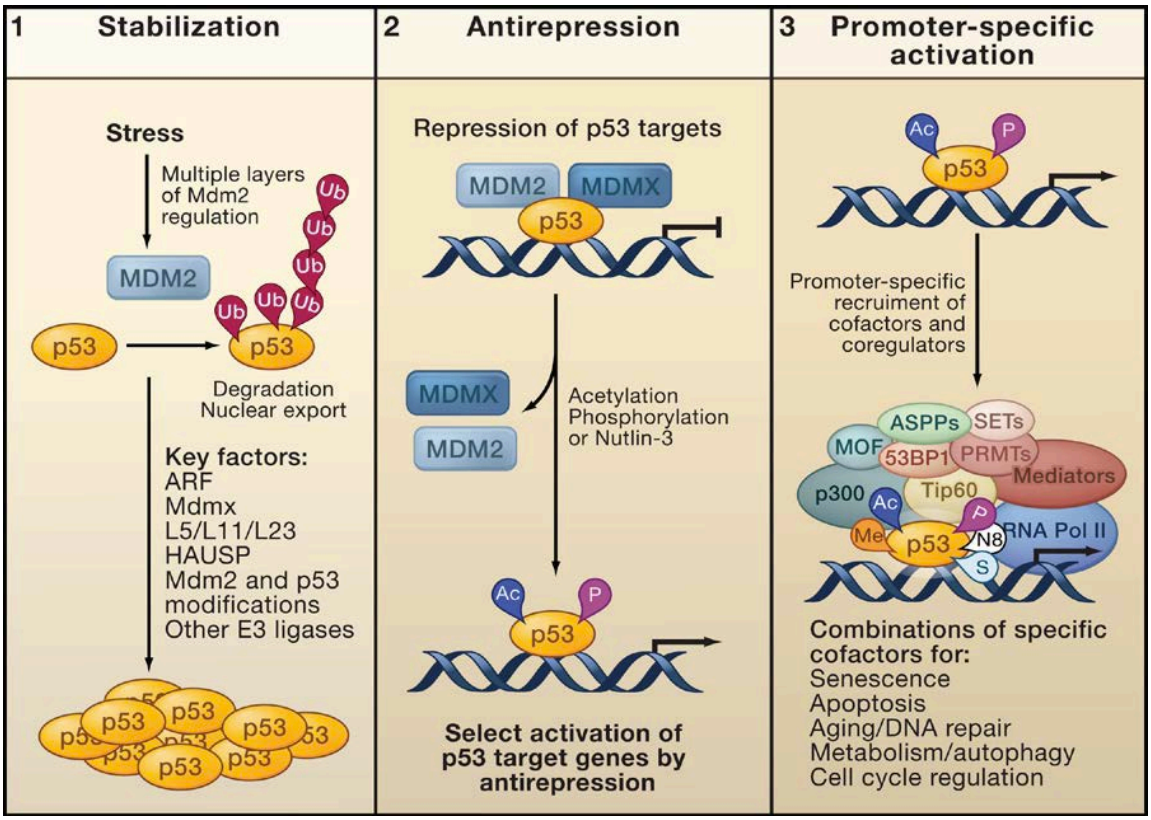

Figure 5.6. Promoter-specific activation of p53.

In this model, p53 activation occurs in three steps: **1)** stabilization, through inhibition of MDM2-mediated ubiquitination and degradation of p53, **2)** antirepression, by releasing p53 from MDM2- and MDMX-mediated inhibition, this requires p53 acetylation and results in the transactivation of select genes such as p21, and **3)** the recruitment and interaction of numerous cofactors by p53 to facilitate the formation of regulatory complexes and various posttranslational modifications, resulting in full activation of target gene expression. Reproduced with permission from (Kruse et al., 2009). Copyright 2009 Elsevier.

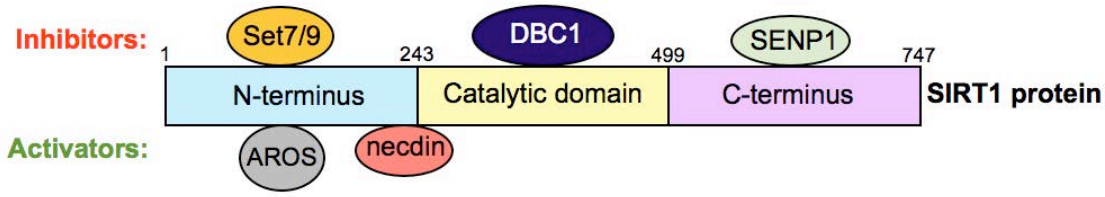

Figure 5.7. Regulation of SIRT1 by direct protein binding.

SIRT1 deacetylase activity can be modulated by direct interaction with other cellular proteins, including active regulator of SIRT1 (AROS), the neuronal specific protein necdin, the tumor suppressor deleted in breast cancer 1 (DBC1), the nuclear desumoylase sentrin-specific protease 1 (SENP1), as well as the methyltransferase Set7/9.

CHAPTER 6. PACS-2 regulates SIRT1-mediated deacetylation of p53 following DNA damage

PACS-2 regulates SIRT1-mediated deacetylation of p53 following DNA damage

Author contributions: In this chapter, Katelyn M. Atkins performed the apoptosis experiments (Figures 6.1A-B, 6.3A), clonogenic assays (Figures 6.1C, 6.3B), cell cycle analysis (Figure 6.2A), HCT116 qRT-PCR (Figures 6.2B-C), p21/p53 western blot analysis (Figures 6.3C-D, 6.6D), endogenous p53 immunoprecipitations and western blot analysis (Figures 6.4A, 6.6B-C), chromatin immunoprecipitations (Figure 6.4D), co-immunoprecipitation analysis (Figures 6.5A-B), *in vivo* p53 deacetylation assay (Figure 6.6A), and nuclear fractionations (Figures 6.7B-C); KMA and Laura L. Thomas (Thomas lab member) performed the thymus western blot and qRT-PCR analysis (Figure 6.4B-C) ; Laurel Thomas (Thomas lab member) performed the microscopy (Figure 6.7A); Jun Yin and Laura L. Thomas (Thomas lab members) performed the *in vitro* binding assay (Figure 6.5C); and Jimmy D. Dikeakos (University of Western Ontario, former Thomas lab member) designed the PACS-2 flag and PACS-2 mcherry constructs. The manuscript was written and prepared by Katelyn Atkins and Gary Thomas.

ABSTRACT

The acetylation of p53 is an essential step controlling promoter-specific activation of p53 target genes following DNA damage. The nicotinamide adenine dinucleotide (NAD^+)-dependent protein deacetylase sirtuin 1 (SIRT1) plays a decisive role in p53-mediated stress responses by deacetylating p53, thereby repressing p53 transcriptional activation. Whereas the cellular functions of SIRT1 have been extensively investigated, less is known regarding how the SIRT1-p53 axis is regulated during the DNA damage response. Here we demonstrate that the membrane trafficking protein PACS-2 inhibits SIRT1-mediated deacetylation of p53 to modulate the cellular response to DNA damage. We demonstrate that PACS-2 directly interacts with SIRT1 and inhibits SIRT1-mediated deacetylation of p53 *in vivo*. Moreover, PACS-2 deficient cells have a SIRT1-dependent reduction in p53 acetylation and p21 expression, resulting in increased apoptosis and reduced clonogenic survival in a p53- and p21-dependent manner following DNA damage. Our findings suggest PACS-2 is a critical regulator of the SIRT1-p53-p21 axis to modulate the DNA damage response.

INTRODUCTION

The tumor suppressor p53 is perhaps the most frequent target of genetic alternations in human cancer, as mutations that disrupt p53 function or its regulatory network have been found in more than half of all human cancers (Hainaut et al., 2000). Following DNA damage, p53 functions as a node for orchestrating diverse biological responses such as cell-cycle arrest, apoptosis, and senescence depending on several factors, including the level and type of stress as well as the cell and tissue type (Zilfou et al., 2009). To coordinate these cellular processes, p53 functions as a sequence-specific transcription factor to promote the transactivation of various target genes, including the cyclin-dependent kinase (CDK) inhibitor p21 to promote growth arrest and facilitate DNA damage repair (el-Deiry et al., 1993, Deng et al., 1995, Brugarolas et al., 1995).

Following DNA damage, the transcriptional activation of p53 is critically dependent on posttranslational modifications, including phosphorylation and acetylation, which coordinately function to stabilize p53 and enhance its transactivation functions, respectively (Meek et al., 2009, Kruse et al., 2009). The acetylation of p53 is a crucial regulatory element controlling promoter-specific activation of p53 target genes (Zilfou et al., 2009, Kruse et al., 2009) and the stress-induced increase of p53 acetylation significantly correlates with p53 activation and stabilization (Luo et al., 2001, Luo et al., 2000, Vaziri et al., 2001,

Ito et al., 2001, Knights et al., 2006). Indeed, mutational loss of acetylation at all major acetylation sites blocks the ability of p53 to induce p21 and suppress cell growth, suggesting acetylation of p53 is indispensable for p53 activation (Tang et al., 2008).

Human sirtuin 1 (SIRT1) is a member of the SIRT family (including SIRT1-7) which has NAD^+-dependent class III histone deacetylase activity. SIRT1 is the mammalian ortholog of yeast Sir2 (silent information regulator 2), which regulates aging and lifespan in several lower organisms (Lin et al., 2000, Tissenbaum et al., 2001, Wood et al., 2004). Recent studies reveal SIRT1 also deacetylates various non-histone proteins that have broad biological functions, including PGC-1α (Rodgers et al., 2005), forkhead transcription factor (FOXO) (Brunet et al., 2004, Motta et al., 2004, van der Horst et al., 2004, Xiong et al., 2011), NF-κB (Yeung et al., 2004, Schug et al., 2010), PTEN (Ikenoue et al., 2008), HIF-1α and HIF-2α (Dioum et al., 2009, Lim et al., 2010, Leiser et al., 2010), Ku70 (Jeong et al., 2007), MyoD (Fulco et al., 2003), and p53 (Luo et al., 2001, Vaziri et al., 2001). These findings implicate SIRT1 in diverse cellular processes, including chromatin remodeling, cell survival, apoptosis, DNA damage responses, as well as fat and glucose metabolism.

SIRT1 negatively regulates p53 transcriptional activation by deacetylating p53 following DNA damage or oxidative stress (Luo et al., 2001, Vaziri et al., 2001, Langley et al., 2002). While the regulation of p53 by modifying enzymes and various cofactors has been heavily studied (Meek et al., 2009), less is known

about the regulation of SIRT1. Transcription of SIRT1 is repressed by p53 as well as the tumor suppressor hypermethylated in cancer 1 (HIC1), which forms a transcription repression complex with SIRT1 on its own promoter (Chen et al., 2005, Nemoto et al., 2004). Moreover, the cell cycle regulator E2F1 transactivates SIRT1 following DNA damage and reciprocally, SIRT1 deacetylates E2F1, inhibiting its transcriptional activities and thereby establishing a negative feedback loop (Wang et al., 2006). SIRT1 is regulated posttranscriptionally by the oncogenic RNA binding protein HuR, which binds the 3'-UTR of *SIRT1* mRNA, stabilizing the transcript and increasing SIRT1 expression (Abdelmohsen et al., 2007) while the p53 target and tumor suppressive microRNA miR-34a represses SIRT1 expression, leading to p53 hyperacetylation and transcriptional activation (Yamakuchi et al., 2008). While these studies illustrate the transcriptional and post-transcriptional control of SIRT1 expression, much less is known about the mechanisms controlling SIRT1 activity.

Recent studies have determined that SIRT1 deacetylase activity can be modulated by direct interaction with other cellular proteins. Active regulator of SIRT1 (AROS) (Kim et al., 2007) and the neuronal specific protein necdin (Hasegawa et al., 2008) are positive modulators that bind SIRT1 to enhance SIRT1-mediated deacetylation of p53 and attenuate p53 transcriptional activation following DNA damage (Kim et al., 2007, Hasegawa et al., 2008). In contrast, the tumor suppressor deleted in breast cancer 1 (DBC1) acts as a direct inhibitor of

SIRT1, reducing SIRT1 deacetylation of p53 and increasing p53 transcriptional activity (Kim et al., 2008, Zhao et al., 2008) while the nuclear desumoylase sentrin-specific protease 1 (SENP1) inhibits SIRT1 deacetylase activity and increases p53 acetylation by desumoylating SIRT1 (Yang et al., 2007). Recently, the methyltransferase Set7/9 was identified as a negative SIRT1 regulator that induces the dissociation of SIRT1 from p53, thereby increasing p53 acetylation following DNA damage (Liu et al., 2011).

The diversity of SIRT1 substrates in pathways such as DNA damage and cell survival, together with the determination that SIRT1 can be modulated by protein binding partners, suggests the regulation of SIRT1 activity is complex, and likely requires additional cellular factors to coordinate these effects. Here we identify the membrane trafficking protein PACS-2 as an inhibitor of SIRT1-mediated deacetylation of p53 following DNA damage. PACS-2 is involved in diverse homeostatic processes (Youker et al., 2009); while initially identified as a regulator of membrane traffic, the role of PACS-2 has expanded to include key functions in viral immunity and death ligand (TRAIL)-induced apoptosis (Youker et al., 2009, Aslan et al., 2009, Werneburg et al., 2012). Here, we demonstrate that PACS-2 directly interacts with SIRT1 and inhibits SIRT1-mediated deacetylation of p53 *in vivo*. We found that PACS-2 deficient cells have a SIRT1-dependent reduction in p53 acetylation and p21 expression, resulting in increased apoptosis and reduced clonogenic survival in a p53- and p21-dependent manner following DNA damage. Based on these observations, we

propose that PACS-2 is a critical regulator of SIRT1-mediated deacetylation of p53 to modulate the DNA damage response.

RESULTS

6.1 Separable roles for PACS-2 in TRAIL- and DNA damage-induced apoptosis

The induction of tumor cell apoptosis can be enhanced when the death ligand TRAIL is combined with DNA damage-inducing chemotherapeutics or irradiation (Shankar et al., 2004), suggesting multiple apoptotic pathways can synergize to kill cancer cells. We recently reported that the membrane trafficking protein PACS-2 is an essential TRAIL effector required for lysosomal/ mitochondria membrane trafficking steps leading to the activation of caspase-3 in cancer cells (Aslan et al., 2009, Werneburg et al., 2012). However, whether the role of PACS-2 in mediating TRAIL-induced apoptosis also extended to p53-regulated apoptosis following DNA damage was not known. To investigate this, we compared the effect of PACS-2 depletion on TRAIL or p53-dependent apoptosis (Figure 6.1A). Parallel plates of control or PACS-2 knockdown human colon carcinoma HCT116 cells or isogenic HCT116 $p53^{-/-}$ cells were treated with the anthracycline chemotherapeutic Doxorubicin or TRAIL and the extent of apoptosis was monitored by caspase-3 activation and poly (ADP-ribose) polymerase (PARP) cleavage. In agreement with earlier studies (Aslan et al., 2009), PACS-2 knockdown blunted TRAIL-induced caspase-3 activation and PARP cleavage and this effect was independent of p53. Surprisingly, however, PACS-2 knockdown sensitized HCT116 cells to Doxorubicin-induced apoptosis in a p53-dependent manner, as PACS-2 deficient HCT116 $p53^{-/-}$ cells failed to elicit

caspase-3 activation or PARP cleavage. Indeed, the sensitization of PACS-2 deficient cells to DNA-damage induced apoptosis was not specific to treatment with Doxorubicin as PACS-2 knockdown also sensitized HCT116 cells to DNA damage-induced apoptosis following treatment with ionizing radiation (IR) (Figure 6.1B).

6.2 PACS-2 regulates p53-mediated apoptosis and clonogenic survival in a p21-dependent manner following DNA damage

The increased sensitivity of PACS-2-deficient cells to Doxorubicin- and IR-induced apoptosis lead us to investigate whether PACS-2 knockdown would similarly alter long-term survival following DNA damage. To test this, control or PACS-2 knockdown HCT116 cells or isogenic $p53^{-/-}$ cells were treated with increasing amounts of Doxorubicin or IR and subsequently analyzed for clonogenic survival. We found that PACS-2 knockdown reduced clonogenic survival of both Doxorubicin- or IR-treated HCT116 cells in a p53-dependent manner, as there was no effect of PACS-2 knockdown on survival of HCT116 $p53^{-/-}$ cells (Figure 6.1C). Moreover, the reduced clonogenic survival of PACS-2-deficient HCT116 cells correlated with the reduced ability of these cells to undergo G_1 cell cycle arrest following DNA damage (Figure 6.2A). Specifically, control or PACS-2 knockdown HCT116 cells were synchronized in G_0/G_1 using serum deprivation and then stimulated to re-enter the cell cycle by the addition of serum and in the presence of bromodeoxyuridine (BrdU). The cells were then

exposed to Doxorubicin and incubated for an additional 24 hours. Flow cytometric analysis revealed that PACS-2 knockdown HCT116 cells had a significantly reduced percentage of cells in G_0/G_1 compared to control knockdown cells (27.2 ± 2.9% versus 16.7 ± 1.2%, respectively), suggesting PACS-2 promotes G_1 growth arrest following DNA damage.

The p53-mediated transactivation of the cyclin-dependent kinase (CDK) inhibitor p21 is required for efficient induction of G_1 cell cycle arrest following DNA damage (el-Deiry et al., 1993, Deng et al., 1995, Brugarolas et al., 1995). Therefore, we tested whether PACS-2 was important for the induction of p21 following DNA damage. Accordingly, we analyzed *p21* mRNA expression in control or PACS-2 knockdown HCT116 cells or isogenic $p53^{-/-}$ cells and found that PACS-2 knockdown repressed the p53-dependent induction of *p21* mRNA following treatment with Doxorubicin (Figures 6.2B-C). However, while knockdown of PACS-2 resulted in reduced expression of p21, the mRNA levels of the proapoptotic BH-3 only protein and p53 target *PUMA* were not significantly changed (Figure 6.2D). This finding is consistent with the determination that PACS-2 deficient cells are sensitized to DNA damage-induced apoptosis and the accumulating evidence identifying p21 as a major inhibitor of p53-dependent apoptosis (Dotto, 2000, Gartel et al., 2002, Cazzalini et al., 2010). Therefore, we investigated whether the reduced p21 in PACS-2 knockdown HCT116 cells was responsible for their aberrant sensitivity to apoptosis and reduced clonogenic survival following DNA damage. Thus, we analyzed the extent of apoptosis and

clonogenic survival in isogenic HCT116 $p21^{-/-}$ cells knocked down for PACS-2. Similar to our results obtained with HCT116 $p53^{-/-}$ cells, PACS-2 knockdown failed to sensitize HCT116 $p21^{-/-}$ cells to apoptosis or affect their clonogenic survival following DNA damage as compared to control knockdown cells (Figures 6.3A-B). These data demonstrate that PACS-2 is critically involved in regulating the cellular response to DNA damage in a p53- and p21-dependent manner.

6.3 PACS-2 regulates p53 acetylation and p53-mediated p21 expression in vivo following DNA damage

Our determination that the p53-mediated induction of p21 was repressed in PACS-2 knockdown cells suggested PACS-2 might modulate p53 function following DNA damage. To test this, we analyzed the ability of Doxorubicin to induce p53 and p21 expression in control or PACS-2 knockdown HCT116 cells (Figure 6.3C). Whereas PACS-2 knockdown had no significant effect on total p53 levels following DNA damage, it resulted in a marked reduction in p21 expression, consistent with the p53-dependent reduction of *p21* mRNA (Figure 6.2B-C). Similar results were observed in human osteosarcoma U2OS cells following exposure to IR, in which knockdown of PACS-2 repressed the induction of p21 but had no measurable effect on the levels of total p53 (Figure 6.3D).

Following DNA damage, the transcriptional activation of p53 is critically dependent on posttranslational modifications, including phosphorylation and acetylation, which coordinately function to stabilize p53 and enhance its

transactivation functions, respectively (Meek et al., 2009, Kruse et al., 2009). Thus, the determination that PACS-2 knockdown repressed p21 expression but had no effect on total p53 levels suggested PACS-2 might modulate p53 activation by controlling p53 posttranslational modifications. To test the above hypothesis, endogenous p53 was immunoprecipitated from control or PACS-2 knockdown HCT116 cells following treatment with Doxorubicin and the extent of p53 Ser_{15} phosphorylation and Lys_{382} acetylation was monitored by western blot (Figure 6.4A). Indeed, while PACS-2 knockdown had no effect on p53 phosphorylation, there was a marked reduction in the level of p53 acetylation, which correlated with impaired induction of p21.

To explore the consequence of PACS-2 loss on the p53-p21 axis *in vivo*, WT and *Pacs2*$^{-/-}$ mice (generated as described in (Aslan et al., 2009)) were exposed to 4.5 Gy IR and thymuses were harvested 6 hours later and analyzed by western blot and qRT-PCR (Figures 6.4B-C). Notably, the induction of both p21 and Puma was repressed in thymuses from *Pacs2*$^{-/-}$ mice whereas the levels of total p53 were unaffected. This repressed induction appeared to result from impaired transcription as qRT-PCR analysis showed *p21* and *Puma* mRNA levels were also reduced (Figure 6.4C). Moreover, the level of p53 Ser_{18} phosphorylation (Ser_{15} in humans) was unaffected but the level of Lys_{379} acetylation (Lys_{382} in humans) was reduced, similar to the results obtained in HCT116 cells (Figure 6.4A). Together, these results suggest PACS-2 is an *in vivo* regulator of p53 transcriptional activation by controlling the extent of p53

acetylation.

6.4 PACS-2 controls the level of acetylated p53 bound to the p21 promoter following DNA damage

Since acetylation of p53 is a crucial regulatory element controlling transcriptional activation of p53 target genes, we analyzed the amount of total and acetylated p53 bound to the p21 promoter following DNA damage. For this, control or PACS-2 knockdown HCT116 cells were treated with Doxorubicin and subjected to chromatin immunoprecipitation (ChIP) analysis using antibodies specific for total p53 or acetylated p53 (K_{382}) (Figure 6.4D). Quantitative PCR (qPCR) of ChIP-associated DNA revealed that PACS-2 knockdown HCT116 cells had reduced levels of acetylated p53 bound to the p21 promoter following DNA damage. By contrast, the amount of total p53 bound to the p21 promoter remained unchanged, suggesting that loss of PACS-2 did not impede the ability of p53 to bind specific DNA sequences, but instead diminished the proportion of promoter-bound p53 that was acetylated.

6.5 PACS-2 regulates SIRT1-dependent deacetylation of p53

The transcriptional activity of p53 is positively modulated by acetylation, catalyzed predominately by the histone acetyltransferase (HAT) activity of CBP/ p300 (Meek et al., 2009). Conversely, the class III histone deacetylase (HDAC) SIRT1 negatively regulates p53 transcriptional activation by deacetylating p53

following DNA damage or oxidative stress (Luo et al., 2001, Vaziri et al., 2001). The determination that loss of PACS-2 resulted in reduced levels of acetylated p53 bound to the p21 promoter following DNA damage led us to investigate whether PACS-2 modulates p53 acetylation by interacting with the acetyltransferase p300 or the deacetylase SIRT1. Therefore, we co-expressed FLAG-tagged PACS-2 with HA-tagged p300 or V5-tagged SIRT1 and found that overexpressed PACS-2 interacted with SIRT1 but not p300 (Figure 6.5A). To examine the interaction between endogenous PACS-2 and SIRT1, cell extracts from HCT116 cells were immunoprecipitated with anti-PACS-2 antibody or control IgG (Figure 6.5B). As expected, western blot analysis revealed that SIRT1 was clearly detected in the immunoprecipitations obtained with anti-PACS-2 antibody, but not with control antibody. We then tested whether PACS-2 binds SIRT1 *in vitro*. As shown in Figure 6.5C, SIRT1 interacts directly with the cargo-binding region (FBR) of PACS-2. These studies, together with the reduced p53 acetylation seen with knockdown of PACS-2 (Figure 6.4), suggest PACS-2 may function to inhibit SIRT1-mediated deacetylation of p53.

To test the above hypothesis, we examined whether PACS-2 expression rescues p53 from SIRT1-mediated deacetylation and repression in human cells. Therefore we coexpressed PACS-2 HA with SIRT1-V5 and p53 FLAG (p53/f) in HCT116 cells, immunoprecipitated p53 with anti-FLAG and monitored p53 acetylation by western blot (Figure 6.6A). While SIRT1 efficiently induced p53 deacetylation, as expected, this effect was inhibited by coexpression with

PACS-2. Moreover, to demonstrate that PACS-2 acts on p53 by repressing SIRT1 function, we tested whether knockdown of PACS-2 indeed reduces acetylation levels of endogenous p53 and, importantly, whether these effects are reversed by the inactivation of SIRT1 genetically or by pharmacologic inhibition. As shown in Figure 6.6B, siRNA-mediated knockdown of PACS-2 markedly reduced the acetylation levels of p53. Notably, the reduced p53 acetylation with PACS-2 knockdown was completely reversed by concomitant knockdown of SIRT1 (Figure 6.6B). Moreover, the findings with siRNA-mediated inactivation of SIRT1 were corroborated pharmacologically, which demonstrated that the SIRT1-specific inhibitor EX-527 also reversed the repressed acetylation of endogenous p53 in PACS-2 knockdown cells (Figure 6.6C). Similar results were also observed with the PACS-2-mediated repression of p21 induction. In these experiments, control or PACS-2 knockdown HCT116 cells were treated with Doxorubicin alone, Doxorubicin plus the class I and II HDAC inhibitor TSA or Doxorubicin plus EX-527 (Figure 6.6D). As expected, we found that the reduced induction of p21 following Doxorubicin treatment in PACS-2 knockdown cells could be prevented by EX-527 but not TSA. Together, these data suggest that the reduced acetylation of p53 in PACS-2-deficient cells is indeed SIRT1-dependent, and that the PACS-2-mediated effects on p53 activation act primarily through SIRT1 *in vivo*.

6.6 PACS-2 interacts with SIRT1 in the nucleus

Whereas SIRT1 localizes predominantly to the nucleus and has well-characterized nuclear functions (Michishita et al., 2005), PACS-2 function thus far has been studied in the regulation of membrane traffic in the cytoplasm (Youker et al., 2009). Interestingly, inspection of the PACS-2 sequence revealed multiple candidate leucine-rich nuclear export signals at Leu_{46}, Leu_{293} and Leu_{295}, suggesting PACS-2 may cycle between the cytosol and the nucleus (la Cour et al., 2004). To test this possibility, we examined the subcellular localization of mcherry-PACS-2 expressed in the absence or presence of the chromosomal region maintenance (CRM1)/exportin 1-dependent nuclear export inhibitor leptomycin B (LMB). We found that mcherry-PACS-2 localized predominantly in the cytosol in control cells but accumulated in the nucleus in the presence of LMB, suggesting PACS-2 shuttles between the nucleus and cytoplasm (Figure 6.7A).

The ability of PACS-2 to traffic to the nucleus led us to ask whether the interaction between SIRT1 and PACS-2 could be detected in the nuclear fraction of cells. Accordingly, we expressed V5-tagged SIRT1 alone or together with FLAG-tagged PACS-2 in the absence or presence of LMB. The lysates were separated into cytoplasmic and nuclear fractions and then PACS-2 was immunoprecipitated with anti-FLAG, and co-precipitating SIRT1 was identified by western blot (Figure 6.7B). We found that SIRT1 interacted with PACS-2 isolated from the nuclear fraction and that this interaction was increased in the presence of LMB. We extended this analysis to determine whether endogenous SIRT1

interacted with nuclear and/or cytoplasmic PACS-2. Accordingly, we immunoprecipitated endogenous PACS-2 from both the cytosolic and high-salt extracted nuclear fractions and found that endogenous SIRT1 interacted preferentially with nuclear PACS-2 following treatment with LMB, as no detectable interaction was seen between SIRT1 and cytoplasmic PACS-2 (Figure 6.7C). Together these findings suggest PACS-2 traffics to the nucleus where it can interact with SIRT1 and that PACS-2 is critically involved in regulating the p53-mediated response following DNA damage by repressing SIRT1 function.

DISCUSSION

The data presented in this study provide evidence that the membrane trafficking protein PACS-2 regulates the SIRT1-mediated deacetylation of p53 to modulate the cellular response to DNA damage. We demonstrate that PACS-2 interacts with SIRT1 in the nucleus and inhibits SIRT1-mediated deacetylation of p53 *in vivo*. We also found that PACS-2 deficient cells have a SIRT1-dependent reduction in p53 acetylation and p21 expression, resulting in increased apoptosis and reduced clonogenic survival in a p53- and p21-dependent manner following DNA damage. Based on these observations, we propose that PACS-2 is a critical regulator of the SIRT1-p53-p21 axis to modulate the DNA damage response.

The observation that apoptosis is increased when cancer cells are treated with TRAIL in combination with chemotherapy or IR (Shankar et al., 2004) suggests various apoptotic pathways have redundant requirements for specific proteins and is consistent with the determination that PACS-2 has distinct roles in TRAIL- and p53-dependent apoptosis. Notably, our data demonstrate that the increased apoptosis and reduced clonogenic survival following DNA damage in PACS-2 deficient cells is both p53- and p21-dependent, as genetic loss of either p53 or p21 mitigates the effect of PACS-2 depletion. Moreover, we observe reduced p53-dependent p21 expression following PACS-2 knockdown that correlates with impaired ability of these cells to undergo G_1 arrest following DNA damage. These findings are consistent with the well-characterized cell cycle

inhibitory functions of p21 as well as with accumulating evidence identifying p21 as a major inhibitor of p53-mediated apoptosis through both cell cycle-dependent and -independent mechanisms (Dotto, 2000, Gartel et al., 2002, Cazzalini et al., 2010). p21 prevents cells harboring DNA damage from aberrantly continuing through mitosis where they become susceptible to mitotic cell death (or mitotic catastrophe) (Bunz et al., 1998, Roninson, 2002); as well as directly represses proapoptotic regulatory proteins such as caspase 3, caspase 2, and apoptosis signal-regulating kinase 1 (ASK1) (Dotto, 2000); and is itself cleaved during DNA damage-induced apoptosis by caspase 3 (Gervais et al., 1998, Zhang et al., 1999).

The determination that acetylation of p53 is essential for transcriptional activation of p21 (Tang et al., 2008, Kruse et al., 2009) is consistent with our observation that PACS-2 knockdown results in reduced levels of acetylated p53 that correlate with impaired induction of p21 following DNA damage. Moreover, ChIP analysis revealed that PACS-2 knockdown induced a selective reduction in acetylated p53 bound to the p21 promoter following DNA damage, while no significant change in total p53 was observed. These results suggest that while PACS-2 has no effect on the ability of p53 to bind DNA in a sequence-specific manner, that it does, however, determine the extent to which promoter-bound p53 is acetylated. This finding is consistent with data demonstrating that reduced acetylation does not impede the DNA-binding ability of p53, as a p53 molecule in which all major acetylation sites are mutated binds DNA as effectively as wild-

type p53 (Tang et al., 2008). Rather, a recent model put forth by Wei Gu and colleagues suggests that acetylation promotes the association of p53 with the transcriptional machinery by inhibiting the association of p53 with its negative regulator MDM2 (Tang et al., 2008, Kruse et al., 2009, Meek et al., 2009). Additional studies are needed to determine the extent to which PACS-2 associates with p53 target gene promoters or modulates MDM2-mediated repression of p53.

Recently, there has been tremendous focus on elucidating the mechanisms modulating p53 acetylation following DNA damage, in particular the regulation of SIRT1-mediated deacetylation of p53. Indeed, multiple protein binding partners have been identified that modulate SIRT1-mediated deacetylation of p53, such as the positive regulators AROS and necdin, and the negative regulators DBC1 and Set7/9 (Kim et al., 2007, Hasegawa et al., 2008, Kim et al., 2008, Zhao et al., 2008, Liu et al., 2011). The determination that PACS-2 interacts with SIRT1 *in vivo* and *in vitro*, as well as inhibits SIRT1-mediated deacetylation of p53 *in vivo*, suggests PACS-2 additionally regulates the SIRT1-p53 axis following DNA damage. Moreover, similar to siRNA knockdown of DBC1 (Kim et al., 2008, Zhao et al., 2008) or Set7/9 (Liu et al., 2011), there is a marked reduction of p53 acetylation in PACS-2 siRNA-treated cells following DNA damage that is completely reversed with concomitant siRNA knockdown or enzymatic inhibition of SIRT1. However, whether these proteins have distinct or redundant roles in SIRT1 regulation is unclear. Therefore, it will

be important to understand the biological context in which these SIRT1 regulators are critical.

Whereas functional regulation of SIRT1 by protein interactions has been investigated in recent studies, much less is known regarding the molecular mechanisms of how these protein binding partners modulate SIRT1 activity. While crystal structures have been solved for human SIRT2, SIRT3, and SIRT5, and SIRT6, structural data for human SIRT1 is lacking, with structures available only for Sirtuin homologs from bacteria (CobB and Sir2Tm), yeast (Sir2 and Hst2), and archea (Sir2-Af1 and Sir2-Af2) (Sanders et al., 2010). Despite this limitation, these studies revealed a structurally conserved catalytic core domain reflective of the high sequence homology among Sir2 proteins within the catalytic domain (Landry et al., 2000, Imai et al., 2000). Notably, recent protein biochemistry studies determined that the evolutionarily diverse N- and C-terminal segments of SIRT1 play critical autoregulatory functions to increase SIRT1 deacetylase activity, and likely substrate-specificity (Pan et al., 2012). Indeed, a SIRT1 holoenzyme is formed by the addition of the N- and C-terminal domains to the catalytic core, dramatically enhancing the catalytic rate and the K_m for NAD^+, respectively (Pan et al., 2012). Binding studies have provided additional insight, as DBC1 binds directly to the catalytic domain to decrease SIRT1 activity (Kim et al., 2008, Zhao et al., 2008), whereas necdin binds both the catalytic domain as well as the noncatalytic N-terminal domain to potentiate SIRT1 activity (Hasegawa et al., 2008), and AROS and Set7/9 both interact with the

noncatalytic N-terminal domain to increase and decrease SIRT1 activity, respectively (Kim et al., 2007, Liu et al., 2011). However, despite these findings, it remains unclear how the binding of various proteins to the same region of SIRT1 can elicit either positive or negative effects on SIRT1 activity. Among other possibilities, this could reflect differences in subcellular localization, as well as conformational changes in SIRT1 induced upon protein-protein interactions that prevent SIRT1 from binding to p53 or a direct competition between regulatory proteins and p53 for binding SIRT1. Thus, detailed mapping and structural analyses remains necessary to further elucidate the mechanisms by which regulatory proteins such as DBC1, Set7/9, AROS, and PACS-2 can modulate SIRT1 activity.

Some membrane-associated cytoplasmic trafficking proteins have additional nuclear gene regulation functions, such as the protein kinase CK2 (Yamane et al., 2005, Pluemsampant et al., 2008) and GSK3β (Hoeflich et al., 2000, Grimes et al., 2001, Zhou et al., 2004, Jope et al., 2004), while many nuclear proteins such as CtBP (Corda et al., 2006), HDAC3 (Longworth et al., 2006), and p53 (Green et al., 2009) have been characterized as having membrane-associated functions, supporting a functional link between the endomembrane system and gene regulation pathways. In these studies we determined that the sorting protein PACS-2 can indeed traffic to the nucleus and interact with a predominantly nuclear SIRT1 protein. While the interaction between endogenous PACS-2 and SIRT1 is enhanced with nuclear accumulation

of PACS-2 following treatment with Leptomycin B, suggesting nuclear specificity of the interaction, the mechanism of PACS-2 nuclear transport is unclear. In future studies it will important to identify the PACS-2 nuclear localization sequence, the regulation of its nuclear import and export, as well as determine whether PACS-2 nuclear localization is required for its ability to modulate the SIRT1-p53 axis.

Our studies identify PACS-2 as a regulator of the SIRT1-p53 axis *in vivo*, leading to p53- and p21-dependent alterations in cell survival. Intriguingly, however, the p53- and p21-dependent sensitivity to apoptosis we observe is in contrast to studies showing that elevated SIRT1 protects cells from apoptosis and promotes cell survival following DNA damage (Luo et al., 2001, Vaziri et al., 2001). This finding is interesting, as the reduced p21 induction we observe with PACS-2 knockdown correlates with an elevated SIRT1 phenotype and is in fact dependent on SIRT1 enzymatic activity, as treatment of PACS-2 depleted cells with Doxorubicin together with the SIRT1 inhibitor EX-527 completely reverses the p21 repression seen with Doxorubicin alone. However, it remains unclear how modulation of SIRT1 affects p53 transcription in a promoter-specific manner, and therefore how alteration of these target genes determine cell fate. For example, knockdown of the SIRT1 inhibitor DBC1 resulted in reduced expression of the proapoptotic p53 targets PUMA, Bax, and Bim, consistent with reduced apoptosis (Kim et al., 2008, Zhao et al., 2008), while the levels of the cell-cycle inhibitor and p53 target GADD45α were conversely increased (Kim et al., 2008).

In our studies, while both p21 and PUMA expression were impaired in *Pacs2*$^{-/-}$ thymuses, only p21 was reduced in HCT116 cells, suggesting the promoter-specific requirement for PACS-2 is different between mice and cancer cells. Indeed, the ability of separate SIRT1 regulators to differentially modulate p53 transcriptional activation is consistent with studies that suggest distinct mechanisms induce different classes of p53 target genes (Tang et al., 2008, Kruse et al., 2009, Zilfou et al., 2009). These classes include: negative regulators of p53, such as MDM2, which are expressed in an acetylation-independent manner and do not require recruitment of coactivators (Tang et al., 2006, Tang et al., 2008); a second class includes those involved in growth arrest, in particular p21, and this requires acetylation and recruitment of coactivators such as CBP/p300 or Tip60/hMOF (Sykes et al., 2006, Tang et al., 2006, Tang et al., 2008); and the third class are apoptotic genes, such as PUMA, which have more stringent requirements given the irreversible nature of the apoptotic response, and require the recruitment of coactivators, specific modifications (e.g. p53 K_{120} acetylation), and complete removal of MDM2-mediated repression (Sykes et al., 2006, Tang et al., 2006, Tang et al., 2008, Li et al., 2009b). It will therefore be important to identify the cofactors required for SIRT1 regulators, such as PACS-2, to modulate p53 function as these interactions may impart additional specificity to SIRT1-mediated p53 regulation.

As mentioned above, while some studies suggest that repression of p53 by SIRT1 promotes cell survival during stress (Luo et al., 2001, Vaziri et al.,

2001), these findings are not universal, and are in contrast to studies proposing SIRT1 negatively regulates cell growth and survival under stress (Wang et al., 2008b, Firestein et al., 2008, Han et al., 2008, Yeung et al., 2004). Intriguingly, SIRT1 promotes transcription-independent p53-mediated apoptosis in response to oxidative stress in mouse embryonic stem cells (Han et al., 2008). SIRT1 also inhibits the expression of antiapoptotic survivin, a member of the inhibitor of apoptosis (IAP) family, by deacetylating histone H3 within nucleosomes at the survivin promoter (Wang et al., 2008b) as well as deacetylates and represses β-catenin (Firestein et al., 2008) and RelA/p65 (Yeung et al., 2004), thereby attenuating Wnt and NF-κB signaling, respectively. These findings, together with the numerous studies demonstrating both oncogenic and tumor suppressive roles for SIRT1 (Li et al., 2011a), illustrate how regulation of SIRT1 may be a double-edged sword that requires tight regulation and a much more thorough understanding of biological context.

Modulation of SIRT1 imparts many p53-dependent effects following cellular stress, however some of the discrepancies between studies could relate to modulation of other SIRT1 substrates that can additionally contribute to p53-mediated effects. Indeed, knockout mouse studies have demonstrated that the developmental defects in SIRT1-null animals cannot be rescued by crossing to p53-null mice (Kamel et al., 2006), likely because SIRT1 regulates a multitude of other critical substrates along with p53. It will therefore be important to test whether PACS-2 additionally regulates SIRT1-mediated deacetylation of histones

or nonhistone substrates such as FOXO, E2F1, Ku70, β-catenin, NF-κB, and PGC-1α, among others.

In summary, our data demonstrate that PACS-2 modulates p53 acetylation and transcriptional activation by negatively regulating the SIRT1-p53 axis following DNA damage. Based on our results and the supporting literature, a more complete understanding of how SIRT1 is regulated is of considerable therapeutic interest and is necessary for understanding the complex network controlling downstream SIRT1 targets.

MATERIALS AND METHODS

Experimental animals

The OHSU Department of Comparative Medicine approved all animal studies described. *Pacs2*$^{-/-}$ mice were maintained on a C57BL/6 background with more than 10 backcrosses. Generation of *Pacs2*$^{-/-}$ mice was described previously (Aslan et al., 2009). All ionizing radiation experiments were performed using a J.L. Shepherd Mark I Model 30 Cesium irradiator (dose rate of 1.475 Gy/min). Mice were exposed to whole body irradiation in a plexiglass pie-plate rotating at approximately 7 revolutions per minute (RPM). Both non-irradiated (control) and irradiated mice were sacrificed at the indicated times post-irradiation. Harvested tissues were snap frozen in liquid nitrogen for RNA isolation or western blot analysis as indicated.

Antibodies and chemical treatments

The following antibodies were obtained as indicated: actin (MAB1501; Chemicon); PACS-2 (193) and PACS-2 (834) (Simmen et al., 2005, Aslan et al., 2009); p53 CMV (#NCL-p53-CM5p; Novocastra), p53 DO-1 (#OP43; Calbiochem), acetyl-p53Lys$_{382}$ (#2525; Cell Signaling Technology), p53 FL-393 (sc-6243; Santa Cruz Biotechnology); acetyl-p53Lys$_{379}$ (#2570; Cell Signaling Technology), phospho-p53Ser$_{15}$ (#9284; Cell Signaling Technology), p21 (#556430; BD Pharmingen), cleaved caspase-3 (Asp$_{175}$) (#9664; Cell Signaling Technology), caspase 3 (3G2) (#9668; Cell Signaling Technology), PARP

(46D11) (#9532; Cell Signaling Technology), PUMA (#969643; Abcam), SIRT1 (H-300) (sc-15404; Santa Cruz Biotechnology), histone 3 (ab1791; Abcam), tubulin (#2148; Cell Signaling Technology), THE-His antibody (#A00186; Genscript), V5 (R960-25; Invitrogen), Flag (F7425; Sigma), and HA mAb clone HA.11 (MMS-101R; Covance). Doxorubicin (Sigma #D1515), Trichostatin A (T8852; Sigma), EX-527 (#2780; Tocris), TRAIL (#375-TL; R&D Systems), Leptomycin B(#431050; Calbiochem) were used as indicated in Legends. Tissue culture cells were irradiated using a J.L. Shepherd Mark I Model 30 Cesium irradiator (dose rate of 1.475 Gy/min).

Plasmids and siRNAs

The following plasmids were obtained as indicated: p300HA (Provided by R.H. Goodman, OHSU); SIRT1-V5 (Provided by J.H. Chung, NIH); His_6-SIRT1 (Provided by J. Denu, UWM); flag-tagged p53 (#10838; addgene). HA-tagged PACS-2 (PACS-2 HA) was previously described (Kottgen et al., 2005, Simmen et al., 2005). mcherry was amplified from a plasmid expressing mcherry-syntaxin (Provided by Wolf Almers, OHSU) and inserted 5 prime to the PACS-2 coding sequence using BamhI and EcorI restriction endonuclease sites. PACS-2 was cloned into a pcdna 3.1 vector containing a sequence encoding for FLAG at the 3 prime end by standard cloning techniques. Plasmids were transfected using Lipofectamine 2000 (#11668-027; Life Technologies) according to manufacture's instructions. Control (non-targeting) siRNA (siGENOME #D-001210; Dharmacon)

and siRNAs specific for PACS-2 (Smartpool #M-022015; Dharmacon) and SIRT1 (Smartpool #M-003540; Dharmacon) were electroporated (Amaxa) according to manufacturer's instructions.

Cell harvest and tissue processing

HCT116 cells (WT, $p53^{-/-}$, $p21^{-/-}$) and U2OS cells were cultured in DMEM supplemented with 10% fetal bovine serum. For experiments monitoring acetylated (ac)-p53, cells were treated as indicated in Legends and harvested in ac-p53 Lysis Buffer [20 mM Tris pH 7.6, containing 0.5% Nonidet P-40 (NP-40), 150 mM NaCl, 1 mM ethylenediaminetetraacetic acid (EDTA), 1 mM eithiothreitol (DTT), 5 uM Trichostatin A (TSA), protease inhibitors (0.5 mM phenylmethanesulfonylfluoride (PMSF) and 0.1 µM each of aprotinin, E-64, and leupeptin) and phosphatase inhibitors (1 mM Na_3VO_4 and 20 mM NaF)]. For all other cell culture experiments, cells were harvest in Protein Lysis Buffer (same as above, minus TSA and DTT). HA-tagged contructs were immunoprecipitated with anti-HA (MMS-101R; Covance), flag-tagged constructs were immunoprecipitated with anti-FLAG mAb M2-agarose (#A2220; Sigma), p53 was immunoprecipitated with anti-p53 DO-1 (#OP43; Calbiochem) and PACS-2 was immunoprecipitated with anti-PACS-2 (834). Horse radish peroxidase (HRP)-conjugated anti-rabbit and anti-mouse secondary antibodies (#OB-4050, #OB-1010, respectively; Fisher Scientific) were used in western blot analysis. Mouse tissues were homogenized in RIPA [50 mM Tris pH 8.0, containing 150 mM NaCl, 1% NP-40,

1% doexycholate, 0.1% sodium dodecyl sulfate (SDS), protease inhibitors (0.5 mM PMSF and 0.1 µM each of aprotinin, E-64, and leupeptin) and phosphatase inhibitors (1 mM Na_3VO_4 and 20 mM NaF)] using a motorized teflon-glass homogenizer. Protein concentration of tissue homogenates was determined using the Biorad protein concentration assay kit (#500-0006; Bio-rad) according to manufacturer's instructions.

Cell cycle analysis

Flow cytomtery was performed in the OHSU Flow Cytometry Core and cells analyzed on a FACSCalibur (BD) by listmode acquisition using CellQuest acquisition/analysis software (BD). Data was analyzed using FCS Express (Version 3). For cell cycle analysis, HCT116 cells were synchronized in G_0/G_1 with serum deprivation (0.1% serum) for 24 hours, and then stimulated to re-enter the cell cycle in the presence of 10 µM Bromodeoxyuridine (BrdU) with or without 0.5 µM Doxorubicin for an additional 24 hours. Cells were then fixed and stained with BrdU-Fluorescein isothiocyanate (FITC) and 7-aminoactinomycin D (7-AAD) (#559619BD; Pharmingen) according to manufacturer's instructions.

Clonogenic assays

HCT116 WT, $p53^{-/-}$, or $p21^{-/-}$ cells were transfected with control or PACS-2 siRNA for 72 hours and then seeded at 300 cells per 35 mM well (each condition seeded in triplicate) and incubated for an additional 24 hours. Cells were then

treated with Doxorubicin or IR as indicated in Legends, 24 hours later cells media was replaced with fresh media and cells were cultured for an additional 12 days prior to fixation and staining with 50% methanol containing 0.5% methylene blue. Colonies were then washed twice with 10% methanol. Colonies were then counted visually and quantified as a fraction of untreated and presented as percent survival.

Quantitative real-time PCR (qRT-PCR) analysis

For mouse tissues, RNA was isolated using Trizol (#15596-026; Sigma) according to manufacturer's instructions. For cell culture studies, RNA was isolated using the RNeasy kit (#74104; Qiagen) according to manufacturer's instruction. For either studies, 5 µg of RNA was reverse transcribed with oligo-dT primers using the Superscript III first strand cDNA synthesis kit (#18080-051; Invitrogen). Real time qRT-PCR reactions were performed in an ABI StepOne Real-Time PCR System with the Power SYBR GREEN PCR Master Mix (#4368706; Applied Biosystems) using the following primer pairs (listed 5' to 3'): mouse *p21* forward-CCATGTCCAATCCTGGTGATG; mouse *p21* reverse-CGAAGAGACAACGGCACACTT; mouse *Puma* forward-GCGGCGGAGACAAGAAGAG; mouse *Puma* reverse-TCCAGGATCCCTGGGTAAGG mouse *glyceraldehyde 3-phosphate dehydrogenase* (*GAPDH*) forward-CTGGAGAAACCTGCCAAGTA; mouse *GAPDH* reverse-TGTTGCTGTAGCCGTATTCA; human *p21* forward-

GACTCTCAGGGTCGAAAACGG; human *p21* reverse-GCGGATTAGGGCTTCCTCT; human *PUMA* forward-CGACCTCAACGCACAGTA; human *PUMA* reverse-ATGCTACATGGTGCAGAGA human *GAPDH* forward-CGGGGCTCTCCAGAACATC; and human *GAPDH* reverse-ATGACCTTGCCCACAGCCT. SYBR-Green fluorescence was analyzed using the ddCt method, the average threshold (Ct) was determined for each gene and normalized to *GAPDH* as an internal control. All reactions were performed in triplicate.

Chromatin immunoprecipitation (ChIP) analysis

10 cm plates of HCT116 cells were washed with phosphate buffered saline (PBS) and fixed in 1% formaldehyde for 10 minutes at room temperature (RT). Reactions were quenched with 125 mM Glycine for 5 minutes at RT and then collected in Harvest Buffer [PBS plus 10 mM DTT, and protease inhibitors (1 mM PMSF, 0.1 µM each of aprotinin, E-64, and leupeptin)]. Cells were then washed once each in 1 mL of Buffer I [10 mM Hepes pH 6.5, containing 0.25% Triton-X100, 10 mM EDTA, 0.5 mM ethylene glycol tetraacetic acid (EGTA), and protease inhibitors (1 mM PMSF, 0.1 µM each of aprotinin, E-64, and leupeptin)], then 1 mL of Buffer II [10 mM Hepes pH 6.5, containing 200 mM NaCl, 1 mM EDTA, 0.5 mM EGTA and protease inhibitors (1 mM PMSF, 0.1 µM each of aprotinin, E-64, and leupeptin)] and then lysed in 300 uL of Nuclear Lysis Buffer

[50 mM Tris pH 8.0, containing 1% SDS, 10 mM EDTA, and protease inhibitors (1 mM PMSF, 0.1 µM each of aprotinin, E-64, and leupeptin)] and incubated on ice for 10 min. Nuclear lysate was diluted 1:2 with ChIP Dilution Buffer [20 mM Tris pH 8.0, containing 0.01% SDS, 1% Triton X100, 2 mM EDTA, 150 mM NaCl and protease inhibitors (1 mM PMSF, 0.1 µM each of aprotinin, E-64, and leupeptin)] and then sonicated 6 times for 10 sec each (power output 6) with at least 30 sec on ice in between each pulse to generate ~400 base pair fragments. Sheared chromatin was centrifuged at 13.2K RPM for 10 minutes at 4°C to pellet cellular debris. Supernatant containing soluble chromatin was diluted 1:5 in ChIP Dilution Buffer and each condition was split into three immunoprecipitation samples (for control immunoglobulin (IgG), anti-p53 DO-1, anti-p53 ac-K_{382}). Samples were pre-cleared by incubation with 10 ug control IgG with 50 uL of pre-blocked Protein A Sepharose beads (50% slurry) containing 3% BSA and 2 ug of sonicated salmon sperm DNA for 2 hours at 4°C. Sample were then immunprecipiated with 3 ug of control IgG, 2.5 ug p53 DO-1, or 10 uL of ac-p53 (K_{382}) antibodies overnight at 4°C. The next day, immune complexes were captured using 50 ul of pre-blocked Protein A Sepharose beads for 2 hours at 4°C. Immune complexes were then washed twice with 1 mL of TSE-I (20 mM Tris pH 8.0, containing 0.1% SDS, 1% Triton X100, 2 mM EDTA, 150 mM NaCl), three times with 1 mL of TSE-II (20 mM Tris pH 8.0, containing 0.1% SDS, 1% Triton X100, 2 mM EDTA, 500 mM NaCl), twice with 1 mL of LiCl Detergent Buffer III (10 mM Tris pH 8.0, containing 0.25 M LiCl, 1% NP-40, 1%

deoxycholate, 1 mM EDTA), and twice with 1 mL of Tris-EDTA Buffer (10 mM Tris and 1 mM EDTA, pH 8.0). After the final wash, samples were eluted with Elution Buffer (50 mM Tris pH 8.0, containing 1% SDS, 1 mM EDTA, 0.1 M NaBicarb-$NaHCO_3$). DNA-protein crosslinks were reversed and proteins digested at 65°C overnight and then DNA was purified using the QIAquick PCR DNA purification kit (Catalog # 28104). DNA was eluted in 20 uL of H_20 (pH 8.0) and then analyzed for quantitative PCR (qPCR) using Taqman Universal PCR mastermix (#4304438; Life Technologies) and the following p21 primers and probe (listed 5' to 3'): p21 promoter forward-GTGGCTCTGATTGGCTTTCTG; p21 promoter reverse-CTGAAAACAGGCAGCCC; and the p21 Taqman probe 6FAM-TGGCATAGAAGAGGCTGGTGGCTATTTTG.

In vitro binding assays

GST-tagged PACS-2 proteins were expressed in Escherichia coli and prepared as previously described (Simmen et al., 2005, Aslan et al., 2009). His_6-SIRT1 (Provided by J. Denu, UWM) was expressed in Escherichia coli and purified using Nickel-nitrilotriacetic acid (NTA)-agarose (QIAGEN) according to manufacturer's instructions and stored in dialysis buffer (25 mM Tris pH 8.0, 100 mM NaCl, 1% glycerol, 5 mM DTT). For protein-protein interaction assays, purified His_6-SIRT1 was incubated with glutathione-Sepharose 4B beads (Sigma) containing GST PACS-2 constructs or GST in Binding Buffer (20 mM Tris pH 7.9, 150 mM NaCl, 0.1% NP-40, 0.1 mM EDTA, 0.3 mM DTT) for 30 minutes at RT,

washed 3x in Wash Buffer (20 mM Tris pH 7.9, 300 mM NaCl, 0.1% NP-40, 0.1 mM EDTA, 3 mM DTT), and then bound proteins were eluted with Laemmli sample buffer, resolved by sodium dodecyl sulfate-polyacrylamide gel electrophoresis (SDS-PAGE), and analyzed by western blot using an anti-His_6 antibody.

Microscopy

U2OS cells were transfected with mcherry PACS-2 using Fugene 6 (Fisher) and then treated with 20 nM Leptomycin B (Calbiochem) for 3 hours prior to fixation. Cells were stained with 4',6-diamidino-2-phenylindole (DAPI, Souther Biotech) and then analyzed by laser scanning confocal microscopy using an Olympus FluoView FV1000 upright microscope (Olympus). The ratio of PACS-2 mcherry signal in the nucleus and cytoplasm was determined using softWoRx Explorer 2.0 (Applied Precision) from > 40 cells from at least three independent experiments.

Nuclear fractionation assays

Cells were harvested in Buffer 1 [50 mM Tris pH 7.9, containing 10 mM KCl, 1 mM EDTA, 0.2% NP-40, 10% glycerol, and protease inhibitors (0.5 mM PMSF and 0.1 µM each of aprotinin, E-64, and leupeptin)] and then centrifuged at 6K RPM for 3 minutes at 4° C to separate nuclei from cytoplasm. Nuclear pellet was lysed with Buffer 2 [20 mM Hepes pH 7.9, containing 400 mM NaCl,

10 mM KCl, 1% NP-40, 20% glycerol, 1 mM EDTA, and protease inhibitors (0.5 mM PMSF and 0.1 µM each of aprotinin, E-64, and leupeptin)] for 20 minutes at 4° C and then centrifugred at 13.2K RPM for 10 minutes to separate the insoluble and soluble nuclear fractions. Soluble nuclear and cytoplasmic fractions were then subjected to immunoprecipitation using anti-FLAG mAb M2-agarose (#A2220; Sigma) or anti-PACS-2 (831) antibodies as indicated in Legends. Immune complexes were captured with Protein G Sepharose (#10-1242; Invitrogen) for 2 hours at 4° C, then washed 3x in Wash Buffer [20 mM Tris pH 7.6, containing 0.5% NP-40, 150 mM NaCl, 1 mM EDTA] and eluted in SDS sample buffer prior to western blot analysis.

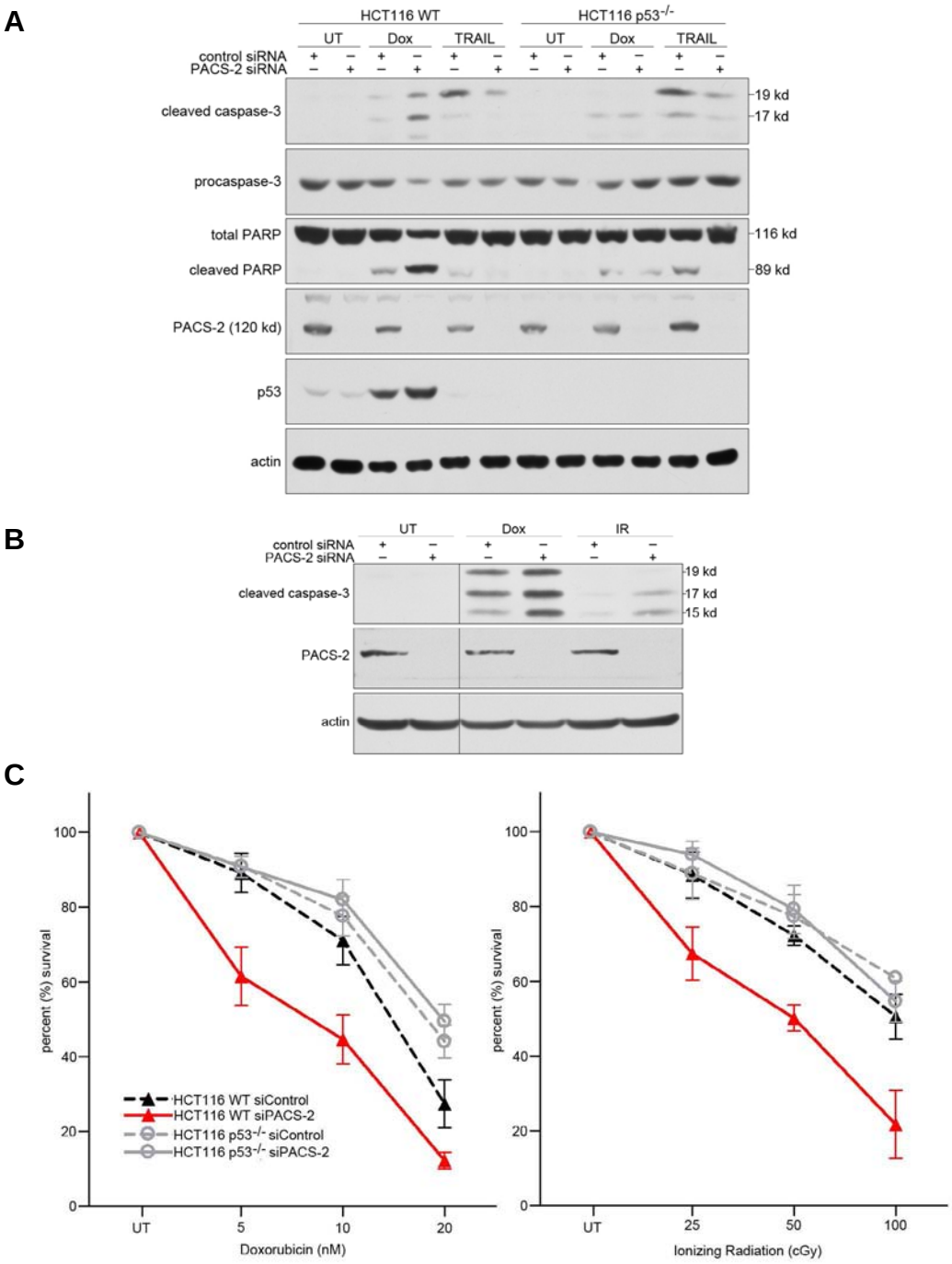

Figure 6.1. PACS-2 deficient cells display increased apoptosis and reduced clonogenic survival in a p53-dependent manner following DNA damage.

(A) HCT116 cells or isogenic p53$^{-/-}$ cells were transfected with control or PACS-2 siRNAs for 48 hours and then treated for an additional 48 hours with Doxorubicin

(0.5 μM) or treated for with TRAIL (20 ng/mL) 5 hours prior to harvest. Cell lysates were subjected to western blotting using cleaved caspase-3, procaspase-3, PARP, PACS-2, and p53 (DO-1) antibodies. Actin served as the loading control. (B) HCT116 cells were transfected with control or PACS-2 siRNAs for 48 hours and then treated for an additional 48 hours with Doxorubicin (0.5 μM) or 20 Gy ionizing radiation (IR). Cell lysates were subjected to western blotting using cleaved caspase-3, PACS-2, and p53 (DO-1) antibodies. Actin served as the loading control. (C) HCT116 cells or isogenic $p53^{-/-}$ cells were transfected with control siRNA (siControl) or PACS-2 siRNA (siPACS-2) for 72 hours and then seeded at 300 cells/well and 24 hours later treated with Doxorubicin (5, 10, or 20 nM) and IR (25, 50, 100 cGy). Following 24 hours of treatment, drug-containing media was replaced with fresh media. Colonies were fixed, stained, and counted 12-14 days following treatment. Error bars represent mean ± SD from ≥ 3 independent experiments.

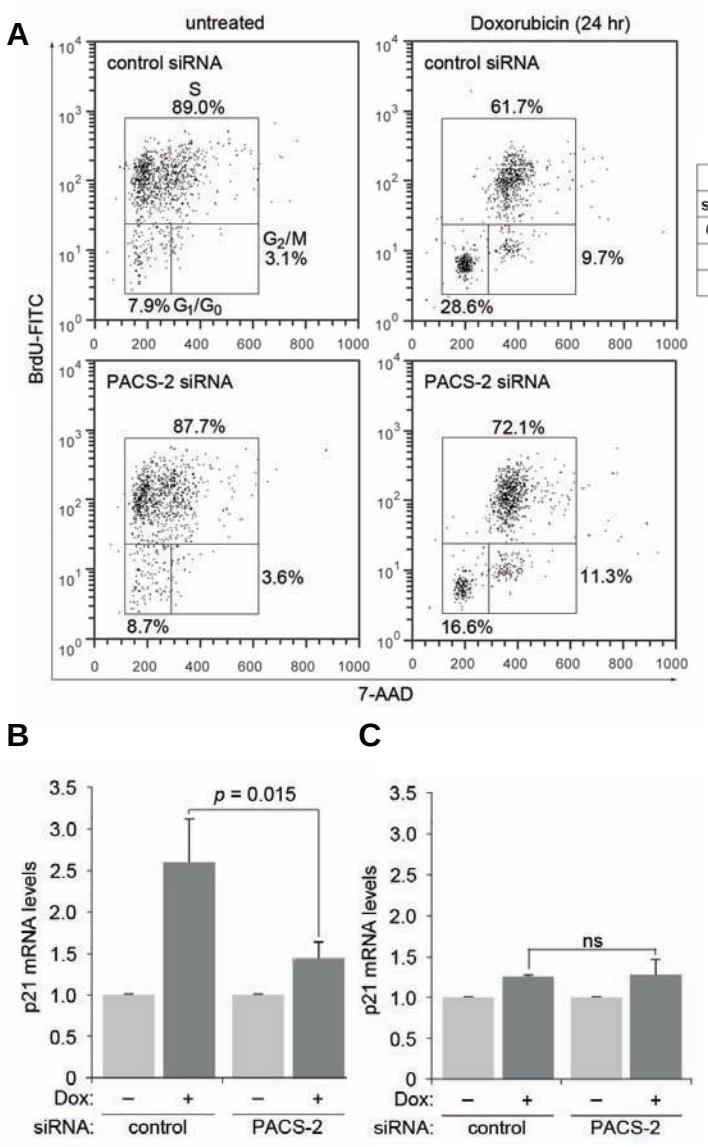

Relative % in each cell cycle phase (±SD)

	untreated		Doxorubicin (24 hr)		
siRNA:	control	PACS-2	control	PACS-2	*p* value
G_1/G_0	8.9±1.0	7.9±1.5	27.2±2.9	16.7±1.2	0.003
S	88±1.2	90.4±2.3	63.3±3.3	72.3±1.8	0.006
G_2M	2.4±0.6	2.4±1.6	9.5±0.4	11.0±0.7	0.01

Figure 6.2. PACS-2 deficient cells have reduced *p21* mRNA and G_1 cell cycle arrest following DNA damage.

(A) HCT116 cells were transfected with control or PACS-2 siRNAs for 48 hours and then synchronized by serum deprivation for an additional 24 hours. Cells were then stimulated to re-enter the cell cycle in the presence of 10 μM Bromodeoxyuridine (BrdU), treated with Doxorubicin (0.5 μM) for an additional 24

hours, and then processed for flow cytometry using anti-BrdU FITC and 7-Aminoactinomycin D (7-AAD). Left, representative scatter plots. Right, statistical analysis depicting mean percentage of cells in each cell cycle phase ± SD from 4 independent experiments. Statistical significance determined using an unpaired Student's t test. (B) HCT116 cells or (C) HCT116 $p53^{-/-}$ cells were transfected with control or PACS-2 specific siRNAs and then treated with doxorubicin (0.5 µM) for 4 hours. RNA was isolated and *p21* mRNA was analyzed by qRT-PCR (normalized to GAPDH). Error bars represent mean ± SD from ≥ 3 independent experiments. Statistical significance determined using Student's t-test. NS, not significant. (D) HCT116 cells were transfected with control or PACS-2 specific siRNAs and then treated with Doxorubicin (0.5 µM) for 4 hours, RNA was isolated and *PUMA* mRNA levels were analyzed by qRT-PCR. Error bars represent mean ± SD from four independent experiments. Statistical significance determined using Student's t-test. ns, not significant.

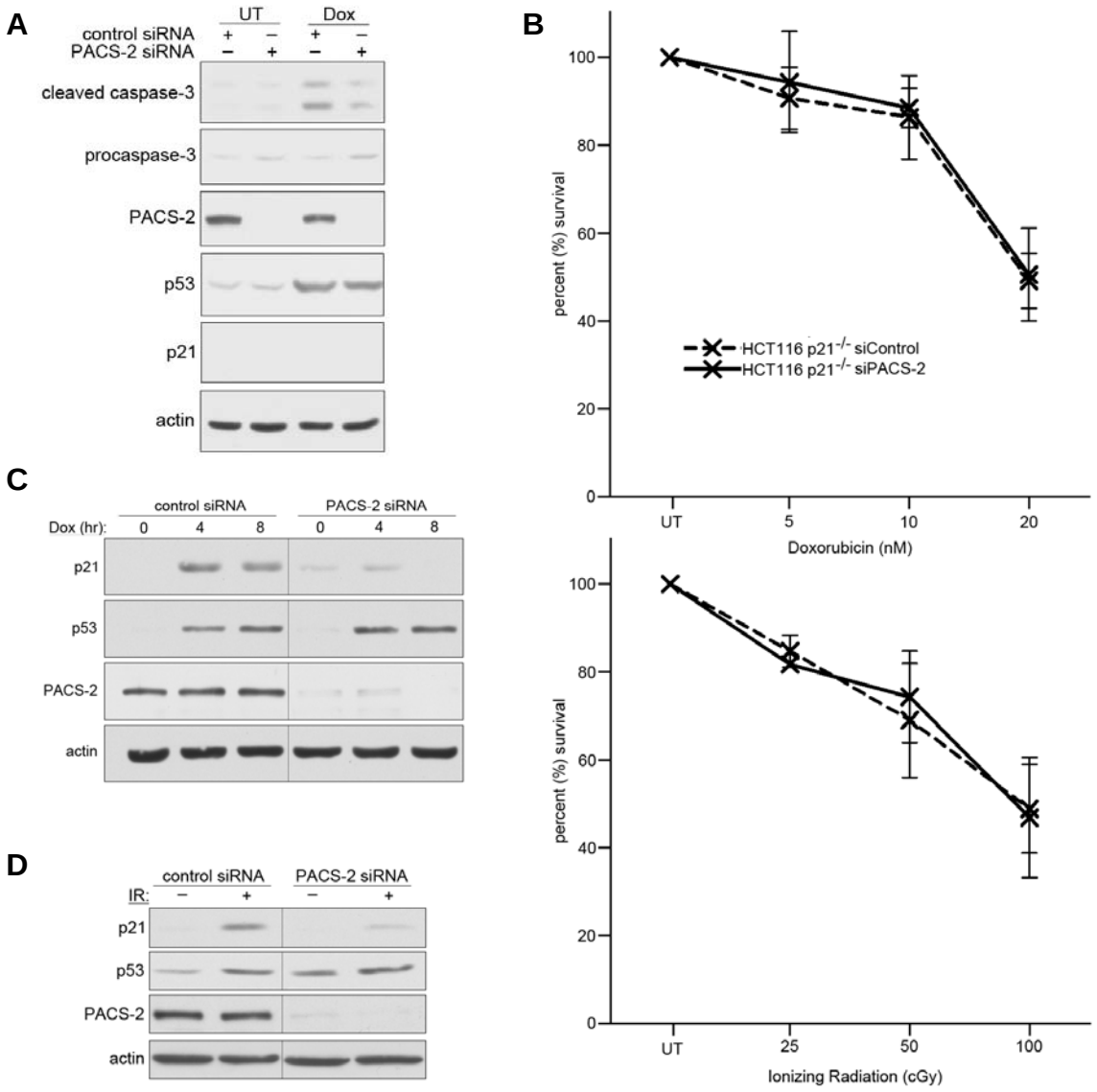

Figure 6.3. The increased apoptosis and reduced clonogenic survival in PACS-2 deficient cells following DNA damage is both p53- and p21-dependent.

(A) HCT116 $p21^{-/-}$ cells were transfected with control or PACS-2 siRNAs for 48 hours and then treated for an additional 48 hours with Doxorubicin (0.5 μM). Cell lysates were subjected to western blotting using cleaved caspase-3,

procaspase-3, PACS-2, p53 (DO-1), and p21 antibodies. Actin served as the loading control. (B) HCT116 $p21^{-/-}$ cells were transfected with control siRNA (siControl) or PACS-2 siRNA (siPACS-2) for 72 hours and then seeded at 300 cells/well and 24 hours later treated with Doxorubicin (5, 10, or 20 nM) and IR (25, 50, 100 cGy). Following 24 hours of treatment, drug-containing media was replaced with fresh media. Colonies were fixed, stained, and counted 12-14 days following following treatment. Error bars represent mean ± SD from ≥ 3 independent experiments. (C) HCT116 cells were transfected with control or PACS-2 siRNAs for 72 hours and then treated with Doxorubicin (0.5 μM) for 0, 4, or 8 hours prior to harvest. Cell lysates were subjected to western blotting using p21, p53 (DO-1), and PACS-2 antibodies. Actin served as the loading control. (D) U2OS cells were transfected with control or PACS-2 siRNAs for 72 hours and then treated with IR (20 Gy) for 24 hours prior to harvest. Cell lysates were subjected to western blotting using p21, p53 (DO-1), and PACS-2 antibodies. Actin served as the loading control.

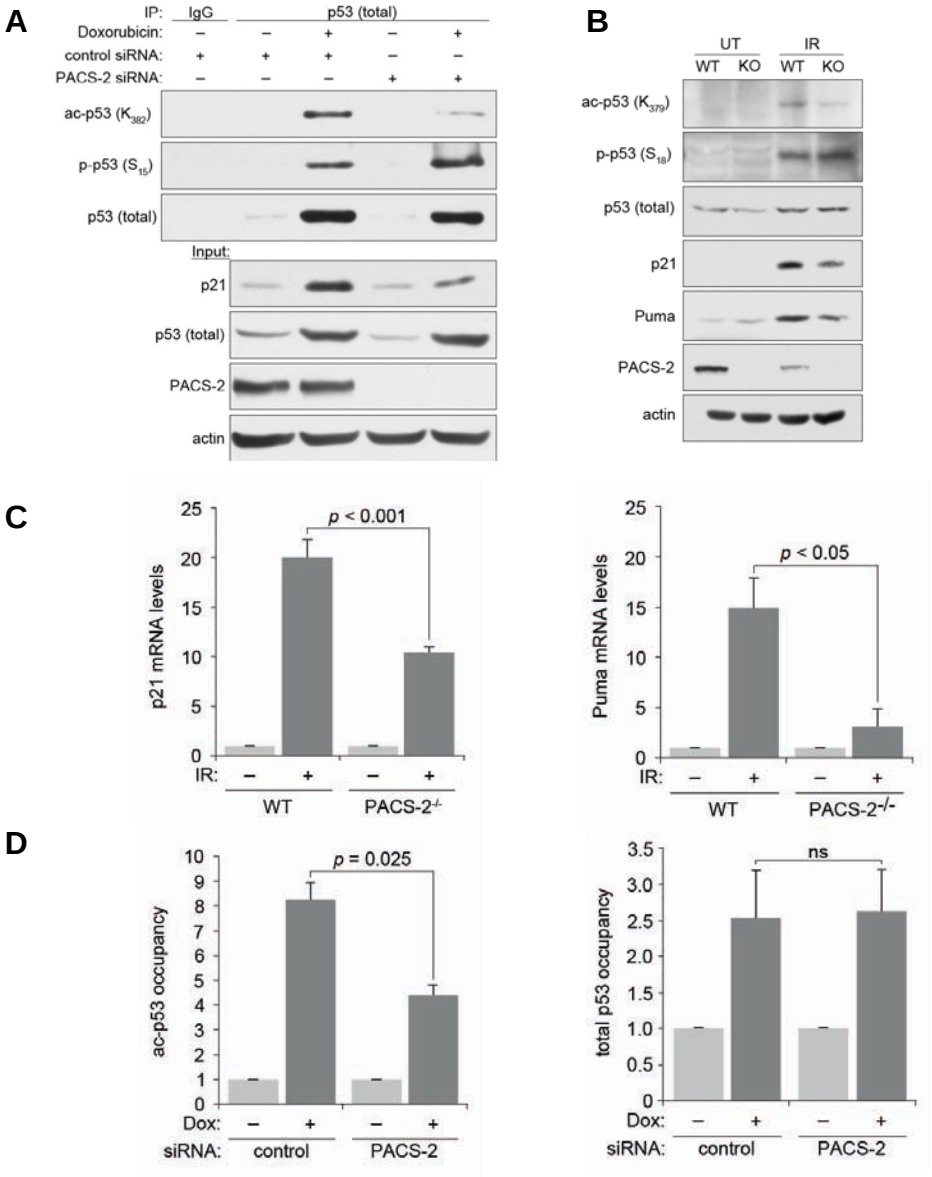

Figure 6.4. p53 acetylation is reduced in PACS-2 deficient cells following DNA Damage.

(A) HCT116 cells transfected with control or PACS-2 specific siRNAs were treated with doxorubicin (0.5 μM) for 6 hours, total p53 was immunoprecipitated with anti-p53 DO-1 antibody. Cell lysates were subjected to western blotting

using acetyl (ac)-p53 (K_{382}), phospho (p)-p53 (S_{15}), p53 (FL-393), p21, p53 (DO-1), and PACS-2 antibodies. Actin served as the loading control. (B) Thymuses from WT and *Pacs2*$^{-/-}$ mice were harvested 6 hours following exposure to 4.5 Gy ionizing radiation (IR) and analyzed by western blot for ac-p53 (K_{379}), p-53 (S_{18}), p53 (CM5), p21, and PACS-2 antibodies. Actin served as the loading control. Representative mice are shown from ≥ 10 mice per condition. (C) Thymuses from WT and *Pacs2*$^{-/-}$ mice were harvested 6 hours following exposure to 4.5 Gy ionizing radiation (IR). RNA was isolated and *p21* and *Puma* mRNA levels were analyzed by qRT-PCR (normalized to GAPDH). Error bars represent mean ± SEM from ≥ 4 mice per condition. Statistical significance determined using Student's t-test. (D) HCT116 cells transfected with control or PACS-2 specific siRNAs were treated with doxorubicin (0.5 μM) for 6 hours and then analyzed by chromatin immunoprecipitation (ChIP)-coupled with qRT-PCR for the p21 promoter using antibodies specific for total p53 (DO-1) or acetylated (ac)-p53 (K_{382}). Error bars represent mean ± SEM from 3 independent experiments. Statistical significance determined using Student's t-test. ns, not significant.

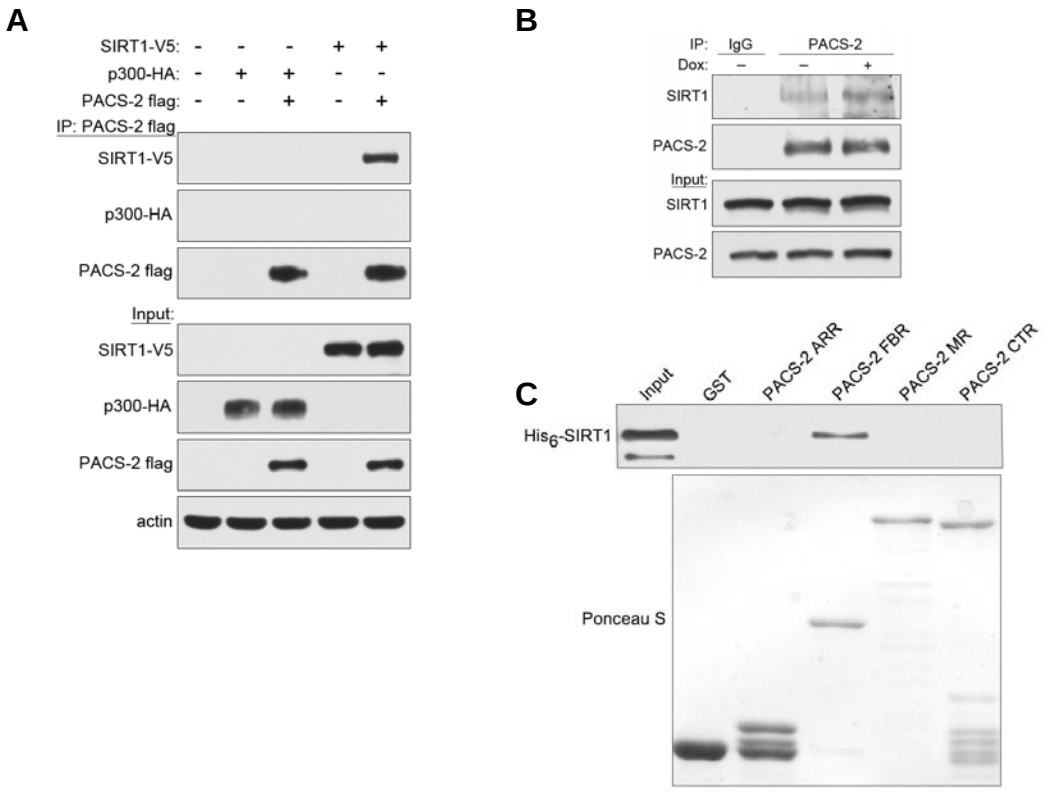

Figure 6.5. PACS-2 interacts with the histone deacetylase SIRT1 both *in vivo* and *in vitro*.

(A) HCT116 cells were transfected with SIRT1-V5 or p300-HA alone or together with PACS-2 flag and the amount of SIRT1-V5 or p300-HA co-immunoprecipitating with PACS-2 flag was detected by western blot. Actin served a loading control. (B) HCT116 cells were treated or not with Doxorubicin (0.5 µM) for 3 hours and then immunoprecipiated with control IgG or anti-PACS-2 (834) antibody and co-immunoprecipitating SIRT1 was detected by western blot. Actin served as a loading control. (C) His_6-SIRT1 was incubated with GST or the indicated GST constructs and the amount of interacting His_6-SIRT1 was detected by western blot using anti-His antibody.

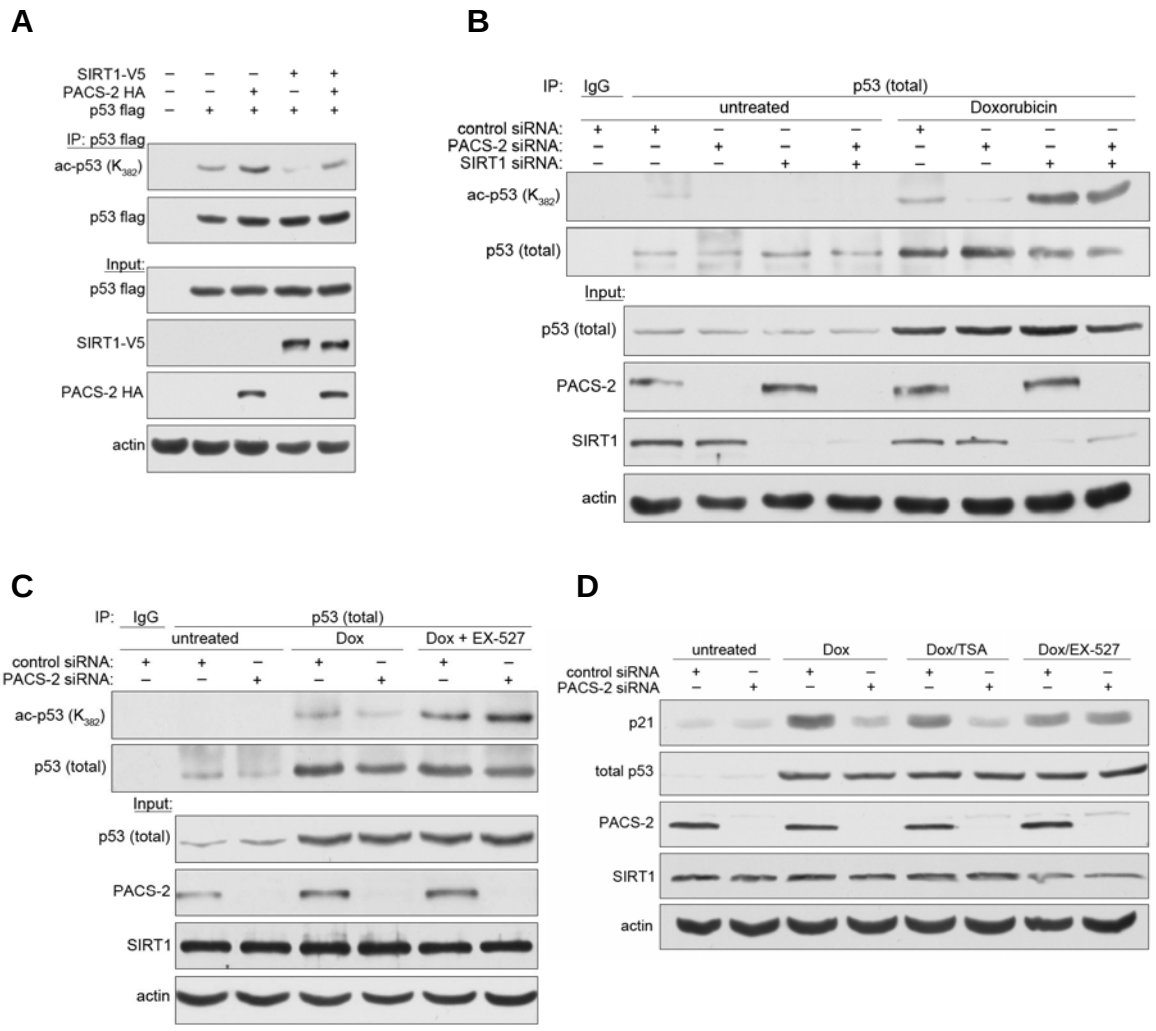

Figure 6.6. PACS-2 regulates SIRT1-mediated deacetylation of p53 *in vivo*.

(A) HCT116 cells were transfected with plasmids expressing p53 flag, PACS-2 HA, or SIRT1-V5 as indicated. p53 was immunoprecipitated and cell extracts were analyzed by western blot using acetylated (ac)-p53 (K_{382}), flag, V5, and HA antibodies. Actin served as a loading control. (B) HCT116 cells were transfected with control, PACS-2, or SIRT1 specific siRNAs as indicated and then treated with doxorubicin (0.5 μM) for 6 hours, total p53 was immunoprecipitated with anti-

p53 antibody (DO-1) and cell extracts were analyzed by western blot using acetylated (ac)-p53 (K_{382}), p53 (FL-393), p53 (DO-1), PACS-2, and SIRT1 antibodies. Actin served as a loading control. (C) HCT116 cells were transfected with control or PACS-2 specific siRNAs and then treated with doxorubicin (0.5 µM) alone or together with the SIRT1 inhibitor EX-527 (1 µM) for 6 hours, total p53 was immunoprecipitated with anti-p53 (DO-1) antibody and cell extracts were analyzed by western blot using acetylated (ac)-p53 (K_{382}), p53 (FL-393), p53 (DO-1), PACS-2, and SIRT1 antibodies. Actin served as a loading control. (D) HCT116 cells were transfected with control or PACS-2 specific siRNAs and then treated for 6 hours with doxorubicin (0.5 µM) alone, or together with the HDACI/II inhibitor Trichostatin A (TSA, 0.5 µM) or EX-527 (1 µM) as indicated. Cell lysates were analyzed by western blot using p21, p53 (DO-1), PACS-2, and SIRT1 antibodies. Actin served as a loading control.

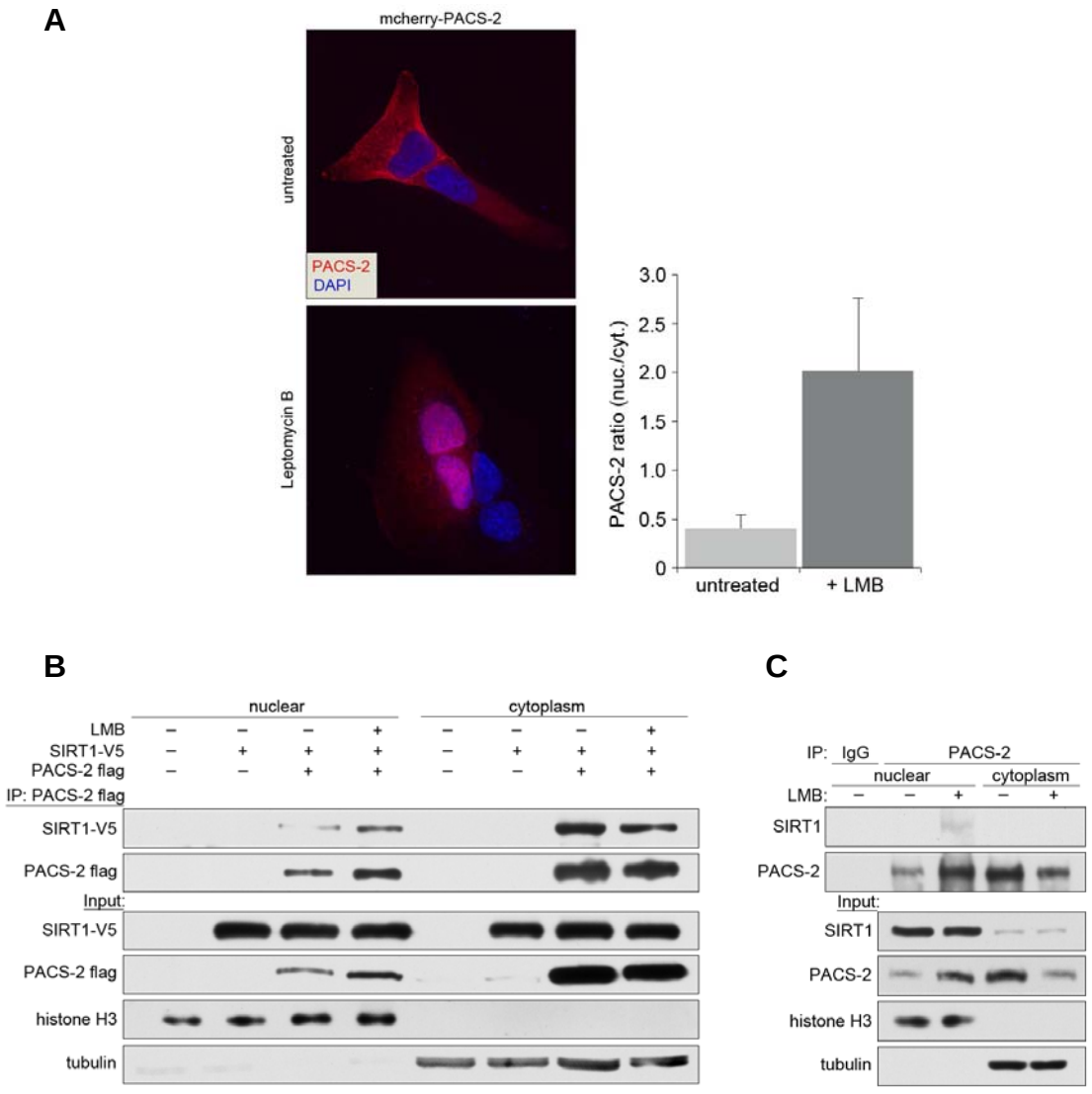

Figure 6.7. PACS-2 interacts with SIRT1 in the nucleus in a Leptomycin B-dependent manner.

(A) Left, U2OS cells expressing mcherry tagged PACS-2 were treated or not with 40 nM of the CRM1-dependent nuclear export inhibitor Leptomycin B (LMB) for 3 hours and PACS-2 localization was monitored by confocal microscopy. Right, the ratio of mcherry PACS-2 signal in the nucleus versus the cytoplasm was

quantified. Error bars represent mean ± SD from 3 independent experiments. (B) HCT116 cells were transfected with plasmids expressing PACS-2 flag or SIRT1-V5 as indicated and then treated with 40 nM Leptomycin B (LMB) for 16 hours prior to harvest and subcellular fractionation. PACS-2 flag was immunoprecipitated from nuclear and cytoplasmic fractions using anti-flag agarose and co-immunoprecipitating SIRT1-V5 was detected by western blot. Histone 3 and tubulin served as nuclear and cytoplasmic markers, respectively. (C) HCT116 cells were treated with 40 nM Leptomycin B (LMB) for 16 hours prior to harvest and subcellular fractionation. PACS-2 was immunoprecipitated from nuclear and cytoplasmic fractions using anti-PACS-2 (831) and co-immunoprecipitating SIRT1 was detected by western blot. Histone 3 and tubulin served as nuclear and cytoplasmic markers, respectively.

CHAPTER 7. DISCUSSION

CHAPTER 7. DISCUSSION

7.1 Summary

The results presented in Part II of this dissertation provide evidence that the membrane trafficking protein PACS-2 regulates the SIRT1-mediated deacetylation of p53 to modulate the cellular response to DNA damage (illustrated in Figure 7.1). We demonstrate that PACS-2 directly interacts with SIRT1 in the nucleus and inhibits SIRT1-mediated deacetylation of p53 *in vivo*. We found that PACS-2 deficient cells have a SIRT1-dependent reduction in p53 acetylation and p21 expression, resulting in increased apoptosis and reduced clonogenic survival in a p53- and p21-dependent manner following DNA damage. Moreover, loss of PACS-2 results in reduced levels of acetylated p53 bound to the p21 promoter following DNA damage. Additionally, we provide evidence that PACS-2 undergoes nucleocytoplasmic trafficking and interacts with SIRT1 in the nucleus of cells. Based on these observations, we propose that PACS-2 is a critical regulator of the SIRT1-p53 axis to modulate the DNA damage response. These results have diverse implications for future research directions regarding novel functions of PACS-2 in cellular processes such as gene regulation, chromatin remodeling, cell growth and survival as well as biological processes such as cancer, aging, and metabolism.

7.2 Novel roles for PACS-2 in apoptosis, cell survival, and tumorigenesis

Recent studies have determined that PACS-2 binds Nef on early endosomes to traffic Nef to the perinuclear region (Dikeakos et al., 2012, Atkins et al., 2008) as well as mediates TRAIL-induced lysosomal/mitochondria membrane trafficking steps leading to the induction of apoptosis in cancer cells (Aslan et al., 2009, Werneburg et al., 2012). Indeed, cells lacking PACS-2 are resistant to apoptosis induced by staurosporine or by the death ligands TNFα or TRAIL (Aslan et al., 2009, Simmen et al., 2005). However, while PACS-2 knockdown cells are resistant to death ligand-induced apoptosis, the studies in this dissertation demonstrate that PACS-2 deficient cells are conversely sensitized to DNA damage-induced apoptosis. Indeed, the observation that apoptosis is increased when cancer cells are treated with TRAIL in combination with chemotherapy or IR (Shankar et al., 2004) suggests various apoptotic pathways have redundant requirements for specific proteins and is consistent with the determination that PACS-2 has distinct roles in TRAIL- and p53-dependent apoptosis.

Notably, while the resistance to TRAIL-induced apoptosis in PACS-2 deficient cells is p53-independent, the sensitivity to DNA damage-induced apoptosis as well as the reduced clonogenic survival are both p53- and p21-dependent, suggesting PACS-2 plays distinct roles in cell survival depending on the nature of the apoptotic stimulus. Together, these data suggest that following DNA damage, PACS-2 deficient tumor cells are more sensitized to DNA damage-inducing chemotherapeutics and ionizing radiation. This finding is significant, as

the *PACS-2* gene is known to be dysregulated in a subset of human cancers. Indeed, the 14q32.33 locus containing *PACS-2* is highly susceptible to chromosomal instability in multiple cancers (Anderson et al., 2001, Gallegos Ruiz et al., 2008, Kang et al., 2006, Dijkman et al., 2006, Bando et al., 1999). Notably, the 14q32.33 locus is deleted in 44% of non-small cell lung carcinomas (NSCLC) (Gallegos Ruiz et al., 2008) and 68% of primary cutaneous large B-cell lymphomas (Dijkman et al., 2006) and is reported as frequently deleted in recurrent breast cancer (Kang et al., 2006) as well as colorectal cancer (Bando et al., 1999, Bartos et al., 2007). Specifically, the *PACS-2* gene has been reported to be deleted in 15-40% of sporadic colorectal cancer (Anderson et al., 2001), consistent with studies from our laboratory showing that PACS-2 protein expression is lost in late stage colorectal cancer (Aslan et al., 2009). These findings suggest tumors that lose *PACS-2*, yet retain wild-type *TP53* status, may be sensitized to chemotherapy or radiation treatment. Indeed, it will be important to test this hypothesis *in vivo* using mouse xenograft tumors from PACS-2 knockdown tumor cell lines treated with chemotherapeutic agents such as Doxorubicin as well as radiation therapy. Along with *in vivo* models, it will be essential to rigorously analyze the nature of PACS-2 expression in a variety of human cancers at various stages. Importantly, it will be essential to analyze the extent to which loss of *PACS-2* occurs independent of *TP53* mutational status. Interestingly, one study suggests that the genomic instability in colorectal cancer, which leads to the frequent loss of the locus containing *PACS-2*, precedes *TP53*

mutation (Kahlenberg et al., 1996). This would suggest that *PACS-2* loss occurs independent of *TP53* mutational status in colorectal cancer. However, a much more comprehensive and rigorous methodology is required to test this hypothesis. Indeed, this analysis is essential for understanding the therapeutic importance of *PACS-2* loss, as tumors with mutated *TP53* and concurrent *PACS-2* loss would likely not be sensitized to DNA damage in the p53- and p21-dependent nature we observed in wild-type *TP53* harboring tumor cell lines. However, tumors with loss of *PACS-2* that retain wild-type *TP53* may be sensitized to particular therapies. Moreover, future studies should analyze how PACS-2 expression correlates with invasiveness, prognosis, and survival in a variety of tumor types. Together, these future studies and analyses will be essential for testing the biological implications of *PACS-2* loss in tumors and whether *PACS-2* status may be a potential marker for identifying tumors likely to benefit from particular DNA damaging therapies.

An additional layer of complexity regarding therapeutic sensitivity of PACS-2 deficient cells exists in PACS-2's role as a TRAIL effector. The determination that PACS-2 is essential for TRAIL-induced apoptosis in multiple cancer cells lines (Aslan et al., 2009, Werneburg et al., 2012), suggests tumors that undergo loss of PACS-2 may be resistant to TRAIL therapy. However, this TRAIL-dependent requirement for PACS-2 is muted by the increasing number of cell lines identified as resistant to TRAIL therapy (Zhang et al., 2005). Importantly, recent studies suggest the induction of tumor cell apoptosis can be increased in

both TRAIL-resistant and TRAIL-sensitive cell lines when TRAIL is combined with DNA damage-inducing chemotherapeutics or irradiation (Shankar et al., 2004), suggesting multiple apoptotic pathways can synergize to kill cancer cells. Indeed, this notion of synergism in preclinical studies (Shankar et al., 2004), together with limited evidence of efficacy using TRAIL agonism as a monotherapy, lead to the clinical testing of recombinant TRAIL or TRAIL receptor agonists in combination with various chemotherapeutic drugs in patients with advanced NSCLC (Soria et al., 2011, Von Pawel J, 2010, Karapetis CS, 2010). These findings, together with the determination that PACS-2 loss sensitizes cells to p53-mediated DNA damage-induced apoptosis and reduced long-term survival, suggests that while PACS-2 loss may be a negative prognostic determinant regarding TRAIL therapy, it may conversely indicate sensitivity to DNA damaging therapeutics. Therefore, similar to that described above, it would be important to analyze how PACS-2 loss correlates with TRAIL resistance or sensitivity as well as clinical response or outcome in patients treated with TRAIL in combination with various chemotherapeutics. However, since the use of TRAIL agonism as a clinical therapeutic is in its infancy, this analysis will take time to acquire adequate tissues from various tumors and patients to rigorously test this hypothesis.

7.3 The role of PACS-2 in p21 function

The function of the G_1/S checkpoint is to prevent cells harboring DNA damage from transitioning into S-phase, thereby replicating the damaged DNA.

This process is largely dependent on the p53-mediated transactivation of the CDK inhibitor p21 (el-Deiry et al., 1993, Deng et al., 1995, Brugarolas et al., 1995). Indeed, in cells lacking p53, expression of p21 alone is sufficient to induce G_1 growth arrest (Rousseau et al., 1999) while conversely, G_1 arrest is abrogated following DNA damage in mouse embryonic fibroblasts and human cancer cells from which p21 has been genetically deleted (Brugarolas et al., 1995, Deng et al., 1995, Waldman et al., 1995). Consistent with this determination, the data in this dissertation demonstrate reduced p53-dependent p21 expression following PACS-2 knockdown that correlates with impaired G_1 arrest following DNA damage. These findings are consistent with the well-characterized cell cycle inhibitory functions of p21 and suggest that PACS-2 functions to promote G_1 growth arrest following DNA damage. However, since the initial discovery of p21 as a cell-cycle inhibitor and p53 effector (el-Deiry et al., 1993, Harper et al., 1993, Gu et al., 1993, Xiong et al., 1993, Noda et al., 1994, Dulic et al., 1994), p21 has been implicated in a multitude of cellular processes including apoptosis, differentiation and senescence, DNA repair, aging, reprogramming of induced pluripotent stem cells (Coqueret, 2003, Garner et al., 2008, Gartel et al., 2002, Li et al., 2009a) as well as tumor suppression and tumor formation (el-Deiry et al., 1993, Efeyan et al., 2007, Barboza et al., 2006, Martin-Caballero et al., 2001, Roninson, 2002, Gartel, 2006, Abbas et al., 2009). Therefore, in future studies it will be important to test whether the role for PACS-2 in regulating p21 expression extends to additional p21-mediated cellular processes following DNA damage,

such as DNA repair and senescence, and to what extent this affects tumorigenesis *in vivo*.

The function of p21 to inhibit cell proliferation is a major determinant of p53-mediated tumor suppression (el-Deiry et al., 1993, Efeyan et al., 2007). Indeed, deletion of p21 accelerates tumor formation in mice expressing a p53 mutant (R_{172}→P) that are deficient in apoptosis but retain some growth arrest activity (Barboza et al., 2006) as well as accelerates the development of chemically induced tumors (Topley et al., 1999, Poole et al., 2004, Jackson et al., 2002, Philipp et al., 1999). However, the first genetic evidence of a tumor suppressor role for p21 resulted from the discovery that p21 knockout mice develop spontaneous tumors at ~16 months of age (Martin-Caballero et al., 2001). However, the relatively late onset of these tumors compared to those that develop in mice lacking other tumor suppressors such as p53 (Donehower et al., 1992, Jacks et al., 1994), p16 (Serrano et al., 1996), or ARF (Kamijo et al., 1999), suggests additional factors likely contribute to malignancy in the absence of p21 (Martin-Caballero et al., 2001). Notably, while many human cancers are associated with reduced p21 expression, such as colorectal (Bukholm et al., 2000, Edmonston et al., 2000, Ogino et al., 2006, Polyak et al., 1996, Zirbes et al., 2000, Mitomi et al., 2005) and NSCLC (Komiya et al., 1997), loss-of-function mutations in p21 are exceptionally rare (Shiohara et al., 1994, McKenzie et al., 1997, Patino-Garcia et al., 1998). Rather, it is suggested that p21 cooperates with other tumor suppressors and antagonizes oncogenes to mediate its tumor

suppressive functions (Abbas et al., 2009). Interestingly, p21 expression is repressed in the same tumor types that frequently undergo loss of PACS-2, namely colorectal cancer and NSCLC (Gallegos Ruiz et al., 2008, Anderson et al., 2001, Bukholm et al., 2000, Edmonston et al., 2000, Ogino et al., 2006, Polyak et al., 1996, Zirbes et al., 2000, Mitomi et al., 2005, Komiya et al., 1997), suggesting perhaps there is a correlation between PACS-2 loss and p21 in human tumors. It would be important in future studies to analyze the correlation between PACS-2 and p21 expression in colorectal and NSCLCs that contain wild-type or mutated p53.

Intriguingly, however, it was the discovery of p21 as an inhibitor of apoptosis that lead to the investigation into oncogenic activities of p21 (Gartel et al., 2002, Roninson, 2002, Gartel, 2006). Indeed, the upregulation of p21 expression in certain cancers positively correlates with tumor grade and invasiveness and is a poor prognostic indicator (Abbas et al., 2009). Limited genetic studies suggest that p21 deletion suppresses the development of spontaneous lymphomas in mice lacking p53 (De la Cueva et al., 2006) or ATM (Wang et al., 1997) as well as suppresses radiation-induced lymphomas in p53-null mice (De la Cueva et al., 2006). Therefore, Gartel et al. proposed that p21 exhibits “antagonistic duality”; in that it can inhibit apoptosis (oncogenic function) to counter its growth arrest effects (tumor suppressive function) (Gartel et al., 2002). Importantly, the studies in this dissertation demonstrate that PACS-2 deficiency leads to impaired induction of p21 that correlates with reduced growth

arrest, resulting in increased apoptosis and reduced clonogenic survival in a p53- and p21-dependent manner. These findings are consistent with both the growth arrest and anti-apoptotic functions of p21 (Dotto, 2000, Gartel et al., 2002, Cazzalini et al., 2010) and suggest that mice harboring PACS-2 deficient xenograft tumors would be sensitized to DNA damage-inducing chemotherapeutics as well as IR due to reduced p21-mediated inhibition of apoptosis. Moreover, PACS-2 deficient mice may also be sensitized to chemically induced tumorigenesis, similar to p21 knockout mice (Topley et al., 1999, Poole et al., 2004, Jackson et al., 2002, Philipp et al., 1999), due to reduced tumor suppressive effects of p21-mediated growth arrest. Moreover, if the tumor suppressive effects in PACS-2 deficient mice were indeed p21-dependent, then *Pacs2*$^{-/-}$*;p21*$^{-/-}$ mice should not be sensitized to tumor formation beyond the extent of p21-null mice. Together, these future studies would be important in testing whether PACS-2 has tumor suppressive functions and the extent to which resulting effects are p21-dependent.

7.4 Mechanisms of SIRT1 regulation

SIRT1 was identified as a p53 deacetylase that binds the lysine-rich C-terminal region of p53 (Langley et al., 2002) to catalyze p53 deacetylation and thereby regulate p53 transcriptional activities and function (Langley et al., 2002, Luo et al., 2001, Vaziri et al., 2001). The experiments in this dissertation identify PACS-2 as a novel regulator of the SIRT1-p53 axis following DNA damage.

Specifically, our studies demonstrate that PACS-2 interacts with SIRT1 *in vivo* and *in vitro*, as well as inhibits SIRT1-mediated deacetylation of p53 *in vivo*. Moreover, similar to siRNA knockdown of the other known SIRT1 inhibitors DBC1 (Kim et al., 2008, Zhao et al., 2008) or Set7/9 (Liu et al., 2011), there is a marked reduction of p53 acetylation in PACS-2 siRNA-treated cells following DNA damage that is completely reversed with concomitant siRNA knockdown or enzymatic inhibition of SIRT1. While our data clearly implicate a role for PACS-2 in modulating the SIRT1-p53 axis *in vivo*, the precise mechanism of this regulation remains to be elucidated. One component of this mechanism is the identification of regions critical for interaction, therefore future studies should include detailed mapping of the binding sites between SIRT1 and PACS-2. While our data demonstrate that the PACS-2 cargo binding region, as expected, is responsible for interacting with full-length SIRT1, it will be important to map the precise region on SIRT1 required for interacting with PACS-2, and vice versa. Subsequent studies could then test the ability of a SIRT1 mutant that fails to bind PACS-2 to mediate p53 deacetylation and regulate p53-induced transcription of target genes. Conversely, the SIRT1-dependent specificity of PACS-2-mediated effects on p53 could be investigated by the generation of a PACS-2 mutant that is unable to bind SIRT1. Future studies should also address whether PACS-2 affects the interaction between SIRT1 and p53 to inhibit SIRT1 function. Indeed, both DBC1 and Set7/9, which bind the catalytic and N-terminal regions of SIRT1, respectively, can disrupt the interaction between SIRT1 and p53 *in vivo* (Zhao et

al., 2008, Liu et al., 2011), however the mechanisms mediating these effects are unknown. In addition, while PACS-2 interacts with SIRT1 directly and clearly has a role in regulating SIRT1-mediated deacetyation of p53 *in vivo*, we cannot eliminate the possibility this effect is due to an indirect mechanism of SIRT1 regulation. For instance, PACS-2 could inhibit the endogenous SIRT1 activator AROS, affect cofactor availability by altering the levels of NAD^+ biosynthesis, affect cellular concentrations of the noncompetitive endogenous inhibitor nicotinamide, or alter SIRT1 subcellular localization. Therefore, it will be important for future studies to more precisely elucidate the mechanism of how PACS-2 regulates SIRT1 to have a greater understanding of the biological context in which this regulation is critical.

One caveat to the elucidation of precise mechanisms regulating SIRT1 activity is the lack of a solved crystal structure for human SIRT1. Indeed, much of the information known regarding the NAD^+-dependent mechanism of the Sirtuin reaction is based on crystal structures solved for human SIRT2, SIRT3, SIRT5, and SIRT6, or other Sirtuin homologs such as bacteria (CobB and Sir2Tm), yeast (Sir2 and Hst2), and archea (Sir2-Af1 and Sir2-Af2) in various ligated forms (Sanders et al., 2010). To note, sequence homology among Sirtuins is limited to the catalytic domain, an ~270 amino acid region that is sufficient for catalytic activity (Landry et al., 2000, Imai et al., 2000). Interestingly, prokaryotic organisms contain only one or two Sirtuins, and these homologs are relatively small, containing few residues outside the highly conserved catalytic domain

(Frye, 2000). Conversely, eukaryotic organisms often have several Sirtuin homologs that contain more extended N- and C-terminal sequences (Frye, 2000). However, human SIRT1 is arguably the most complex of the Sirtuins, as it contains the most extended N- and C-terminal segments flanking the catalytic core and by far has the most number of identified substrates (Stunkel et al., 2011, Pan et al., 2012). These findings, together with recent protein biochemistry studies determining that the evolutionarily diverse N- and C-terminal segments of SIRT1 play critical autoregulatory functions to increase SIRT1 deacetylase activity (Pan et al., 2012), suggest that various protein binding partners can dramatically alter SIRT1 activity by interacting with or affecting the conformation of the N- and C-terminal domains. Therefore, it will continue to be of great interest and heavy pursuit in the field to co-crystalize substrate-ligated SIRT1 with various binding parters to further elucidate the mechanisms by which proteins such as DBC1, Set7/9, AROS, and PACS-2 can modulate SIRT1 activity.

7.5 Implications of modulating SIRT1 function

Given the tremendous number of SIRT1 substrates and the biologic complexity of these targets, SIRT1 has been associated with diverse normal and abnormal processes such as aging, neural plasticity, memory, metabolism, inflammation, immunity, neurodegeneration, and cancer (Haigis et al., 2010, Saunders et al., 2007). Because of these pleiotropic functions, SIRT1 has been widely investigated as a prospective therapeutic target for multiple disease

processes. Indeed, studies suggest that SIRT1 activators may be therapeutically beneficial in inflammatory or metabolic diseases as well as in neurodegeneration (Stunkel et al., 2011).

The most well-characterized function of SIRT1 is the regulation of multiple targets involved in metabolism and energy homeostasis. These studies have identified SIRT1 as having robust protective effects against pathologies associated with chronic intake of high-fat diet, such as glucose intolerance and liver steatosis (Herranz et al., 2010, Pfluger et al., 2008, Banks et al., 2008). In particular, these studies have identified SIRT1 as a master regulator of metabolic pathways such as gluconeogenesis and lipogenesis, as well as implicated SIRT1 in the control of the central regulation of food intake (Sasaki et al., 2010) and circadian clock function (Bellet et al., 2010). SIRT1 mediates these effects through transcriptional silencing as well as through direct interaction with specific corepressors (Stunkel et al., 2011). For instance, the SIRT1-mediated deacetylation of PGC-1α promotes gluconeogenic gene induction and increases hepatic glucose output during caloric restriction (Rodgers et al., 2005), while deacetylation of LXR and downregulation of PTP1B enhances reverse cholesterol transport and decreases insulin resistance, respectively (Sun et al., 2007, Li et al., 2007). In addition, SIRT1 enhances fatty acid mobilization from adipose tissue as well as positively regulates insulin secretion in pancreatic β-cells through the deacetylation of PPARγ (Picard et al., 2004, Moynihan et al., 2005, Banks et al., 2008). Interestingly, overexpression of SIRT1 in the liver

enhances insulin sensitivity (Li et al., 2011b) while SIRT1 knockdown results in insulin resistance, likely through PTP1B silencing at the chromatin level (Sun et al., 2007). Moreover, SIRT1 activation has been linked to insulin sensitivity, enhanced fatty acid oxidation, and decreased lipogenesis (Haigis et al., 2006, Liang et al., 2009), further supporting the therapeutic implications of SIRT1 activation for metabolic diseases. The determination that PACS-2 inhibits SIRT1 function at the level of p53, suggests that perhaps PACS-2 plays a role in modulating SIRT1 activity toward other substrates, such as those involved in metabolic pathways. This hypothesis is currently being tested in the laboratory, with ongoing experiments working toward characterizing the metabolic phenotype of PACS-2 deficient animals basally, as well as in response to high-fat diet induced obesity. These ongoing and future studies will be essential for determining if PACS-2-mediated SIRT1 regulation extends to additional pathways beyond p53.

While the role of SIRT1 in metabolism is complex, accumulating evidence continues to support well-defined protective roles for SIRT1 in regulating energy metabolism. However, in the context of cancer, the role for SIRT1 is much less clear. A function for SIRT1 in cancer initially stemmed from the ability of SIRT1 to deacetylate the tumor suppressor p53, thereby inhibiting its transactivation functions (Luo et al., 2001, Vaziri et al., 2001). Consistent with this determination, p53 is hyperacetylated in SIRT1 deficient mice, resulting in increased thymocyte apoptosis (Cheng et al., 2003), although this result could not be confirmed by

other investigators (Kamel et al., 2006). Subsequent studies determined that SIRT1 is elevated in multiple cancers (Deng, 2009), supporting the notion that SIRT1 may be oncogenic. However, the majority of *in vivo* studies with genetically modified SIRT1 support the idea that SIRT1 has tumor suppressive functions (Firestein et al., 2008, Herranz et al., 2010, Oberdoerffer et al., 2008, Wang et al., 2008a). Notably, increased SIRT1 expression results in delayed development of lymphomas and sarcomas in $p53^{+/-}$ mice, while loss of SIRT1 accelerates tumor formation (Wang et al., 2008a, Oberdoerffer et al., 2008). Moreover, the ability of SIRT1 overexpression to protect $Apc^{+/min}$ mice from intestinal tumors lead to the determination that SIRT1 deacetylates and inhibits β-catenin to mediate this effect (Firestein et al., 2008). Intriguingly, the first direct evidence of an oncogenic function for SIRT1 *in vivo* was a study that reported that increased SIRT1 expression in mice lacking the tumor suppress PTEN, a PIP_3 phosphatase that attenuates PI3K signaling, produced aggressive thyroid and prostate carcinomas (Serrano, 2011). Together, these studies illustrate how regulation of SIRT1 may be a double-edged sword that requires tight control and a much more thorough understanding of biological context. Therefore, it will be important to test in future studies if PACS-2 additionally regulates SIRT1-mediated deacetylation of histones or other nonhistone substrates, to better understand the extent to which PACS-2 modulates SIRT1 function.

7.6 Nuclear functions for PACS-2

Prior to the studies in this dissertation, PACS-2 function had thus far been studied in the context of various cytoplasmic membrane trafficking roles (Youker et al., 2009). Therefore, the determination that PACS-2 was regulating cell fate processes in a manner dependent on the predominantly nuclear SIRT1, p53 and p21 proteins, lead us to test whether PACS-2 could additionally localize to the nucleus. Indeed, our studies determined that PACS-2 could shuttle between the nucleus and the cytoplasm, as well as interact with endogenous SIRT1 in the nucleus. This determination was noteworthy regarding known PACS protein functions, and suggested PACS may have additional uncharacterized nuclear roles. This notion was consistent with accumulating data demonstrating that some membrane-associated cytoplasmic trafficking proteins have additional nuclear gene regulation functions, such as the protein kinase CK2 (Yamane et al., 2005, Pluemsampant et al., 2008) and GSK3β (Hoeflich et al., 2000, Grimes et al., 2001, Zhou et al., 2004, Jope et al., 2004). Conversely, many nuclear proteins such as CtBP (Corda et al., 2006), HDAC3 (Longworth et al., 2006), and p53 (Green et al., 2009) have been characterized as having membrane-associated functions. Together, these findings support a functional link between the endomembrane system and gene regulation pathways, and support a potential nuclear role for PACS-2 in SIRT1-mediated transcriptional regulation of p53 target genes, such as p21. Therefore, it will be essential for future studies to discern the mechanism of PACS-2 nuclear transport. It will be critical to identify the PACS-2 nuclear localization and nuclear export sequences, as well as to

determine what cellular factors regulate the shuttling of PACS-2 between the nucleus and cytoplasm. Importantly, future studies should also address whether PACS-2 nuclear localization is required for its ability to modulate the SIRT1-p53 axis.

The determination that PACS-2 has nuclear trafficking capabilities opens the door to analyzing novel nuclear functions of PACS-2. One manner in which this could be performed would be by overexpressing PACS-2 or a PACS-2 mutant deficient in nuclear localization, immunoprecipitating PACS-2 from the nucleus of cells and then identifying co-immunoprecipitating proteins by mass spectrometry. This type of analysis would provide useful information as to the scope of nuclear proteins that interact with PACS-2 and suggest clues to subsequent experimental approaches to investigate. Moreover, the determination that PACS-2 traffics to the nucleus, as well as binds SIRT1 and modulate p53 transcription in a SIRT1-dependent manner suggests that perhaps PACS-2 associates with these factors at DNA promoters or even binds DNA itself. In future studies, it will be important to investigate this hypothesis by coupling chromatin immunoprecipitation using anti-PACS-2 antibodies with massively parallel sequencing (ChIP-seq) to identify DNA regions that associate with PACS-2. This type of analysis would provide useful information to whether PACS-2 associates with transcription factors at the chromatin level on specific genes, such as p21; moreover, whether PACS-2 associates with additional promoters in a sequence-specific manner. Together, these studies would

provides clues as to the nuclear functions of PACS-2 and what gene regulation pathways or networks in which PACS-2 may function.

7.7 Systematic approach to the role of PACS-2 in gene regulation, cancer, and beyond

The studies in this dissertation implicate PACS-2 in regulating a SIRT1-p53-p21 axis, thereby modulating cellular fate following DNA damage. Importantly, SIRT1, p53, and p21 have complex, even conflicting, roles in tumor suppression and tumor formation as well as in cell death and cell survival. Indeed, both SIRT1 and p21 have been identified as having both tumor suppressive and oncogenic roles depending on the cellular context, and both can mediate these effects in a p53-dependent and -independent manner (Abbas et al., 2009, Stunkel et al., 2011), illustrating the complexity of these gene regulation networks. These complex and conflicting findings suggest that to understand the role of PACS-2 in modulating these processes will require a comprehensive and systematic approach. Thus far, studies regarding the role of PACS in cancer and tumor cell signaling have relied primarily on the analysis of specific cellular effects following PACS-2 knockdown or overexpression in a limited number of cancer types/cell lines. Therefore, to comprehensively analyze the role of PACS-2 in various cell death and survival pathways, future experiments should be performed using a systems biology approach. This type of methodology would computationally analyze high throughput genomic, transcriptomic, and proteomic

data gathered from multiple tumor cell lines after knockdown or overexpession of PACS-2. Importantly, this approach could be used with PACS-2 mutants, such as one deficient in nuclear localization, or that cannot bind SIRT1, etc. This computational analysis could then correlate experimental conditions, such as DNA damage or radiation treatment, to changes in genomic, transcriptomic, and proteomic profiles depicting various cellular processes and signaling pathways. This type of unbiased analysis would help identify which signaling and gene regulation pathways PACS-2 functions, as well as analyze how the role of PACS-2 in particular pathways might change depending on tumor cell type; ultimately yielding critical information as to the cellular context of PACS-2 dysregulation and how this might be useful in understanding the role of PACS-2 in cancer and other disease processes.

Importantly, performing a systems biology approach to understanding the role of PACS-2 in signaling pathways and gene regulation networks by comprehensively analyzing tumor cell lines or tissues would help facilitate subsequent studies to test these functions *in vivo* in mouse tumorigenesis models. However, the strength of these tumor models lies, in part, in the types of animals used for the analysis. Currently, our laboratory has analyzed *Pacs2* loss using a gene trap knockout strategy. Although gene trap knockout mice can be very effective, there are limitations regarding potential differential or alternative splicing, and this strategy does not always generate null alleles and animals can indeed become hypomorphic. Moreover, in any constitutive knockout model there

is always the possibility that compensatory mechanisms may arise during embryonic development which may mask cellular processes regulated by the gene of interest. This is consistent with studies showing that the single Caenorhabditis elegans PACS protein localizes to early endosomes and was identified in a genetic screen as a mediator of synaptic transmission, as knockdown of *PACS* lead to severe defects at the neuromuscular junction (Sieburth et al., 2005). This striking defect is in contrast to *Pacs2* gene trap knockout mice, which are developmentally normal and contain no obvious physical or behavioral defect. Therefore, in future studies it may be useful to develop tamoxifen-inducible tissue specific-*Pacs2* knockout mice, thereby controlling the timing and location of *Pacs2* knockdown in various tumor models. This type of methodology would also be very useful for studying PACS-2 function in a variety of contexts related to other known PACS-2 functions, such as polycystic kidney disease, TRAIL action, and viral pathogenesis (Youker et al., 2009).

7.8 Conclusion to PART II

The results presented in Part II of this dissertation provide evidence that the membrane trafficking protein PACS-2 regulates the SIRT1-mediated deacetylation of p53 to modulate the cellular response to DNA damage (illustrated in Figure 7.1). We demonstrate that PACS-2 directly interacts with SIRT1 in the nucleus and inhibits SIRT1-mediated deacetylation of p53 *in vivo*.

We found that PACS-2 deficient cells have a SIRT1-dependent reduction in p53 acetylation and p21 expression, resulting in increased apoptosis and reduced clonogenic survival in a p53- and p21-dependent manner following DNA damage. Moreover, loss of PACS-2 results in reduced levels of acetylated p53 bound to the p21 promoter following DNA damage. Additionally, we provide evidence that PACS-2 undergoes nucleocytoplasmic trafficking and interacts with SIRT1 in the nucleus of cells. Based on these observations, we propose that PACS-2 is a critical regulator of the SIRT1-p53 axis to modulate the DNA damage response. These results have diverse implications for future research directions regarding novel functions of PACS-2 in cellular processes such as gene regulation, chromatin remodeling, cell growth and survival as well as biological processes such as cancer, aging, and metabolism.

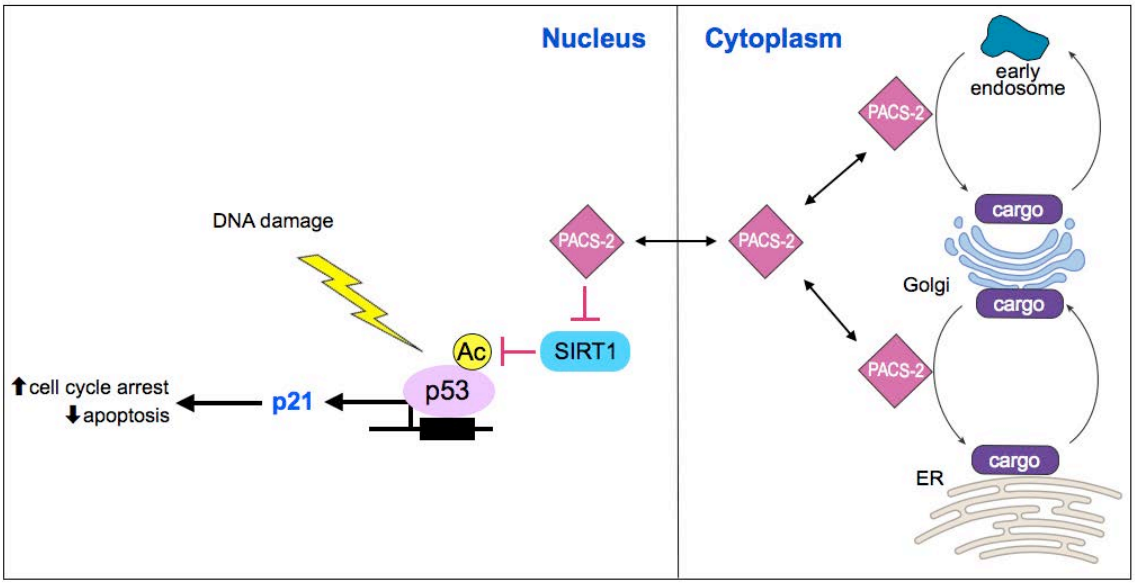

Figure 7.1. Model of PACS-2 dual-function in membrane traffic and p53 transcriptional activation.

In the cytoplasm, PACS-2 mediates the TGN-localization of cargo such as Nef and CI-MPR (Atkins et al., 2008), as well the ER-localization of cargo such as profurin, PKD2, and calnexin (Feliciangeli et al., 2006, Kottgen et al., 2005, Myhill et al., 2008). In the nucleus, PACS-2 inhibits SIRT1-mediated deacetylation of p53 following DNA damage, thereby increasing p53 transcriptional activation, including the expression of p21, resulting in p21-mediated growth arrest and inhibition of apoptosis.

CHAPTER 8. Conclusion

The studies in this dissertation describe how the identification of PACS-2 as essential for HIV-1 Nef-mediated immune evasion lead to the discovery of a small molecule inhibitor that targets a critical PACS-2-dependent step in Nef action, as well as identify PACS-2 as a negative regulator of SIRT1 and as an essential mediator of p53 activation and p21 expression following DNA damage. These studies significantly contribute to the understanding of how a membrane trafficking protein can have diverse cellular roles linking viral pathogenesis to DNA damage and tumor suppression pathways. Future studies must systematically determine how PACS-2 coordinates these various functional roles and the cellular and biological contexts for which these regulatory networks are essential.

In the context of HIV-1 Nef-mediated pathogenesis, future studies should investigate whether disruption of the Nef-PACS-2 interaction may be an effective strategy to prevent downstream Nef-SFK-, or potentially other Nef $PXXP_{75}$-dependent events. Indeed, future studies should including solving a high resolution crystal structure of Nef with PACS-2, as the identification of how this interaction is mediated will facilitate the development of small molecule compounds that can disrupt the Nef-PACS-2 interaction. In addition, studies in which transgenic mice expressing wild-type Nef or Nef mutated for PACS-protein interactions, $Nef^{E4A,W113A}$, would provide critical *in vivo* evidence for the

importance of PACS-mediated Nef trafficking steps in determining the extent of Nef-induced disease pathogenesis. Together, these studies would provide essential information about how the interaction of Nef with cellular proteins such as PACS-2 could identify potential pharmacologic targets for inhibition of Nef action. In addition, future studies should more precisely elucidate the mechanism of how Nef switches from the signaling to the stoichiometric mode of MHC-I downregulation to have a greater understanding of the biological context in which this regulation is critical. These studies should analyze whether the signaling and stoichiometric pathways occur only in activated $CD4^+$ T-cells or monocyte-macrophage cells, or whether one or both of these pathways exist in longer-lived HIV-1 reservoir populations such as resting $CD4^+$ T-cells. Together, the proposed studies would provide critical information about how these identified mechanisms of Nef action could be used to understand how HIV-1 functions in distinct cellular reservoirs to mediate disease pathogenesis.

The studies in this dissertation suggest tumors that lose *PACS-2*, yet retain wild-type *TP53* status, may be sensitized to chemotherapy or radiation treatment. Therefore, it will be essential to rigorously analyze the nature of PACS-2 expression in a variety of human cancers at various stages. Importantly, it will be essential to analyze the extent to which loss of *PACS-2* occurs independent of *TP53* mutational status. Indeed, this analysis is essential for understanding the therapeutic importance of *PACS-2* loss, as tumors with mutated *TP53* and concurrent *PACS-2* loss would likely not be sensitized to DNA

damage in the p53- and p21-dependent nature we observed in wild-type *TP53* harboring tumor cell lines. However, tumors with loss of *PACS-2* that retain wild-type *TP53* may be sensitized to particular therapies, such as Doxorubicin or ionizing radiation. Moreover, future studies should analyze how PACS-2 expression correlates with invasiveness, prognosis, and survival in a variety of tumor types. In addition, it would be important to analyze the correlation between PACS-2 and p21 expression in cancers that contain wild-type or mutated p53. Together, these future studies and analyses will be essential for testing the biological implications of *PACS-2* loss in tumors and whether *PACS-2* status may be a potential biomarker for identifying tumors likely to benefit from particular DNA damaging therapies, such as Doxorubicin or ionizing radiation.

The studies presented in this dissertation were limited to the analysis of p53 Lys_{382} acetylation as a readout of PACS-2-mediated regulation of SIRT1 deacetylase activity. Therefore, it will be important in future studies to test whether PACS-2 affects the acetylation of additional p53 lysine residues in a SIRT1-dependent manner. Moreover, future studies should further probe the mechanism by which acetylation of p53 leads to promoter-specific activation of p53 target genes, including the role of components of the basal transcriptional machinery and the affinity of p53 to specific DNA regions. In particular, future studies should address how acetylation of specific p53 lysine residues or combinations of residues leads to activation of various target genes and different cellular fates following DNA damage. These studies will be critical for

understanding how proteins such as PACS-2 are able to modulate p53 transcriptional activation through the regulation of p53 acetylation.

To address whether PACS-2-mediated inhibition of SIRT1 is specific to p53 or includes additional SIRT1 substrates, comprehensive studies should include a rigorous testing of the acetylation status of additional SIRT1 targets in the presence or absence of PACS-2. In addition, Pacs2$^{-/-}$ mice should be analyzed for evidence of a SIRT1-overexpressing phenotype, such as that seen in mice treated with SIRT1 activators, which are resistance to diet-induced obesity and more efficiently clear glucose. Together, these studies will be essential for determining if the effect of PACS-2 on modulating SIRT1 activity is specific to p53 or includes additional SIRT1 targets. These studies are critical, because it is currently unknown whether any of the previously identified SIRT1 modulators, such as AROS or DBC1, broadly affect SIRT1 activity, or if they predominantly target SIRT1-mediated deacetylation of p53.

Therefore, given the diverse nature of the cellular proteins and processes modulated by PACS-2, the implications of this data are far reaching and suggest that PACS-2 may function in various cellular processes such as gene regulation, chromatin remodeling, cell growth and survival as well as biological processes such as cancer, viral immunity, and metabolism.

APPENDIX A. A HIF-Regulated VHL-PTP1B-Src Signaling Axis Identifies a Therapeutic Target in Renal Cell Carcinoma

A HIF-Regulated VHL-PTP1B-Src Signaling Axis Identifies a Therapeutic Target in Renal Cell Carcinoma

Natsuko Suwaki,[1*†] Elsa Vanhecke,[1*‡] Katelyn M. Atkins,[2] Manuela Graf,[1] Katherine Swabey,[1] Paul Huang,[1] Peter Schraml,[3] Holger Moch,[3] Amy Mulick Cassidy,[4] Daniel Brewer,[5] Bissan Al-Lazikani,[6] Paul Workman,[6] Johann De-Bono,[4] Stan B. Kaye,[4] James Larkin,[7] Martin. E. Gore,[7] Charles L. Sawyers,[8] Peter Nelson,[9] Tomasz M. Beer,[10] Hao Geng,[10] Lina Gao,[10] David Z. Qian,[10] Joshi J. Alumkal,[10] Gary Thomas,[2] George V. Thomas[1,10§]

[1]Section of Cell and Molecular Biology, Institute of Cancer Research, Sutton, Surrey SM2 5NG, UK. [2]Vollum Institute, Oregon Health and Science University, Portland, OR 97239, USA. [3]Institute of Surgical Pathology, University Hospital Zurich, Zurich CH-8091, Switzerland. [4]Section of Medicine, Institute of Cancer Research, Sutton, Surrey SM2 5NG, UK. [5]Section of Molecular Carcinogenesis, Institute of Cancer Research, Sutton, Surrey SM2 5NG, UK. [6]Cancer Research UK Center for Therapeutics, Division of Cancer Therapeutics, Institute of Cancer Research, Sutton, Surrey SM2 5NG, UK. [7]Royal Marsden Hospital, London SW3 6JJ, UK. [8]Human Oncology and Pathogenesis Program, Memorial Sloan-Kettering Cancer Center, New York, NY 10065, USA. [9]Divisions of Human Biology and Clinical Research, Fred Hutchinson Cancer Research Center,

Seattle, WA 98109, USA. [10]OHSU Knight Cancer Institute, Oregon Health and Science University, Portland, OR 97239, USA.

*These authors contributed equally to this work.

†Present address: Gray Institute for Radiation Oncology and Biology, University of Oxford, Oxford OX3 7DQ, UK.

‡Present address: INSERM U981, Institut de Cancérologie Gustave-Roussy, 94805 Villejuif Cedex, France.

§To whom correspondence should be addressed.

Author contributions: N.S., E.V., K.S., H.G., and D.Z.Q. performed the cellular and biochemical experiments; M.G. conducted the immunohistochemical assays; P.S. and H.M. performed and analyzed the survival correlations; B.A.-L., D.B., and A.M.C. performed the statistical analysis on the tissue microarray and network interaction map; P.H. conducted the proteomics experiments; P.H., B.A.-L., and P.N. analyzed the proteomics data; K.M.A. and G.T. performed the *in vitro* kinase assays; L.G. and J.J.A. Performed ChIP experiments; M.E.G., J.L., S.B.K., J.D.-B., and T.M.B. provided clinical samples for analysis and clinical insight; N.S., E.V., K.M.A., G.T., C.L.S., and P.W. provided critical input into the overall research direction; G.V.T. directed the research and wrote the manuscript with input from all the co-authors.

Science Translational Medicine. 2011 Jun 1;3(85):85ra47

ABSTRACT

Metastatic renal cell carcinoma (RCC) is a molecularly heterogeneous disease that is intrinsically resistant to chemotherapy and radiotherapy. Although therapies targeted to the molecules vascular endothelial growth factor and mammalian target of rapamycin have shown clinical effectiveness, their effects are variable and short-lived, underscoring the need for improved treatment strategies for RCC. Here, we used quantitative phosphoproteomics and immunohistochemical profiling of 346 RCC specimens and determined that Src kinase signaling is elevated in RCC cells that retain wild-type von Hippel-Lindau (VHL) protein expression. RCC cell lines and xenografts with wild-type VHL exhibited sensitivity to the Src inhibitor dasatinib, in contrast to cell lines that lacked the VHL protein, which were resistant. Forced expression of hypoxia-inducible factor (HIF) in RCC cells with wild-type VHL diminished Src signaling output by repressing transcription of the Src activator protein tyrosine phosphatase 1B (PTP1B), conferring resistance to dasatinib. Our results suggest that a HIF-regulated VHL-PTP1B-Src signaling pathway determines the sensitivity of RCC to Src inhibitors and that stratification of RCC patients with antibody-based profiling may identify patients likely to respond to Src inhibitors in RCC clinical trials.

INTRODUCTION

Renal cell carcinoma (RCC) is the most lethal genitourinary cancer, accounting for about 209,000 new cancer occurrences and 102,000 deaths per year worldwide (Gupta et al., 2008). Cure rates in RCC are modest because more than a quarter of patients have metastatic disease at presentation, and patients treated surgically for localized cancers frequently relapse with metastatic disease (Janzen et al., 2003, Lam et al., 2005). RCC is histologically heterogeneous. Although ~75% of RCC are clear cell carcinomas, papillary, chromophobe, sarcomatoid, collecting duct, and medullary carcinomas also occur (Bonsib, 2009). Inactivation of the von Hippel-Lindau (VHL) tumor suppressor gene is the most prevalent driver mutation, accounting for ~60% of all RCC tumors and occurring primarily in the clear cell subtype (Dalgliesh et al., 2010, Kim et al., 2004). VHL loss stabilizes hypoxiainducible factor–1a (HIF-1α) andHIF-2α, leading to increased expression of HIF-responsive genes, including VEGF-A, PDGF-B, and TGF-A (Kim et al., 2004). HIF-dependent gene expression is further elevated by mammalian target of rapamycin (mTOR), thereby identifying several therapeutic targets in VHL-negative RCC (Thomas et al., 2006). Indeed, drugs that target vascular endothelial growth factor (VEGF) and mTOR show clinical activity in patients with metastatic RCC, although these responses are often variable and short-lived (Rini et al., 2009a, Rini et al., 2009b).

The remaining ~40% of patients with VHL-positive RCCs suffer from a lack of biologically rational treatment options, a result of a paucity of identified molecular drivers. Furthermore, patients with papillary RCC and other non–clear cell RCC are often excluded from clinical trials (Motzer et al., 2002, Ronnen et al., 2006), suggesting that identification of predictive biomarkers that stratify patients for rational treatment strategies is urgently required. Indeed, the ability of the Bcr-Abl inhibitor imatinib to successfully treat chronic myeloid leukemia supports such an approach and has led to the development of targeted therapies for other cancers (Demetri et al., 2002, Druker et al., 2001, Flaherty et al., 2010). Targeted therapies are most effective in treating homogenous cancers driven by a single activating oncogene and are much less effective against molecularly heterogeneous cancers such as RCC (Rini et al., 2009a). Indeed, quantitative phosphoproteomic studies show that cancer is driven by aberrant networks rather than discrete signaling pathways (Huang et al., 2007, Stommel et al., 2007). This observation is exemplified by Src kinase, which, despite its pivotal role in tumor growth, angiogenesis, and metastasis, is rarely mutated in cancer. Rather, Src's signaling output is controlled posttranslationally by the convergent action of the lipid raft–localized inhibitory receptor tyrosine kinase Csk and the activating tyrosine phosphatase PTP1B (protein tyrosine phosphatase 1B) (Yeatman, 2004).

Here, we report a personalized medicine approach for stratifying tumors on the basis of the HIF-regulated VHL-PTP1B-Src signaling axis in patients with

VHL-positive RCC that may identify patients likely to respond to Src inhibitors as a co- or monotherapy.

RESULTS

A.1 Src is expressed in RCC and correlates with VHL expression

To identify cellular signaling networks differentially regulated in RCC subgroups, we performed quantitative phosphoproteomics on SN12C clear cell carcinoma cells, which retain VHL protein expression, and its isogenic subline SN12C-shVHL, which has reduced VHL by short hairpin RNA (shRNA) knockdown (Thomas et al., 2006, Pan et al., 2006, Pantuck et al., 2010, Turcotte et al., 2008). Lysates from parallel cultures of serum-stimulated SN12C and SN12C-shVHL cells were labeled with iTRAQ 8-plex reagent, and phosphotyrosine-containing peptides were subjected to immobilized metal affinity chromatography–tandem mass spectrometry (MS/MS) analysis (Huang et al., 2007). Quantitative phosphorylation profiles were generated for 22 phosphorylation sites, whereas cluster analysis revealed a >50% reduction of pTyr at numerous phosphorylation sites in SN12C-shVHL lysates (Figure A.1A and Table A.1). Specifically, the proportion of pY419 autophosphorylated Src as well as several Src substrates, including annexin II, paxillin, and inositol polyphosphate phosphatase-like 1 (INPPL1), were diminished in SN12C-shVHL lysates. The ability of serum to increase pTyr levels of Src substrates in SN12C cells but not SN12C-shVHL cells suggested that VHL expression is a key determinant of Src kinase activity. Consistent with this possibility, *in vitro* kinase assays showed that SN12C cells contained about twice as much dasatinib-

sensitive Src kinase activity as did SN12C-shVHL cells (Figure A.1B). Together, these data suggest that VHL may regulate Src kinase activity as well as its downstream signaling.

Because both the amount of total Src protein and its enzyme activity are implicated in cancer development (Yeatman, 2004, Ishizawar et al., 2004, Wheeler et al., 2009), we analyzed a human RCC tissue microarray (TMA) with samples from 215 patients for Src protein expression by immunohistochemistry (Figure A.1C). We found a significant positive association between total Src protein, which correlates with cytoplasmic staining, and active Src, which correlates with membranous staining (P = 0.0185, Table A.2A). RCC samples with strong Src immunostaining came from patients with reduced survival when compared to patients whose samples had weak expression (P = 0.0367; Figure A.1D). In addition, multivariate analysis with stage [grouped as organ-confined (pT1, 2) or advanced (pT3, 4)] and Fuhrman grade revealed that strong Src levels independently predicted poorer survival (P = 0.02, Table A.2B). Indeed, there was a tendency for tumors staining negatively for VHL to have weaker Src staining (Table A.2C).

A.2 VHL-WT RCC cells are sensitive to dasatinib

To evaluate whether VHL expression determined sensitivity to Src inhibitors, we treated SN12C and SN12C-shVHL cells as well as ACHN or ACHN-shVHL papillary RCC cells with dasatinib (Thomas et al., 2006, Pan et al.,

2006, Pantuck et al., 2010, Turcotte et al., 2008). We found that dasatinib reduced proliferation of VHL-WT SN12C and ACHN cells but not their shVHL counterparts (Figure A.2A). The inhibition of proliferation by dasatinib correlated with an increase in G1-arrested cells and a corresponding decrease in S-phase cells as determined by propidium iodide (PI) staining (Table A.3). Moreover, 5-bromo-2′-deoxyuridine (BrdU) staining showed that dasatinib caused a dosedependent decrease in DNA synthesis in VHL-WT SN12C and ACHN cells but not in their shVHL counterparts (Figure A.2B). No accumulation of a sub-G1 population was observed, suggesting that dasatinib is cytostatic in the cell lines tested. Similar results were obtained with VHL-WT RXF-393 and Caki-1 RCC cells compared to VHL-null 786-0 cells (Figures A.3 and A.4). Correspondingly, ectopic expression of VHL in 786-0 cells conferred increased sensitivity to dasatinib (Figure A.4).

Our determination that dasatinib inhibited proliferation of VHLWT RCC cells prompted us to test whether dasatinib inhibited Src kinase activation and the phosphorylation of Src substrates. Indeed, flow cytometric and immunoblot analyses showed that dasatinib reduced pY419 Src levels irrespective of VHL status (Figure A.2C). In agreement with the *in vitro* kinase assay (Figure A.1B), Western blot analysis showed that pY419 Src levels were higher in VHL-WT SN12C or ACHN cells compared to their shVHL counterparts. Dasatinib also caused total Src protein levels to increase regardless of VHL status (Figure A.2C and Figure A.4). This dasatinib-induced increase in total Src protein has been

observed in other tumor types as well as with other classes of Src inhibitors and is consistent with the increased stability of dephosphorylated Src *in vivo* (Buettner et al., 2008, Gwanmesia et al., 2009, Schweppe et al., 2009, Frame, 2002). In addition to inhibiting pY419 Src, dasatinib inhibited phosphorylation of the Src substrate FAK in VHL-WT cells (Figure A.2C). Surprisingly, pY576/577 FAK was undetectable in VHL knockdown cells despite the presence of total FAK protein. These results suggest that dasatinib may selectively inhibit proliferation of VHL-WT cells compared to their VHL-null or VHL-low counterparts by repressing Src's signaling output.

To evaluate the effect of dasatinib on tumor growth *in vivo*, we implanted SN12C and SN12C-shVHL cells subcutaneously into the flanks of nude mice. Daily treatment with dasatinib significantly reduced the growth of VHL-WT SN12C cells but had no effect on SN12C-shVHL cells, recapitulating our *in vitro* findings (compare Figures A.2, A and D). Dasatinib had no statistically significant effect on apoptosis in the xenograft tumors. Notably, administration of dasatinib resulted in a statistically significant reduction of Ki-67–positive proliferating SN12C cells but not SN12C-shVHL cells (Figure A.2E). Together, these results demonstrate that VHL-WT RCC cells are more sensitive than shVHL cells to dasatinib in xenograft tumors as well as *in vitro* and that this sensitivity is mediated through a blockade on proliferation.

Next, we asked whether the dasatinibinduced growth inhibitory effects on VHLWT RCC cells were due to Src inhibition. Indeed, SN12C cells knocked down

for Src (SN12C-shSrc) were resistant to dasatinib treatment (Figure A.5A). By contrast, rescue of SN12C-shSrc cells by expression of chicken Src, which is resistant to the human-specific shRNA (Zhang et al., 2009), restored dasatinib sensitivity. Moreover, stable expression of a dasatinib-resistant Src encoding a T388I gatekeeper mutation, which prevents access of adenosine 5′-triphosphate (ATP)– competitive inhibitors to the ATP-binding pocket in Src, thereby protecting pY419 autophosphorylation, conferred resistance of SN12C cells to dasatinib (Figure A.5B) (Zhang et al., 2009, Lombardo et al., 2004). Similarly, expression of v-Src, which naturally expresses the T→I gatekeeper mutation (Liu et al., 1999), rendered VHL-WT SN12C and ACHN cells resistant to dasatinib (Figures A.5C and A.6). Accordingly, SN12C–v-Src xenograft tumors grown in severe combined immunodeficient (SCID) mice were resistant to dasatinib, whereas parental SN12C tumors remained dasatinib-sensitive (Figure A.5D).

Several controls supported our findings that dasatinib suppressed proliferation in VHL-WT cells by inhibiting Src. First, SN12C cells expressing the BCR-ABL T315I gatekeeper mutant were sensitive to dasatinib, suggesting the dasatinib resistance mediated by Src T388I or v-Src was specific (Figure A.7). Second, treatment with imatinib, which inhibits ABL, PDGFR (platelet-derived growth factor receptor), and c-KIT but not Src, had no effect on the proliferation of SN12C or SN12CshVHL cells (Figure A.8A). Finally, saracatinib, a structurally unrelated Src inhibitor (Ple et al., 2004), repressed proliferation of control SN12C cells but not

shVHL cells (Figure A.8B).

A.3 Constitutively stabilized HIF confers resistance to dasatinib in VHL-WT cells

Because the E3 ligase activity of VHL negatively regulates HIF, we asked whether expression of constitutively stable HIF would phenocopy VHL loss by conferring resistance to dasatinib in VHL-WT RCC cells. Indeed, SN12C and ACHN cells expressing constitutively stable HIF-1α–P564A or HIF-2α–P405A,P531A mutants (Kondo et al., 2002) contained reduced levels of Src mRNA and were resistant to the dasatinib-mediated G1 arrest observed in parental SN12C and ACHN cells (Figures A.9, A to C, Figure A.10, and Table A. 4). Correspondingly, constitutively stable HIF-1α and HIF-2α inhibited Src signaling output in VHL-WT RCC cells as determined by immunoblot of pY419 Src and phosphorylated Src substrates, including pY576/577 FAK, pY703STAT3, and pY204ERK (Figure A.9D). Conversely, ectopic expression of VHL in VHL-null 786-0 RCC cells resulted in an increase in both total and pY419 Src, as well as the phosphorylation and activation of its downstream targets when compared to the parental cells (Figures A.4 and A.11). Together, these results suggest that HIF represses VHL-mediated Src signaling output.

The ability of constitutively stable HIF mutants to promote dasatinib resistance and repress Src signaling output suggested that HIF may repress an activator of Src activity. Consistent with this possibility, expression of PTP1B protein and mRNA, which activates Src by dephosphorylation of Y530, was

consistently lower in shVHL or RCC cells that ectopically express constitutively stable HIF (Figure A.9, D and E). Correspondingly, PTP1B protein was decreased in VHL-null 786-0 cells compared to VHL-restored 786-0–VHL cells (Figure A.11). Biochemical analysis of Src signaling output suggested that PTP1B knockdown phenocopied expression of constitutively stable HIF in VHL-WT cells. SN12CshPTP1B cells contained reduced pY419 Src and the levels of phosphorylated Src substrates, including pY576/577FAK, and pY204ERK (Figure A.9F), and were relatively resistant to dasatinib-mediated growth inhibition (Figure A.9G). Only pY703STAT3 was unaffected by PTP1B knockdown, which may result from a PTP1B-specific effect on STAT3 (signal transducer and activator of transcription 3) and its regulator, JAK (Janus kinase) (Lund et al., 2005). As a control, SN12C cells were exposed to hypoxia *in vitro* or in xenograft tumors. We found that HIF was stabilized but PTP1B was unaffected, suggesting that HIF-regulated PTP1B expression may be different under hypoxic conditions (Figure A.12).

Consistent with the reduced activation of Src, PTP1B knockdown cells were less sensitive to dasatinib than control cells (Figures A.9G and A.13). By contrast, overexpression of the Src regulator Csk in SN12C cells had no effect on dasatinib sensitivity or Src signaling output (Figure A.14), which is consistent with work by others that Csk phosphorylation of Src pY530 is complex (Boerner et al., 1996, Moarefi et al., 1997, Sun et al., 1998, Matsubara et al., 2010, Veracini et

al., 2008) (see Discussion). Together, these results suggest that sensitivity to dasatinib correlates with the inhibition of Src's signaling output.

In addition to repressed levels of PTP1B protein, RCC cells with VHL knockdown or expression of constitutively stable HIF had reduced PTP1B mRNA (Figure A.9E), suggesting that HIF may repress PTP1B transcription. In support of this finding, chromatin immunoprecipitation (ChIP) revealed that HIF is enriched at a putative hypoxia response element in the PTP1B promoter in ACHN cells expressing constitutively stable HIF-1α–P564A but not in parental ACHN cells (Figure A.15). This result suggests that HIF-mediated transcriptional regulation of the PTP1B gene contributes to the repression of Src signaling output in VHL-null RCC cells.

A.4 Interaction of VHL, HIF, PTP1B, and Src in RCC patients

Our identification of a HIF-regulated VHL-PTP1B-Src signaling axis in RCC cell lines provided us with additional markers to interrogate the presence of this pathway in RCC patients. We constructed a TMA from a second cohort of 131 patients with RCC and performed immunohistochemistry for VHL, HIF-2α, which is the primary driver in VHL-null RCC (Kaelin, 2008), Src, and PTP1B. As controls, we analyzed the HIF transcriptional target CA-IX, as well as the Src substrate pFAK. Quantification was performed with automated digital image analysis algorithms to rigorously and systematically measure staining intensity (Figure A.16A). An unsupervised hierarchical clustering of the tumors on the

basis of the expression of VHL, Src, pFAK, and PTP1B was used to generate a heat map (Figure A.17). VHL, Src, PTP1B, and pFAK showed the most similar expression patterns, although pFAK expression was generally lower than the other markers.

In agreement with the initial RCC clinical data set (Table A.2A), a Spearman rank correlation test of the second RCC clinical data set again revealed a positive correlation between VHL and Src ($r = 0.409$; $P < 0.001$; Figure A.16B). Using these more stringent analyses, only 8% (1 of 12) of VHL-negative tumors had strong Src expression, whereas 58% (69 of 119) of VHL strong tumors had strong Src expression, suggesting a correlative relationship between VHL and Src ($P = 0.0018$; Figure A.16C and Table A.5). Conversely, the relationship between VHL and HIF-2α revealed a significant negative correlation ($r = -0.132$; $P = 0.036$). In agreement with our *in vitro* findings, PTP1B positively correlated with VHL ($r = 0.293$; $P < 0.001$) but negatively correlated with HIF-2α ($r = -0.212$; $P = 0.001$), suggesting that patient tumors with VHL loss or HIF-2α overexpression may have reduced PTP1B expression. Controls showed positive correlations between HIF-2α and CA-IX and between Src and pFAK as expected (Figure A.16B). A multiple linear regression showed VHL ($P < 0.0001$) and PTP1B ($P < 0.0001$) to be predictors of Src expression. Additionally, VHL ($P < 0.0001$) and HIF-2α ($P = 0.0021$) were independent predictors of PTP1B levels (Table A.6). Next, we extracted the data points and organized them into a scatter plot representing patient subgroups defined by VHL and Src expression (Figure

A.16D). Indeed, 28.6% of the patients were VHL strong/Src strong, representing the potential candidates for a prospective Phase II clinical trial with dasatinib (Table A.5).

Next, we tested whether this RCC immunohistochemistry profile could be applied to other cancers to predict sensitivity to dasatinib. Using a clinical data set of transitional cell carcinomas of the bladder, we found the same correlations among VHL, Src, HIF-2α, and PTP1B (Figure A.18). Together, these findings suggest that the immunophenotype of the VHL-PTP1B-Src signaling axis comprises a signature that not only defines a biologically distinct subgroup of RCC that may benefit from dasatinib or similar Src inhibitors but also points to a wider clinical applicability for these predictive markers in identifying sensitivity to Src inhibitors.

We then explored the cooperating events involved in mediating sensitivity to dasatinib by applying a systems-based approach to map the potential protein-protein interactions, transcriptional information, and the signaling networks they affect by using the ROCK-BCFG database (Richardson et al., 2009). We seeded the interaction network searches with targets identified in our experiments and defined a protein interaction network containing 82 nodes that suggest an underlying signaling network involving Src, PTP1B, CA-IX, FAK, and VHL together with the transcriptional regulators HIF-1α, HIF-2α, and Sp1 (Figure A. 19).

DISCUSSION

Although targeted therapies have been successful in treating cancers driven by the activation of a single oncogene, these drugs are much less effective in molecularly heterogeneous cancers driven by a multitude of dysregulated signaling networks (Stommel et al., 2007). Successful treatment therefore requires a personalized medicine approach based on robust predictive biomarkers that can stratify patients toward appropriate targeted therapies. Here, we used a quantitative phosphoproteomic screen to identify Src as a potential pharmacologic target in metastatic RCC. Immunohistochemistry of 346 human RCC tumors identified a positive correlation between Src and VHL expression, whereas treatment of VHL-WT xenografts with dasatinib blocked tumor growth *in vivo*. Conversely, forced expression of HIF, which phenocopied VHL loss, diminished Src's signaling output by down-regulation of PTP1B, thereby conferring resistance to dasatinib. HIF binds the PTP1B promoter and reduces PTP1B expression, suggesting that HIF controls Src signaling output by regulating PTP1B transcription. Our data suggest that stratifying RCC patients by profiling for expression of VHL and Src, as well as downstream effector molecules may identify patients likely to respond to Src inhibitors in future RCC clinical trials.

Despite playing a central role in multiple tumorigenic signaling networks, Src itself is rarely mutated in cancers (Yeatman, 2004). Our data suggest that

one mechanism by which tumor cells amplify Src kinase activity is by using gene-autonomous drivers such as PTP1B to dephosphorylate the kinase autoinhibitory domain. The ability of PTP1B knockdown to confer resistance to dasatinib (Figures A.9G and A.13) suggests that PTP1B may augment Src signaling in RCC cells by channeling inputs from upstream oncogenes, including Ras (Dube et al., 2004). Unlike PTP1B knockdown, overexpression of Csk did not alter Src pY419 status (Figure A.14), suggesting that the regulation of Src activation by Csk is complex. Our findings are consistent with reports that Csk phosphorylation of Src Y530 requires interaction of Csk with Csk-binding protein (Cbp) in lipid rafts (Boerner et al., 1996, Moarefi et al., 1997, Sun et al., 1998, Matsubara et al., 2010, Veracini et al., 2008), suggesting that analysis of Src pY419 or pY530 levels by immunoblot is insufficient to detect minute or compartment-specific changes in Src activation. Our finding that hypoxia-induced stabilization of HIF failed to affect PTP1B expression is in agreement with the HIF-dependent but hypoxia-independent regulation of Ror2 (Figure A.12) (Wright et al., 2010), and is consistent with the model that HIF-mediated inhibition of PTP1B requires that HIF be constitutively stabilized by VHL loss and not by fluctuating O2 levels present in VHL-WT tumors (Chan et al., 2002). Finally, although our studies cannot exclude the possibility that dasatinib may mediate its effects by inhibiting additional Src family kinases (SFKs), they highlight the therapeutic utility of a pan-SFK inhibitor such as dasatinib.

Successful implementation of targeted therapies in molecularly heterogeneous cancers requires robust predictive biomarkers. The development of epidermal growth factor receptor (EGFR) mutation analysis for stratification of patients with non–small cell lung cancer to EGFR inhibitors supports the feasibility of this approach (Gridelli et al., 2011). Therefore, our initial examination of VHL and Src on routinely processed human RCC samples assessed the clinical significance of Src expression. Indeed, RCC patient samples with strong Src expression had a statistically significant reduced overall survival when compared to those with weak expression. This analysis also suggested a positive correlation between VHL and Src with a semiquantitative scoring protocol that was biased toward sensitivity relative to specificity. We then more rigorously interrogated the VHL-Src relationship with enhanced specificity by analyzing VHL, Src, as well as their downstream effector molecules in a second cohort of human RCC tumors. This analysis used unbiased digital image analysis algorithms to objectively quantify staining intensities and to determine correlations between these molecules. The VHL-Src relationship was one of the strongest correlations found. In addition, the relationships among VHL, Src, HIF-2α, PTP1B, pFAK, and CA-IX were recapitulated in patient tumors, consistent with our *in vitro* results. The presence of these associations in clinical samples reveals the strength of the molecular networks identified and supports the testing of these markers in future clinical trials.

Inactivation of the VHL tumor suppressor gene is the most prevalent driver mutation in RCC, accounting for ~60% of all tumors (Dalgliesh et al., 2010, Kim et al., 2004). Thus, even though ~40% of RCC patients have VHL-positive cancer, they are treated as if they have VHL-negative cancers. Unfortunately, the absence of biomarker-driven treatment protocols in RCC, together with the fact that VHL-positive patients are excluded from many registration trials, precludes meaningful understanding of the mechanisms of response or resistance. Thus, the singular approach targeting VEGF or mTOR, which is currently used to treat metastatic RCC, underscores the need for alternative treatment strategies for VHL-positive metastatic RCC. Our findings suggest that Src inhibition may represent a rational treatment option in renal cancers that retain VHL protein expression. Additionally, analyzing functional readouts of VHL and Src activity by means of HIF, CA-IX, and pFAK expression could enhance specificity because functional VHL would confer low HIF and CA-IX expression, whereas elevated Src signaling output would correlate with increased pFAK levels. Although the ideal treatment subgroup would include those tumors that are VHL strong, Src strong, pFAK strong, HIF weak, and CA-IX weak, the most effective biomarker combination can only be determined from future clinical studies in which outcomes after Src inhibitor treatment are known. Because Src inhibitors such as dasatinib and saracatinib already have been clinically tested, our data suggest that analysis of these potential biomarkers can occur rapidly in a Phase II clinical trial in patients with metastatic RCC.

Collectively, our results suggest that a fundamental change in RCC treatment may be warranted. Specifically, patients should be selected initially on the basis of a molecular phenotype. The simplicity of our approach lies in two elements: use of an immunohistochemical-based assay on routinely processed clinical samples and the targeting of src, a well-characterized oncogene for which there already exist clinically active drugs. The key challenges ahead are assessing intratumor heterogeneity and standardization of methods across diagnostic laboratories. In summary, stratifying RCC patients on the basis of the presence of an active VHL-PTP1B-Src signaling axis in the tumor will identify a subgroup likely to respond to Src inhibitors.

MATERIAL AND METHODS

Sample preparation, peptide immunoprecipitation, and MS analysis

SN12C and SN12C-shVHL cells were maintained in Dulbecco's modified Eagle's medium (DMEM) supplemented with 10% fetal bovine serum (FBS). Cells (40 to 50% confluence per 10-cm plate) were seeded for 24 hours, washed twice with phosphate-buffered saline (PBS), and then incubated for 24 hours in serum-free media. Cells were stimulated with 10% serum for 10 min and harvested in 900-ml dish/8 M urea. Unstimulated cells were used as controls. Cells were lysed in 8 M urea and subjected to reduction, alkylation, and trypsin digestion as previously described (Huang et al., 2007). Peptides were desalted on a C18 Sep-Pak Plus cartridge (Waters), eluted with 25% acetonitrile, and lyophilized to dryness. Lyophilized peptides were subjected to labeling with the iTRAQ 8-plex reagent (Applied Biosystems). Peptide immunoprecipitation was performed as described (Huang et al., 2007). Briefly, 30 mg of protein G Plus-agarose beads (Sigma) was incubated with 12 mg of each of the antiphosphotyrosine antibodies [pTyr100 (Cell Signaling Technology), PT66 (Perkin Elmer), and 4G10 (Millipore)] in 200 ml of immunoprecipitation buffer (100 mM tris, 100 mM NaCl, 1% NP-40, pH 7.4) for 8 hours at 4°C. Beads were washed with rinse buffer (100 mM tris, 100 mM NaCl, pH 7.4), and retained peptides were eluted from antibody with 70 ml of elution buffer (100 mM glycine, pH 2.5) for 1 hour at room temperature. Immobilized metal affinity

chromatography was performed to enrich for phosphorylated peptides, and peptides retained on the column were eluted with 250 mM sodium phosphate (pH 8.0) and analyzed by electrospray ionization liquid chromatography–MS/MS on a QqTof (QSTAR Elite, Applied Biosystems) as described (Huang et al., 2007).

Phosphopeptide sequencing, quantification, and analysis

MS/MS spectra were extracted, searched, and quantified with Protein Pilot (Applied Biosystems). Phosphorylation sites and peptide sequence assignments were validated by manual confirmation of raw MS/MS data. Peak areas of iTRAQ marker ions [mass/charge ratio (m/z) 113, 114, 115, 116, 117, 118, 119, and 121] were normalized with values from the iTRAQ marker ion peak areas of nonphosphorylated peptides in supernatant of the immunoprecipitation. Each condition was normalized against the 113 channels to obtain fold changes across all eight conditions. Table A.1 represents the mean and SD of two biological replicate experiments.

Tissue microarrays

Two separate RCC patient clinical databases were used to construct the TMAs described in our experiment. The first TMA comprised 215 clear cell RCCs collected from nephrectomies performed at the University Hospital of Zurich. All RCC samples were histologically reviewed by one pathologist (H.M.). This study was approved by the local commission of ethics. Tumor-specific survival data

were obtained by reviewing the hospital records and by the cancer registry of the Canton of Zurich. The second RCC TMA consisted of 131 nephrectomies performed for kidney cancer at the Royal Marsden Hospital, London. This study protocol was approved by the hospital ethics review board. All tumors arrayed from this second data set were histologically reviewed by one pathologist (G.V.T.).

Immunohistochemistry

The first TMA was stained with the ultraView Universal DAB Detection Kit (Ventana). A clear cell RCC tumor with strong membranous Src positivity was used as positive control. Negative controls were identical array sections stained in the absence of the primary antibody. Immunohistochemistry can yield false positivity at the margin or edges of tissue (that is, edge effect), and this needs to be considered when scoring TMA cores. Therefore, to minimize false positivity, we used a conservative 5% cutoff; that is, any tumors with <5% cytoplasmic and/or membranous staining were considered negative, and any tumors with >5% cytoplasmic and/or membranous staining were considered positive. Next, positive Src expression was analyzed subjectively based on antibody staining intensity as having either weak or strong cytoplasmic and/or membranous immunoreactivity by an experienced pathologist (H.M.). VHL immunostaining was similarly scored (Dahinden et al., 2010). The second TMA was processed with EnVision Kits (Dako), SuperSensitive IHC Detection Systems (BioGenex), or

Vectastain ABC Kit (Vector Labs) according to the manufacturer's instruction. Negative control slides were used in every run (incubated in Dako Universal Negative Control Mouse/Rabbit). Diaminobenzidine tetrahydrochloride (DAB) was used as the enzyme substrate for visualization and counterstained with hematoxylin.

Image acquisition, management, and automated analysis

The Aperio ScanScope CS slide scanner (Aperio Technologies) was used to capture whole-slide digital images with a 20x objective. Slides were de-arrayed to visualize individual cores with the TMA Lab (Aperio). A color deconvolution algorithm (Aperio) was used to develop a quantitative scoring model for measuring cytoplasmic immunoreactivity in TMAs consecutively stained with VHL, Src, CA-IX, PTP1B, and pFAK. A nuclear algorithm was used to quantify HIF-2α and Ki-67 nuclear positivity. The algorithm was calibrated to individual staining patterns (range of hues and saturation), and three intensity ranges were generated: weak, yellow; moderate, orange; strong, red; and immunonegative, blue. For pixels that satisfy the color specification, the algorithm counted the number and intensity sum in each intensity range, along with three additional quantities: average intensity, ratio of strong/total number, and average intensity of weak positive pixels. The algorithm was calibrated for both cytoplasmic and nuclear expression by constructing receiver operator curves for hue, hue width, and color saturation. A pseudocolor "markup" image was generated from the

algorithm and verified to ensure that specified inputs were measuring the desired color and intensity ranges. All markup images were inspected by a pathologist (G.V.T.) to confirm the accuracy of the algorithm. The final automated score was assessed for each core as the product of corrected average intensity and corrected positive pixel percentage.

Cell culture

RCC isogenic pairs of VHL WT ACHN and SN12C and counterparts expressing shRNA targeting VHL have already been described (Thomas et al., 2006). ACHN and SN12C cells expressing a VHL-resistant version of HIF-1α or HIF-2α were generated by transducing a retrovirus expressing HIF-1α (P564A) and HIF-2α (P405A; P853A) in which the proline hydroxylation sites are mutated to alanine (a kind gift of Dr. William Kaelin). Transduction of empty retroviral vector (pBabe) served as a negative control. 786-0 VHL-WT and vector controls were a kind gift of Dr. William Ohh. To assess the role of Src we generated stable SN12C (i) shRNA mediated knock down of Src using pSuper-Retro-puro system; (ii) a c-Src rescued lines resistant to the shRNA targeting using a retroviral expression vector pBabe-hygro encoding the chicken c-Src protein and (iii) a dasatinib resistant with a mutant form of c-Src (T338I). These plasmids were a kind gift of Dr. Joan Massagué and procedures were followed as described (Zhang et al., 2009). In addition, SN12C cells expressing lower level of PTP1B was developed by viral transduction with PTP1BshRNA (V2SHS_170902; Open

Biosystems and TRC 0000002777; Sigma). SN12C cell line stably transduced with GFP shRNA (Addgene) or with Non-Targeting shRNA Control (Sigma) served as a controls, respectively. SN12C cells overexpressing CSK were generated by stable transfection of pCSK-N1 (kind gift from Dr. M. Okada and Dr. S. Nada). All cell lines were routinely grown in monolayer cultures in Dulbecco's Modified Eagle Medium (DMEM) supplemented with 10% FBS and penicillin/ streptomycin.

Drugs and antibodies

Dasatinib, saracatinib, and imatinib were purchased from JS Research Chemicals Trading, Germany. The antibodies used in western blotting and immunohistochemistry staining were: pY419 Src, pY530 Src, Src, pY576/577 FAK, FAK, pY705 STAT3, CSK (C74C1), ERK1/2, cleaved caspase-3 (Asp175) from New England Biolabs, α-tubulin (TU02), β-actin, (C4), pY204 ERK1/2 (E-4) from Santa Cruz Biotechnology, Src, VHL, HIF-1α, PTP1B from BD Biosciences, HIF-2α, PTP1B (EP1841Y), STAT3 (STAAD22A) from Abcam, HIF2-α from Millipore, CA-IX from Novus Biologicals, Ki-67 from DAKO and Pimonidazole was purchased from Hypoxyprobe, Inc.

Cell proliferation assay

5 x 10^4 cells were plated and treated with a single dose of 25, 50 or 100 nM dasatinib or vehicle (DMSO). Cells were trypsinized, resuspended in DMEM/

10% FBS and counted using the VI-Cell XR automated cell-viability analyzer (Beckmann Coulter) at 96h post-treatment, unless otherwise stated. Cell counts were performed in triplicate and experiments were repeated on at least three independent occasions. Cells were split to sustain log phase growth.

Xenografts

5 x 10^6 SN12C and SN12C shVHL cells or 1x106 SN12C and SN12C v-Src cells diluted in 100 ml of matrigel (Collaborative Biomedical) were subcutaneously injected into both flanks of nude or SCID mice, respectively. When tumor volume reached 150 mm3, mice were randomized to daily treatment with vehicle or 10 mg/kg of dasatinib (six animals/group). Nude mice were injected with pimonidazole (Hypoxyprobe, Inc) 1h prior to sacrifice. All mouse experiments were performed in compliance with the guidelines of the Animal Research Committee of the University of California at Los Angeles and in accordance with UK Home Office and UK CCCR guidelines for animal experimentation with local Ethical Committee approval.

Flow cytometry

Cells were plated at a density such that they were no more than 70% confluent on the day of analysis. Cells were treated with dasatinib for 48h unless otherwise stated. For PI staining, cells were trypsinized, collected by centrifugation and washed in PBS prior to fixing in 70% v/v ethanol. Ethanol was

removed by washing in PBS. Cells were incubated with 100 µg/ml RNase A (Sigma) for 5 min and stained with 50 µg/ml PI for 30 min. For BrdU analysis, dasatinib-treated cells were incubated for 30 min with 10 µM BrdU (Sigma) prior to harvesting. Cells were stained with fluorescein isothiocyanate (FITC)-conjugated anti-BrdU antibodies (BD Biosciences) according to the manufacturer instruction. Following multiple washes in blocking solution and PBS, cells were stained with 5 µg/ml PI for 30 min. The PI or BrdU/PI-stained samples were analyzed by LSR FACS machine (Becton Dickinson) and the cell cycle profile was analyzed with the FlowJo software (Tree Star Inc.). Phosphoprotein flow cytometry analysis was performed as previously described (Shah et al., 2008).

Real-time PCR

Total RNA was extracted from cells with the RNeasy kit (Qiagen) and the reverse transcription performed with 1 µg of RNAs and 200 units of Superscript II enzyme (Invitrogen). Real time PCR amplifications were performed using the Brilliant II Fast SYBR Green QPCR Master Mix (Agilent Technologies) with 2 µl of 1/10 cDNA and 300-500 nM of primers. The primers used were as follows for RPLP0 5'-GTGATGTGCAGCTGATCAAGACT-3' and 5'-GATGACCAGCCCAAAGGAGA-3', from SuperArray Biosciences for Src and PTP1B. Reactions proceeded with initial 2 min incubation at 95°C followed by 40 cycles of amplification: 95°C for 5s and 60°C for 2 0s in a Mx3000p thermal cycler (Agilent Technologies). Fluorescence was measured in real time with

dissociation curves option; the cycle threshold (Ct) values were calculated using the Mx3000p algorithm (Agilent Technologies). Standard curves were performed on serial dilutions of genomic human DNA or RT-transcripts. Comparative quantitation was performed using the MxPro QPCR software by comparing the Ct value obtained from the amplification of a given target with that determined for the normalizer, RPLP0 (human acidic ribosomal phosphoprotein P0). Relative mRNA abundance was calculated using the Ct method.

Chromatin immunoprecipitation

Sheared, formaldehyde crosslinked chromatin derived from 0.5 X 10^6 cells was incubated with 1µl of anti-HI-1α antibody (Abcam ab2185) or 2 µg of normal rabbit (IgG) antibody (Millipore) to immunoprecipitate DNA overnight at 4°C. 1% of chromatin was removed prior to immunoprecipitation as input. Immune complexes were collected with protein A/G (3:1)-magnetic beads (Dynabeads, Invitrogen). After extensive washing, immune complexes were released, crosslinks were reversed, and DNA was purified with mini-elute PCR purification kit (Qiagen) and eluted with 60ul EB. A putative palindromic HRE sequence, localized at -214 to -224, was found in the PTP1B promoter region using CLCbio Genomics workbench software. The primers designed by the software were as follow forward 5'- ATGGAATTTGTGCTCTGCT-3' and reverse 5'-CTCTATTTCCTGCCTCCCA-3'. Real-time PCR was performed in triplicate on

2ul of the immunoprecipitated DNA or 2ul of the 1% input. Immunoprecipitated DNA was calculated as “% of input” with ddCt method.

Western blot analysis

Cells were seeded to have approximately 50% confluence upon lysis. Cells were lysed after 18h of exposure to vehicle or dasatinib in EBC lysis buffer (50 mM Tris, pH 8.0, 120 mM NaCl, 0.5% Nonidet P-40) supplemented with complete protease (Roche) and phosphatase inhibitor (Calbiochem) cocktails. Xenograft tumors were lysed in a protein lysis buffer (150 mM NaCl, 1 mM EDTA, 50 mM Tris, 1% v/v Triton X-100, 1 nM NaF, 1 mM NaVO3, 5 µM bpVphen, 1 mM PMSF), supplemented with phosphatase inhibitors I & II, protease inhibitor cocktail and TLCK (Sigma). Protein extracts (40-100 µg) were resolved by SDS-PAGE, transferred on to polyvinylidene fluoride membrane (Millipore) and probed with appropriate antibodies. The primary antibodies were detected using horseradish peroxidase-linked goat anti-mouse or anti-rabbit secondary antibodies (Jackson Laboratories) and visualized by SuperSignal West Pico Chemiluminescent substrate (Thermo Scientific). Images were collected by UVP BioSpectrum(R) AC Chemi HR 410 Imaging System. Blots were analyzed and quantified using UVP VisionWorksLS Image Acquision and Analysis software.

In vitro Src kinase assay

Equal number of subconfluent SN12C and SN12C-shVHL cells were harvested is NETN lysis buffer [20 mM Tris (pH 8.0), 150 mM NaCl, 0.5% NP-40, 1 mM EDTA] supplemented with protease inhibitors (0.5 mM phenylmethylsulfonyl fluoride and 0.1 µM each of aprotinin, E-64, and leupeptin), and phosphatase inhibitors (1 mM sodium orthovanadate and 20 mM sodium fluoride). Endogenous Src was immunoprecipitated with anti-Src 327 ascites (Jonathan Cooper, Fred Hutchinson Cancer Research Center, USA) and captured with Protein G-sepharose 4B (Invitrogen). Immunoprecipitated Src kinase activity from SN12C and SN12C-shVHL cells was measured using a commercial Src Assay Kit (Millipore #17-131) accordingly to the manufacturer's instructions. Briefly, Src immunoprecipitates or control immunoprecipitates (lysates incubated with Protein G in the absence of antibody) were incubated in Src Kinase Reaction Buffer [100 mM Tris (pH 7.2), 125 mM MgCl2, 5 mM MnCl2, 2 mM EGTA, 250 µM sodium orthovanadate, 2 mM dithiothreitol] at 30° C for 10 min with Src substrate peptide (KVEKIGEGTYGVVYK), 10 µCi [g-32P] ATP in manganese/ATP buffer [75 mM MnCl2, 500 µM ATP in 75 mM MOPS (pH 7.2), 25 mM b-glycerol phosphate, 5 mM EGTA, 1 mM sodium orthovanadate, 1 mM dithiothreitol] and 50 nM Dasatinib where indicated. Reactions were spotted onto P81 phosphocellulose paper, precipitated with 40% TCA, then washed five times with 0.75% phosphoric acid, once with acetone and transferred to vials containing 5 ml of scintillation fluid (CytoScint, Fisher #BP458-4) and 32P-labeled substrate peptide was measured in a Packard 1900TR Liquid Scintillation

Analyzer. Data are presented as the mean CPM ± S.D. from three independent experiments assayed in duplicate. Statistical analysis between mean CPM of SN12C and SN12C-shVHL Src kinase activity was performed using a 2-tailed Student's t-test. For immunoblot analysis, the amount of Src was quantified with NIH Image J and presented numerically as the fold-change.

Statistical analysis

Contingency table analysis and Chi-square test were used for the analysis of the association between membranous and cytoplasmic Src expression as well as between Src and VHL protein expression. Overall survival rates were determined according to the Kaplan–Meier method and analyzed for statistical differences using a log rank test. Spearman Rho correlation coefficients were used to assess the association between different biomarkers expression and was performed using the GraphPad Prism software. To analyze whether level of a protein can be predicted by other proteins, multiple linear regression was performed in the R statistical programming language (R v 2.10.1). All model variables, both response and explanatory, have been log transformed to improve normality. No model selection was performed. Two models were examined based on previous biological knowledge and the correlation results: Src level as the response variable with VHL and PTP1B as the explanatory variables, and PTP1B level as the response variable with VHL and HIF-2α as the explanatory variables. The statistical significance of differences for the *in vitro* experiments was

determined by 2-tailed Student's t-test (GraphPad statistics software). Any difference with a P-value less than 0.05 was considered significant. The heatmap was generated using Spotfire software. Scatter plots were generated using Statistica software and thresholds gated as stated in figure legend.

ACKNOWLEDGMENTS

Acknowledgments: We thank C. W. Ryan, W. Y. Kim, K. Ellwood-Yen, M. Ashcroft, S. Mittnacth, I. K. Mellinghoff, J. T. Erler, and R. Dresbeck for helpful discussions; J. G. Braun for academic support; L. Iwai, N. Martin, C. Garcia, P. Clarke, S. Eccles, and J. Dukes for technical expertise; M. C. Costello for artwork; W. Kaelin [Howard Hughes Medical Institute (HHMI)] for the HIF-1α and HIF-2α prolyl hydroxylase mutants; J. Massagué (HHMI) for the Src shRNA, chicken Src, and Src T388I mutant; M. Ohh for the 786-0 VHL-WT plasmid; M. Okada and S. Nada for the Csk plasmids; and T. Mori, S. McWeeney, and S. Mongue-Tchokote from the Biostatistics Shared Resource of the Knight Cancer Institute (National Cancer Institute P30 CA 069533). M.E.G. thanks the Royal Marsden Hospital foundation. Funding: K.M.A. is supported by National Research Service Award T32 GM71338 and award RMS1112 from the Radiological Society of North America. P.W. is supported by Cancer Research UK program grant C309/A8274 and is a Cancer Research UK Life Fellow. This study was supported by NIH grants DK37274, CA151564 (G.T.), 1KL2 RR024141 01 through OCTRI and UL1 RR024140 (J.J.A.), R01CA149253-01 (D.Z.Q.), P30 CA069533 13S5 through OHSU Knight Cancer Institute and the Pacific Northwest Prostate Specialized Programs of Research Excellence (G.V.T.), Knight Cancer Institute award (G.T.), VHL Family Alliance, STOP Cancer Foundation, Experimental Cancer Medicine Center network and the Institute of Cancer Research (G.V.T.).

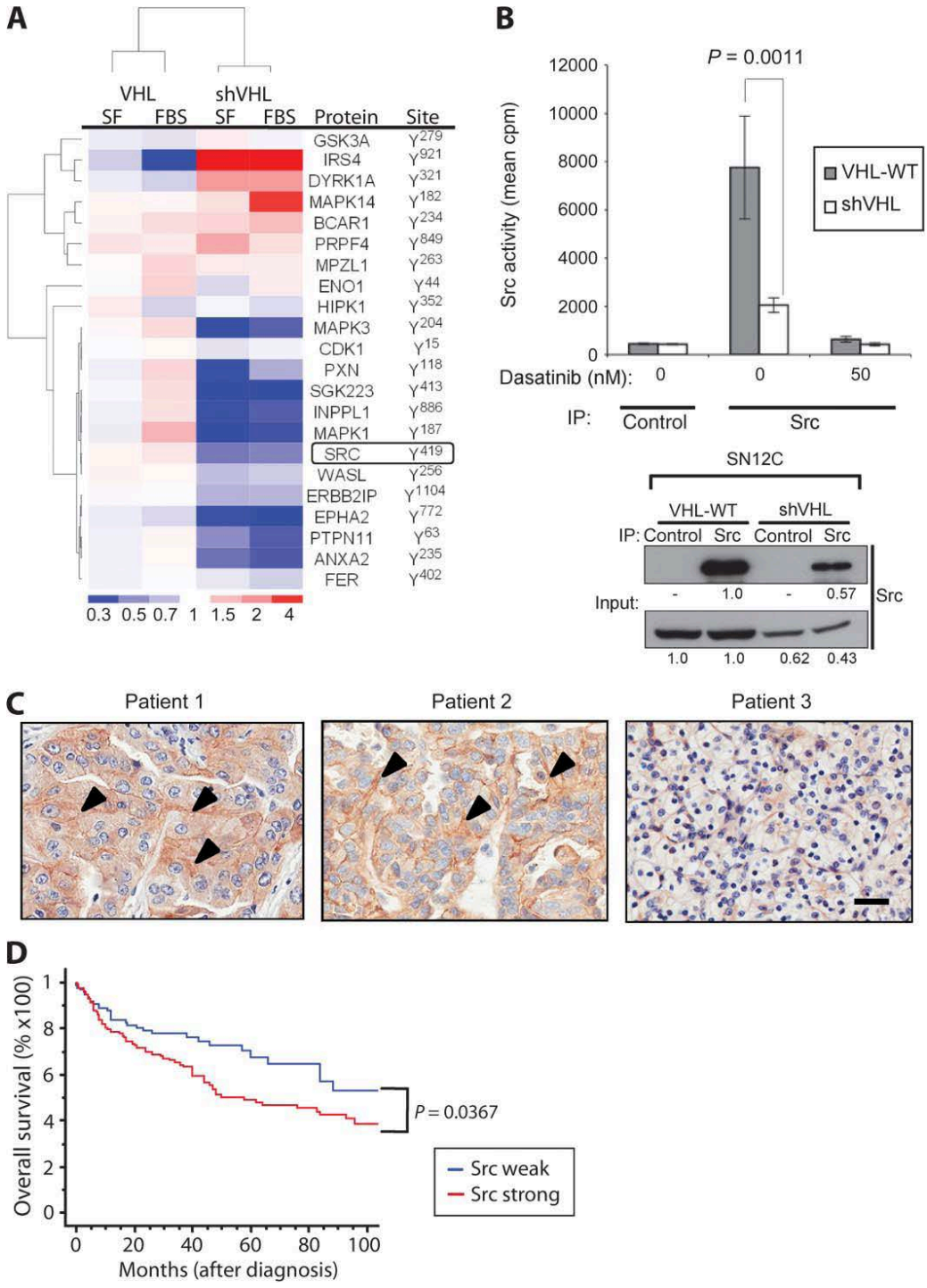

Figure A.1. Src is expressed in RCC and is associated with poor outcome.

(A) Lysates from parallel cultures of serum-stimulated SN12C and SN12C-shVHL cells were labeled with iTRAQ 8-plex reagent and phosphotyrosine-containing peptides were subjected to immobilized metal affinity chromatography–MS/MS analysis. Quantitative phosphorylation profiles were generated for 22 phosphorylation sites. Mean ratios to SN12C control were log-transformed and partitioned according to similarity of phosphorylation status by unsupervised hierarchical clustering with Cluster 3.0 and visualized with TreeView. Heat map is pseudocolored to indicate direction and magnitude of mean ratios relative to SN12C control cells. SF, serum free; FBS, fetal bovine serum. See also table S1 and Materials and Methods. (B) Src was immunoprecipitated from SN12C and SN12C shVHL cells, and Src kinase activity was measured in the absence or presence of 50 nM dasatinib as described in Materials andMethods. Data are presented as the mean cpm (counts per minute) ± SD from three independent experiments assayed in duplicate. (Lower panel) Corresponding Western blot showing control (no primary antibody) or Src immunoprecipitates and relative Src expression in SN12C and SN12CshVHL cells. The amount of Src was quantified with ImageJ and presented as mean cpm. (C) Immunohistochemistry for Src from samples from three representative RCC patients with strong (left and middle panels) or weak expression (right panel). Arrowheads indicate membranous localization. Scale bar, 20 mm. (D) Kaplan-Meier survival analysis of clear cell RCC patients with tumors expressing weak or strong Src immunohistochemical staining (n = 117, P = 0.0367).

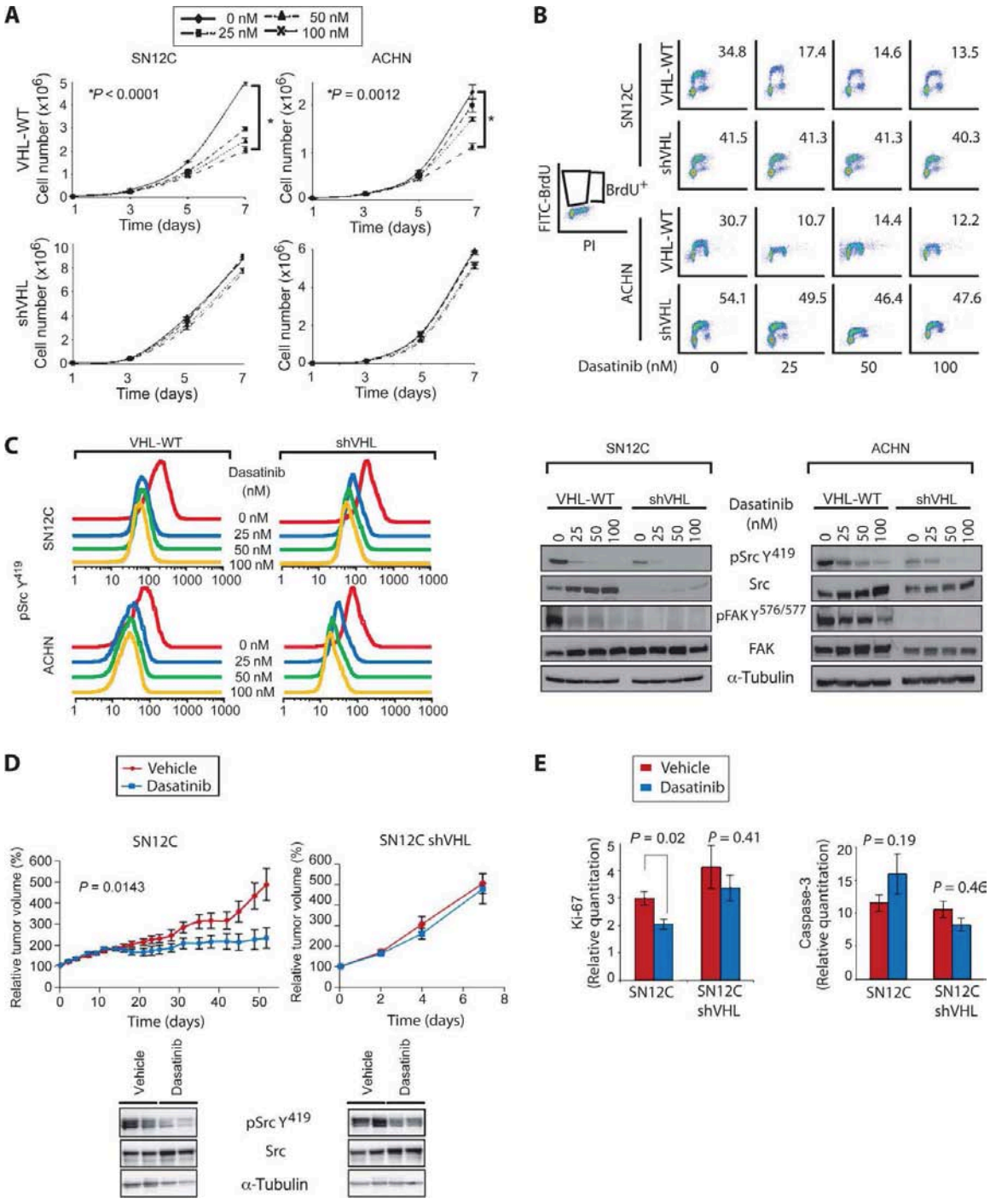

Figure A.2. Dasatinib induces growth arrest in VHL-WT RCC cells.

(A) VHL-WT SN12C and ACHN or shVHL cells (5 X 10^4) were treated with vehicle and 25, 50, or 100 nM dasatinib 24 hours after seeding. The effect of dasatinib on cell growth was monitored by cell counting at indicated time points (n = 3). Data are presented as means ± SD. (B) Subconfluent SN12C and ACHN VHL-WT or shVHL cells were treated with the indicated doses of dasatinib for 48 hours and labeled with 10 mM BrdU for 30 min before harvesting. Cells were dual-stained with fluorescein isothiocyanate (FITC)–BrdU antibody and PI and analyzed by flow cytometry. (C) Subconfluent SN12C and ACHN VHL-WT or shVHL cells were treated with vehicle and 25, 50, or 100 nM dasatinib. Inhibitory effect of dasatinib on Src kinase activity was assessed by flow cytometry with anti-pY419 Src (left panel). Levels of total and phospho-specific forms of Src and FAK were determined by immunoblotting (right panel). α-Tubulin was used as the loading control. (D) Nude mice bearing SN12C and SN12C shVHL xenografts were treated daily with vehicle or dasatinib (10 mg/kg) by oral gavage. Fold increase in tumor volume is plotted against days following tumor injection. Xenografts were analyzed by immunoblot for levels of pY419 Src and total Src. a-Tubulin was used as the loading control. Data are presented as means ± SEM of six mice in each group. (E) Xenograft tumors from (D) were analyzed for cell proliferation and apoptosis by immunohistochemistry against Ki-67 and cleaved caspase-3, respectively, and subjected to quantitative image analysis. Data are presented as means ± SEM (n = 11 to 21).

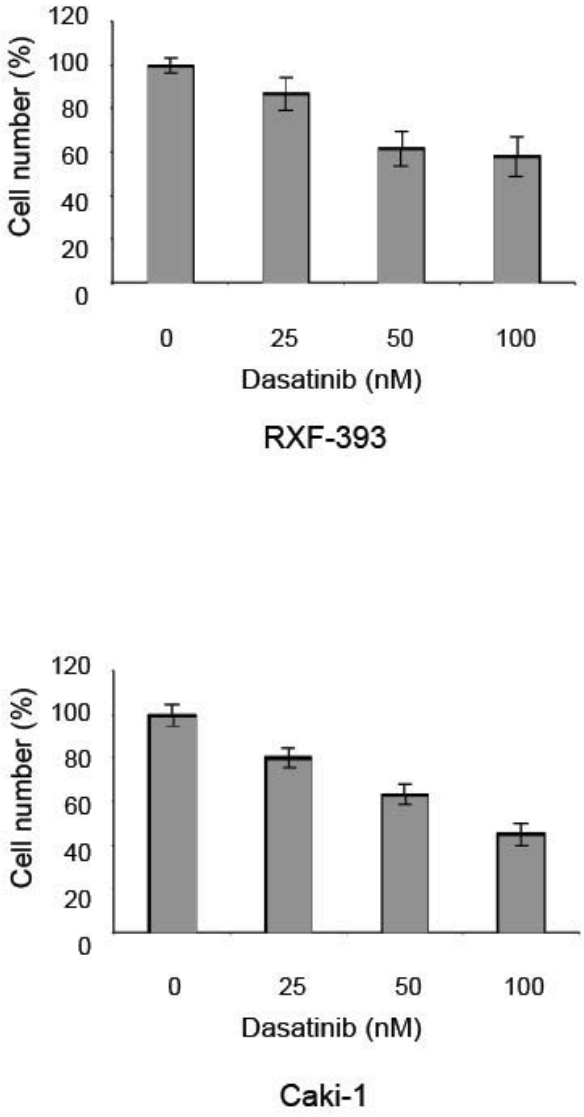

Figure A.3. VHL-WT RXF-393 and Caki-1 cells are sensitive to dasatinib.

5 x 10^4 RXF-393 or Caki-1 cells were treated with vehicle, 25, 50 or 100 nM dasatinib 24h post-seeding. Effect of dasatinib on cell growth was recorded by cell count after 96h. Data are presented as the mean ± S.D. (n = 3).

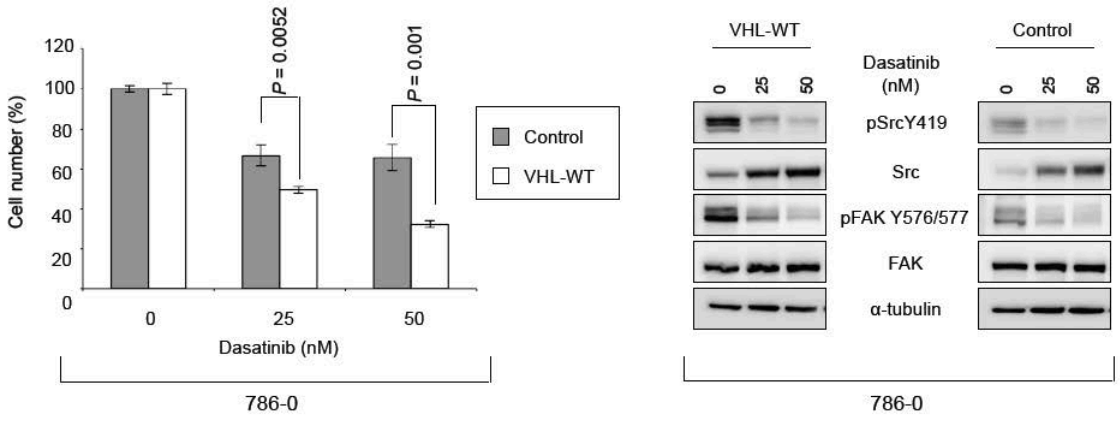

Figure A.4. Reconstitution of VHL enhances sensitivity to dasatinib in VHL null 786-0 cells.

5 x 10^4 786-0 control or 786-0 cells expressing VHL (VHL-WT) were treated with vehicle, 25 or 50 nM dasatinib 24h post-seeding. Effect of dasatinib on cell proliferation was monitored by cell count after 96h. Levels of total and phosphospecific forms of Src and FAK after 24h vehicle/dasatinib treatments were determined by immunoblot. α-tubulin, loading control.

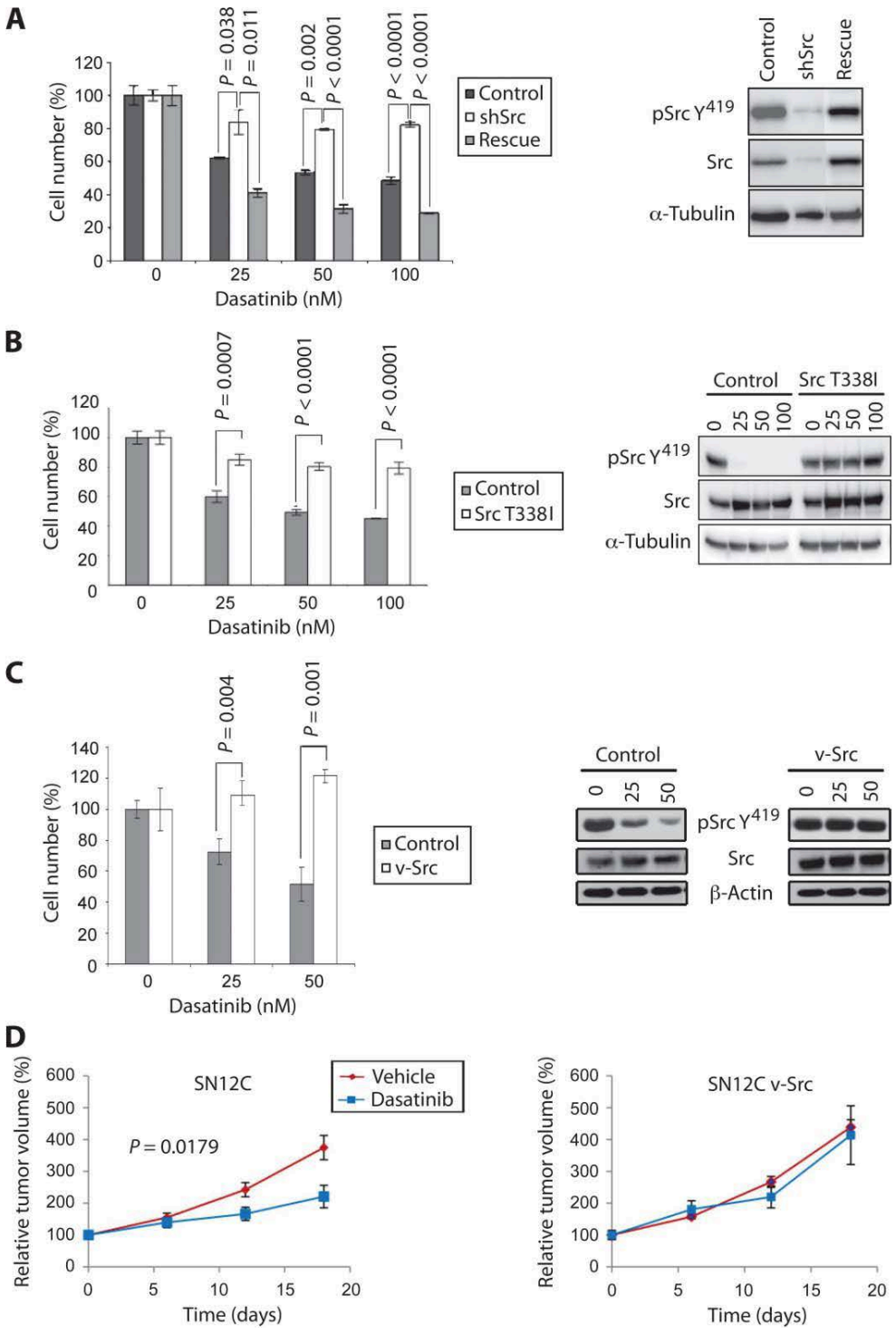

Figure A.5. Src is the relevant target of dasatinib in RCC.

(A) SN12C, SN12C-shSrc, or SN12-shSrc cells expressing shRNA-resistant Src (Rescue) were treated with vehicle and 25, 50, or 100 nM dasatinib for 96 hours and then cell growth was analyzed by cell count. Data are presented as means ± SD (n = 3). Src expression or knockdown was verified by immunoblot with antibodies against total and pY419 Src. a-Tubulin was used as the loading control. (B and C) SN12C cells (Control) or SN12C cells stably expressing (B) dasatinib-resistant Src (Src T338I) or (C) v-Src were treated with vehicle alone or with 25 or 50 nM dasatinib for 96 hours and then cell growth was analyzed by cell count. Data are presented as means ± SD (n = 3). The levels of total Src and pY419 Src were assessed by immunoblot. a-Tubulin and β-actin were used as loading controls. (D) SCID mice bearing SN12C and SN12C v-Src xenografts were treated daily with vehicle or dasatinib (10 mg/kg) by oral gavage. Percent (%) increase in tumor volume is plotted against days after tumor injection. Data are presented as means ± SEM (n = 24).

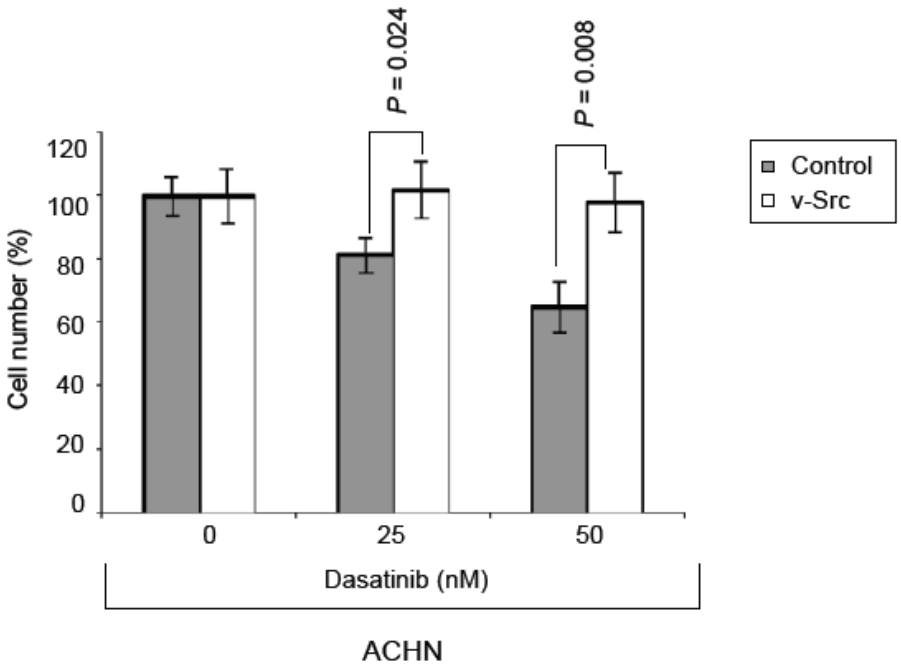

Figure A.6. Expression of v-Src renders VHL-WT cells resistant to dasatinib.

5 x 10^4 ACHN cells expressing either a control vector or v-Src were treated with vehicle, 25 or 50nM dasatinib 24h post-seeding. Effect of dasatinib on cell growth was monitored by cell count after 96h. Data are presented as the mean ± S.D. (n = 3).

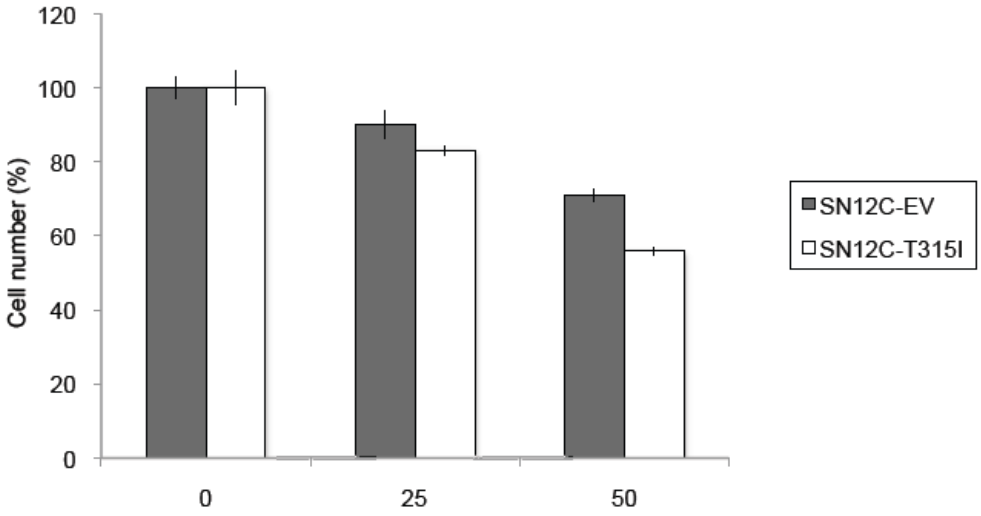

Figure A.7. Overexpression of Bcr-Abl T315I mutant does not rescue sensitivity to dasatinib.

5 x 10^4 SN12C cells expressing either a control vector (EV) or BCR-Abl T315I were treated with vehicle, 25 or 50 nM dasatinib 24h post-seeding. Effect of dasatinib on cell proliferation was monitored by cell count after 96h. Data are presented as the mean ± S.D. (n = 3).

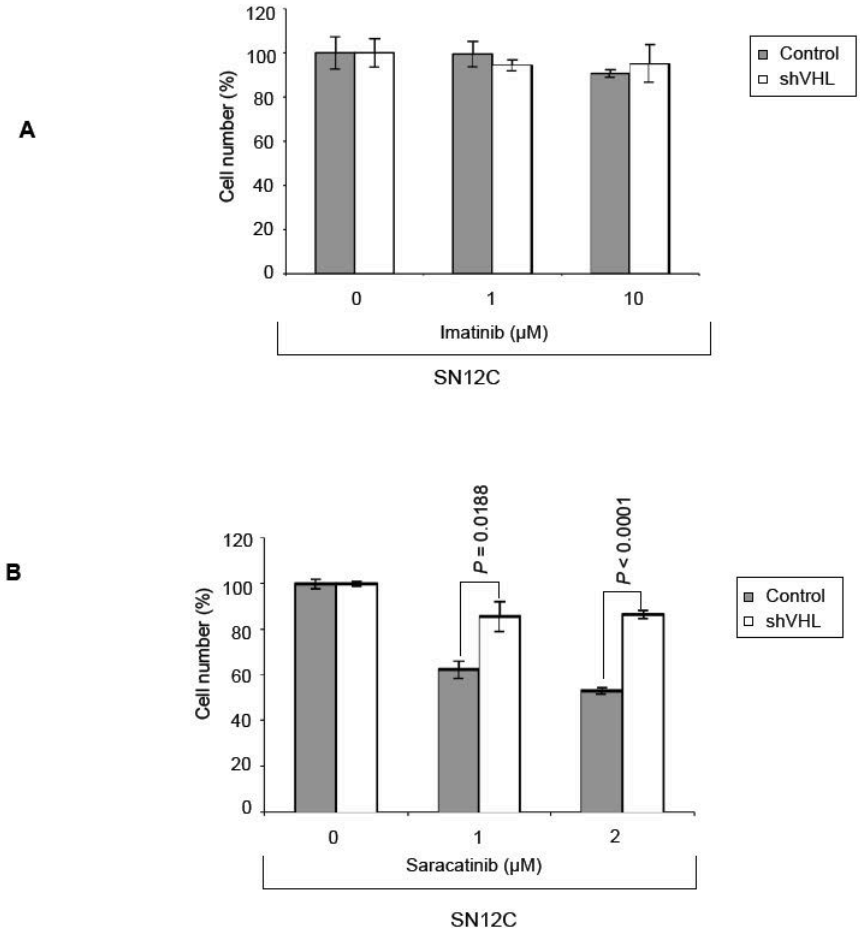

Figure A.8. Growth inhibition of VHL-WT cells by dasatinib is due to Src inhibition.

(A, B) 5 x 10^4 cells SN12C VHL-WT or shVHL cells were treated with indicated doses of (A) imatinib or (B) saracatinib. Effect of these drugs on cell proliferation was monitored by cell count 96h post-treatment. Data are presented as the mean ± S.D. (n = 3).

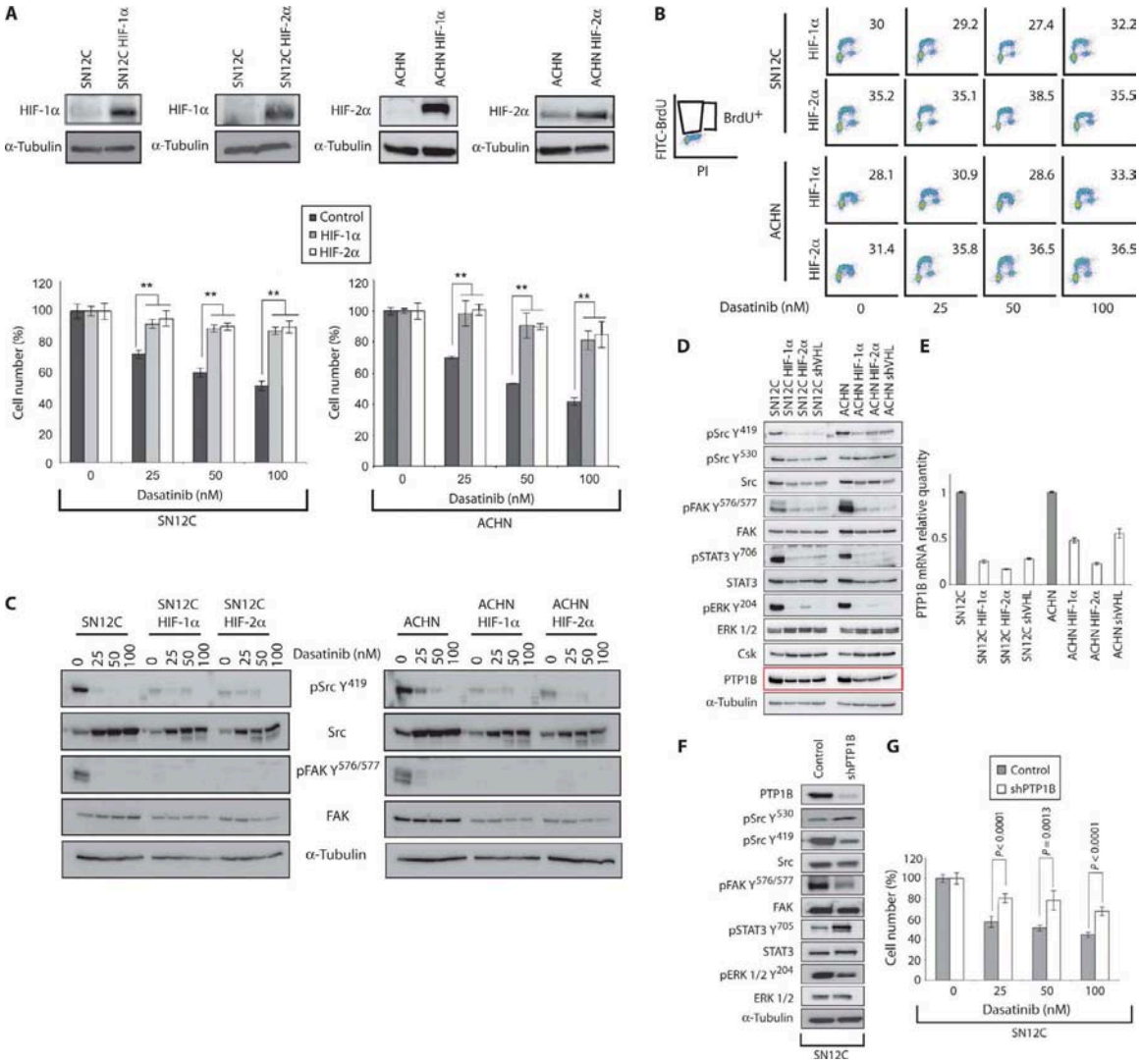

Figure A.9. HIF-α and PTP1B are involved in dasatinib-induced growth inhibition.

(A) SN12C and ACHN cells stably expressing mutant HIF-1α (P564A) or HIF-2α (P405A; P531A) were treated with vehicle and 25, 50, or 100 nM dasatinib for 96 hours and then cell growth was analyzed by cell count. Data are presented as means ± SD (n = 3, **P < 0.01). Overexpression of the mutant forms of HIF-α was validated by immunoblot. α-Tubulin was used as the loading control. (B)

SN12C and ACHN cells stably expressing mutant HIF-1α (P564A) or HIF-2α (P405A; P531A) were treated with vehicle and 25, 50, or 100 nM dasatinib for 48 hours and then analyzed for BrdU incorporation by flow cytometry as described in Materials and Methods. (C) SN12C and ACHN cells stably expressing constitutively stable HIF-1α P564A (SN12C HIF-1α) or HIF-2α P405A; P531A (SN12C HIF-2α) were treated with vehicle alone or with 25, 50, or 100 nM dasatinib for 18 hours. Levels of total Src and FAK, as well as pSrc Y419 and pFAK Y576/577 were determined by immunoblot. α-Tubulin was used as the loading control. (D) Lysates from the SN12C and ACHN mutant HIF-α–overexpressing lines, shVHL cells, and the parental cell lines were examined for expression of total and/or phosphospecific forms of Src, FAK, ERK1/2 (extracellular signal–regulated kinase 1/2), STAT3, Csk, and PTP1B by immunoblot. α-Tubulin was used as the loading control. (E) The levels of PTP1B mRNA were measured by real-time polymerase chain reaction (PCR) in SN12C and ACHN HIF-α–overexpressing and shVHL cell lines. Levels of PTP1B mRNA in the parental cell lines were normalized to 1. Data are presented as means ± SD (n = 3). (F) SN12C cells expressing an shRNA targeting PTP1B (shPTP1B) were analyzed by immunoblot for expression levels of total and/or phospho-specific forms of PTP1B, Src, FAK, STAT3, ERK1/2, and a-tubulin. (G) SN12C or shPTP1B cells were treated with vehicle and 25, 50, or 100 nM dasatinib, and cell growth was assessed by cell count. Data are presented as means ± SD (n = 3).

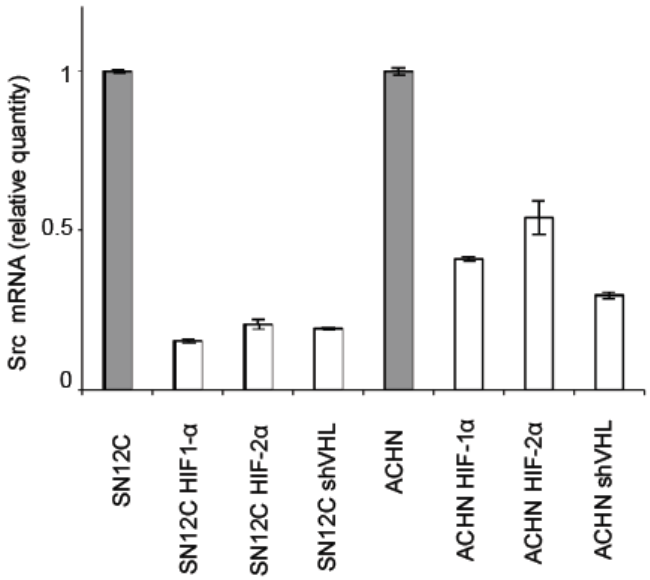

Figure A.10. VHL status modulates Src expression at the transcriptional level.

Transcriptional level of Src in SN12C or ACHN parental cells, SN12C or ACHN cells overexpressing constitutively stable HIF-1α-P564A (HIF-1α) or HIF-2α-P405A,P853A (HIF-2α) mutants, or isogenic shVHL knockdown cells (n = 3). Data are presented as the mean ± S.D. Levels of mRNA in the parental cell lines are normalized to 1.

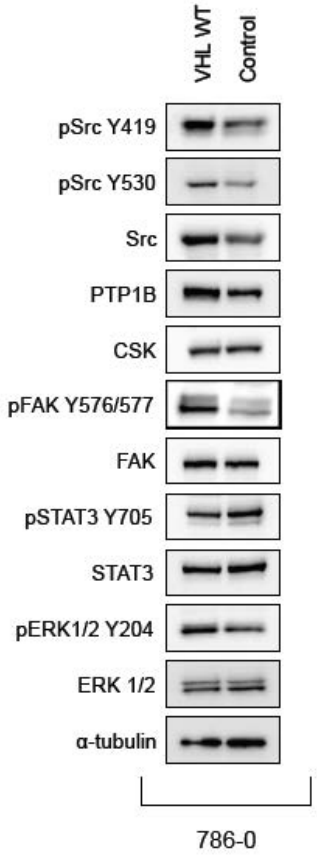

Figure A.11. Reconstitution of VHL alters S signaling output.

786-0 Control and VHL-WT expressing cells were analyzed for total and phospho-specific forms of Src, PTP1B, CSK, FAK, STAT3 and ERK1/2 by immunoblot. α-tubulin, loading control.

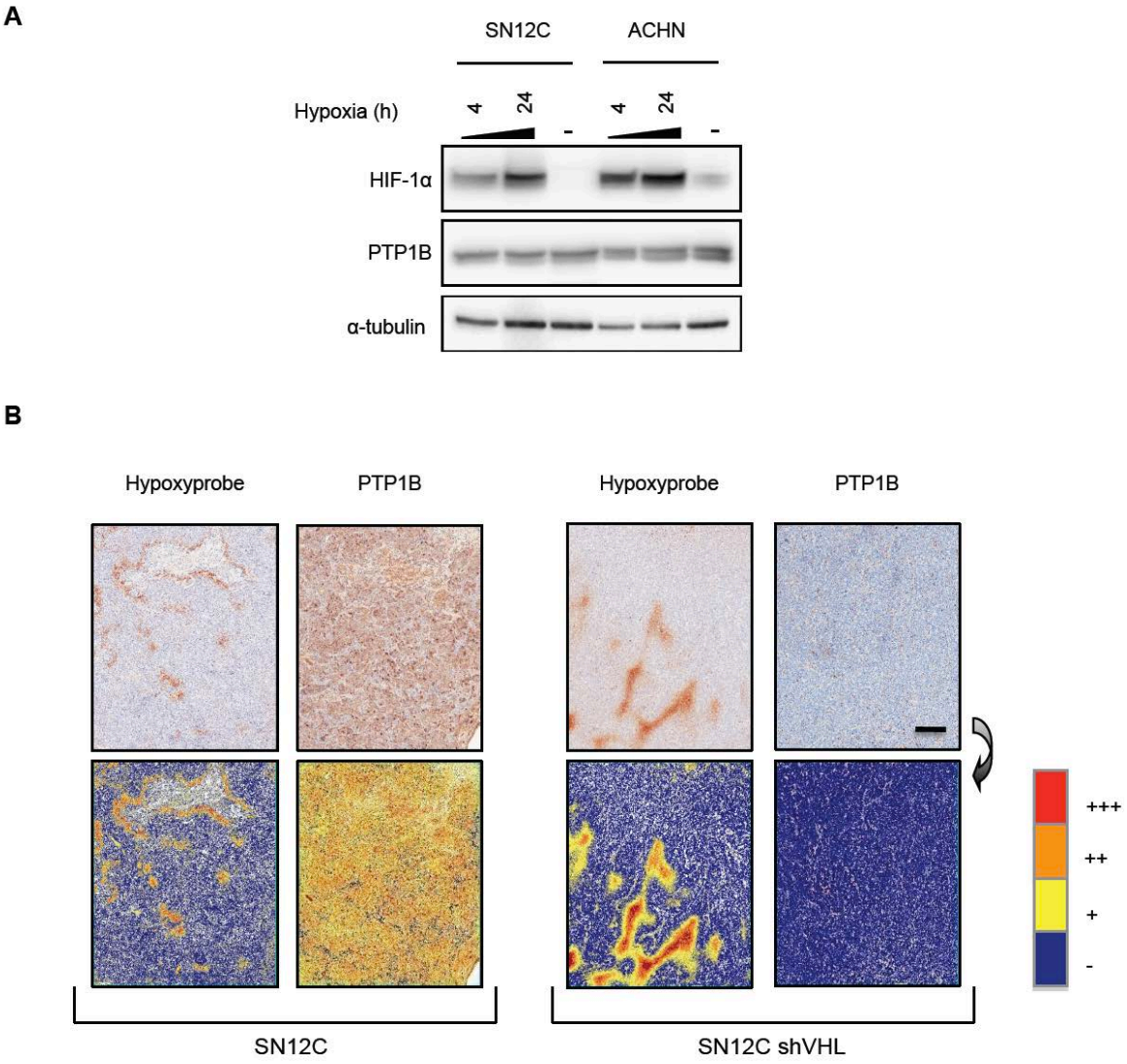

Figure A.12. PTP1B expression levels and hypoxia.

(A) Changes in levels of PTP1B and HIF1α in SN12C and ACHN cells were monitored by immunoblot following exposure to hypoxia (1% oxygen) for the indicated times. α-tubulin, loading control. (B) Xenograft tumors from SN12C and SN12C shVHL cells were immunostained with pimonidazole (Hypoxyprobe) and

PTP1B. Corresponding markup images of the color deconvolution algorithm with intensity ranges are shown (Red = strong, orange = moderate, yellow = weak, blue = negative immunoreactivity). Scale bar is 100 µm.

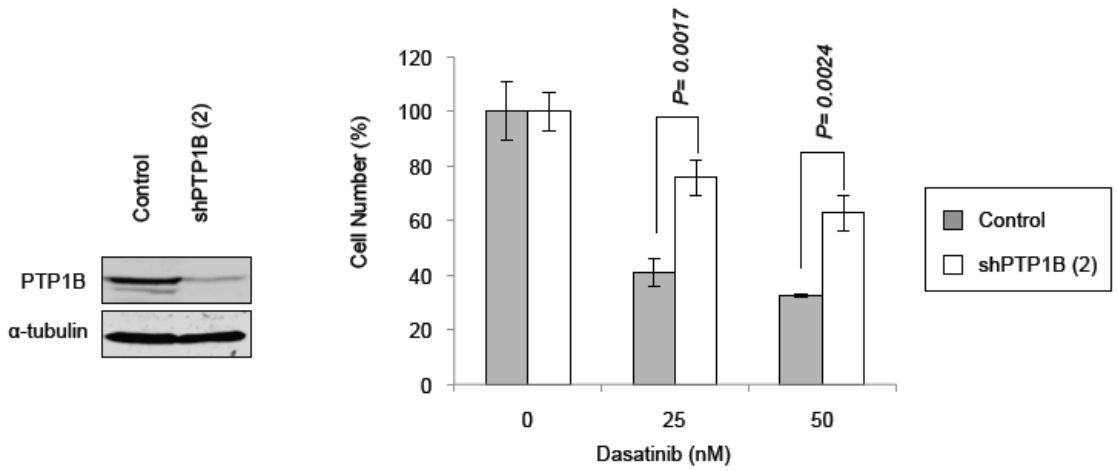

Figure A.13. Second PTP1B shRNA also rescues sensitivity to dasatinib.

SN12C (control) and SN12C-shPTP1B (targeting sequence #2) cells were analyzed for expression of PTP1B by immunoblot. α-tubulin, loading control. Cell proliferation following 96h exposure to vehicle alone or to 25 or 50 nM dasatinib was assessed by cell count. Data are presented as the mean ± S.D. (n = 3).

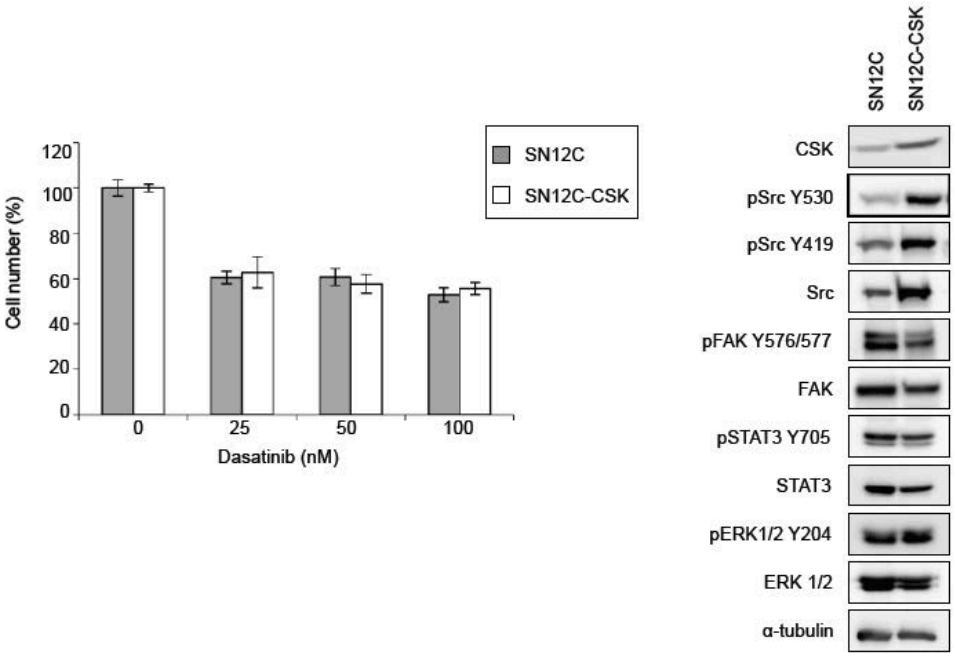

Figure A.14. Csk overexpression does not confer dasatinib-resistance in SN12C cells.

Control SN12C cells or CSK-overexpressing SN12C cells were analyzed by cell count following 96h treatment with vehicle, 25, 50 or 100 nM dasatinib. Data are presented as the mean ± S.D. (n = 3). The levels of CSK, as well as total and phospho-specific forms of Src, FAK, STAT3, and ERK 1/2 were monitored by immunoblot. α-tubulin, loading control.

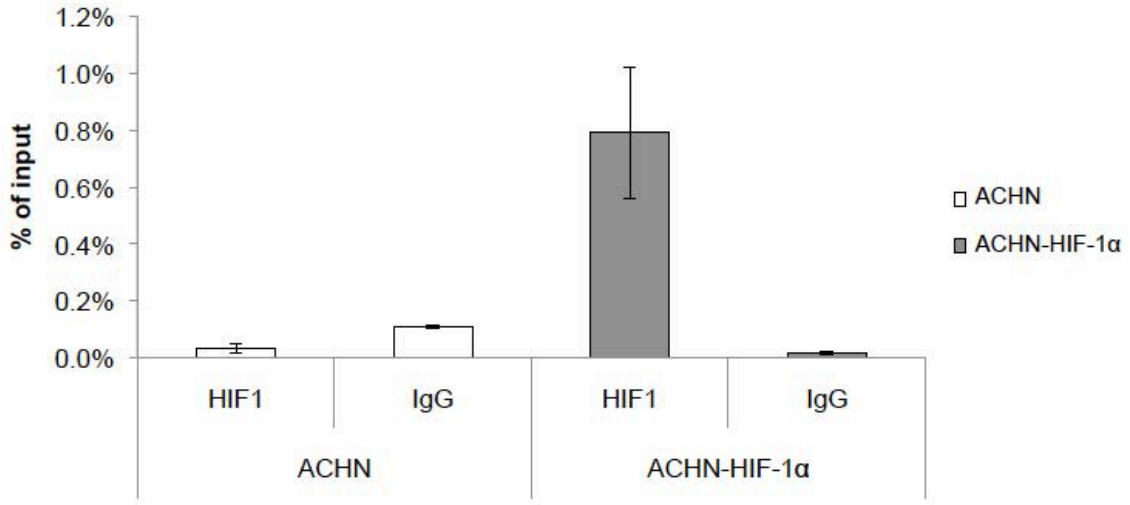

Figure A.15. Chromatin Immunoprecipitation analysis at the PTP1B promoter.

ChIP analysis using anti-HIF1α or non-specific IgG antibodies was performed on sheared chromatin from ACHN or ACHN-HIF-1α cells. Co-immunoprecipitated DNA containing the PTP1B hypoxia response element (HRE) was quantified using using real-time PCR and presented as percent (%) of input.

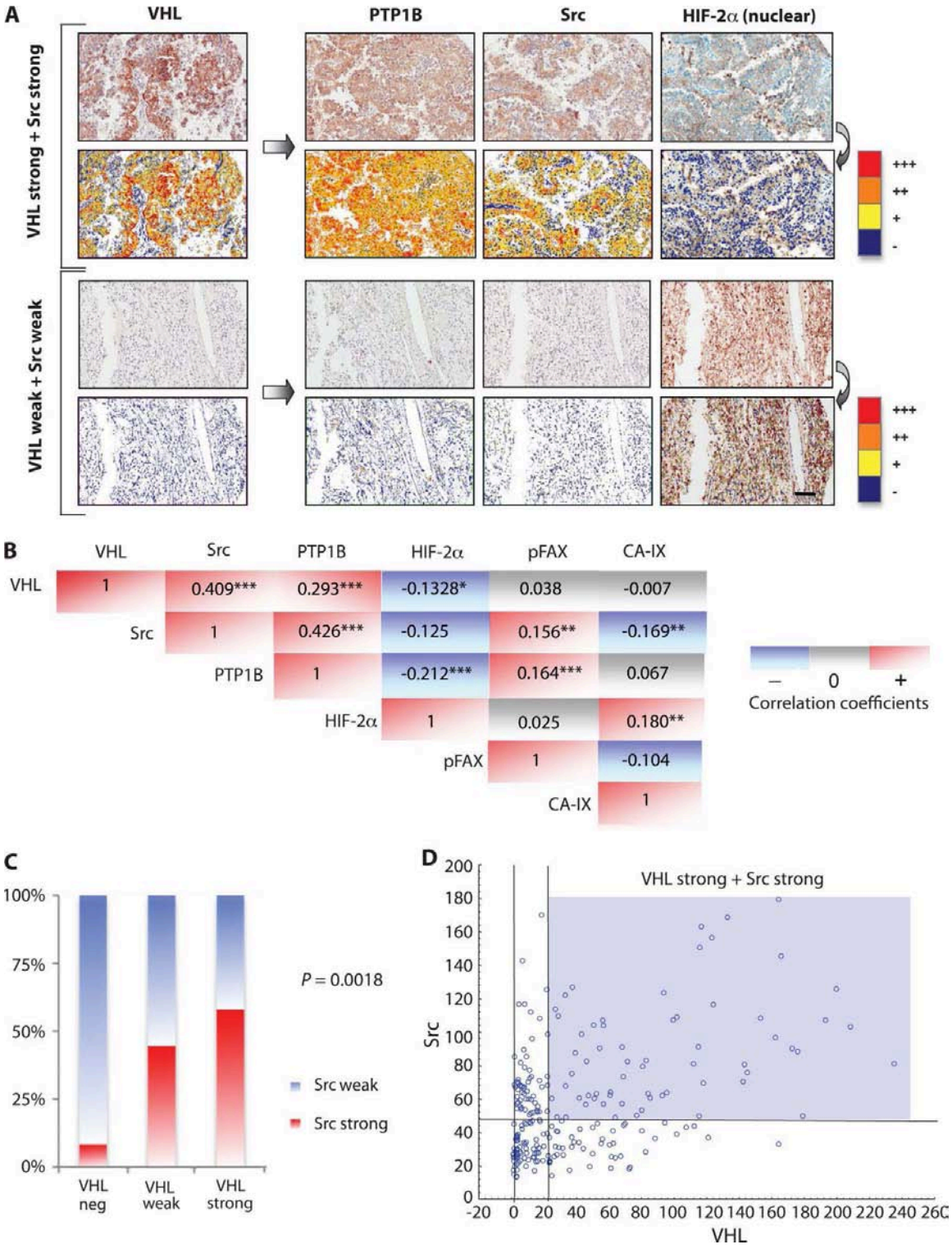

Figure A.16. VHL, HIF-α, Src, and PTP1B levels are related in RCC patients.

(A) Quantitative assessment of VHL, PTP1B, Src, and HIF-2α expression by immunostaining of RCC TMA. Representative staining images from a patient with strong VHL protein expression (top panel) and from a patient with weak VHL expression (bottom panel) are shown. Corresponding markup images of the color deconvolution algorithm with intensity ranges are shown (red = strong, orange = moderate, yellow = weak, blue = negative immunoreactivity). For HIF-2α, the nuclear immunostaining algorithm was applied. Scale bar, 50 mm. (B) Spearman Rho correlation coefficients among the biomarkers. Red indicates positive correlation and blue indicates negative correlation. P values for these correlations are represented as follows: *P < 0.05; **P < 0.001; ***P < 0.0001 (n = 131). (C) Comparison between Src and VHL protein expression in the samples of the RCC tissue microarray (TMA). (D) Scatter plot of the VHL and Src scores generated from automated image analysis intensity algorithm. The vertical lines represent fifth percentile and median VHL scores, corresponding to thresholds for negative and weak expression, respectively. The horizontal line represents the median for the Src score, where levels below are considered weak expression and levels above are considered strong expression. The upper right (shaded) quadrant depicts the molecular phenotype of tumors with both strong VHL and strong Src expression.

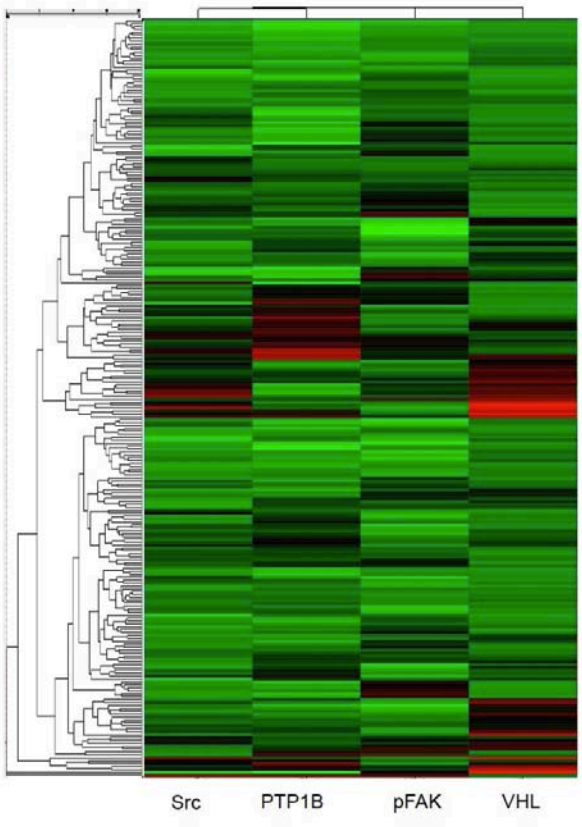

Figure A.17. Heat map showing hierarchical clustering of the protein expression data of VHL, Src, pFAK and PTP1B.

The data was generated from the cytoplasmic staining intensity scores as measured by quantitative digital image analysis and normalized by centering on the median. HIF-2α immunostaining is not shown, as its reported values were scored by quantifying nuclear positivity. Each row corresponds to a patient sample and each column represents the indicated biomarker (Src, PTP1B, pFAK, VHL). Color represents expression level from black to red, with red indicating high expression and green indicating low expression. The columns were also clustered as shown by the simple tree at the top of the figure.

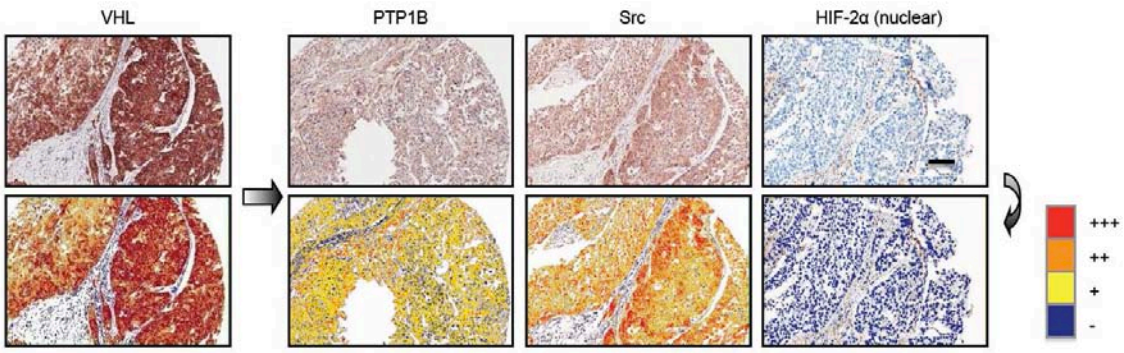

	Correlation Coefficient	*P*
VHL		
SRC	0.493	0.027
PTP1B	0.477	0.034
HIF-2α	- 0.408	0.07
HIF-2α		
PTP1B	- 0.582	0.007

Figure A.18. Correlation between the expression levels of VHL, PTP1B, Src and HIF-2α immunostaining in transitional cell carcinoma of the bladder.

A tumor from a representative transitional cell carcinomas patient was immunostained with VHL, PTP1B, Src and HIF-2α using DAB based detection method and subsequently counterstained with hematoxylin. The scanned slides were then subjected to quantitative digital image analysis. Corresponding markup images of the color deconvolution algorithm with intensity ranges are shown (Red = strong, orange = moderate, yellow = weak, blue = negative immunoreactivity). For HIF-2α, the algorithm was applied for nuclear immunostaining. Scale bar is 50µm.

Table, Spearman Rho correlations between the biomarkers

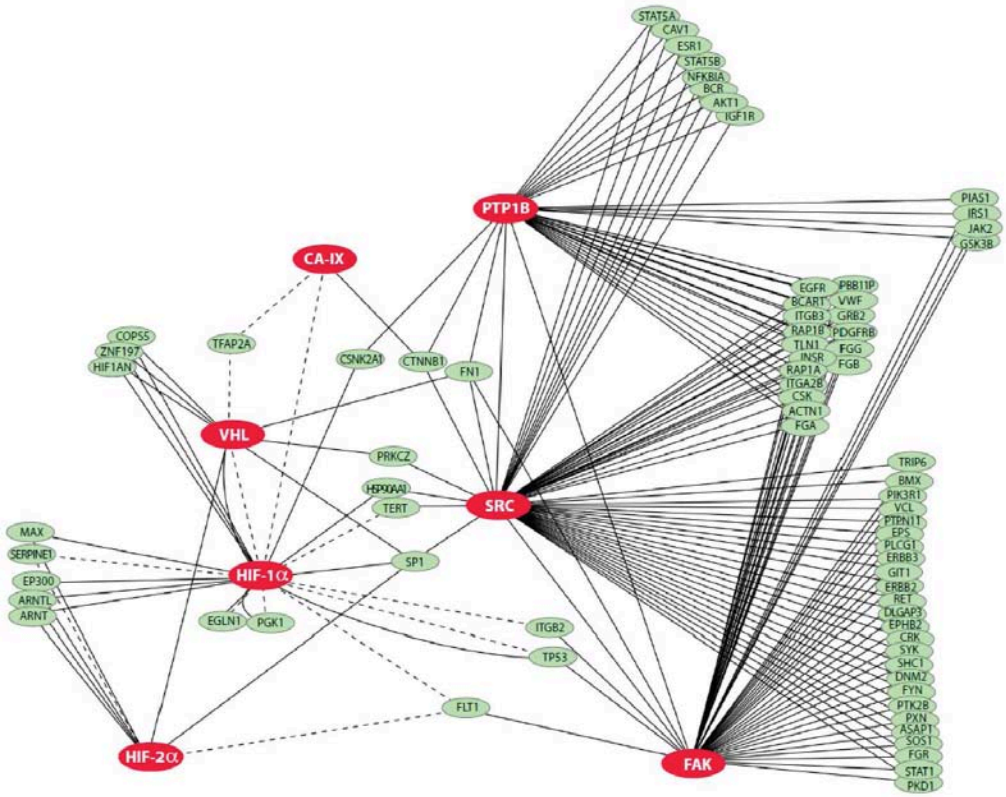

Figure A.19. Analysis of interrelationships among VHL, HIF-α, Src and PTP1B in RCC patients.

ROCK-BCFG network interaction map: Red nodes indicate the markers experimentally analyzed *in vitro* and *in vivo*. Solid lines denote physical interactions and dotted lines denote transcriptional regulation events.

Accession	Protein Name	Protein	pY site	Mean				Standard Deviation			
				SN12C	SN12C+FBS	SN12C shVHL	SN12C shVHL+FBS	SN12C	SN12C+FBS	SN12C shVHL	SN12C shVHL+FBS
P06733	Alpha-enolase	ENO1	Y44	0.98	1.36	0.78	1.14	0.03	0.23	0.05	0.16
Q96RT1	Erbb2-interacting protein	Erbin	Y1104	0.98	0.99	0.60	0.61	0.03	0.08	0.02	0.15
Q86Z02	Homeodomain-interacting protein kinase 1	HIPK1	Y352	1.15	0.74	0.95	0.79	0.21	0.14	0.23	0.06
O14654	Insulin receptor substrate 4	IRS-4	Y921	0.72	0.03	8.85	6.29	0.39	0.00	2.30	1.78
Q86YV5	Tyrosine-protein kinase SgK223	SGK223	Y413	0.96	1.24	0.09	0.17	0.05	0.17	0.04	0.03
P49840	Glycogen synthase kinase-3 alpha	GSK3A	Y279	0.89	0.84	1.11	0.94	0.15	0.08	0.17	0.14
Q16539	Mitogen-activated protein kinase 14	p38-alpha	Y182	1.06	1.05	1.22	4.21	0.09	0.35	0.51	0.28
P27361	Mitogen-activated protein kinase 3	ERK1	Y204	1.04	1.26	0.04	0.31	0.05	0.40	0.05	0.01
P06493	Cyclin-dependent kinase 1	CDK1	Y15	0.99	1.04	0.84	0.94	0.02	0.03	0.04	0.04
Q06124	protein tyrosine phosphatase, non-receptor type 11	SHP-2	Y63	0.92	1.05	0.47	0.30	0.12	0.05	0.04	0.19
Q13627	Dual specificity tyrosine-phosphorylation-regulated kinase 1A	DYRK1A	Y321	0.89	0.73	2.00	1.99	0.15	0.27	0.25	0.15
Q13523	Serine/threonine-protein kinase PRP4 homolog	PRP4	Y849	1.19	1.14	1.81	1.23	0.27	0.33	0.07	0.03
P12931	Proto-oncogene tyrosine-protein kinase Src	SRC	Y419	1.06	1.15	0.41	0.44	0.09	0.02	0.01	0.31
O15357	Phosphatidylinositol-3,4,5-trisphosphate 5-phosphatase 2	SHIP-2	Y886	0.91	1.21	0.20	0.30	0.12	0.14	0.04	0.14
O95297	Myelin protein zero-like protein 1	PZR	Y263	1.02	1.29	1.15	1.13	0.03	0.10	0.40	0.26
P07355	Annexin A2	ANXA2	Y235	0.92	1.04	0.39	0.28	0.11	0.23	0.03	0.03
P28482	Mitogen-activated protein kinase 1	ERK2	Y187	0.90	1.67	0.09	0.23	0.14	0.08	0.02	0.13
P49023	Paxillin	PXN	Y118	0.91	1.31	0.19	0.57	0.13	0.01	0.03	0.10
P56945	Breast cancer anti-estrogen resistance protein 1	P130Cas	Y234	1.07	1.25	1.31	1.56	0.10	0.07	0.68	0.12
O00401	Neural Wiskott-Aldrich syndrome protein	N-WASP	Y256	1.07	1.03	0.66	0.71	0.10	0.27	0.02	0.11
P29317	Ephrin type-A receptor 2	EphA2	Y772	0.90	0.78	0.20	0.18	0.15	0.03	0.04	0.06
P16591	Proto-oncogene tyrosine-protein kinase FER	Fer	Y402	0.93	0.99	0.86	0.73	0.10	0.03	0.12	0.25

Table A.1. Summary of differentially phosphorylated proteins between SN12C and SN12C VHL cells

A

Src	cytoplasm neg/weak N(%)	cytoplasm strong N(%)	total	*P*
membrane neg/weak N(%)	102 (94.4)	6 (6.6)	108 (100)	*0.0185*
membrane strong N(%)	94 (84.7)	17 (15.3)	111 (100)	

B

Variables	**95% CI for RR**	**RR**	*P*
Fuhrman grade	1.228 – 2.177	1.635	*0.001*
Tumor stage (pT1/2 vs pT3/4)	1.616 – 4.158	2.592	*<0.001*
Src cyt/mem (n/n,n/w,w/w,w/n vs n/s,w/s,s/s,s/w,s/n)	1.083 – 2.524	1.654	*0.02*

C

		VHL		
	Strong	Weak	Negative	
Src	N (%)	N (%)	N (%)	
Strong	57 (62)	53 (52)	7 (33)	*P=0.04**
Weak	35 (38)	49 (48)	14 (67)	

Table A.2. Clinicopathological correlations for Src in patients with RCC sampled on tissue microarray (cohort 1).

(A) Association between membranous and cytoplasmic Src expression. Contingency table analysis and Chi Square test. (B) Multivariate analysis with tumor stage, Fuhrman grade, Src cytoplasmic and membranous expression (combined). Cox proportional hazard regression analysis. CI = Confidence interval; RR = Relative risk; n = negative; w = weak; s = strong expression. (C) Correlation between Src and VHL expression in RCC. *Contingency table analysis and Chi-square test. 215 tumor cores from 215 patients.

	Dasatinib (nM)			
	0	**25**	**50**	**100**
SN12C				
VHL-WT				
G_1	52.4	59.5	63.6	70.0
S	30.9	23.9	22.8	16.3
G_2-M	15.4	15.0	11.7	11.7
shVHL				
G_1	45.0	45.2	45.4	46.1
S	35.6	36.9	38.5	35.3
G_2-M	19.1	17.5	15.7	18.5
ACHN				
VHL-WT				
G_1	54.7	59.7	62.1	64.5
S	26.5	25.8	17.6	15.7
G_2-M	16.8	12.6	16.0	14.9
shVHL				
G_1	51.4	50.2	47.6	46.1
S	33.0	37.4	36.7	40.8
G_2-M	13.9	9.8	14.2	10.9

Table A.3. Cell cycle analysis of shVHL lines.

VHL-WT or shVHL SN12C and ACHN cell lines were treated with the indicated concentration of dasatinib, and cell cycle profiles were examined by flow cytometry. Cell population (%) in each cell cycle phase was quantified.

	Dasatinib (nM)			
	0	**25**	**50**	**100**
SN12C				
HIF-1α				
G_1	58.3	60.1	59.2	60.4
S	26.7	25.1	27.6	26.5
G_2-M	13.3	13.3	11.4	11.1
HIF-2α				
G_1	56.4	54.8	55.7	49.7
S	20.9	23.6	21.4	27.8
G_2-M	21.5	20.6	22.1	21.3
ACHN				
HIF-1α				
G_1	57.3	59.2	56.4	60.1
S	21.6	21.6	25.1	17.6
G_2-M	17.7	17.1	16.0	22.0
HIF-2α				
G_1	59.4	53.9	51.9	55.3
S	20.8	27.7	27.0	24.2
G_2-M	17.5	16.1	19.3	17.7

Table A.4. Cell cycle analyses of HIF-α mutant cell lines.

Cell cycle profiles of SN12C and ACHN cells expressing constitutively stable HIF-1α–P564A (HIF-1α) or HIF-2α–P405A, P853A (HIF-2α) mutants were analyzed by flow cytometry 48 hours after treatment with dasatinib. Cell population (%) in each cell cycle phase was quantified.

		VHL		
	Strong	Weak	Negative	
Src	N (%)	N (%)	N (%)	
Strong	69 (58)	49 (45)	1 (8)	*P =0.0018*
Weak	50 (42)	61 (55)	11 (92)	

Table A.5. Correlation between Src and VHL expression in patients with RCC sampled on tissue microarray (cohort 2).

*Contingency table analysis and Chi-square test. 262 tumor cores from 131 patients Numbers may not add up to 262 because of missing cores

Outcome and covariates	Estimated coefficient	95% CI	*P*
Src			
VHL	0.146	0.096 to 0.196	2.55×10^{-8}
PTP1B	0.257	0.155 to 0.359	1.20×10^{-6}
Intercept	2.382	1.987 to 2.778	$<2 \times 10^{-16}$
PTP1B			
VHL	0.164	0.104 to 0.225	2.11×10^{-7}
HIF-2α	−0.228	−0.373 to −0.084	0.00211
Intercept	4.298	3.796 to 4.800	$<2 \times 10^{-16}$

Table A.6. Multiple linear regression.

Coefficient estimates for two predefined models PTP1B and Src. All variables have been log-transformed. CI, confidence interval.

APPENDIX B. Preliminary and Supplementary Data

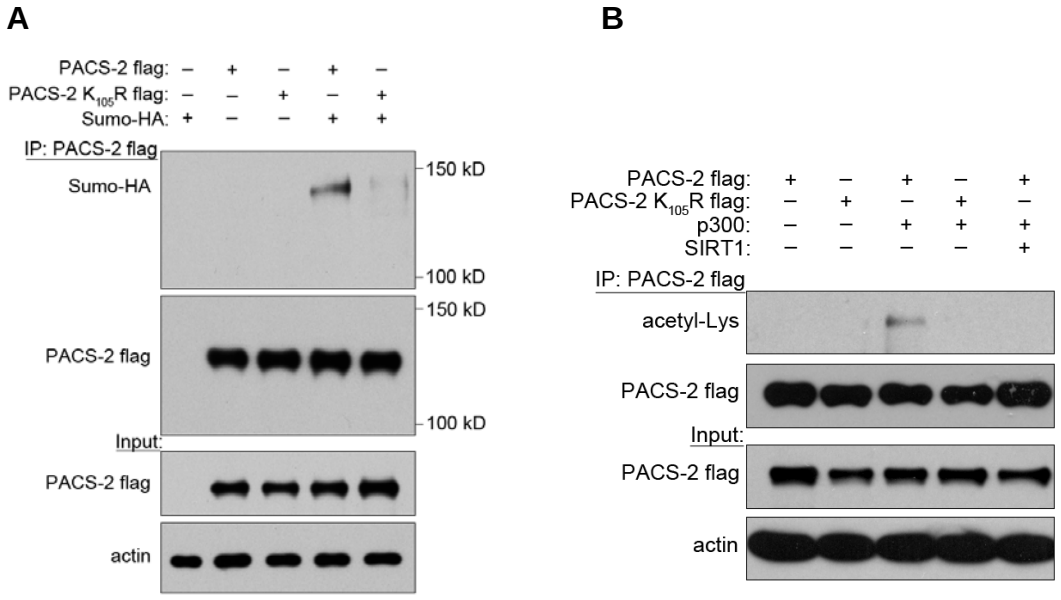

Figure B.1. PACS-2 is sumoylated and acetylated at Lys$_{105}$.

(A) U2OS cells were cotransfected with PACS-2 flag or PACS-2 K_{105}→R flag and Sumo-HA. PACS-2 flag was immunoprecipitated and Sumo-HA was detected by western blot. (B) U2OS cells were cotransfected with PACS-2 flag or PACS-2 K_{105}→R flag, p300, and SIRT1 as indicated. PACS-2 flag was immunoprecipitated and the amount of acetylated PACS-2 was detected by western using acetyl lysine antibody.

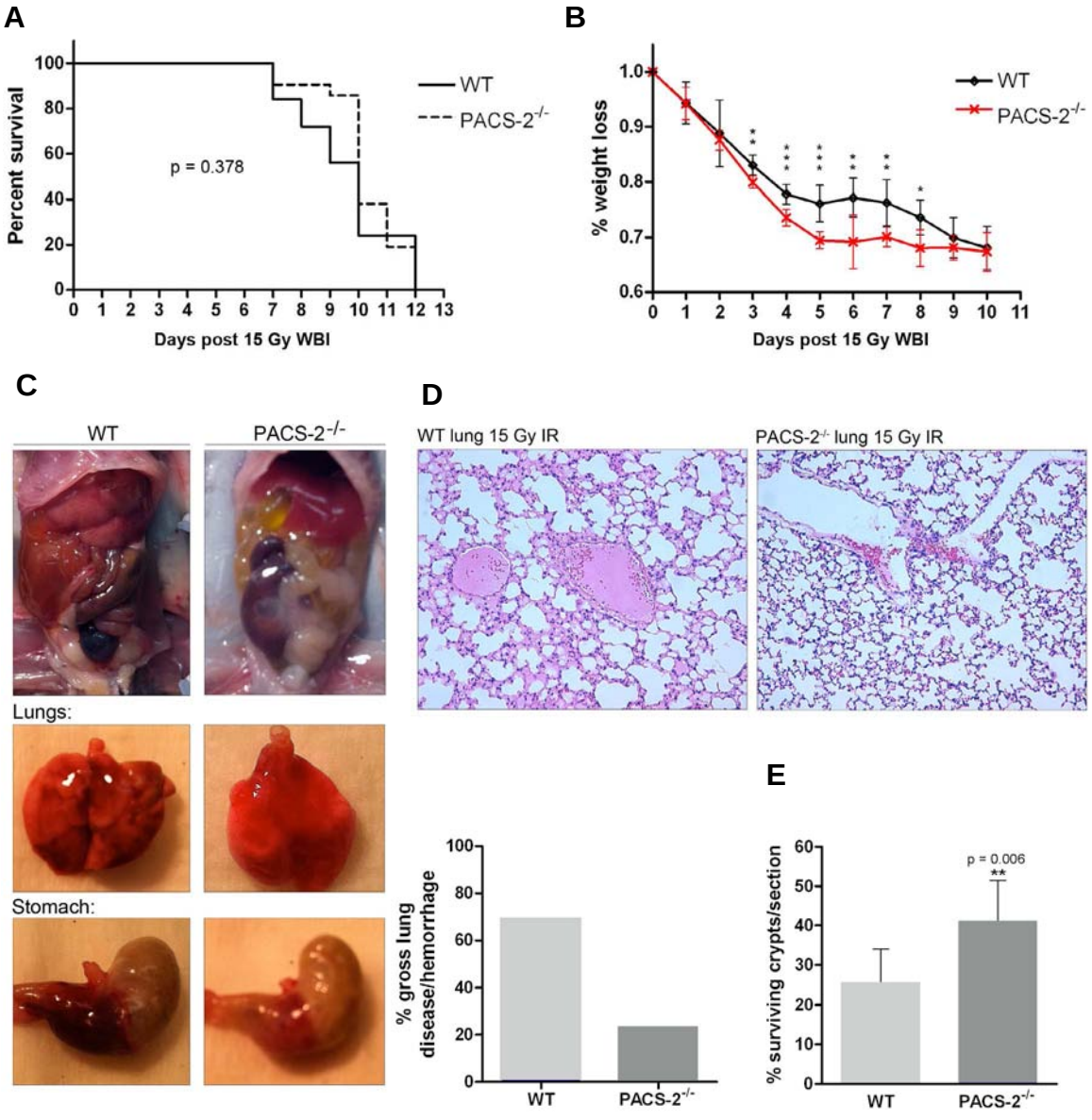

Figure B.2. Survival analysis of wild-type and *Pacs2*$^{-/-}$ mice following 15 Gy whole body irradiation.

(A) Wilde-type (WT) (n = 25) and *Pacs2*$^{-/-}$ (n = 21) mice were exposed to 15 Gy whole body irradiation (WBI) and analyzed for overall survival by the Kaplan Meier method and statistical significance determined using the log-rank test. (B)

Weights were recorded daily from male mice and calculated as a percentage of total body weight lost. Error bars represent mean ± SD. Statistical significance determined using a two-sided t-test. (C) Left, representative autopsy photos of WT and *Pacs2*$^{-/-}$ mice following 15 Gy WBI. Right, graphical representation of the occurrence of gross lung disease and hemorrhage from 29 autopsied mice (11/16 WT, 3/13 *Pacs2*$^{-/-}$). (D) Lungs from autopsied mice exposed to 15 Gy WBI were processed for hematoxylin & eosin (H&E) staining. (E) Surviving crypts from the small intestine of WT and *Pacs2*$^{-/-}$ mice were analyzed 3.5 days following 15 Gy WBI using the crypt microcolony survival assay. Error bars represent mean ± SD. Statistical significance determined using a two-sided t-test.

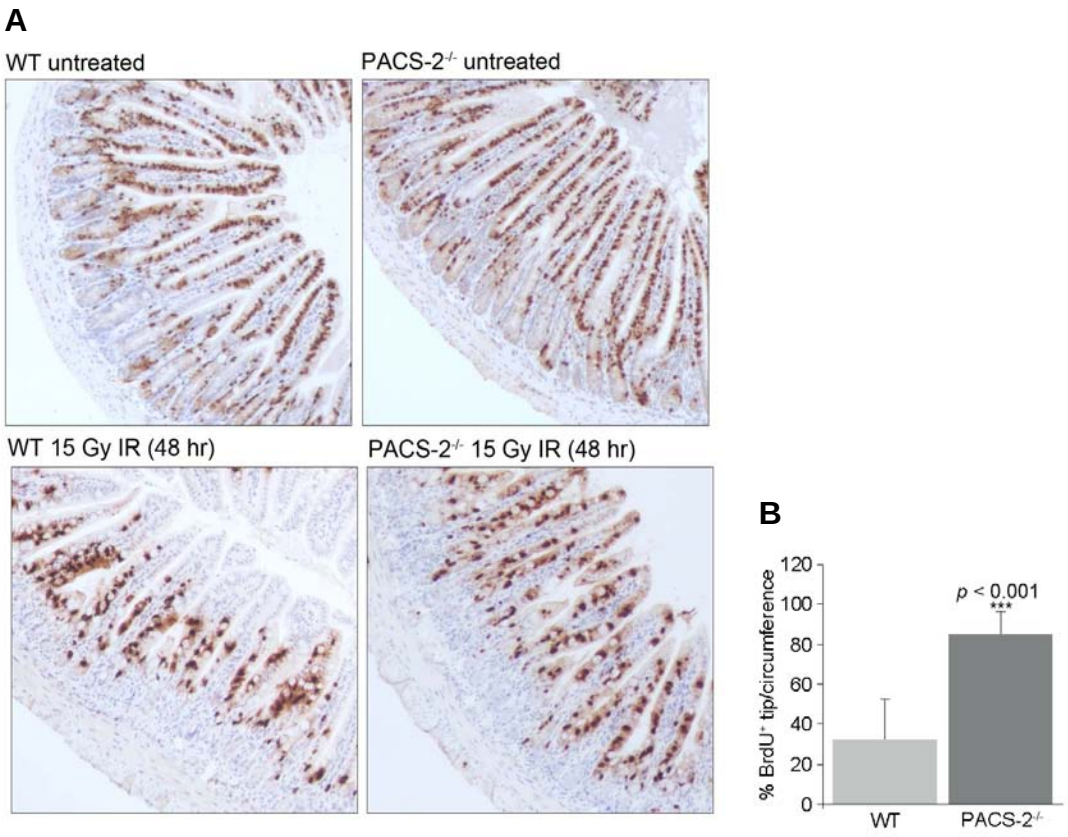

Figure B.3. Migration of BrdU$^+$ cells along the crypt-villus axis following IR.

(A) WT and *Pacs2*$^{-/-}$ mice were injected with 50 mg/kg BrdU and immediately exposed to 15 Gy WBI or left untreated. 48 hours following BrdU injection, small intestine was dissected and a 3 cm segment of ileum just proximal to the cecum was processed for IHC using anti-BrdU antibody. (B) The number of villi with BrdU$^+$ cells reaching the upper 1/4th of the villus were counted and presented as the mean percentage of BrdU$^+$ villus tips per circumference (or cross-section). Error bars represent mean ± SD. Statistical significance determined using a two-sided t-test. Quantification from untreated mice was not depicted, as all villi from untreated mice (both WT and *Pacs2*$^{-/-}$) had Brdu$^+$ cells at the villus tips.

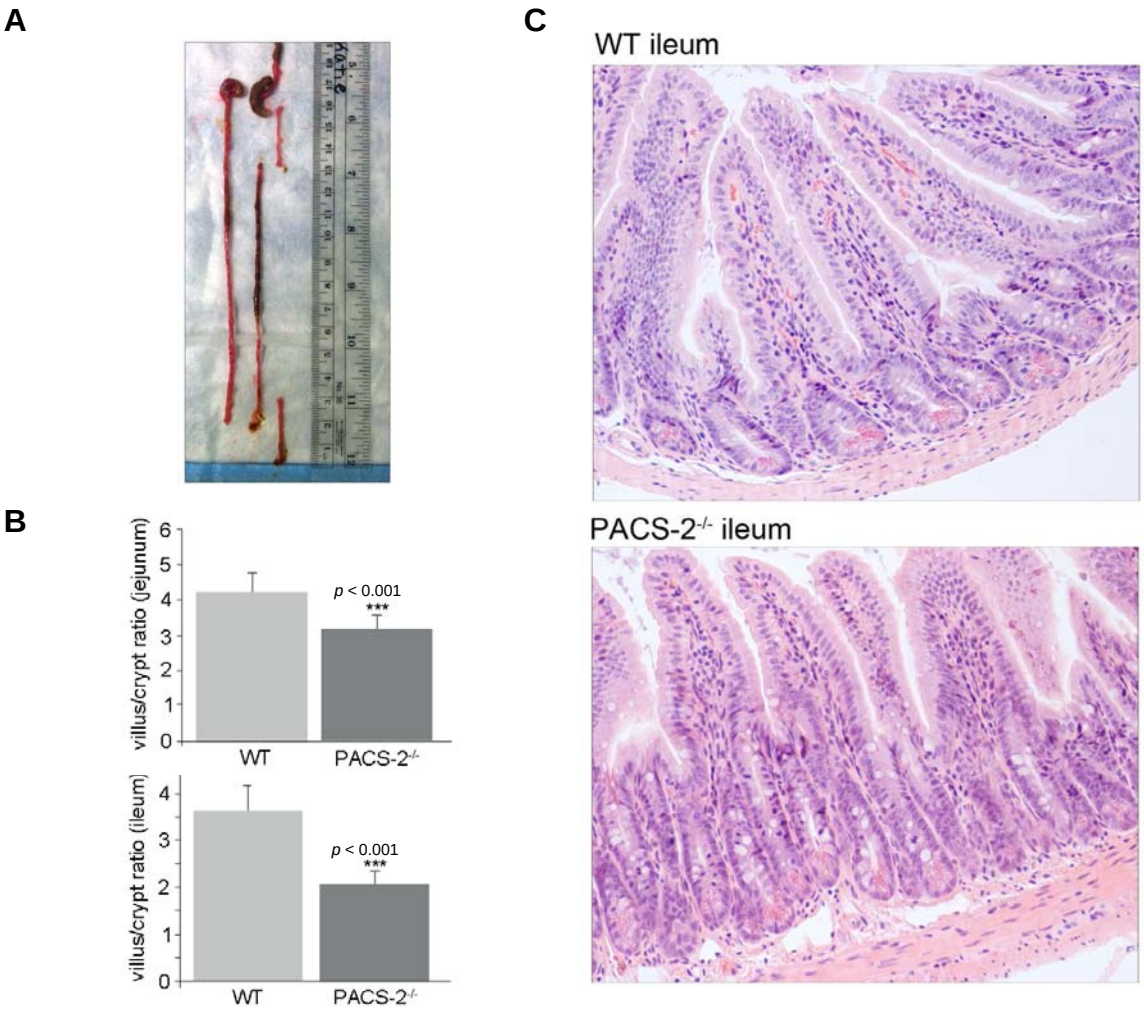

B.4. Analysis of villus-crypt ratio in WT and *Pacs2*$^{-/-}$ mice.

(A) 10 week old male WT and *Pacs2*$^{-/-}$ mice were sacrificed and 3 cm segments of ileum (just proximal to cecum) and jejunum (mid-way between stomach and cecum) were processed for H&E. (B) Ratio of villus height to crypt depth was quantified from ≧ 100 villi per genotype from n = 4 mice. Error bars represent mean ± SEM. Statistical significance determined using a two-sided t-test. Upper, jejunum. Lower, ileum. (C) Representative images from ileum.

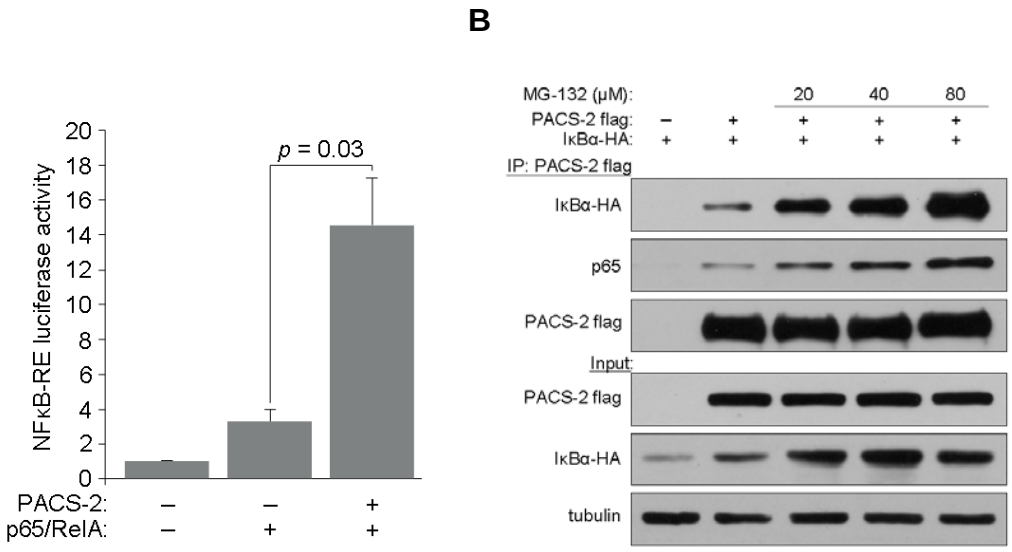

Figure B.5. PACS-2 promotes NF-κB transcriptional activity and interacts with p65 and IκBα.

(A) HCT116 cells were cotransfected with plasmids encoding the NF-κB response element (RE) (firefly luciferase) and thymidine kinase (renilla luciferase) together with PACS-2-HA and the NF-κB subunit p65/RelA as indicated. The relative luciferase activity was determined by the ratio of firefly to renilla. Error bars represent mean ± SD. Statistical significance determined using a two-sided t-test. (B) HCT116 cells were cotransfected with PACS-2 flag and Inhibitor of κB-α (IκBα)-HA and treated with MG-132 for 6 hours. PACS-2 flag was immunoprecipitated and coimmunoprecipitating IκBα-HA and endogenous p65 was detected by western blot.

REFERENCES

Abbas, T. and Dutta, A. (2009). P21 in Cancer: Intricate Networks and Multiple Activities. *Nature reviews.Cancer* **9,** 400-414.

Abdelmohsen, K., Pullmann, R., Jr., Lal, A., Kim, H.H., Galban, S., Yang, X.*, et al.* (2007). Phosphorylation of HuR by Chk2 regulates SIRT1 expression. *Mol Cell* **25,** 543-557.

Abida, W.M., Nikolaev, A., Zhao, W., Zhang, W. and Gu, W. (2007). FBXO11 promotes the Neddylation of p53 and inhibits its transcriptional activity. *J Biol Chem* **282,** 1797-1804.

Achleitner, G., Gaigg, B., Krasser, A., Kainersdorfer, E., Kohlwein, S.D., Perktold, A.*, et al.* (1999). Association between the endoplasmic reticulum and mitochondria of yeast facilitates interorganelle transport of phospholipids through membrane contact. *European journal of biochemistry / FEBS* **264,** 545-553.

Adams, E.J. and Parham, P. (2001). Species-specific evolution of MHC class I genes in the higher primates. *Immunological reviews* **183,** 41-64.

Adamson, C.S. and Freed, E.O. (2007). Human immunodeficiency virus type 1 assembly, release, and maturation. *Adv Pharmacol* **55,** 347-387.

Agopian, K., Wei, B.L., Garcia, J.V. and Gabuzda, D. (2007). CD4 and MHC-I downregulation are conserved in primary HIV-1 Nef alleles from brain and lymphoid tissues, but Pak2 activation is highly variable. *Virology* **358,** 119-135.

Ahn, K., Angulo, A., Ghazal, P., Peterson, P.A., Yang, Y. and Fruh, K. (1996). Human cytomegalovirus inhibits antigen presentation by a sequential multistep process. *Proc Natl Acad Sci U S A* **93,** 10990-10995.

Aiken, C., Konner, J., Landau, N.R., Lenburg, M.E. and Trono, D. (1994). Nef induces CD4 endocytosis: requirement for a critical dileucine motif in the membrane-proximal CD4 cytoplasmic domain. *Cell* **76,** 853-864.

Akari, H., Arold, S., Fukumori, T., Okazaki, T., Strebel, K. and Adachi, A. (2000). Nef-induced major histocompatibility complex class I down-regulation is functionally dissociated from its virion incorporation, enhancement of viral infectivity, and CD4 down-regulation. *Journal of virology* **74,** 2907-2912.

Alexaki, A., Liu, Y. and Wigdahl, B. (2008). Cellular reservoirs of HIV-1 and their role in viral persistence. *Current HIV research* **6,** 388-400.

Allende-Vega, N., Sparks, A., Lane, D.P. and Saville, M.K. (2010). MdmX is a substrate for the deubiquitinating enzyme USP2a. *Oncogene* **29,** 432-441.

An, W., Kim, J. and Roeder, R.G. (2004). Ordered cooperative functions of PRMT1, p300, and CARM1 in transcriptional activation by p53. *Cell* **117,** 735-748.

Anderson, G.R., Brenner, B.M., Swede, H., Chen, N., Henry, W.M., Conroy, J.M.*, et al.* (2001). Intrachromosomal genomic instability in human sporadic

colorectal cancer measured by genome-wide allelotyping and inter-(simple sequence repeat) PCR. *Cancer research* **61,** 8274-8283.

Anderson, M.E., Woelker, B., Reed, M., Wang, P. and Tegtmeyer, P. (1997). Reciprocal interference between the sequence-specific core and nonspecific C-terminal DNA binding domains of p53: implications for regulation. *Mol Cell Biol* **17,** 6255-6264.

Anderson, S.J., Lenburg, M., Landau, N.R. and Garcia, J.V. (1994). The cytoplasmic domain of CD4 is sufficient for its down-regulation from the cell surface by human immunodeficiency virus type 1 Nef. *Journal of virology* **68,** 3092-3101.

Appella, E. and Anderson, C.W. (2001). Post-translational modifications and activation of p53 by genotoxic stresses. *European journal of biochemistry / FEBS* **268,** 2764-2772.

Arhel, N.J. and Kirchhoff, F. (2009). Implications of Nef: host cell interactions in viral persistence and progression to AIDS. *Current topics in microbiology and immunology* **339,** 147-175.

Arien, K.K. and Verhasselt, B. (2008). HIV Nef: role in pathogenesis and viral fitness. *Current HIV research* **6,** 200-208.

Arold, S., Franken, P., Strub, M.P., Hoh, F., Benichou, S., Benarous, R. and Dumas, C. (1997). The crystal structure of HIV-1 Nef protein bound to the Fyn kinase SH3 domain suggests a role for this complex in altered T cell receptor signaling. *Structure* **5,** 1361-1372.

Arold, S., Hoh, F., Domergue, S., Birck, C., Delsuc, M.A., Jullien, M. and Dumas, C. (2000). Characterization and molecular basis of the oligomeric structure of HIV-1 nef protein. *Protein science : a publication of the Protein Society* **9,** 1137-1148.

Ashcroft, M., Kubbutat, M.H. and Vousden, K.H. (1999). Regulation of p53 function and stability by phosphorylation. *Mol Cell Biol* **19,** 1751-1758.

Ashcroft, M., Taya, Y. and Vousden, K.H. (2000). Stress signals utilize multiple pathways to stabilize p53. *Mol Cell Biol* **20,** 3224-3233.

Asher, G., Gatfield, D., Stratmann, M., Reinke, H., Dibner, C., Kreppel, F.*, et al.* (2008). SIRT1 regulates circadian clock gene expression through PER2 deacetylation. *Cell* **134,** 317-328.

Aslan, J.E., You, H., Williamson, D.M., Endig, J., Youker, R.T., Thomas, L.*, et al.* (2009). Akt and 14-3-3 control a PACS-2 homeostatic switch that integrates membrane traffic with TRAIL-induced apoptosis. *Molecular cell* **34,** 497-509.

Astoul, E., Edmunds, C., Cantrell, D.A. and Ward, S.G. (2001). PI 3-K and T-cell activation: limitations of T-leukemic cell lines as signaling models. *Trends in immunology* **22,** 490-496.

Atkins, K.M., Thomas, L., Youker, R.T., Harriff, M.J., Pissani, F., You, H. and Thomas, G. (2008). HIV-1 Nef binds PACS-2 to assemble a multikinase cascade that triggers major histocompatibility complex class I (MHC-I)

down-regulation: analysis using short interfering RNA and knock-out mice. *J Biol Chem* **283,** 11772-11784.

AVERT. (2011). AVERTing HIV and AIDS. HIV & AIDS statistics from around the world. [WWW document]. URL http://www.avert.org/aids-statistics.htm

Baker, S.J., Fearon, E.R., Nigro, J.M., Hamilton, S.R., Preisinger, A.C., Jessup, J.M.*, et al.* (1989). Chromosome 17 deletions and p53 gene mutations in colorectal carcinomas. *Science* **244,** 217-221.

Balotta, C., Bagnarelli, P., Riva, C., Valenza, A., Antinori, S., Colombo, M.C.*, et al.* (1997). Comparable biological and molecular determinants in HIV type 1-infected long-term nonprogressors and recently infected individuals. *AIDS research and human retroviruses* **13,** 337-341.

Bamshad, M.J., Mummidi, S., Gonzalez, E., Ahuja, S.S., Dunn, D.M., Watkins, W.S.*, et al.* (2002). A strong signature of balancing selection in the 5' cis-regulatory region of CCR5. *Proc Natl Acad Sci U S A* **99,** 10539-10544.

Bando, T., Kato, Y., Ihara, Y., Yamagishi, F., Tsukada, K. and Isobe, M. (1999). Loss of heterozygosity of 14q32 in colorectal carcinoma. *Cancer Genet Cytogenet* **111,** 161-165.

Banks, A.S., Kon, N., Knight, C., Matsumoto, M., Gutierrez-Juarez, R., Rossetti, L.*, et al.* (2008). SirT1 gain of function increases energy efficiency and prevents diabetes in mice. *Cell metabolism* **8,** 333-341.

Barboza, J.A., Liu, G., Ju, Z., El-Naggar, A.K. and Lozano, G. (2006). P21 Delays Tumor Onset by Preservation of Chromosomal Stability. *Proceedings of the National Academy of Sciences of the United States of America* **103,** 19842-19847.

Bargonetti, J., Friedman, P.N., Kern, S.E., Vogelstein, B. and Prives, C. (1991). Wild-type but not mutant p53 immunopurified proteins bind to sequences adjacent to the SV40 origin of replication. *Cell* **65,** 1083-1091.

Barisoni, L., Bruggeman, L.A., Mundel, P., D'Agati, V.D. and Klotman, P.E. (2000a). HIV-1 induces renal epithelial dedifferentiation in a transgenic model of HIV-associated nephropathy. *Kidney international* **58,** 173-181.

Barisoni, L., Kriz, W., Mundel, P. and D'Agati, V. (1999). The dysregulated podocyte phenotype: a novel concept in the pathogenesis of collapsing idiopathic focal segmental glomerulosclerosis and HIV-associated nephropathy. *Journal of the American Society of Nephrology : JASN* **10,** 51-61.

Barisoni, L., Mokrzycki, M., Sablay, L., Nagata, M., Yamase, H. and Mundel, P. (2000b). Podocyte cell cycle regulation and proliferation in collapsing glomerulopathies. *Kidney international* **58,** 137-143.

Barre-Sinoussi, F., Chermann, J.C., Rey, F., Nugeyre, M.T., Chamaret, S., Gruest, J.*, et al.* (1983). Isolation of a T-lymphotropic retrovirus from a patient at risk for acquired immune deficiency syndrome (AIDS). *Science* **220,** 868-871.

Bartek, J., Lukas, C. and Lukas, J. (2004). Checking on DNA damage in S phase. *Nature reviews. Molecular cell biology* **5,** 792-804.

Bartos, J.D., Gaile, D.P., McQuaid, D.E., Conroy, J.M., Darbary, H., Nowak, N.J., *et al.* (2007). aCGH local copy number aberrations associated with overall copy number genomic instability in colorectal cancer: coordinate involvement of the regions including BCR and ABL. *Mutation research* **615,** 1-11.

Bell, I., Schaefer, T.M., Trible, R.P., Amedee, A. and Reinhart, T.A. (2001). Down-modulation of the costimulatory molecule, CD28, is a conserved activity of multiple SIV Nefs and is dependent on histidine 196 of Nef. *Virology* **283,** 148-158.

Bellet, M.M. and Sassone-Corsi, P. (2010). Mammalian circadian clock and metabolism - the epigenetic link. *J Cell Sci* **123,** 3837-3848.

Belzile, J.P., Duisit, G., Rougeau, N., Mercier, J., Finzi, A. and Cohen, E.A. (2007). HIV-1 Vpr-mediated G2 arrest involves the DDB1-CUL4AVPRBP E3 ubiquitin ligase. *PLoS pathogens* **3,** e85.

Benson, R.E., Sanfridson, A., Ottinger, J.S., Doyle, C. and Cullen, B.R. (1993). Downregulation of cell-surface CD4 expression by simian immunodeficiency virus Nef prevents viral super infection. *The Journal of experimental medicine* **177,** 1561-1566.

Berger, S.L. (2010). Keeping p53 in check: a high-stakes balancing act. *Cell* **142,** 17-19.

Berke, G. (1995). The CTL's kiss of death. *Cell* **81,** 9-12.

Berridge, M.J. (2002). The endoplasmic reticulum: a multifunctional signaling organelle. *Cell calcium* **32,** 235-249.

Betzi, S., Restouin, A., Opi, S., Arold, S.T., Parrot, I., Guerlesquin, F*., et al.* (2007). Protein protein interaction inhibition (2P2I) combining high throughput and virtual screening: Application to the HIV-1 Nef protein. *Proc Natl Acad Sci U S A* **104,** 19256-19261.

Blagoveshchenskaya, A.D., Thomas, L., Feliciangeli, S.F., Hung, C.H. and Thomas, G. (2002). HIV-1 Nef downregulates MHC-I by a PACS-1- and PI3K-regulated ARF6 endocytic pathway. *Cell* **111,** 853-866.

Blais, M.E., Dong, T. and Rowland-Jones, S. (2011). HLA-C as a mediator of natural killer and T-cell activation: spectator or key player? *Immunology* **133,** 1-7.

Blander, G., Olejnik, J., Krzymanska-Olejnik, E., McDonagh, T., Haigis, M., Yaffe, M.B. and Guarente, L. (2005). SIRT1 shows no substrate specificity in vitro. *J Biol Chem* **280,** 9780-9785.

Blattner, C., Tobiasch, E., Litfen, M., Rahmsdorf, H.J. and Herrlich, P. (1999). DNA damage induced p53 stabilization: no indication for an involvement of p53 phosphorylation. *Oncogene* **18,** 1723-1732.

Boehm, M. and Bonifacino, J.S. (2001). Adaptins: the final recount. *Mol Biol Cell* **12,** 2907-2920.

Boerner, R.J., Kassel, D.B., Barker, S.C., Ellis, B., DeLacy, P. and Knight, W.B. (1996). Correlation of the phosphorylation states of pp60c-src with

tyrosine kinase activity: the intramolecular pY530-SH2 complex retains significant activity if Y419 is phosphorylated. *Biochemistry* **35,** 9519-9525.
Bogerd, H.P. and Cullen, B.R. (2008). Single-stranded RNA facilitates nucleocapsid: APOBEC3G complex formation. *RNA* **14,** 1228-1236.
Bonifacino, J.S. and Glick, B.S. (2004). The mechanisms of vesicle budding and fusion. *Cell* **116,** 153-166.
Bonifacino, J.S. and Traub, L.M. (2003). Signals for sorting of transmembrane proteins to endosomes and lysosomes. *Annual review of biochemistry* **72,** 395-447.
Bonsib, S.M. (2009). Renal cystic diseases and renal neoplasms: a mini-review. *Clinical journal of the American Society of Nephrology : CJASN* **4,** 1998-2007.
Bosque, A. and Planelles, V. (2009). Induction of HIV-1 latency and reactivation in primary memory CD4+ T cells. *Blood* **113,** 58-65.
Bouard, D., Sandrin, V., Boson, B., Negre, D., Thomas, G., Granier, C. and Cosset, F.L. (2007). An acidic cluster of the cytoplasmic tail of the RD114 virus glycoprotein controls assembly of retroviral envelopes. *Traffic* **8,** 835-847.
Bouras, T., Fu, M., Sauve, A.A., Wang, F., Quong, A.A., Perkins, N.D*., et al.* (2005). SIRT1 deacetylation and repression of p300 involves lysine residues 1020/1024 within the cell cycle regulatory domain 1. *J Biol Chem* **280,** 10264-10276.
Boya, P., Andreau, K., Poncet, D., Zamzami, N., Perfettini, J.L., Metivier, D*., et al.* (2003a). Lysosomal membrane permeabilization induces cell death in a mitochondrion-dependent fashion. *The Journal of experimental medicine* **197,** 1323-1334.
Boya, P., Gonzalez-Polo, R.A., Poncet, D., Andreau, K., Vieira, H.L., Roumier, T*., et al.* (2003b). Mitochondrial membrane permeabilization is a critical step of lysosome-initiated apoptosis induced by hydroxychloroquine. *Oncogene* **22,** 3927-3936.
Braunstein, M., Rose, A.B., Holmes, S.G., Allis, C.D. and Broach, J.R. (1993). Transcriptional silencing in yeast is associated with reduced nucleosome acetylation. *Genes Dev* **7,** 592-604.
Braunstein, M., Sobel, R.E., Allis, C.D., Turner, B.M. and Broach, J.R. (1996). Efficient transcriptional silencing in Saccharomyces cerevisiae requires a heterochromatin histone acetylation pattern. *Mol Cell Biol* **16,** 4349-4356.
Breckenridge, D.G., Stojanovic, M., Marcellus, R.C. and Shore, G.C. (2003). Caspase cleavage product of BAP31 induces mitochondrial fission through endoplasmic reticulum calcium signals, enhancing cytochrome c release to the cytosol. *J Cell Biol* **160,** 1115-1127.
Briant, L. (2011). HIV-1 Assembly, Release and Maturation. *World Journal of AIDS* **01,** 111-130.

Brodsky, M.H., Nordstrom, W., Tsang, G., Kwan, E., Rubin, G.M. and Abrams, J.M. (2000). Drosophila p53 binds a damage response element at the reaper locus. *Cell* **101,** 103-113.

Brooks, C.L. and Gu, W. (2003). Ubiquitination, phosphorylation and acetylation: the molecular basis for p53 regulation. *Current opinion in cell biology* **15,** 164-171.

Brooks, C.L. and Gu, W. (2006). p53 ubiquitination: Mdm2 and beyond. *Mol Cell* **21,** 307-315.

Brooks, C.L. and Gu, W. (2011). The impact of acetylation and deacetylation on the p53 pathway. *Protein & cell* **2,** 456-462.

Buettner, R., Mesa, T., Vultur, A., Lee, F. and Jove, R. (2008). Inhibition of Src family kinases with dasatinib blocks migration and invasion of human melanoma cells. *Mol Cancer Res* **6,** 1766-1774.

Brugarolas, J., Chandrasekaran, C., Gordon, J.I., Beach, D., Jacks, T. and Hannon, G.J. (1995). Radiation-induced cell cycle arrest compromised by p21 deficiency. *Nature* **377,** 552-557.

Bruggeman, L.A., Ross, M.D., Tanji, N., Cara, A., Dikman, S., Gordon, R.E.*, et al.* (2000). Renal epithelium is a previously unrecognized site of HIV-1 infection. *Journal of the American Society of Nephrology : JASN* **11,** 2079-2087.

Brunet, A., Sweeney, L.B., Sturgill, J.F., Chua, K.F., Greer, P.L., Lin, Y.*, et al.* (2004). Stress-dependent regulation of FOXO transcription factors by the SIRT1 deacetylase. *Science* **303,** 2011-2015.

Bryk, M., Banerjee, M., Murphy, M., Knudsen, K.E., Garfinkel, D.J. and Curcio, M.J. (1997). Transcriptional silencing of Ty1 elements in the RDN1 locus of yeast. *Genes Dev* **11,** 255-269.

Bukholm, I.K. and Nesland, J.M. (2000). Protein expression of p53, p21 (WAF1/CIP1), bcl-2, Bax, cyclin D1 and pRb in human colon carcinomas. *Virchows Archiv : an international journal of pathology* **436,** 224-228.

Bunnik, E.M., Swenson, L.C., Edo-Matas, D., Huang, W., Dong, W., Frantzell, A.*, et al.* (2011). Detection of inferred CCR5- and CXCR4-using HIV-1 variants and evolutionary intermediates using ultra-deep pyrosequencing. *PLoS pathogens* **7,** e1002106.

Bunz, F., Dutriaux, A., Lengauer, C., Waldman, T., Zhou, S., Brown, J.P.*, et al.* (1998). Requirement for p53 and p21 to sustain G2 arrest after DNA damage. *Science (New York, N.Y.)* **282,** 1497-1501.

Burgos, P.V., Mardones, G.A., Rojas, A.L., daSilva, L.L., Prabhu, Y., Hurley, J.H. and Bonifacino, J.S. (2010). Sorting of the Alzheimer's disease amyloid precursor protein mediated by the AP-4 complex. *Developmental cell* **18,** 425-436.

Burtey, A., Rappoport, J.Z., Bouchet, J., Basmaciogullari, S., Guatelli, J., Simon, S.M.*, et al.* (2007). Dynamic interaction of HIV-1 Nef with the clathrin-mediated endocytic pathway at the plasma membrane. *Traffic* **8,** 61-76.

Cai, H., Reinisch, K. and Ferro-Novick, S. (2007). Coats, tethers, Rabs, and SNAREs work together to mediate the intracellular destination of a transport vesicle. *Developmental cell* **12,** 671-682.

Cai, Y., Maeda, Y., Cedzich, A., Torres, V.E., Wu, G., Hayashi, T*., et al.* (1999). Identification and characterization of polycystin-2, the PKD2 gene product. *J Biol Chem* **274,** 28557-28565.

Cain, C., Miller, S., Ahn, J. and Prives, C. (2000). The N terminus of p53 regulates its dissociation from DNA. *J Biol Chem* **275,** 39944-39953.

Canbay, A., Guicciardi, M.E., Higuchi, H., Feldstein, A., Bronk, S.F., Rydzewski, R*., et al.* (2003). Cathepsin B inactivation attenuates hepatic injury and fibrosis during cholestasis. *J Clin Invest* **112,** 152-159.

Caplan, S., Naslavsky, N., Hartnell, L.M., Lodge, R., Polishchuk, R.S., Donaldson, J.G. and Bonifacino, J.S. (2002). A tubular EHD1-containing compartment involved in the recycling of major histocompatibility complex class I molecules to the plasma membrane. *EMBO J* **21,** 2557-2567.

Caron de Fromentel, C. and Soussi, T. (1992). TP53 tumor suppressor gene: a model for investigating human mutagenesis. *Genes Chromosomes Cancer* **4,** 1-15.

Carrington, M., Dean, M., Martin, M.P. and O'Brien, S.J. (1999). Genetics of HIV-1 infection: chemokine receptor CCR5 polymorphism and its consequences. *Human molecular genetics* **8,** 1939-1945.

Carrington, M., Kissner, T., Gerrard, B., Ivanov, S., O'Brien, S.J. and Dean, M. (1997). Novel alleles of the chemokine-receptor gene CCR5. *American journal of human genetics* **61,** 1261-1267.

Carter, S., Bischof, O., Dejean, A. and Vousden, K.H. (2007). C-terminal modifications regulate MDM2 dissociation and nuclear export of p53. *Nat Cell Biol* **9,** 428-435.

Casartelli, N., Giolo, G., Neri, F., Haller, C., Potesta, M., Rossi, P*., et al.* (2006). The Pro78 residue regulates the capacity of the human immunodeficiency virus type 1 Nef protein to inhibit recycling of major histocompatibility complex class I molecules in an SH3-independent manner. *The Journal of general virology* **87,** 2291-2296.

Cawley, S., Bekiranov, S., Ng, H.H., Kapranov, P., Sekinger, E.A., Kampa, D*., et al.* (2004). Unbiased mapping of transcription factor binding sites along human chromosomes 21 and 22 points to widespread regulation of noncoding RNAs. *Cell* **116,** 499-509.

Cazzalini, O., Scovassi, A.I., Savio, M., Stivala, L.A. and Prosperi, E. (2010). Multiple roles of the cell cycle inhibitor p21(CDKN1A) in the DNA damage response. *Mutat Res* **704,** 12-20.

CDC (2011) HIV in the United States. V.H. National Center for HIV/AIDS, STD, and TB Prevention, Division of HIV/AIDS Prevention (ed.).

Cen, Y., Youn, D.Y. and Sauve, A.A. (2011). Advances in characterization of human sirtuin isoforms: chemistries, targets and therapeutic applications. *Current medicinal chemistry* **18,** 1919-1935.

Chan, D.A., Sutphin, P.D., Denko, N.C. and Giaccia, A.J. (2002). Role of prolyl hydroxylation in oncogenically stabilized hypoxia-inducible factor-1alpha. *J Biol Chem* **277,** 40112-40117.

Chan, H.M. and La Thangue, N.B. (2001). p300/CBP proteins: HATs for transcriptional bridges and scaffolds. *J Cell Sci* **114,** 2363-2373.

Chang, T.C., Wentzel, E.A., Kent, O.A., Ramachandran, K., Mullendore, M., Lee, K.H.*, et al.* (2007). Transactivation of miR-34a by p53 broadly influences gene expression and promotes apoptosis. *Mol Cell* **26,** 745-752.

Chang, Y., Cesarman, E., Pessin, M.S., Lee, F., Culpepper, J., Knowles, D.M. and Moore, P.S. (1994). Identification of herpesvirus-like DNA sequences in AIDS-associated Kaposi's sarcoma. *Science* **266,** 1865-1869.

Chao, C., Hergenhahn, M., Kaeser, M.D., Wu, Z., Saito, S., Iggo, R.*, et al.* (2003). Cell type- and promoter-specific roles of Ser18 phosphorylation in regulating p53 responses. *J Biol Chem* **278,** 41028-41033.

Chao, C., Herr, D., Chun, J. and Xu, Y. (2006). Ser18 and 23 phosphorylation is required for p53-dependent apoptosis and tumor suppression. *EMBO J* **25,** 2615-2622.

Chaudhry, A., Das, S.R., Jameel, S., George, A., Bal, V., Mayor, S. and Rath, S. (2008). HIV-1 Nef induces a Rab11-dependent routing of endocytosed immune costimulatory proteins CD80 and CD86 to the Golgi. *Traffic* **9,** 1925-1935.

Chaudhuri, R., Lindwasser, O.W., Smith, W.J., Hurley, J.H. and Bonifacino, J.S. (2007). Downregulation of CD4 by human immunodeficiency virus type 1 Nef is dependent on clathrin and involves direct interaction of Nef with the AP2 clathrin adaptor. *Journal of virology* **81,** 3877-3890.

Chaudhuri, R., Mattera, R., Lindwasser, O.W., Robinson, M.S. and Bonifacino, J.S. (2009). A basic patch on alpha-adaptin is required for binding of human immunodeficiency virus type 1 Nef and cooperative assembly of a CD4-Nef-AP-2 complex. *Journal of virology* **83,** 2518-2530.

Chavrier, P. and Goud, B. (1999). The role of ARF and Rab GTPases in membrane transport. *Current opinion in cell biology* **11,** 466-475.

Chen, W.Y., Wang, D.H., Yen, R.C., Luo, J., Gu, W. and Baylin, S.B. (2005). Tumor suppressor HIC1 directly regulates SIRT1 to modulate p53-dependent DNA-damage responses. *Cell* **123,** 437-448.

Chen, X., Ko, L.J., Jayaraman, L. and Prives, C. (1996). p53 levels, functional domains, and DNA damage determine the extent of the apoptotic response of tumor cells. *Genes Dev* **10,** 2438-2451.

Cheng, H.L., Mostoslavsky, R., Saito, S., Manis, J.P., Gu, Y., Patel, P.*, et al.* (2003). Developmental defects and p53 hyperacetylation in Sir2 homolog (SIRT1)-deficient mice. *Proc Natl Acad Sci U S A* **100,** 10794-10799.

Cheng, J.P. and Lane, J.D. (2010). Organelle dynamics and membrane trafficking in apoptosis and autophagy. *Histology and histopathology* **25,** 1457-1472.

Chipuk, J.E., Bouchier-Hayes, L., Kuwana, T., Newmeyer, D.D. and Green, D.R. (2005). PUMA couples the nuclear and cytoplasmic proapoptotic function of p53. *Science (New York, N.Y.)* **309,** 1732-1735.

Chipuk, J.E., Kuwana, T., Bouchier-Hayes, L., Droin, N.M., Newmeyer, D.D., Schuler, M. and Green, D.R. (2004). Direct activation of Bax by p53 mediates mitochondrial membrane permeabilization and apoptosis. *Science (New York, N.Y.)* **303,** 1010-1014.

Cho, Y., Gorina, S., Jeffrey, P.D. and Pavletich, N.P. (1994). Crystal structure of a p53 tumor suppressor-DNA complex: understanding tumorigenic mutations. *Science* **265,** 346-355.

Choi, H.J., Lee, H., Kim, H., Kwon, J.E., Kang, H.J., You, K.T*., et al.* (2010). MicroRNA expression profile of gastrointestinal stromal tumors is distinguished by 14q loss and anatomic site. *International journal of cancer. Journal international du cancer* **126,** 1640-1650.

Choi, H.J. and Smithgall, T.E. (2004). Conserved residues in the HIV-1 Nef hydrophobic pocket are essential for recruitment and activation of the Hck tyrosine kinase. *Journal of molecular biology* **343,** 1255-1268.

Choudhary, C., Kumar, C., Gnad, F., Nielsen, M.L., Rehman, M., Walther, T.C*., et al.* (2009). Lysine acetylation targets protein complexes and co-regulates major cellular functions. *Science* **325,** 834-840.

Chuikov, S., Kurash, J.K., Wilson, J.R., Xiao, B., Justin, N., Ivanov, G.S*., et al.* (2004). Regulation of p53 activity through lysine methylation. *Nature* **432,** 353-360.

Chun, T.W., Finzi, D., Margolick, J., Chadwick, K., Schwartz, D. and Siliciano, R.F. (1995). In vivo fate of HIV-1-infected T cells: quantitative analysis of the transition to stable latency. *Nat Med* **1,** 1284-1290.

Chun, T.W., Justement, J.S., Lempicki, R.A., Yang, J., Dennis, G., Jr., Hallahan, C.W*., et al.* (2003). Gene expression and viral prodution in latently infected, resting CD4+ T cells in viremic versus aviremic HIV-infected individuals. *Proc Natl Acad Sci U S A* **100,** 1908-1913.

Chutiwitoonchai, N., Hiyoshi, M., Mwimanzi, P., Ueno, T., Adachi, A., Ode, H*., et al.* (2011). The identification of a small molecule compound that reduces HIV-1 Nef-mediated viral infectivity enhancement. *PloS one* **6,** e27696.

Ciani, L. and Salinas, P.C. (2005). WNTs in the vertebrate nervous system: from patterning to neuronal connectivity. *Nature reviews. Neuroscience* **6,** 351-362.

Clarke, A.R., Purdie, C.A., Harrison, D.J., Morris, R.G., Bird, C.C., Hooper, M.L. and Wyllie, A.H. (1993). Thymocyte apoptosis induced by p53-dependent and independent pathways. *Nature* **362,** 849-852.

Clore, G.M., Ernst, J., Clubb, R., Omichinski, J.G., Kennedy, W.M., Sakaguchi, K*., et al.* (1995a). Refined solution structure of the oligomerization domain of the tumour suppressor p53. *Nature structural biology* **2,** 321-333.

Clore, G.M., Omichinski, J.G., Sakaguchi, K., Zambrano, N., Sakamoto, H., Appella, E. and Gronenborn, A.M. (1994). High-resolution structure of the

oligomerization domain of p53 by multidimensional NMR. *Science* **265,** 386-391.

Clore, G.M., Omichinski, J.G., Sakaguchi, K., Zambrano, N., Sakamoto, H., Appella, E. and Gronenborn, A.M. (1995b). Interhelical angles in the solution structure of the oligomerization domain of p53: correction. *Science* **267,** 1515-1516.

Cohen, G.B., Gandhi, R.T., Davis, D.M., Mandelboim, O., Chen, B.K., Strominger, J.L. and Baltimore, D. (1999). The selective downregulation of class I major histocompatibility complex proteins by HIV-1 protects HIV-infected cells from NK cells. *Immunity* **10,** 661-671.

Coleman, S.H., Madrid, R., Van Damme, N., Mitchell, R.S., Bouchet, J., Servant, C.*, et al.* (2006). Modulation of cellular protein trafficking by human immunodeficiency virus type 1 Nef: role of the acidic residue in the ExxxLL motif. *Journal of virology* **80,** 1837-1849.

Collins, K.L., Chen, B.K., Kalams, S.A., Walker, B.D. and Baltimore, D. (1998). HIV-1 Nef protein protects infected primary cells against killing by cytotoxic T lymphocytes. *Nature* **391,** 397-401.

Connor, R.I., Sheridan, K.E., Ceradini, D., Choe, S. and Landau, N.R. (1997). Change in coreceptor use correlates with disease progression in HIV-1--infected individuals. *The Journal of experimental medicine* **185,** 621-628.

Conticello, S.G., Thomas, C.J., Petersen-Mahrt, S.K. and Neuberger, M.S. (2005). Evolution of the AID/APOBEC family of polynucleotide (deoxy)cytidine deaminases. *Molecular biology and evolution* **22,** 367-377.

Cooper, D.A., Gold, J., Maclean, P., Donovan, B., Finlayson, R., Barnes, T.G.*, et al.* (1985). Acute AIDS retrovirus infection. Definition of a clinical illness associated with seroconversion. *Lancet* **1,** 537-540.

Coqueret, O. (2003). New roles for p21 and p27 cell-cycle inhibitors: a function for each cell compartment? *Trends in cell biology* **13,** 65-70.

Corda, D., Colanzi, A. and Luini, A. (2006). The multiple activities of CtBP/BARS proteins: the Golgi view. *Trends Cell Biol* **16,** 167-173.

Crump, C.M., Hung, C.H., Thomas, L., Wan, L. and Thomas, G. (2003). Role of PACS-1 in trafficking of human cytomegalovirus glycoprotein B and virus production. *Journal of virology* **77,** 11105-11113.

Crump, C.M., Xiang, Y., Thomas, L., Gu, F., Austin, C., Tooze, S.A. and Thomas, G. (2001). PACS-1 binding to adaptors is required for acidic cluster motif-mediated protein traffic. *EMBO J* **20,** 2191-2201.

Csordas, G., Renken, C., Varnai, P., Walter, L., Weaver, D., Buttle, K.F.*, et al.* (2006). Structural and functional features and significance of the physical linkage between ER and mitochondria. *J Cell Biol* **174,** 915-921.

Cummins, J.M., Rago, C., Kohli, M., Kinzler, K.W., Lengauer, C. and Vogelstein, B. (2004). Tumour suppression: disruption of HAUSP gene stabilizes p53. *Nature* **428,** 1 p following 486.

Dacks, J.B. and Field, M.C. (2007). Evolution of the eukaryotic membrane-trafficking system: origin, tempo and mode. *J Cell Sci* **120,** 2977-2985.

Dacks, J.B., Peden, A.A. and Field, M.C. (2009). Evolution of specificity in the eukaryotic endomembrane system. *The international journal of biochemistry & cell biology* **41,** 330-340.

D'Agati, V. and Appel, G.B. (1998). Renal pathology of human immunodeficiency virus infection. *Seminars in nephrology* **18,** 406-421.

Dahinden, C., Ingold, B., Wild, P., Boysen, G., Luu, V.D., Montani, M.*, et al.* (2010). Mining tissue microarray data to uncover combinations of biomarker expression patterns that improve intermediate staging and grading of clear cell renal cell cancer. *Clin Cancer Res* **16,** 88-98.

Dai, J.M., Wang, Z.Y., Sun, D.C., Lin, R.X. and Wang, S.Q. (2007). SIRT1 interacts with p73 and suppresses p73-dependent transcriptional activity. *Journal of cellular physiology* **210,** 161-166.

Dai, M.S., Zeng, S.X., Jin, Y., Sun, X.X., David, L. and Lu, H. (2004). Ribosomal protein L23 activates p53 by inhibiting MDM2 function in response to ribosomal perturbation but not to translation inhibition. *Mol Cell Biol* **24,** 7654-7668.

Dalgliesh, G.L., Furge, K., Greenman, C., Chen, L., Bignell, G., Butler, A.*, et al.* (2010). Systematic sequencing of renal carcinoma reveals inactivation of histone modifying genes. *Nature* **463,** 360-363.

Dameron, K.M., Volpert, O.V., Tainsky, M.A. and Bouck, N. (1994). Control of angiogenesis in fibroblasts by p53 regulation of thrombospondin-1. *Science* **265,** 1582-1584.

Dang, W., Steffen, K.K., Perry, R., Dorsey, J.A., Johnson, F.B., Shilatifard, A.*, et al.* (2009). Histone H4 lysine 16 acetylation regulates cellular lifespan. *Nature* **459,** 802-807.

daSilva, L.L., Sougrat, R., Burgos, P.V., Janvier, K., Mattera, R. and Bonifacino, J.S. (2009). Human immunodeficiency virus type 1 Nef protein targets CD4 to the multivesicular body pathway. *Journal of virology* **83,** 6578-6590.

De la Cueva, E., Garcia-Cao, I., Herranz, M., Lopez, P., Garcia-Palencia, P., Flores, J.M.*, et al.* (2006). Tumorigenic activity of p21Waf1/Cip1 in thymic lymphoma. *Oncogene* **25,** 4128-4132.

de Rozieres, S., Maya, R., Oren, M. and Lozano, G. (2000). The loss of mdm2 induces p53-mediated apoptosis. *Oncogene* **19,** 1691-1697.

Deacon, N.J., Tsykin, A., Solomon, A., Smith, K., Ludford-Menting, M., Hooker, D.J.*, et al.* (1995). Genomic structure of an attenuated quasi species of HIV-1 from a blood transfusion donor and recipients. *Science* **270,** 988-991.

Dean, M., Carrington, M., Winkler, C., Huttley, G.A., Smith, M.W., Allikmets, R.*, et al.* (1996). Genetic restriction of HIV-1 infection and progression to AIDS by a deletion allele of the CKR5 structural gene. Hemophilia Growth and Development Study, Multicenter AIDS Cohort Study, Multicenter Hemophilia Cohort Study, San Francisco City Cohort, ALIVE Study. *Science* **273,** 1856-1862.

Dehart, J.L. and Planelles, V. (2008). Human immunodeficiency virus type 1 Vpr links proteasomal degradation and checkpoint activation. *Journal of virology* **82,** 1066-1072.

DeHart, J.L., Zimmerman, E.S., Ardon, O., Monteiro-Filho, C.M., Arganaraz, E.R. and Planelles, V. (2007). HIV-1 Vpr activates the G2 checkpoint through manipulation of the ubiquitin proteasome system. *Virology journal* **4,** 57.

DeLeo, A.B., Jay, G., Appella, E., Dubois, G.C., Law, L.W. and Old, L.J. (1979). Detection of a transformation-related antigen in chemically induced sarcomas and other transformed cells of the mouse. *Proc Natl Acad Sci U S A* **76,** 2420-2424.

Delmas, P., Padilla, F., Osorio, N., Coste, B., Raoux, M. and Crest, M. (2004). Polycystins, calcium signaling, and human diseases. *Biochem Biophys Res Commun* **322,** 1374-1383.

Demetri, G.D., von Mehren, M., Blanke, C.D., Van den Abbeele, A.D., Eisenberg, B., Roberts, P.J.*, et al.* (2002). Efficacy and safety of imatinib mesylate in advanced gastrointestinal stromal tumors. *N Engl J Med* **347,** 472-480.

Deng, C., Zhang, P., Harper, J.W., Elledge, S.J. and Leder, P. (1995). Mice lacking p21CIP1/WAF1 undergo normal development, but are defective in G1 checkpoint control. *Cell* **82,** 675-684.

Deng, C.X. (2009). SIRT1, is it a tumor promoter or tumor suppressor? *International journal of biological sciences* **5,** 147-152.

Detels, R., Munoz, A., McFarlane, G., Kingsley, L.A., Margolick, J.B., Giorgi, J.*, et al.* (1998). Effectiveness of potent antiretroviral therapy on time to AIDS and death in men with known HIV infection duration. Multicenter AIDS Cohort Study Investigators. *JAMA : the journal of the American Medical Association* **280,** 1497-1503.

Di Lello, P., Jenkins, L.M., Jones, T.N., Nguyen, B.D., Hara, T., Yamaguchi, H.*, et al.* (2006). Structure of the Tfb1/p53 complex: Insights into the interaction between the p62/Tfb1 subunit of TFIIH and the activation domain of p53. *Mol Cell* **22,** 731-740.

Dijkman, R., Tensen, C.P., Jordanova, E.S., Knijnenburg, J., Hoefnagel, J.J., Mulder, A.A.*, et al.* (2006). Array-based comparative genomic hybridization analysis reveals recurrent chromosomal alterations and prognostic parameters in primary cutaneous large B-cell lymphoma. *Journal of clinical oncology : official journal of the American Society of Clinical Oncology* **24,** 296-305.

Dikeakos, J.D., Thomas, L., Kwon, G., Elferich, J., Shinde, U. and Thomas, G. (2012). An interdomain binding site on HIV-1 Nef interacts with PACS-1 and PACS-2 on endosomes to down-regulate MHC-I. *Mol Biol Cell* **23,** 2184-2197.

Dinkins, C., Arko-Mensah, J. and Deretic, V. (2010). Autophagy and HIV. *Seminars in cell & developmental biology* **21,** 712-718.

Dioum, E.M., Chen, R., Alexander, M.S., Zhang, Q., Hogg, R.T., Gerard, R.D. and Garcia, J.A. (2009). Regulation of hypoxia-inducible factor 2alpha

signaling by the stress-responsive deacetylase sirtuin 1. *Science* **324,** 1289-1293.

Dittie, A.S., Thomas, L., Thomas, G. and Tooze, S.A. (1997). Interaction of furin in immature secretory granules from neuroendocrine cells with the AP-1 adaptor complex is modulated by casein kinase II phosphorylation. *EMBO J* **16,** 4859-4870.

Donehower, L.A., Harvey, M., Slagle, B.L., McArthur, M.J., Montgomery, C.A., Jr., Butel, J.S. and Bradley, A. (1992). Mice deficient for p53 are developmentally normal but susceptible to spontaneous tumours. *Nature* **356,** 215-221.

Doray, B., Lee, I., Knisely, J., Bu, G. and Kornfeld, S. (2007). The gamma/sigma1 and alpha/sigma2 hemicomplexes of clathrin adaptors AP-1 and AP-2 harbor the dileucine recognition site. *Mol Biol Cell* **18,** 1887-1896.

Dornan, D., Wertz, I., Shimizu, H., Arnott, D., Frantz, G.D., Dowd, P*., et al.* (2004). The ubiquitin ligase COP1 is a critical negative regulator of p53. *Nature* **429,** 86-92.

Dotto, G.P. (2000). p21(WAF1/Cip1): more than a break to the cell cycle? *Biochim Biophys Acta* **1471,** M43-56.

Douek, D.C., Picker, L.J. and Koup, R.A. (2003). T cell dynamics in HIV-1 infection. *Annual review of immunology* **21,** 265-304.

Druker, B.J., Sawyers, C.L., Kantarjian, H., Resta, D.J., Reese, S.F., Ford, J.M*., et al.* (2001). Activity of a specific inhibitor of the BCR-ABL tyrosine kinase in the blast crisis of chronic myeloid leukemia and acute lymphoblastic leukemia with the Philadelphia chromosome. *N Engl J Med* **344,** 1038-1042.

Dube, N., Cheng, A. and Tremblay, M.L. (2004). The role of protein tyrosine phosphatase 1B in Ras signaling. *Proc Natl Acad Sci U S A* **101,** 1834-1839.

Duden, R. (2003). ER-to-Golgi transport: COP I and COP II function (Review). *Molecular membrane biology* **20,** 197-207.

Dulic, V., Kaufmann, W.K., Wilson, S.J., Tlsty, T.D., Lees, E., Harper, J.W*., et al.* (1994). p53-dependent inhibition of cyclin-dependent kinase activities in human fibroblasts during radiation-induced G1 arrest. *Cell* **76,** 1013-1023.

Dulic, V., Stein, G.H., Far, D.F. and Reed, S.I. (1998). Nuclear accumulation of p21Cip1 at the onset of mitosis: a role at the G2/M-phase transition. *Mol Cell Biol* **18,** 546-557.

Edmonston, T.B., Cuesta, K.H., Burkholder, S., Barusevicius, A., Rose, D., Kovatich, A.J*., et al.* (2000). Colorectal carcinomas with high microsatellite instability: defining a distinct immunologic and molecular entity with respect to prognostic markers. *Human pathology* **31,** 1506-1514.

Efeyan, A., Collado, M., Velasco-Miguel, S. and Serrano, M. (2007). Genetic dissection of the role of p21Cip1/Waf1 in p53-mediated tumour suppression. *Oncogene* **26,** 1645-1649.

Egger, M., Hirschel, B., Francioli, P., Sudre, P., Wirz, M., Flepp, M.*, et al.* (1997). Impact of new antiretroviral combination therapies in HIV infected patients in Switzerland: prospective multicentre study. Swiss HIV Cohort Study. *BMJ* **315,** 1194-1199.

Efeyan, A., Collado, M., Velasco-Miguel, S. and Serrano, M. (2007). Genetic dissection of the role of p21Cip1/Waf1 in p53-mediated tumour suppression. *Oncogene* **26,** 1645-1649.

Eisfeld, A.J., Yee, M.B., Erazo, A., Abendroth, A. and Kinchington, P.R. (2007). Downregulation of class I major histocompatibility complex surface expression by varicella-zoster virus involves open reading frame 66 protein kinase-dependent and -independent mechanisms. *Journal of virology* **81,** 9034-9049.

el-Deiry, W.S., Kern, S.E., Pietenpol, J.A., Kinzler, K.W. and Vogelstein, B. (1992). Definition of a consensus binding site for p53. *Nat Genet* **1,** 45-49.

el-Deiry, W.S., Tokino, T., Velculescu, V.E., Levy, D.B., Parsons, R., Trent, J.M.*, et al.* (1993). WAF1, a potential mediator of p53 tumor suppression. *Cell* **75,** 817-825.

Elias, M. (2010). Patterns and processes in the evolution of the eukaryotic endomembrane system. *Molecular membrane biology* **27,** 469-489.

Emert-Sedlak, L., Kodama, T., Lerner, E.C., Dai, W., Foster, C., Day, B.W.*, et al.* (2009). Chemical library screens targeting an HIV-1 accessory factor/host cell kinase complex identify novel antiretroviral compounds. *ACS chemical biology* **4,** 939-947.

Engels, H., Schuler, H.M., Zink, A.M., Wohlleber, E., Brockschmidt, A., Hoischen, A.*, et al.* (2012). A phenotype map for 14q32.3 terminal deletions. *American journal of medical genetics. Part A* **158A,** 695-706.

Espinosa, J.M., Verdun, R.E. and Emerson, B.M. (2003). p53 functions through stress- and promoter-specific recruitment of transcription initiation components before and after DNA damage. *Mol Cell* **12,** 1015-1027.

Fackler, O.T. and Baur, A.S. (2002). Live and let die: Nef functions beyond HIV replication. *Immunity* **16,** 493-497.

Fan, W. and Luo, J. (2010). SIRT1 regulates UV-induced DNA repair through deacetylating XPA. *Mol Cell* **39,** 247-258.

Farmer, G., Colgan, J., Nakatani, Y., Manley, J.L. and Prives, C. (1996). Functional interaction between p53, the TATA-binding protein (TBP), andTBP-associated factors in vivo. *Mol Cell Biol* **16,** 4295-4304.

Feliciangeli, S.F., Thomas, L., Scott, G.K., Subbian, E., Hung, C.H., Molloy, S.S.*, et al.* (2006). Identification of a pH sensor in the furin propeptide that regulates enzyme activation. *J Biol Chem* **281,** 16108-16116.

Fellay, J., Ge, D., Shianna, K.V., Colombo, S., Ledergerber, B., Cirulli, E.T.*, et al.* (2009). Common genetic variation and the control of HIV-1 in humans. *PLoS genetics* **5,** e1000791.

Fellay, J., Shianna, K.V., Ge, D., Colombo, S., Ledergerber, B., Weale, M.*, et al.* (2007). A whole-genome association study of major determinants for host control of HIV-1. *Science* **317,** 944-947.

Feng, L., Lin, T., Uranishi, H., Gu, W. and Xu, Y. (2005). Functional analysis of the roles of posttranslational modifications at the p53 C terminus in regulating p53 stability and activity. *Mol Cell Biol* **25,** 5389-5395.

Fields, S. and Jang, S.K. (1990). Presence of a potent transcription activating sequence in the p53 protein. *Science* **249,** 1046-1049.

Finlay, C.A., Hinds, P.W. and Levine, A.J. (1989). The p53 proto-oncogene can act as a suppressor of transformation. *Cell* **57,** 1083-1093.

Finzi, D. and Siliciano, R.F. (1998). Viral dynamics in HIV-1 infection. *Cell* **93,** 665-671.

Firestein, R., Blander, G., Michan, S., Oberdoerffer, P., Ogino, S., Campbell, J.*, et al.* (2008). The SIRT1 deacetylase suppresses intestinal tumorigenesis and colon cancer growth. *PloS one* **3,** e2020.

Flaherty, K.T., Puzanov, I., Kim, K.B., Ribas, A., McArthur, G.A., Sosman, J.A.*, et al.* (2010). Inhibition of mutated, activated BRAF in metastatic melanoma. *N Engl J Med* **363,** 809-819.

Ford, J., Jiang, M. and Milner, J. (2005). Cancer-specific functions of SIRT1 enable human epithelial cancer cell growth and survival. *Cancer Res* **65,** 10457-10463.

Foster, J.L., Denial, S.J., Temple, B.R. and Garcia, J.V. (2011). Mechanisms of HIV-1 Nef function and intracellular signaling. *Journal of neuroimmune pharmacology : the official journal of the Society on NeuroImmune Pharmacology* **6,** 230-246.

Foster, J.L. and Garcia, J.V. (2008). HIV-1 Nef: at the crossroads. *Retrovirology* **5,** 84.

Frame, M.C. (2002). Src in cancer: deregulation and consequences for cell behaviour. *Biochim Biophys Acta* **1602,** 114-130.

Franke, W.W. and Kartenbeck, J. (1971). Outer mitochondrial membrane continuous with endoplasmic reticulum. *Protoplasma* **73,** 35-41.

Frantz, S. (2001). Role model. *Nature reviews. Molecular cell biology* **2,** 872-873.

Freed, E.O. (1998). HIV-1 gag proteins: diverse functions in the virus life cycle. *Virology* **251,** 1-15.

Friedman, P.N., Chen, X., Bargonetti, J. and Prives, C. (1993). The p53 protein is an unusually shaped tetramer that binds directly to DNA. *Proc Natl Acad Sci U S A* **90,** 3319-3323.

Friedrich, T.C., Dodds, E.J., Yant, L.J., Vojnov, L., Rudersdorf, R., Cullen, C.*, et al.* (2004). Reversion of CTL escape-variant immunodeficiency viruses in vivo. *Nat Med* **10,** 275-281.

Friedrich, T.C., Piaskowski, S.M., Leon, E.J., Furlott, J.R., Maness, N.J., Weisgrau, K.L.*, et al.* (2010). High viremia is associated with high levels of in vivo major histocompatibility complex class I Downregulation in rhesus

macaques infected with simian immunodeficiency virus SIVmac239. *Journal of virology* **84,** 5443-5447.

Frye, R.A. (2000). Phylogenetic classification of prokaryotic and eukaryotic Sir2-like proteins. *Biochem Biophys Res Commun* **273,** 793-798.

Fu, M., Liu, M., Sauve, A.A., Jiao, X., Zhang, X., Wu, X.*, et al.* (2006). Hormonal control of androgen receptor function through SIRT1. *Mol Cell Biol* **26,** 8122-8135.

Fu, X., Wang, Y., Schetle, N., Gao, H., Putz, M., von Gersdorff, G.*, et al.* (2008). The subcellular localization of TRPP2 modulates its function. *Journal of the American Society of Nephrology : JASN* **19,** 1342-1351.

Fukushima, Y., Oshika, Y., Tsuchida, T., Tokunaga, T., Hatanaka, H., Kijima, H.*, et al.* (1998). Brain-specific angiogenesis inhibitor 1 expression is inversely correlated with vascularity and distant metastasis of colorectal cancer. *International journal of oncology* **13,** 967-970.

Fulco, M., Schiltz, R.L., Iezzi, S., King, M.T., Zhao, P., Kashiwaya, Y.*, et al.* (2003). Sir2 regulates skeletal muscle differentiation as a potential sensor of the redox state. *Mol Cell* **12,** 51-62.

Funk, W.D., Pak, D.T., Karas, R.H., Wright, W.E. and Shay, J.W. (1992). A transcriptionally active DNA-binding site for human p53 protein complexes. *Mol Cell Biol* **12,** 2866-2871.

Gaigg, B., Simbeni, R., Hrastnik, C., Paltauf, F. and Daum, G. (1995). Characterization of a microsomal subfraction associated with mitochondria of the yeast, Saccharomyces cerevisiae. Involvement in synthesis and import of phospholipids into mitochondria. *Biochim Biophys Acta* **1234,** 214-220.

Gail, M.H., Tan, W.Y., Pee, D. and Goedert, J.J. (1997). Survival after AIDS diagnosis in a cohort of hemophilia patients. Multicenter Hemophilia Cohort Study. *Journal of acquired immune deficiency syndromes and human retrovirology : official publication of the International Retrovirology Association* **15,** 363-369.

Gallegos Ruiz, M.I., Floor, K., Roepman, P., Rodriguez, J.A., Meijer, G.A., Mooi, W.J.*, et al.* (2008). Integration of gene dosage and gene expression in non-small cell lung cancer, identification of HSP90 as potential target. *PloS one* **3,** e0001722.

Gallo, R., Wong-Staal, F., Montagnier, L., Haseltine, W.A. and Yoshida, M. (1988). HIV/HTLV gene nomenclature. *Nature* **333,** 504.

Gallo, R.C., Salahuddin, S.Z., Popovic, M., Shearer, G.M., Kaplan, M., Haynes, B.F.*, et al.* (1984). Frequent detection and isolation of cytopathic retroviruses (HTLV-III) from patients with AIDS and at risk for AIDS. *Science* **224,** 500-503.

Gandhi, R.T. and Walker, B.D. (2002). Immunologic control of HIV-1. *Annual review of medicine* **53,** 149-172.

Ganem, D. (2006). KSHV infection and the pathogenesis of Kaposi's sarcoma. *Annual review of pathology* **1,** 273-296.

Ganser-Pornillos, B.K., Yeager, M. and Sundquist, W.I. (2008). The structural biology of HIV assembly. *Current opinion in structural biology* **18,** 203-217.
Garcia, J.V. and Miller, A.D. (1991). Serine phosphorylation-independent downregulation of cell-surface CD4 by nef. *Nature* **350,** 508-511.
Garner, E. and Raj, K. (2008). Protective mechanisms of p53-p21-pRb proteins against DNA damage-induced cell death. *Cell cycle (Georgetown, Tex.)* **7,** 277-282.
Gartel, A.L. (2006). Is p21 an oncogene? *Molecular cancer therapeutics* **5,** 1385-1386.
Gartel, A.L. and Tyner, A.L. (2002). The role of the cyclin-dependent kinase inhibitor p21 in apoptosis. *Molecular cancer therapeutics* **1,** 639-649.
Geoffrey Bodenhausen, D.J.R. (1980). Natural abundance nitrogen-15 NMR by enhanced heteronuclear spectroscopy. *Chemical Physics Letters* **69,** 185–189.
Gervais, J.L., Seth, P. and Zhang, H. (1998). Cleavage of CDK inhibitor p21(Cip1/Waf1) by caspases is an early event during DNA damage-induced apoptosis. *J Biol Chem* **273,** 19207-19212.
Geyer, M., Fackler, O.T. and Peterlin, B.M. (2001). Structure--function relationships in HIV-1 Nef. *EMBO reports* **2,** 580-585.
Geyer, M., Munte, C.E., Schorr, J., Kellner, R. and Kalbitzer, H.R. (1999). Structure of the anchor-domain of myristoylated and non-myristoylated HIV-1 Nef protein. *Journal of molecular biology* **289,** 123-138.
Giamarchi, A., Padilla, F., Coste, B., Raoux, M., Crest, M., Honore, E. and Delmas, P. (2006). The versatile nature of the calcium-permeable cation channel TRPP2. *EMBO reports* **7,** 787-793.
Giolo, G., Neri, F., Casartelli, N., Potesta, M., Belleudi, F., Torrisi, M.R. and Doria, M. (2007). Internalization and intracellular retention of CD4 are two separate functions of the human immunodeficiency virus type 1 Nef protein. *The Journal of general virology* **88,** 3133-3138.
Giono, L.E. and Manfredi, J.J. (2006). The p53 tumor suppressor participates in multiple cell cycle checkpoints. *Journal of cellular physiology* **209,** 13-20.
Gondois-Rey, F., Biancotto, A., Pion, M., Chenine, A.L., Gluschankof, P., Horejsi, V*., et al.* (2001). Production of HIV-1 by resting memory T lymphocytes. *AIDS* **15,** 1931-1940.
Gonzalez, P.A., Carreno, L.J., Coombs, D., Mora, J.E., Palmieri, E., Goldstein, B*., et al.* (2005). T cell receptor binding kinetics required for T cell activation depend on the density of cognate ligand on the antigen-presenting cell. *Proc Natl Acad Sci U S A* **102,** 4824-4829.
Goodman, R.H. and Smolik, S. (2000). CBP/p300 in cell growth, transformation, and development. *Genes Dev* **14,** 1553-1577.
Gottlieb, S. and Esposito, R.E. (1989). A new role for a yeast transcriptional silencer gene, SIR2, in regulation of recombination in ribosomal DNA. *Cell* **56,** 771-776.

Gottschling, D.E., Aparicio, O.M., Billington, B.L. and Zakian, V.A. (1990). Position effect at S. cerevisiae telomeres: reversible repression of Pol II transcription. *Cell* **63,** 751-762.

Grantham, J.J. (2008). Clinical practice. Autosomal dominant polycystic kidney disease. *N Engl J Med* **359,** 1477-1485.

Green, D.R. and Kroemer, G. (2009). Cytoplasmic functions of the tumour suppressor p53. *Nature* **458,** 1127-1130.

Greenberg, M.E., Bronson, S., Lock, M., Neumann, M., Pavlakis, G.N. and Skowronski, J. (1997). Co-localization of HIV-1 Nef with the AP-2 adaptor protein complex correlates with Nef-induced CD4 down-regulation. *EMBO J* **16,** 6964-6976.

Greenberg, M.E., Iafrate, A.J. and Skowronski, J. (1998). The SH3 domain-binding surface and an acidic motif in HIV-1 Nef regulate trafficking of class I MHC complexes. *EMBO J* **17,** 2777-2789.

Gridelli, C., De Marinis, F., Di Maio, M., Cortinovis, D., Cappuzzo, F. and Mok, T. (2011). Gefitinib as first-line treatment for patients with advanced non-small-cell lung cancer with activating Epidermal Growth Factor Receptor mutation: implications for clinical practice and open issues. *Lung Cancer* **72,** 3-8.

Griffiths, G., Hoflack, B., Simons, K., Mellman, I. and Kornfeld, S. (1988). The mannose 6-phosphate receptor and the biogenesis of lysosomes. *Cell* **52,** 329-341.

Grimes, C.A. and Jope, R.S. (2001). The multifaceted roles of glycogen synthase kinase 3beta in cellular signaling. *Progress in neurobiology* **65,** 391-426.

Grzesiek, S., Bax, A., Clore, G.M., Gronenborn, A.M., Hu, J.S., Kaufman, J.*, et al.* (1996a). The solution structure of HIV-1 Nef reveals an unexpected fold and permits delineation of the binding surface for the SH3 domain of Hck tyrosine protein kinase. *Nature structural biology* **3,** 340-345.

Grzesiek, S., Bax, A., Hu, J.S., Kaufman, J., Palmer, I., Stahl, S.J.*, et al.* (1997). Refined solution structure and backbone dynamics of HIV-1 Nef. *Protein science : a publication of the Protein Society* **6,** 1248-1263.

Grzesiek, S., Stahl, S.J., Wingfield, P.T. and Bax, A. (1996b). The CD4 determinant for downregulation by HIV-1 Nef directly binds to Nef. Mapping of the Nef binding surface by NMR. *Biochemistry* **35,** 10256-10261.

Gu, F., Crump, C.M. and Thomas, G. (2001). Trans-Golgi network sorting. *Cell Mol Life Sci* **58,** 1067-1084.

Gu, W., Malik, S., Ito, M., Yuan, C.X., Fondell, J.D., Zhang, X.*, et al.* (1999). A novel human SRB/MED-containing cofactor complex, SMCC, involved in transcription regulation. *Mol Cell* **3,** 97-108.

Gu, W. and Roeder, R.G. (1997). Activation of p53 sequence-specific DNA binding by acetylation of the p53 C-terminal domain. *Cell* **90,** 595-606.

Gu, Y., Turck, C.W. and Morgan, D.O. (1993). Inhibition of CDK2 activity in vivo by an associated 20K regulatory subunit. *Nature* **366,** 707-710.

Guarani, V., Deflorian, G., Franco, C.A., Kruger, M., Phng, L.K., Bentley, K.*, et al.* (2011). Acetylation-dependent regulation of endothelial Notch signalling by the SIRT1 deacetylase. *Nature* **473,** 234-238.

Guicciardi, M.E., Deussing, J., Miyoshi, H., Bronk, S.F., Svingen, P.A., Peters, C.*, et al.* (2000). Cathepsin B contributes to TNF-alpha-mediated hepatocyte apoptosis by promoting mitochondrial release of cytochrome c. *J Clin Invest* **106,** 1127-1137.

Guicciardi, M.E., Leist, M. and Gores, G.J. (2004). Lysosomes in cell death. *Oncogene* **23,** 2881-2890.

Gupta, K., Miller, J.D., Li, J.Z., Russell, M.W. and Charbonneau, C. (2008). Epidemiologic and socioeconomic burden of metastatic renal cell carcinoma (mRCC): a literature review. *Cancer treatment reviews* **34,** 193-205.

Gupta, K.K. (1993). Acute immunosuppression with HIV seroconversion. *N Engl J Med* **328,** 288-289.

Guss, D.A. (1994). The acquired immune deficiency syndrome: an overview for the emergency physician, Part 1. *The Journal of emergency medicine* **12,** 375-384.

Gwanmesia, P.M., Romanski, A., Schwarz, K., Bacic, B., Ruthardt, M. and Ottmann, O.G. (2009). The effect of the dual Src/Abl kinase inhibitor AZD0530 on Philadelphia positive leukaemia cell lines. *BMC cancer* **9,** 53.

Haigis, M.C. and Guarente, L.P. (2006). Mammalian sirtuins--emerging roles in physiology, aging, and calorie restriction. *Genes Dev* **20,** 2913-2921.

Haigis, M.C. and Sinclair, D.A. (2010). Mammalian sirtuins: biological insights and disease relevance. *Annual review of pathology* **5,** 253-295.

Hainaut, P. and Hollstein, M. (2000). p53 and human cancer: the first ten thousand mutations. *Advances in cancer research* **77,** 81-137.

Haller, C. and Fackler, O.T. (2008). HIV-1 at the immunological and T-lymphocytic virological synapse. *Biological chemistry* **389,** 1253-1260.

Hallows, W.C., Lee, S. and Denu, J.M. (2006). Sirtuins deacetylate and activate mammalian acetyl-CoA synthetases. *Proc Natl Acad Sci U S A* **103,** 10230-10235.

Hammer, S.M., Eron, J.J., Jr., Reiss, P., Schooley, R.T., Thompson, M.A., Walmsley, S.*, et al.* (2008). Antiretroviral treatment of adult HIV infection: 2008 recommendations of the International AIDS Society-USA panel. *JAMA : the journal of the American Medical Association* **300,** 555-570.

Han, L., Zhou, R., Niu, J., McNutt, M.A., Wang, P. and Tong, T. (2010). SIRT1 is regulated by a PPAR{gamma}-SIRT1 negative feedback loop associated with senescence. *Nucleic Acids Res* **38,** 7458-7471.

Han, M.K., Song, E.K., Guo, Y., Ou, X., Mantel, C. and Broxmeyer, H.E. (2008). SIRT1 regulates apoptosis and Nanog expression in mouse embryonic stem cells by controlling p53 subcellular localization. *Cell stem cell* **2,** 241-251.

Hanna, Z., Kay, D.G., Cool, M., Jothy, S., Rebai, N. and Jolicoeur, P. (1998a). Transgenic mice expressing human immunodeficiency virus type 1 in immune cells develop a severe AIDS-like disease. *Journal of virology* **72,** 121-132.

Hanna, Z., Kay, D.G., Rebai, N., Guimond, A., Jothy, S. and Jolicoeur, P. (1998). Nef harbors a major determinant of pathogenicity for an AIDS-like disease induced by HIV-1 in transgenic mice. *Cell* **95,** 163-175.

Hanna, Z., Weng, X., Kay, D.G., Poudrier, J., Lowell, C. and Jolicoeur, P. (2001). The pathogenicity of human immunodeficiency virus (HIV) type 1 Nef in CD4C/HIV transgenic mice is abolished by mutation of its SH3-binding domain, and disease development is delayed in the absence of Hck. *Journal of virology* **75,** 9378-9392.

Hansen, T.H. and Bouvier, M. (2009). MHC class I antigen presentation: learning from viral evasion strategies. *Nature reviews. Immunology* **9,** 503-513.

Harper, J.W., Adami, G.R., Wei, N., Keyomarsi, K. and Elledge, S.J. (1993). The p21 Cdk-interacting protein Cip1 is a potent inhibitor of G1 cyclin-dependent kinases. *Cell* **75,** 805-816.

Harper, J.W., Elledge, S.J., Keyomarsi, K., Dynlacht, B., Tsai, L.H., Zhang, P*., et al.* (1995). Inhibition of cyclin-dependent kinases by p21. *Molecular biology of the cell* **6,** 387-400.

Harris, R.S. and Liddament, M.T. (2004). Retroviral restriction by APOBEC proteins. *Nature reviews. Immunology* **4,** 868-877.

Hasegawa, K. and Yoshikawa, K. (2008). Necdin regulates p53 acetylation via Sirtuin1 to modulate DNA damage response in cortical neurons. *The Journal of neuroscience : the official journal of the Society for Neuroscience* **28,** 8772-8784.

Hassan, R., Suzu, S., Hiyoshi, M., Takahashi-Makise, N., Ueno, T., Agatsuma, T*., et al.* (2009). Dys-regulated activation of a Src tyroine kinase Hck at the Golgi disturbs N-glycosylation of a cytokine receptor Fms. *Journal of cellular physiology* **221,** 458-468.

Haupt, Y., Maya, R., Kazaz, A. and Oren, M. (1997). Mdm2 promotes the rapid degradation of p53. *Nature* **387,** 296-299.

He, L., He, X., Lim, L.P., de Stanchina, E., Xuan, Z., Liang, Y*., et al.* (2007). A microRNA component of the p53 tumour suppressor network. *Nature* **447,** 1130-1134.

He, J.C., Husain, M., Sunamoto, M., D'Agati, V.D., Klotman, M.E., Iyengar, R. and Klotman, P.E. (2004). Nef stimulates proliferation of glomerular podocytes through activation of Src-dependent Stat3 and MAPK1,2 pathways. *J Clin Invest* **114,** 643-651.

Heigele, A., Schindler, M., Gnanadurai, C.W., Leonard, J.A., Collins, K.L. and Kirchhoff, F. (2012). Down-modulation of CD8alphabeta is a fundamental activity of primate lentiviral Nef proteins. *Journal of virology* **86,** 36-48.

Hellerstein, M., Hanley, M.B., Cesar, D., Siler, S., Papageorgopoulos, C., Wieder, E.*, et al.* (1999). Directly measured kinetics of circulating T lymphocytes in normal and HIV-1-infected humans. *Nat Med* **5,** 83-89.

Hermeking, H., Lengauer, C., Polyak, K., He, T.C., Zhang, L., Thiagalingam, S.*, et al.* (1997). 14-3-3 sigma is a p53-regulated inhibitor of G2/M progression. *Mol Cell* **1,** 3-11.

Herranz, D., Munoz-Martin, M., Canamero, M., Mulero, F., Martinez-Pastor, B., Fernandez-Capetillo, O. and Serrano, M. (2010). Sirt1 improves healthy ageing and protects from metabolic syndrome-associated cancer. *Nature communications* **1,** 3.

HHS. (2012). Panel on Antiretroviral Guidelines for Adults and Adolescents. Guidelines for the use of antiretroviral agents in HIV-1-infected adults and adolescents. Department of Health and Human Services. [WWW document]. URL http://aidsinfo.nih.gov/contentfiles/lvguidelines/AdultandAdolescentGL.pdf

Hiby, S.E., Walker, J.J., O'Shaughnessy K, M., Redman, C.W., Carrington, M., Trowsdale, J. and Moffett, A. (2004). Combinations of maternal KIR and fetal HLA-C genes influence the risk of preeclampsia and reproductive success. *The Journal of experimental medicine* **200,** 957-965.

Hill, A., Jugovic, P., York, I., Russ, G., Bennink, J., Yewdell, J.*, et al.* (1995). Herpes simplex virus turns off the TAP to evade host immunity. *Nature* **375,** 411-415.

Hill, M., Tachedjian, G. and Mak, J. (2005). The packaging and maturation of the HIV-1 Pol proteins. *Current HIV research* **3,** 73-85.

Hirst, J., Barlow, L.D., Francisco, G.C., Sahlender, D.A., Seaman, M.N., Dacks, J.B. and Robinson, M.S. (2011). The fifth adaptor protein complex. *PLoS biology* **9,** e1001170.

Hiyoshi, M., Suzu, S., Yoshidomi, Y., Hassan, R., Harada, H., Sakashita, N.*, et al.* (2008). Interaction between Hck and HIV-1 Nef negatively regulates cell surface expression of M-CSF receptor. *Blood* **111,** 243-250.

Hoeflich, K.P., Luo, J., Rubie, E.A., Tsao, M.S., Jin, O. and Woodgett, J.R. (2000). Requirement for glycogen synthase kinase-3beta in cell survival and NF-kappaB activation. *Nature* **406,** 86-90.

Holder, J.L., Jr., Lotze, T.E., Bacino, C. and Cheung, S.W. (2012). A child with an inherited 0.31 Mb microdeletion of chromosome 14q32.33: Further delineation of a critical region for the 14q32 deletion syndrome. *American journal of medical genetics. Part A* **158A,** 1962-1966.

Hollstein, M., Sidransky, D., Vogelstein, B. and Harris, C.C. (1991). p53 mutations in human cancers. *Science* **253,** 49-53.

Holmes, R.K., Malim, M.H. and Bishop, K.N. (2007). APOBEC-mediated viral restriction: not simply editing? *Trends in biochemical sciences* **32,** 118-128.

Honda, R., Tanaka, H. and Yasuda, H. (1997). Oncoprotein MDM2 is a ubiquitin ligase E3 for tumor suppressor p53. *FEBS letters* **420,** 25-27.

Horio, Y., Hayashi, T., Kuno, A. and Kunimoto, R. (2011). Cellular and molecular effects of sirtuins in health and disease. *Clin Sci (Lond)* **121,** 191-203.

Hrecka, K., Gierszewska, M., Srivastava, S., Kozaczkiewicz, L., Swanson, S.K., Florens, L.*, et al.* (2007). Lentiviral Vpr usurps Cul4-DDB1[VprBP] E3 ubiquitin ligase to modulate cell cycle. *Proc Natl Acad Sci U S A* **104,** 11778-11783.

Hreidarsson, S.J. and Stamberg, J. (1983). Distal monosomy 14 not associated with ring formation. *Journal of medical genetics* **20,** 147-149.

Hu, D.J., Dondero, T.J., Rayfield, M.A., George, J.R., Schochetman, G., Jaffe, H.W.*, et al.* (1996). The emerging genetic diversity of HIV. The importance of global surveillance for diagnostics, research, and prevention. *JAMA : the journal of the American Medical Association* **275,** 210-216.

Huang, J., Perez-Burgos, L., Placek, B.J., Sengupta, R., Richter, M., Dorsey, J.A.*, et al.* (2006). Repression of p53 activity by Smyd2-mediated methylation. *Nature* **444,** 629-632.

Huang, J., Sengupta, R., Espejo, A.B., Lee, M.G., Dorsey, J.A., Richter, M.*, et al.* (2007). p53 is regulated by the lysine demethylase LSD1. *Nature* **449,** 105-108.

Huang, P.H., Mukasa, A., Bonavia, R., Flynn, R.A., Brewer, Z.E., Cavenee, W.K.*, et al.* (2007). Quantitative analysis of EGFRvIII cellular signaling networks reveals a combinatorial therapeutic strategy for glioblastoma. *Proc Natl Acad Sci U S A* **104,** 12867-12872.

Hughes, A.L. and Nei, M. (1988). Pattern of nucleotide substitution at major histocompatibility complex class I loci reveals overdominant selection. *Nature* **335,** 167-170.

Hughes, M.D., Johnson, V.A., Hirsch, M.S., Bremer, J.W., Elbeik, T., Erice, A.*, et al.* (1997). Monitoring plasma HIV-1 RNA levels in addition to CD4+ lymphocyte count improves assessment of antiretroviral therapeutic response. ACTG 241 Protocol Virology Substudy Team. *Annals of internal medicine* **126,** 929-938.

Hung, C.H., Thomas, L., Ruby, C.E., Atkins, K.M., Morris, N.P., Knight, Z.A.*, et al.* (2007). HIV-1 Nef assembles a Src family kinase-ZAP-70/Syk-PI3K cascade to downregulate cell-surface MHC-I. *Cell host & microbe* **1,** 121-133.

Huotari, J. and Helenius, A. (2011). Endosome maturation. *EMBO J* **30,** 3481-3500.

Hupp, T.R., Meek, D.W., Midgley, C.A. and Lane, D.P. (1992). Regulation of the specific DNA binding function of p53. *Cell* **71,** 875-886.

Huppa, J.B. and Davis, M.M. (2003). T-cell-antigen recognition and the immunological synapse. *Nature reviews. Immunology* **3,** 973-983.

Hwang, B.J., Ford, J.M., Hanawalt, P.C. and Chu, G. (1999). Expression of the p48 xeroderma pigmentosum gene is p53-dependent and is involved in global genomic repair. *Proc Natl Acad Sci U S A* **96,** 424-428.

Ikenoue, T., Inoki, K., Zhao, B. and Guan, K.L. (2008). PTEN acetylation modulates its interaction with PDZ domain. *Cancer Res* **68,** 6908-6912.

Imai, S., Armstrong, C.M., Kaeberlein, M. and Guarente, L. (2000). Transcriptional silencing and longevity protein Sir2 is an NAD-dependent histone deacetylase. *Nature* **403,** 795-800.

Inga, A., Storici, F., Darden, T.A. and Resnick, M.A. (2002). Differential transactivation by the p53 transcription factor is highly dependent on p53 level and promoter target sequence. *Mol Cell Biol* **22,** 8612-8625.

Ishido, S., Goto, E., Matsuki, Y. and Ohmura-Hoshino, M. (2009). E3 ubiquitin ligases for MHC molecules. *Current opinion in immunology* **21,** 78-83.

Ishizawar, R. and Parsons, S.J. (2004). c-Src and cooperating partners in human cancer. *Cancer cell* **6,** 209-214.

Ito, A., Lai, C.H., Zhao, X., Saito, S., Hamilton, M.H., Appella, E. and Yao, T.P. (2001). p300/CBP-mediated p53 acetylation is commonly induced by p53-activating agents and inhibited by MDM2. *EMBO J* **20,** 1331-1340.

Iwabuchi, K., Bartel, P.L., Li, B., Marraccino, R. and Fields, S. (1994). Two cellular proteins that bind to wild-type but not mutant p53. *Proc Natl Acad Sci U S A* **91,** 6098-6102.

Iwakuma, T. and Lozano, G. (2007). Crippling p53 activities via knock-in mutations in mouse models. *Oncogene* **26,** 2177-2184.

Iyer, N.G., Ozdag, H. and Caldas, C. (2004). p300/CBP and cancer. *Oncogene* **23,** 4225-4231.

Jabbar, M.A. and Nayak, D.P. (1990). Intracellular interaction of human immunodeficiency virus type 1 (ARV-2) envelope glycoprotein gp160 with CD4 blocks the movement and maturation of CD4 to the plasma membrane. *Journal of virology* **64,** 6297-6304.

Jacks, T., Remington, L., Williams, B.O., Schmitt, E.M., Halachmi, S., Bronson, R.T. and Weinberg, R.A. (1994). Tumor spectrum analysis in p53-mutant mice. *Current biology : CB* **4,** 1-7.

Jackson, R.J., Adnane, J., Coppola, D., Cantor, A., Sebti, S.M. and Pledger, W.J. (2002). Loss of the cell cycle inhibitors p21(Cip1) and p27(Kip1) enhances tumorigenesis in knockout mouse models. *Oncogene* **21,** 8486-8497.

Jackson, L.P., Kelly, B.T., McCoy, A.J., Gaffry, T., James, L.C., Collins, B.M., *et al.* (2010). A large-scale conformational change couples membrane recruitment to cargo binding in the AP2 clathrin adaptor complex. *Cell* **141,** 1220-1229.

Janeway, C.A., Paul Travers, Mark Walport, Mark J. Shlomchik. (2005) Immunobiology The Immune System in Health and Disease New York, New York, Garland Publishing.

Jansson, M., Durant, S.T., Cho, E.C., Sheahan, S., Edelmann, M., Kessler, B. and La Thangue, N.B. (2008). Arginine methylation regulates the p53 response. *Nat Cell Biol* **10,** 1431-1439.

Janzen, N.K., Kim, H.L., Figlin, R.A. and Belldegrun, A.S. (2003). Surveillance after radical or partial nephrectomy for localized renal cell carcinoma and

management of recurrent disease. *The Urologic clinics of North America* **30,** 843-852.

Jarvis, M.A., Jones, T.R., Drummond, D.D., Smith, P.P., Britt, W.J., Nelson, J.A. and Baldick, C.J. (2004). Phosphorylation of human cytomegalovirus glycoprotein B (gB) at the acidic cluster casein kinase 2 site (Ser900) is required for localization of gB to the trans-Golgi network and efficient virus replication. *Journal of virology* **78,** 285-293.

Jay, P., Rougeulle, C., Massacrier, A., Moncla, A., Mattei, M.G., Malzac, P*., et al.* (1997). The human necdin gene, NDN, is maternally imprinted and located in the Prader-Willi syndrome chromosomal region. *Nat Genet* **17,** 357-361.

Jeffers, J.R., Parganas, E., Lee, Y., Yang, C., Wang, J., Brennan, J*., et al.* (2003). Puma is an essential mediator of p53-dependent and -independent apoptotic pathways. *Cancer cell* **4,** 321-328.

Jeffrey, P.D., Gorina, S. and Pavletich, N.P. (1995). Crystal structure of the tetramerization domain of the p53 tumor suppressor at 1.7 angstroms. *Science* **267,** 1498-1502.

Jenkins, P.M., Zhang, L., Thomas, G. and Martens, J.R. (2009). PACS-1 mediates phosphorylation-dependent ciliary trafficking of the cyclic-nucleotide-gated channel in olfactory sensory neurons. *The Journal of neuroscience : the official journal of the Society for Neuroscience* **29,** 10541-10551.

Jenuwein, T. and Allis, C.D. (2001). Translating the histone code. *Science* **293,** 1074-1080.

Jeong, J., Juhn, K., Lee, H., Kim, S.H., Min, B.H., Lee, K.M*., et al.* (2007). SIRT1 promotes DNA repair activity and deacetylation of Ku70. *Experimental & molecular medicine* **39,** 8-13.

Jia, X., Singh, R., Homann, S., Yang, H., Guatelli, J. and Xiong, Y. (2012). Structural basis of evasion of cellular adaptive immunity by HIV-1 Nef. *Nature structural & molecular biology* **19,** 701-706.

Jin, S., Martinek, S., Joo, W.S., Wortman, J.R., Mirkovic, N., Sali, A*., et al.* (2000). Identification and characterization of a p53 homologue in Drosophila melanogaster. *Proc Natl Acad Sci U S A* **97,** 7301-7306.

Jin, Y.J., Cai, C.Y., Zhang, X. and Burakoff, S.J. (2008). Lysine 144, a ubiquitin attachment site in HIV-1 Nef, is required for Nef-mediated CD4 down-regulation. *J Immunol* **180,** 7878-7886.

Jin, Y.J., Cai, C.Y., Zhang, X., Zhang, H.T., Hirst, J.A. and Burakoff, S.J. (2005). HIV Nef-mediated CD4 down-regulation is adaptor protein complex 2 dependent. *J Immunol* **175,** 3157-3164.

Johansson, A.C., Appelqvist, H., Nilsson, C., Kagedal, K., Roberg, K. and Ollinger, K. (2010). Regulation of apoptosis-associated lysosomal membrane permeabilization. *Apoptosis* **15,** 527-540.

Johnson, T.M., Hammond, E.M., Giaccia, A. and Attardi, L.D. (2005). The p53QS transactivation-deficient mutant shows stress-specific apoptotic activity and induces embryonic lethality. *Nat Genet* **37,** 145-152.

Jones, B.G., Thomas, L., Molloy, S.S., Thulin, C.D., Fry, M.D., Walsh, K.A. and Thomas, G. (1995). Intracellular trafficking of furin is modulated by the phosphorylation state of a casein kinase II site in its cytoplasmic tail. *EMBO J* **14,** 5869-5883.

Jope, R.S. and Johnson, G.V. (2004). The glamour and gloom of glycogen synthase kinase-3. *Trends in biochemical sciences* **29,** 95-102.

Juven, T., Barak, Y., Zauberman, A., George, D.L. and Oren, M. (1993). Wild type p53 can mediate sequence-specific transactivation of an internal promoter within the mdm2 gene. *Oncogene* **8,** 3411-3416.

Kaeberlein, M., McVey, M. and Guarente, L. (1999). The SIR2/3/4 complex and SIR2 alone promote longevity in Saccharomyces cerevisiae by two different mechanisms. *Genes Dev* **13,** 2570-2580.

Kaelin, W.G., Jr. (2008). Kidney cancer: now available in a new flavor. *Cancer cell* **14,** 423-424.

Kaeser, M.D. and Iggo, R.D. (2002). Chromatin immunoprecipitation analysis fails to support the latency model for regulation of p53 DNA binding activity in vivo. *Proc Natl Acad Sci U S A* **99,** 95-100.

Kahlenberg, M.S., Stoler, D.L., Basik, M., Petrelli, N.J., Rodriguez-Bigas, M. and Anderson, G.R. (1996). p53 tumor suppressor gene status and the degree of genomic instability in sporadic colorectal cancers. *Journal of the National Cancer Institute* **88,** 1665-1670.

Kahn, J.O. and Walker, B.D. (1998). Acute human immunodeficiency virus type 1 infection. *N Engl J Med* **339,** 33-39.

Kahraman, A., Barreyro, F.J., Bronk, S.F., Werneburg, N.W., Mott, J.L., Akazawa, Y.*, et al.* (2008). TRAIL mediates liver injury by the innate immune system in the bile duct-ligated mouse. *Hepatology* **47,** 1317-1330.

Kalergis, A.M., Boucheron, N., Doucey, M.A., Palmieri, E., Goyarts, E.C., Vegh, Z.*, et al.* (2001). Efficient T cell activation requires an optimal dwell-time of interaction between the TCR and the pMHC complex. *Nature immunology* **2,** 229-234.

Kamel, C., Abrol, M., Jardine, K., He, X. and McBurney, M.W. (2006). SirT1 fails to affect p53-mediated biological functions. *Aging cell* **5,** 81-88.

Kamijo, T., Bodner, S., van de Kamp, E., Randle, D.H. and Sherr, C.J. (1999). Tumor spectrum in ARF-deficient mice. *Cancer Res* **59,** 2217-2222.

Kang, T.W. and Han, K.T. (2006). Genomic DNA Aberration Profiles in Paraffin-Embedded Breast Tumor Using Array-CHG on c-erbB-2 Overexpression. *J Korean Surg Soc* **79,** 265.

Kao, S.Y., Calman, A.F., Luciw, P.A. and Peterlin, B.M. (1987). Anti-termination of transcription within the long terminal repeat of HIV-1 by tat gene product. *Nature* **330,** 489-493.

Karapetis CS, C.P., Leighl NB, Durbin-Johnson B, O'Neill V, Spigel DR (2010) Phase II study of PRO95780 plus paclitaxel, carboplatin, and bevacizumab (PCB) in non-small cell lung cancer (NSCLC). *J Clin Oncol***28**, Suppl:7s. Abstract 7535.

Kasper, M.R. and Collins, K.L. (2003). Nef-mediated disruption of HLA-A2 transport to the cell surface in T cells. *Journal of virology* **77,** 3041-3049.

Kasper, M.R., Roeth, J.F., Williams, M., Filzen, T.M., Fleis, R.I. and Collins, K.L. (2005). HIV-1 Nef disrupts antigen presentation early in the secretory pathway. *J Biol Chem* **280,** 12840-12848.

Kastan, M.B., Onyekwere, O., Sidransky, D., Vogelstein, B. and Craig, R.W. (1991). Participation of p53 protein in the cellular response to DNA damage. *Cancer Res* **51,** 6304-6311.

Kaufmann, G.R., Cunningham, P., Kelleher, A.D., Zaunders, J., Carr, A., Vizzard, J.*, et al.* (1998). Patterns of viral dynamics during primary human immunodeficiency virus type 1 infection. The Sydney Primary HIV Infection Study Group. *The Journal of infectious diseases* **178,** 1812-1815.

Kay, D.G., Yue, P., Hanna, Z., Jothy, S., Tremblay, E. and Jolicoeur, P. (2002). Cardiac disease in transgenic mice expressing human immunodeficiency virus-1 nef in cells of the immune system. *Am J Pathol* **161,** 321-335.

Keele, B.F., Giorgi, E.E., Salazar-Gonzalez, J.F., Decker, J.M., Pham, K.T., Salazar, M.G.*, et al.* (2008). Identification and characterization of transmitted and early founder virus envelopes in primary HIV-1 infection. *Proc Natl Acad Sci U S A* **105,** 7552-7557.

Keele, B.F., Van Heuverswyn, F., Li, Y., Bailes, E., Takehisa, J., Santiago, M.L.*, et al.* (2006). Chimpanzee reservoirs of pandemic and nonpandemic HIV-1. *Science* **313,** 523-526.

Kerkau, T., Schmitt-Landgraf, R., Schimpl, A. and Wecker, E. (1989). Downregulation of HLA class I antigens in HIV-1-infected cells. *AIDS research and human retroviruses* **5,** 613-620.

Kern, S.E., Kinzler, K.W., Bruskin, A., Jarosz, D., Friedman, P., Prives, C. and Vogelstein, B. (1991). Identification of p53 as a sequence-specific DNA-binding protein. *Science* **252,** 1708-1711.

Kerppola, T.K. (2008). Bimolecular fluorescence complementation (BiFC) analysis as a probe of protein interactions in living cells. *Annual review of biophysics* **37,** 465-487.

Kestler, H.W., 3rd, Ringler, D.J., Mori, K., Panicali, D.L., Sehgal, P.K., Daniel, M.D. and Desrosiers, R.C. (1991). Importance of the nef gene for maintenance of high virus loads and for development of AIDS. *Cell* **65,** 651-662.

Kim, E., Rohaly, G., Heinrichs, S., Gimnopoulos, D., Meissner, H. and Deppert, W. (1999). Influence of promoter DNA topology on sequence-specific DNA binding and transactivation by tumor suppressor p53. *Oncogene* **18,** 7310-7318.

Kim, E.J., Kho, J.H., Kang, M.R. and Um, S.J. (2007). Active regulator of SIRT1 cooperates with SIRT1 and facilitates suppression of p53 activity. *Mol Cell* **28,** 277-290.

Kim, J.E., Chen, J. and Lou, Z. (2008). DBC1 is a negative regulator of SIRT1. *Nature* **451,** 583-586.

Kim, S.C., Sprung, R., Chen, Y., Xu, Y., Ball, H., Pei, J.*, et al.* (2006). Substrate and functional diversity of lysine acetylation revealed by a proteomics survey. *Mol Cell* **23,** 607-618.

Kim, W.Y. and Kaelin, W.G. (2004). Role of VHL gene mutation in human cancer. *Journal of clinical oncology : official journal of the American Society of Clinical Oncology* **22,** 4991-5004.

Kirchhoff, F. (2009). Is the high virulence of HIV-1 an unfortunate coincidence of primate lentiviral evolution? *Nature reviews. Microbiology* **7,** 467-476.

Kirchhoff, F., Greenough, T.C., Brettler, D.B., Sullivan, J.L. and Desrosiers, R.C. (1995). Brief report: absence of intact nef sequences in a long-term survivor with nonprogressive HIV-1 infection. *N Engl J Med* **332,** 228-232.

Kitahata, M.M., Gange, S.J., Abraham, A.G., Merriman, B., Saag, M.S., Justice, A.C.*, et al.* (2009). Effect of early versus deferred antiretroviral therapy for HIV on survival. *N Engl J Med* **360,** 1815-1826.

Knights, C.D., Catania, J., Di Giovanni, S., Muratoglu, S., Perez, R., Swartzbeck, A.*, et al.* (2006). Distinct p53 acetylation cassettes differentially influence gene-expression patterns and cell fate. *J Cell Biol* **173,** 533-544.

Koblin, B.A., van Benthem, B.H., Buchbinder, S.P., Ren, L., Vittinghoff, E., Stevens, C.E.*, et al.* (1999). Long-term survival after infection with human immunodeficiency virus type 1 (HIV-1) among homosexual men in hepatitis B vaccine trial cohorts in Amsterdam, New York City, and San Francisco, 1978-1995. *American journal of epidemiology* **150,** 1026-1030.

Komiya, T., Hosono, Y., Hirashima, T., Masuda, N., Yasumitsu, T., Nakagawa, K.*, et al.* (1997). p21 expression as a predictor for favorable prognosis in squamous cell carcinoma of the lung. *Clin Cancer Res* **3,** 1831-1835.

Kondo, K., Klco, J., Nakamura, E., Lechpammer, M. and Kaelin, W.G., Jr. (2002). Inhibition of HIF is necessary for tumor suppression by the von Hippel-Lindau protein. *Cancer cell* **1,** 237-246.

Koot, M., Keet, I.P., Vos, A.H., de Goede, R.E., Roos, M.T., Coutinho, R.A.*, et al.* (1993). Prognostic value of HIV-1 syncytium-inducing phenotype for rate of CD4+ cell depletion and progression to AIDS. *Annals of internal medicine* **118,** 681-688.

Kottgen, M., Benzing, T., Simmen, T., Tauber, R., Buchholz, B., Feliciangeli, S.*, et al.* (2005). Trafficking of TRPP2 by PACS proteins represents a novel mechanism of ion channel regulation. *EMBO J* **24,** 705-716.

Koulen, P., Cai, Y., Geng, L., Maeda, Y., Nishimura, S., Witzgall, R.*, et al.* (2002). Polycystin-2 is an intracellular calcium release channel. *Nat Cell Biol* **4,** 191-197.

Krummel, K.A., Lee, C.J., Toledo, F. and Wahl, G.M. (2005). The C-terminal lysines fine-tune P53 stress responses in a mouse model but are not required for stability control or transactivation. *Proc Natl Acad Sci U S A* **102,** 10188-10193.

Kruse, J.P. and Gu, W. (2008). SnapShot: p53 posttranslational modifications. *Cell* **133,** 930-930 e931.

Kruse, J.P. and Gu, W. (2009). Modes of p53 regulation. *Cell* **137,** 609-622.
Kubbutat, M.H., Jones, S.N. and Vousden, K.H. (1997). Regulation of p53 stability by Mdm2. *Nature* **387,** 299-303.
Kume, S., Haneda, M., Kanasaki, K., Sugimoto, T., Araki, S., Isshiki, K.*, et al.* (2007). SIRT1 inhibits transforming growth factor beta-induced apoptosis in glomerular mesangial cells via Smad7 deacetylation. *J Biol Chem* **282,** 151-158.
la Cour, T., Kiemer, L., Molgaard, A., Gupta, R., Skriver, K. and Brunak, S. (2004). Analysis and prediction of leucine-rich nuclear export signals. *Protein engineering, design & selection : PEDS* **17,** 527-536.
Lam, J.S., Leppert, J.T., Figlin, R.A. and Belldegrun, A.S. (2005). Surveillance following radical or partial nephrectomy for renal cell carcinoma. *Current urology reports* **6,** 7-18.
Lama, J., Mangasarian, A. and Trono, D. (1999). Cell-surface expression of CD4 reduces HIV-1 infectivity by blocking Env incorporation in a Nef- and Vpu-inhibitable manner. *Current biology : CB* **9,** 622-631.
Landry, J., Sutton, A., Tafrov, S.T., Heller, R.C., Stebbins, J., Pillus, L. and Sternglanz, R. (2000). The silencing protein SIR2 and its homologs are NAD-dependent protein deacetylases. *Proc Natl Acad Sci U S A* **97,** 5807-5811.
Lane, D.P. (1992). Cancer. p53, guardian of the genome. *Nature* **358,** 15-16.
Lane, D.P. and Crawford, L.V. (1979). T antigen is bound to a host protein in SV40-transformed cells. *Nature* **278,** 261-263.
Langley, E., Pearson, M., Faretta, M., Bauer, U.M., Frye, R.A., Minucci, S.*, et al.* (2002). Human SIR2 deacetylates p53 and antagonizes PML/p53-induced cellular senescence. *EMBO J* **21,** 2383-2396.
Laptenko, O. and Prives, C. (2006). Transcriptional regulation by p53: one protein, many possibilities. *Cell Death Differ* **13,** 951-961.
Larsen, J.E., Massol, R.H., Nieland, T.J. and Kirchhausen, T. (2004). HIV Nef-mediated major histocompatibility complex class I down-modulation is independent of Arf6 activity. *Mol Biol Cell* **15,** 323-331.
Lasky, L.A., Nakamura, G., Smith, D.H., Fennie, C., Shimasaki, C., Patzer, E.*, et al.* (1987). Delineation of a region of the human immunodeficiency virus type 1 gp120 glycoprotein critical for interaction with the CD4 receptor. *Cell* **50,** 975-985.
Le Gall, S., Buseyne, F., Trocha, A., Walker, B.D., Heard, J.M. and Schwartz, O. (2000). Distinct trafficking pathways mediate Nef-induced and clathrin-dependent major histocompatibility complex class I down-regulation. *Journal of virology* **74,** 9256-9266.
Le Gall, S., Erdtmann, L., Benichou, S., Berlioz-Torrent, C., Liu, L., Benarous, R.*, et al.* (1998). Nef interacts with the mu subunit of clathrin adaptor complexes and reveals a cryptic sorting signal in MHC I molecules. *Immunity* **8,** 483-495.

Lee, C.H., Leung, B., Lemmon, M.A., Zheng, J., Cowburn, D., Kuriyan, J. and Saksela, K. (1995). A single amino acid in the SH3 domain of Hck determines its high affinity and specificity in binding to HIV-1 Nef protein. *EMBO J* **14,** 5006-5015.

Lee, C.H., Saksela, K., Mirza, U.A., Chait, B.T. and Kuriyan, J. (1996). Crystal structure of the conserved core of HIV-1 Nef complexed with a Src family SH3 domain. *Cell* **85,** 931-942.

Lee, W., Harvey, T.S., Yin, Y., Yau, P., Litchfield, D. and Arrowsmith, C.H. (1994). Solution structure of the tetrameric minimum transforming domain of p53. *Nature structural biology* **1,** 877-890.

Lefrere, J.J., Morand-Joubert, L., Mariotti, M., Bludau, H., Burghoffer, B., Petit, J.C. and Roudot-Thoraval, F. (1997). Even individuals considered as long-term nonprogressors show biological signs of progression after 10 years of human immunodeficiency virus infection. *Blood* **90,** 1133-1140.

Leiser, S.F. and Kaeberlein, M. (2010). A role for SIRT1 in the hypoxic response. *Mol Cell* **38,** 779-780.

Lenassi, M., Cagney, G., Liao, M., Vaupotic, T., Bartholomeeusen, K., Cheng, Y*., et al.* (2010). HIV Nef is secreted in exosomes and triggers apoptosis in bystander CD4+ T cells. *Traffic* **11,** 110-122.

Leng, R.P., Lin, Y., Ma, W., Wu, H., Lemmers, B., Chung, S*., et al.* (2003). Pirh2, a p53-induced ubiquitin-protein ligase, promotes p53 degradation. *Cell* **112,** 779-791.

Leonard, J.A., Filzen, T., Carter, C.C., Schaefer, M. and Collins, K.L. (2011). HIV-1 Nef disrupts intracellular trafficking of major histocompatibility complex class I, CD4, CD8, and CD28 by distinct pathways that share common elements. *Journal of virology* **85,** 6867-6881.

Lerner, E.C. and Smithgall, T.E. (2002). SH3-dependent stimulation of Src-family kinase autophosphorylation without tail release from the SH2 domain in vivo. *Nature structural biology* **9,** 365-369.

Leslie, A.J., Pfafferott, K.J., Chetty, P., Draenert, R., Addo, M.M., Feeney, M*., et al.* (2004). HIV evolution: CTL escape mutation and reversion after transmission. *Nat Med* **10,** 282-289.

Levine, A.J. (1997). p53, the cellular gatekeeper for growth and division. *Cell* **88,** 323-331.

Levine, A.J., Momand, J. and Finlay, C.A. (1991). The p53 tumour suppressor gene. *Nature* **351,** 453-456.

Lewis, M.J., Balamurugan, A., Ohno, A., Kilpatrick, S., Ng, H.L. and Yang, O.O. (2008). Functional adaptation of Nef to the immune milieu of HIV-1 infection in vivo. *J Immunol* **180,** 4075-4081.

Li, H., Collado, M., Villasante, A., Strati, K., Ortega, S., Canamero, M*., et al.* (2009a). The Ink4/Arf locus is a barrier for iPS cell reprogramming. *Nature* **460,** 1136-1139.

Li, K. and Luo, J. (2011a). The role of SIRT1 in tumorigenesis. *North American journal of medicine & science* **4,** 104-106.

Li, M., Brooks, C.L., Kon, N. and Gu, W. (2004). A dynamic role of HAUSP in the p53-Mdm2 pathway. *Mol Cell* **13,** 879-886.
Li, M., Chen, D., Shiloh, A., Luo, J., Nikolaev, A.Y., Qin, J. and Gu, W. (2002a). Deubiquitination of p53 by HAUSP is an important pathway for p53 stabilization. *Nature* **416,** 648-653.
Li, M., Luo, J., Brooks, C.L. and Gu, W. (2002b). Acetylation of p53 inhibits its ubiquitination by Mdm2. *J Biol Chem* **277,** 50607-50611.
Li, R., Waga, S., Hannon, G.J., Beach, D. and Stillman, B. (1994a). Differential effects by the p21 CDK inhibitor on PCNA-dependent DNA replication and repair. *Nature* **371,** 534-537.
Li, S.S. (2005b). Specificity and versatility of SH3 and other proline-recognition domains: structural basis and implications for cellular signal transduction. *Biochem J* **390,** 641-653.
Li, T., Kon, N., Jiang, L., Tan, M., Ludwig, T., Zhao, Y*., et al.* (2012). Tumor Suppression in the Absence of p53-Mediated Cell-Cycle Arrest, Apoptosis, and Senescence. *Cell* **149,** 1269-1283.
Li, X., Wu, L., Corsa, C.A., Kunkel, S. and Dou, Y. (2009b). Two mammalian MOF complexes regulate transcription activation by distinct mechanisms. *Mol Cell* **36,** 290-301.
Li, X., Zhang, S., Blander, G., Tse, J.G., Krieger, M. and Guarente, L. (2007). SIRT1 deacetylates and positively regulates the nuclear receptor LXR. *Mol Cell* **28,** 91-106.
Li, Y., Jenkins, C.W., Nichols, M.A. and Xiong, Y. (1994b). Cell cycle expression and p53 regulation of the cyclin-dependent kinase inhibitor p21. *Oncogene* **9,** 2261-2268.
Li, Y., Wright, J.M., Qian, F., Germino, G.G. and Guggino, W.B. (2005). Polycystin 2 interacts with type I inositol 1,4,5-trisphosphate receptor to modulate intracellular Ca2+ signaling. *J Biol Chem* **280,** 41298-41306.
Li, Y., Xu, S., Giles, A., Nakamura, K., Lee, J.W., Hou, X*., et al.* (2011b). Hepatic overexpression of SIRT1 in mice attenuates endoplasmic reticulum stress and insulin resistance in the liver. *FASEB journal : official publication of the Federation of American Societies for Experimental Biology* **25,** 1664-1679.
Li, Y., Xu, W., McBurney, M.W. and Longo, V.D. (2008). SirT1 inhibition reduces IGF-I/IRS-2/Ras/ERK1/2 signaling and protects neurons. *Cell metabolism* **8,** 38-48.
Liang, F., Kume, S. and Koya, D. (2009). SIRT1 and insulin resistance. *Nature reviews. Endocrinology* **5,** 367-373.
Lieberman, J. (2003). The ABCs of granule-mediated cytotoxicity: new weapons in the arsenal. *Nature reviews. Immunology* **3,** 361-370.
Lim, J.H., Lee, Y.M., Chun, Y.S., Chen, J., Kim, J.E. and Park, J.W. (2010). Sirtuin 1 modulates cellular responses to hypoxia by deacetylating hypoxia-inducible factor 1alpha. *Mol Cell* **38,** 864-878.
Lin, D., Shields, M.T., Ullrich, S.J., Appella, E. and Mercer, W.E. (1992). Growth arrest induced by wild-type p53 protein blocks cells prior to or near the

restriction point in late G1 phase. *Proc Natl Acad Sci U S A* **89,** 9210-9214.

Lin, S.J., Defossez, P.A. and Guarente, L. (2000). Requirement of NAD and SIR2 for life-span extension by calorie restriction in Saccharomyces cerevisiae. *Science* **289,** 2126-2128.

Lindwasser, O.W., Smith, W.J., Chaudhuri, R., Yang, P., Hurley, J.H. and Bonifacino, J.S. (2008). A diacidic motif in human immunodeficiency virus type 1 Nef is a novel determinant of binding to AP-2. *Journal of virology* **82,** 1166-1174.

Linzer, D.I. and Levine, A.J. (1979). Characterization of a 54K dalton cellular SV40 tumor antigen present in SV40-transformed cells and uninfected embryonal carcinoma cells. *Cell* **17,** 43-52.

Lippincott-Schwartz, J. and Liu, W. (2006). Insights into COPI coat assembly and function in living cells. *Trends Cell Biol* **16,** e1-4.

Litchfield, D.W. (2003). Protein kinase CK2: structure, regulation and role in cellular decisions of life and death. *Biochem J* **369,** 1-15.

Liu, J., Chung, H.J., Vogt, M., Jin, Y., Malide, D., He, L.*, et al.* (2011a). JTV1 co-activates FBP to induce USP29 transcription and stabilize p53 in response to oxidative stress. *EMBO J* **30,** 846-858.

Liu, L., Scolnick, D.M., Trievel, R.C., Zhang, H.B., Marmorstein, R., Halazonetis, T.D. and Berger, S.L. (1999). p53 sites acetylated in vitro by PCAF and p300 are acetylated in vivo in response to DNA damage. *Mol Cell Biol* **19,** 1202-1209.

Liu, L.X., Heveker, N., Fackler, O.T., Arold, S., Le Gall, S., Janvier, K.*, et al.* (2000). Mutation of a conserved residue (D123) required for oligomerization of human immunodeficiency virus type 1 Nef protein abolishes interaction with human thioesterase and results in impairment of Nef biological functions. *Journal of virology* **74,** 5310-5319.

Liu, R., Paxton, W.A., Choe, S., Ceradini, D., Martin, S.R., Horuk, R.*, et al.* (1996). Homozygous defect in HIV-1 coreceptor accounts for resistance of some multiply-exposed individuals to HIV-1 infection. *Cell* **86,** 367-377.

Liu, T., Liu, P.Y. and Marshall, G.M. (2009). The critical role of the class III histone deacetylase SIRT1 in cancer. *Cancer Res* **69,** 1702-1705.

Liu, X., Wang, D., Zhao, Y., Tu, B., Zheng, Z., Wang, L.*, et al.* (2011b). Methyltransferase Set7/9 regulates p53 activity by interacting with Sirtuin 1 (SIRT1). *Proc Natl Acad Sci U S A* **108,** 1925-1930.

Liu, Y., Bishop, A., Witucki, L., Kraybill, B., Shimizu, E., Tsien, J.*, et al.* (1999). Structural basis for selective inhibition of Src family kinases by PP1. *Chemistry & biology* **6,** 671-678.

Liu, Y., Lagowski, J.P., Vanderbeek, G.E. and Kulesz-Martin, M.F. (2004). Facilitated search for specific genomic targets by p53 C-terminal basic DNA binding domain. *Cancer biology & therapy* **3,** 1102-1108.

Lohrum, M.A., Ludwig, R.L., Kubbutat, M.H., Hanlon, M. and Vousden, K.H. (2003). Regulation of HDM2 activity by the ribosomal protein L11. *Cancer cell* **3,** 577-587.

Lombardo, L.J., Lee, F.Y., Chen, P., Norris, D., Barrish, J.C., Behnia, K.*, et al.* (2004). Discovery of N-(2-chloro-6-methyl- phenyl)-2-(6-(4-(2-hydroxyethyl)- piperazin-1-yl)-2-methylpyrimidin-4- ylamino)thiazole-5-carboxamide (BMS-354825), a dual Src/Abl kinase inhibitor with potent antitumor activity in preclinical assays. *Journal of medicinal chemistry* **47,** 6658-6661.

Longworth, M.S. and Laimins, L.A. (2006). Histone deacetylase 3 localizes to the plasma membrane and is a substrate of Src. *Oncogene* **25,** 4495-4500.

Lowe, S.W. and Ruley, H.E. (1993a). Stabilization of the p53 tumor suppressor is induced by adenovirus 5 E1A and accompanies apoptosis. *Genes Dev* **7,** 535-545.

Lowe, S.W., Schmitt, E.M., Smith, S.W., Osborne, B.A. and Jacks, T. (1993b). P53 is Required for Radiation-Induced Apoptosis in Mouse Thymocytes. *Nature* **362,** 847-849.

Lowe, S.W. and Sherr, C.J. (2003). Tumor suppression by Ink4a-Arf: progress and puzzles. *Current opinion in genetics & development* **13,** 77-83.

Lozano, G. (2010). Mouse models of p53 functions. *Cold Spring Harbor perspectives in biology* **2,** a001115.

Lu, H. and Levine, A.J. (1995). Human TAFII31 protein is a transcriptional coactivator of the p53 protein. *Proc Natl Acad Sci U S A* **92,** 5154-5158.

Lund, I.K., Hansen, J.A., Andersen, H.S., Moller, N.P. and Billestrup, N. (2005). Mechanism of protein tyrosine phosphatase 1B-mediated inhibition of leptin signalling. *Journal of molecular endocrinology* **34,** 339-351.

Luo, J., Nikolaev, A.Y., Imai, S., Chen, D., Su, F., Shiloh, A.*, et al.* (2001). Negative control of p53 by Sir2alpha promotes cell survival under stress. *Cell* **107,** 137-148.

Luo, J., Su, F., Chen, D., Shiloh, A. and Gu, W. (2000). Deacetylation of p53 modulates its effect on cell growth and apoptosis. *Nature* **408,** 377-381.

Luo, T., Anderson, S.J. and Garcia, J.V. (1996). Inhibition of Nef- and phorbol ester-induced CD4 degradation by macrolide antibiotics. *Journal of virology* **70,** 1527-1534.

Luzio, J.P., Pryor, P.R. and Bright, N.A. (2007). Lysosomes: fusion and function. *Nature reviews. Molecular cell biology* **8,** 622-632.

MacPherson, D., Kim, J., Kim, T., Rhee, B.K., Van Oostrom, C.T., DiTullio, R.A.*, et al.* (2004). Defective apoptosis and B-cell lymphomas in mice with p53 point mutation at Ser 23. *EMBO J* **23,** 3689-3699.

Maddocks, O.D. and Vousden, K.H. (2011). Metabolic regulation by p53. *J Mol Med (Berl)* **89,** 237-245.

Mahlknecht, U. and Voelter-Mahlknecht, S. (2009). Fluorescence in situ hybridization and chromosomal organization of the sirtuin 4 gene (Sirt4) in the mouse. *Biochem Biophys Res Commun* **382,** 685-690.

Malim, M.H. and Emerman, M. (2008). HIV-1 accessory proteins--ensuring viral survival in a hostile environment. *Cell host & microbe* **3,** 388-398.

Malumbres, M. and Barbacid, M. (2001). To cycle or not to cycle: a critical decision in cancer. *Nature reviews. Cancer* **1,** 222-231.

Malumbres, M. and Barbacid, M. (2005). Mammalian cyclin-dependent kinases. *Trends in biochemical sciences* **30,** 630-641.

Malumbres, M. and Barbacid, M. (2009). Cell cycle, CDKs and cancer: a changing paradigm. *Nature reviews.Cancer* **9,** 153-166.

Mangasarian, A., Piguet, V., Wang, J.K., Chen, Y.L. and Trono, D. (1999). Nef-induced CD4 and major histocompatibility complex class I (MHC-I) down-regulation are governed by distinct determinants: N-terminal alpha helix and proline repeat of Nef selectively regulate MHC-I trafficking. *Journal of virology* **73,** 1964-1973.

Mansouri, M., Douglas, J., Rose, P.P., Gouveia, K., Thomas, G., Means, R.E.*, et al.* (2006). Kaposi sarcoma herpesvirus K5 removes CD31/PECAM from endothelial cells. *Blood* **108,** 1932-1940.

Margottin, F., Bour, S.P., Durand, H., Selig, L., Benichou, S., Richard, V.*, et al.* (1998). A novel human WD protein, h-beta TrCp, that interacts with HIV-1 Vpu connects CD4 to the ER degradation pathway through an F-box motif. *Mol Cell* **1,** 565-574.

Marine, J.C., Francoz, S., Maetens, M., Wahl, G., Toledo, F. and Lozano, G. (2006). Keeping p53 in check: essential and synergistic functions of Mdm2 and Mdm4. *Cell Death Differ* **13,** 927-934.

Marine, J.C. and Jochemsen, A.G. (2005). Mdmx as an essential regulator of p53 activity. *Biochem Biophys Res Commun* **331,** 750-760.

Marlink, R., Kanki, P., Thior, I., Travers, K., Eisen, G., Siby, T.*, et al.* (1994). Reduced rate of disease development after HIV-2 infection as compared to HIV-1. *Science* **265,** 1587-1590.

Marras, D., Bruggeman, L.A., Gao, F., Tanji, N., Mansukhani, M.M., Cara, A.*, et al.* (2002). Replication and compartmentalization of HIV-1 in kidney epithelium of patients with HIV-associated nephropathy. *Nat Med* **8,** 522-526.

Martin-Caballero, J., Flores, J.M., Garcia-Palencia, P. and Serrano, M. (2001). Tumor susceptibility of p21(Waf1/Cip1)-deficient mice. *Cancer research* **61,** 6234-6238.

Matsubara, T., Ikeda, F., Hata, K., Nakanishi, M., Okada, M., Yasuda, H.*, et al.* (2010). Cbp recruitment of Csk into lipid rafts is critical to c-Src kinase activity and bone resorption in osteoclasts. *Journal of bone and mineral research : the official journal of the American Society for Bone and Mineral Research* **25,** 1068-1076.

Matsuda, D., Nakayama, Y., Horimoto, S., Kuga, T., Ikeda, K., Kasahara, K. and Yamaguchi, N. (2006). Involvement of Golgi-associated Lyn tyrosine kinase in the translocation of annexin II to the endoplasmic reticulum under oxidative stress. *Exp Cell Res* **312,** 1205-1217.

Maurin, M.L., Brisset, S., Le Lorc'h, M., Poncet, V., Trioche, P., Aboura, A.*, et al.* (2006). Terminal 14q32.33 deletion: genotype-phenotype correlation. *American journal of medical genetics. Part A* **140,** 2324-2329.

May, M., Sterne, J.A., Sabin, C., Costagliola, D., Justice, A.C., Thiebaut, R.*, et al.* (2007). Prognosis of HIV-1-infected patients up to 5 years after initiation of HAART: collaborative analysis of prospective studies. *AIDS* **21,** 1185-1197.

McCutchan, F.E. (2006). Global epidemiology of HIV. *Journal of medical virology* **78 Suppl 1,** S7-S12.

McKenzie, K.E., Siva, A., Maier, S., Runnebaum, I.B., Seshadri, R. and Sukumar, S. (1997). Altered WAF1 genes do not play a role in abnormal cell cycle regulation in breast cancers lacking p53 mutations. *Clin Cancer Res* **3,** 1669-1673.

McLure, K.G. and Lee, P.W. (1998). How p53 binds DNA as a tetramer. *EMBO J* **17,** 3342-3350.

McMahon, H.T. and Mills, I.G. (2004). COP and clathrin-coated vesicle budding: different pathways, common approaches. *Current opinion in cell biology* **16,** 379-391.

Means, R.E., Lang, S.M. and Jung, J.U. (2007). The Kaposi's sarcoma-associated herpesvirus K5 E3 ubiquitin ligase modulates targets by multiple molecular mechanisms. *Journal of virology* **81,** 6573-6583.

Meek, D.W. and Anderson, C.W. (2009). Posttranslational modification of p53: cooperative integrators of function. *Cold Spring Harbor perspectives in biology* **1,** a000950.

Mehle, A., Goncalves, J., Santa-Marta, M., McPike, M. and Gabuzda, D. (2004). Phosphorylation of a novel SOCS-box regulates assembly of the HIV-1 Vif-Cul5 complex that promotes APOBEC3G degradation. *Genes Dev* **18,** 2861-2866.

Melchior, F. and Hengst, L. (2002). SUMO-1 and p53. *Cell Cycle* **1,** 245-249.

Mellman, I. and Warren, G. (2000). The road taken: past and future foundations of membrane traffic. *Cell* **100,** 99-112.

Mellors, J.W., Kingsley, L.A., Rinaldo, C.R., Jr., Todd, J.A., Hoo, B.S., Kokka, R.P. and Gupta, P. (1995). Quantitation of HIV-1 RNA in plasma predicts outcome after seroconversion. *Annals of internal medicine* **122,** 573-579.

Mellors, J.W., Rinaldo, C.R., Jr., Gupta, P., White, R.M., Todd, J.A. and Kingsley, L.A. (1996). Prognosis in HIV-1 infection predicted by the quantity of virus in plasma. *Science* **272,** 1167-1170.

Mettenleiter, T.C., Klupp, B.G. and Granzow, H. (2006). Herpesvirus assembly: a tale of two membranes. *Current opinion in microbiology* **9,** 423-429.

Michael, D. and Oren, M. (2003). The p53-Mdm2 module and the ubiquitin system. *Seminars in cancer biology* **13,** 49-58.

Michel, N., Allespach, I., Venzke, S., Fackler, O.T. and Keppler, O.T. (2005). The Nef protein of human immunodeficiency virus establishes superinfection

immunity by a dual strategy to downregulate cell-surface CCR5 and CD4. *Current biology : CB* **15,** 714-723.

Michishita, E., Park, J.Y., Burneskis, J.M., Barrett, J.C. and Horikawa, I. (2005). Evolutionarily conserved and nonconserved cellular localizations and functions of human SIRT proteins. *Mol Biol Cell* **16,** 4623-4635.

Migliorini, D., Lazzerini Denchi, E., Danovi, D., Jochemsen, A., Capillo, M., Gobbi, A.*, et al.* (2002). Mdm4 (Mdmx) regulates p53-induced growth arrest and neuronal cell death during early embryonic mouse development. *Mol Cell Biol* **22,** 5527-5538.

Migueles, S.A., Laborico, A.C., Imamichi, H., Shupert, W.L., Royce, C., McLaughlin, M.*, et al.* (2003). The differential ability of HLA B*5701+ long-term nonprogressors and progressors to restrict human immunodeficiency virus replication is not caused by loss of recognition of autologous viral gag sequences. *Journal of virology* **77,** 6889-6898.

Mihara, M., Erster, S., Zaika, A., Petrenko, O., Chittenden, T., Pancoska, P. and Moll, U.M. (2003). P53 has a Direct Apoptogenic Role at the Mitochondria. *Molecular cell* **11,** 577-590.

Min, S.W., Cho, S.H., Zhou, Y., Schroeder, S., Haroutunian, V., Seeley, W.W.*, et al.* (2010). Acetylation of tau inhibits its degradation and contributes to tauopathy. *Neuron* **67,** 953-966.

Ming, L., Wang, P., Bank, A., Yu, J. and Zhang, L. (2006). PUMA Dissociates Bax and Bcl-X(L) to induce apoptosis in colon cancer cells. *The Journal of biological chemistry* **281,** 16034-16042.

Mitchell, R.S., Chaudhuri, R., Lindwasser, O.W., Tanaka, K.A., Lau, D., Murillo, R.*, et al.* (2008). Competition model for upregulation of the major histocompatibility complex class II-associated invariant chain by human immunodeficiency virus type 1 Nef. *Journal of virology* **82,** 7758-7767.

Mitomi, H., Mori, A., Kanazawa, H., Nishiyama, Y., Ihara, A., Otani, Y.*, et al.* (2005). Venous invasion and down-regulation of p21(WAF1/CIP1) are associated with metastasis in colorectal carcinomas. *Hepato-gastroenterology* **52,** 1421-1426.

Miyashita, T. and Reed, J.C. (1995). Tumor suppressor p53 is a direct transcriptional activator of the human bax gene. *Cell* **80,** 293-299.

Moarefi, I., LaFevre-Bernt, M., Sicheri, F., Huse, M., Lee, C.H., Kuriyan, J. and Miller, W.T. (1997). Activation of the Src-family tyrosine kinase Hck by SH3 domain displacement. *Nature* **385,** 650-653.

Mohri, H., Perelson, A.S., Tung, K., Ribeiro, R.M., Ramratnam, B., Markowitz, M.*, et al.* (2001). Increased turnover of T lymphocytes in HIV-1 infection and its reduction by antiretroviral therapy. *The Journal of experimental medicine* **194,** 1277-1287.

Molloy, S.S., Anderson, E.D., Jean, F. and Thomas, G. (1999). Bi-cycling the furin pathway: from TGN localization to pathogen activation and embryogenesis. *Trends Cell Biol* **9,** 28-35.

Molloy, S.S., Thomas, L., Kamibayashi, C., Mumby, M.C. and Thomas, G. (1998). Regulation of endosome sorting by a specific PP2A isoform. *J Cell Biol* **142,** 1399-1411.

Molloy, S.S., Thomas, L., VanSlyke, J.K., Stenberg, P.E. and Thomas, G. (1994). Intracellular trafficking and activation of the furin proprotein convertase: localization to the TGN and recycling from the cell surface. *EMBO J* **13,** 18-33.

Montagnoli, A., Tenca, P., Sola, F., Carpani, D., Brotherton, D., Albanese, C. and Santocanale, C. (2004). Cdc7 inhibition reveals a p53-dependent replication checkpoint that is defective in cancer cells. *Cancer Res* **64,** 7110-7116.

Montes de Oca Luna, R., Wagner, D.S. and Lozano, G. (1995). Rescue of early embryonic lethality in mdm2-deficient mice by deletion of p53. *Nature* **378,** 203-206.

Morgan, D.O. (1995). Principles of CDK regulation. *Nature* **374,** 131-134.

Moss, A.R., Bacchetti, P., Osmond, D., Krampf, W., Chaisson, R.E., Stites, D*., et al.* (1988). Seropositivity for HIV and the development of AIDS or AIDS related condition: three year follow up of the San Francisco General Hospital cohort. *Br Med J (Clin Res Ed)* **296,** 745-750.

Motta, M.C., Divecha, N., Lemieux, M., Kamel, C., Chen, D., Gu, W*., et al.* (2004). Mammalian SIRT1 represses forkhead transcription factors. *Cell* **116,** 551-563.

Motzer, R.J., Bacik, J., Mariani, T., Russo, P., Mazumdar, M. and Reuter, V. (2002). Treatment outcome and survival associated with metastatic renal cell carcinoma of non-clear-cell histology. *Journal of clinical oncology : official journal of the American Society of Clinical Oncology* **20,** 2376-2381.

Moutouh, L., Corbeil, J. and Richman, D.D. (1996). Recombination leads to the rapid emergence of HIV-1 dually resistant mutants under selective drug pressure. *Proc Natl Acad Sci U S A* **93,** 6106-6111.

Moynihan, K.A., Grimm, A.A., Plueger, M.M., Bernal-Mizrachi, E., Ford, E., Cras-Meneur, C*., et al.* (2005). Increased dosage of mammalian Sir2 in pancreatic beta cells enhances glucose-stimulated insulin secretion in mice. *Cell metabolism* **2,** 105-117.

Muesing, M.A., Smith, D.H., Cabradilla, C.D., Benton, C.V., Lasky, L.A. and Capon, D.J. (1985). Nucleic acid structure and expression of the human AIDS/lymphadenopathy retrovirus. *Nature* **313,** 450-458.

Mukerji, J., Olivieri, K.C., Misra, V., Agopian, K.A. and Gabuzda, D. (2012). Proteomic analysis of HIV-1 Nef cellular binding partners reveals a role for exocyst complex proteins in mediating enhancement of intercellular nanotube formation. *Retrovirology* **9,** 33.

Muratori, C., Cavallin, L.E., Kratzel, K., Tinari, A., De Milito, A., Fais, S*., et al.* (2009). Massive secretion by T cells is caused by HIV Nef in infected cells and by Nef transfer to bystander cells. *Cell host & microbe* **6,** 218-230.

Murray-Zmijewski, F., Slee, E.A. and Lu, X. (2008). A complex barcode underlies the heterogeneous response of p53 to stress. *Nature reviews. Molecular cell biology* **9,** 702-712.

Muthumani, K., Choo, A.Y., Hwang, D.S., Premkumar, A., Dayes, N.S., Harris, C.*, et al.* (2005). HIV-1 Nef-induced FasL induction and bystander killing requires p38 MAPK activation. *Blood* **106,** 2059-2068.

Myhill, N., Lynes, E.M., Nanji, J.A., Blagoveshchenskaya, A.D., Fei, H., Carmine Simmen, K.*, et al.* (2008). The subcellular distribution of calnexin is mediated by PACS-2. *Mol Biol Cell* **19,** 2777-2788.

Nakahata, Y., Kaluzova, M., Grimaldi, B., Sahar, S., Hirayama, J., Chen, D.*, et al.* (2008). The NAD+-dependent deacetylase SIRT1 modulates CLOCK-mediated chromatin remodeling and circadian control. *Cell* **134,** 329-340.

Nakano, K. and Vousden, K.H. (2001). PUMA, a novel proapoptotic gene, is induced by p53. *Mol Cell* **7,** 683-694.

Naslavsky, N., Weigert, R. and Donaldson, J.G. (2003). Convergence of non-clathrin- and clathrin-derived endosomes involves Arf6 inactivation and changes in phosphoinositides. *Mol Biol Cell* **14,** 417-431.

Natarajan, K., Dimasi, N., Wang, J., Mariuzza, R.A. and Margulies, D.H. (2002). Structure and function of natural killer cell receptors: multiple molecular solutions to self, nonself discrimination. *Annual review of immunology* **20,** 853-885.

Nauli, S.M., Alenghat, F.J., Luo, Y., Williams, E., Vassilev, P., Li, X.*, et al.* (2003). Polycystins 1 and 2 mediate mechanosensation in the primary cilium of kidney cells. *Nat Genet* **33,** 129-137.

Nekhai, S. and Jeang, K.T. (2006). Transcriptional and post-transcriptional regulation of HIV-1 gene expression: role of cellular factors for Tat and Rev. *Future microbiology* **1,** 417-426.

Nemoto, S., Fergusson, M.M. and Finkel, T. (2004). Nutrient availability regulates SIRT1 through a forkhead-dependent pathway. *Science* **306,** 2105-2108.

Noda, A., Ning, Y., Venable, S.F., Pereira-Smith, O.M. and Smith, J.R. (1994). Cloning of senescent cell-derived inhibitors of DNA synthesis using an expression screen. *Experimental cell research* **211,** 90-98.

North, B.J. and Sinclair, D.A. (2007). Sirtuins: a conserved key unlocking AceCS activity. *Trends in biochemical sciences* **32,** 1-4.

Noda, A., Ning, Y., Venable, S.F., Pereira-Smith, O.M. and Smith, J.R. (1994). Cloning of senescent cell-derived inhibitors of DNA synthesis using an expression screen. *Experimental cell research* **211,** 90-98.

Noviello, C.M., Benichou, S. and Guatelli, J.C. (2008). Cooperative binding of the class I major histocompatibility complex cytoplasmic domain and human immunodeficiency virus type 1 Nef to the endosomal AP-1 complex via its mu subunit. *Journal of virology* **82,** 1249-1258.

Nurse, P. (1990). Universal control mechanism regulating onset of M-phase. *Nature* **344,** 503-508.

Nyberg, K.A., Michelson, R.J., Putnam, C.W. and Weinert, T.A. (2002). Toward maintaining the genome: DNA damage and replication checkpoints. *Annual review of genetics* **36,** 617-656.

Oberdoerffer, P., Michan, S., McVay, M., Mostoslavsky, R., Vann, J., Park, S.K.*, et al.* (2008). SIRT1 redistribution on chromatin promotes genomic stability but alters gene expression during aging. *Cell* **135,** 907-918.

Oda, E., Ohki, R., Murasawa, H., Nemoto, J., Shibue, T., Yamashita, T.*, et al.* (2000a). Noxa, a BH3-only member of the Bcl-2 family and candidate mediator of p53-induced apoptosis. *Science* **288,** 1053-1058.

Oda, K., Arakawa, H., Tanaka, T., Matsuda, K., Tanikawa, C., Mori, T.*, et al.* (2000b). p53AIP1, a potential mediator of p53-dependent apoptosis, and its regulation by Ser-46-phosphorylated p53. *Cell* **102,** 849-862.

Ogino, S., Kawasaki, T., Kirkner, G.J., Ogawa, A., Dorfman, I., Loda, M. and Fuchs, C.S. (2006). Down-regulation of p21 (CDKN1A/CIP1) is inversely associated with microsatellite instability and CpG island methylator phenotype (CIMP) in colorectal cancer. *J Pathol* **210,** 147-154.

Okamoto, K. and Beach, D. (1994). Cyclin G is a transcriptional target of the p53 tumor suppressor protein. *EMBO J* **13,** 4816-4822.

Okamoto, K., Li, H., Jensen, M.R., Zhang, T., Taya, Y., Thorgeirsson, S.S. and Prives, C. (2002). Cyclin G recruits PP2A to dephosphorylate Mdm2. *Mol Cell* **9,** 761-771.

Older Aguilar, A.M., Guethlein, L.A., Adams, E.J., Abi-Rached, L., Moesta, A.K. and Parham, P. (2010). Coevolution of killer cell Ig-like receptors with HLA-C to become the major variable regulators of human NK cells. *J Immunol* **185,** 4238-4251.

Oliner, J.D., Pietenpol, J.A., Thiagalingam, S., Gyuris, J., Kinzler, K.W. and Vogelstein, B. (1993). Oncoprotein MDM2 conceals the activation domain of tumour suppressor p53. *Nature* **362,** 857-860.

Ollmann, M., Young, L.M., Di Como, C.J., Karim, F., Belvin, M., Robertson, S.*, et al.* (2000). Drosophila p53 is a structural and functional homolog of the tumor suppressor p53. *Cell* **101,** 91-101.

Oneyama, C., Agatsuma, T., Kanda, Y., Nakano, H., Sharma, S.V., Nakano, S.*, et al.* (2003). Synthetic inhibitors of proline-rich ligand-mediated protein-protein interaction: potent analogs of UCS15A. *Chemistry & biology* **10,** 443-451.

Oren, M. (1991) The role of p53 in neoplasia New York, Academic.

Ortigas, A.P., Stein, C.K., Thomson, L.L. and Hoo, J.J. (1997). Delineation of 14q32.3 deletion syndrome. *Journal of medical genetics* **34,** 515-517.

Owen-Schaub, L.B., Zhang, W., Cusack, J.C., Angelo, L.S., Santee, S.M., Fujiwara, T.*, et al.* (1995). Wild-type human p53 and a temperature-sensitive mutant induce Fas/APO-1 expression. *Mol Cell Biol* **15,** 3032-3040.

Paabo, S., Severinsson, L., Andersson, M., Martens, I., Nilsson, T. and Peterson, P.A. (1989). Adenovirus proteins and MHC expression. *Advances in cancer research* **52,** 151-163.

Palella, F.J., Jr., Delaney, K.M., Moorman, A.C., Loveless, M.O., Fuhrer, J., Satten, G.A.*, et al.* (1998). Declining morbidity and mortality among patients with advanced human immunodeficiency virus infection. HIV Outpatient Study Investigators. *N Engl J Med* **338,** 853-860.

Pan, J., Mestas, J., Burdick, M.D., Phillips, R.J., Thomas, G.V., Reckamp, K.*, et al.* (2006). Stromal derived factor-1 (SDF-1/CXCL12) and CXCR4 in renal cell carcinoma metastasis. *Molecular cancer* **5,** 56.

Pan, P.W., Feldman, J.L., Devries, M.K., Dong, A., Edwards, A.M. and Denu, J.M. (2011). Structure and biochemical functions of SIRT6. *J Biol Chem* **286,** 14575-14587.

Pan, Z.Q., Reardon, J.T., Li, L., Flores-Rozas, H., Legerski, R., Sancar, A. and Hurwitz, J. (1995). Inhibition of nucleotide excision repair by the cyclin-dependent kinase inhibitor p21. *J Biol Chem* **270,** 22008-22016.

Pan, X., Rudolph, J.M., Abraham, L., Habermann, A., Haller, C., Krijnse-Locker, J. and Fackler, O.T. (2012b). HIV-1 Nef compensates for disorganization of the immunological synapse by inducing trans-Golgi network-associated Lck signaling. *Blood* **119,** 786-797.

Pan, M., Yuan, H., Brent, M., Ding, E.C. and Marmorstein, R. (2012). SIRT1 contains N- and C-terminal regions that potentiate deacetylase activity. *J Biol Chem* **287,** 2468-2476.

Pantuck, A.J., An, J., Liu, H. and Rettig, M.B. (2010). NF-kappaB-dependent plasticity of the epithelial to mesenchymal transition induced by Von Hippel-Lindau inactivation in renal cell carcinomas. *Cancer Res* **70,** 752-761.

Pantaleo, G., Demarest, J.F., Schacker, T., Vaccarezza, M., Cohen, O.J., Daucher, M.*, et al.* (1997). The qualitative nature of the primary immune response to HIV infection is a prognosticator of disease progression independent of the initial level of plasma viremia. *Proc Natl Acad Sci U S A* **94,** 254-258.

Pantaleo, G., Graziosi, C. and Fauci, A.S. (1993). New concepts in the immunopathogenesis of human immunodeficiency virus infection. *N Engl J Med* **328,** 327-335.

Parant, J., Chavez-Reyes, A., Little, N.A., Yan, W., Reinke, V., Jochemsen, A.G. and Lozano, G. (2001). Rescue of embryonic lethality in Mdm4-null mice by loss of Trp53 suggests a nonoverlapping pathway with MDM2 to regulate p53. *Nat Genet* **29,** 92-95.

Patino-Garcia, A., Sotillo-Pineiro, E. and Sierrasesumaga-Ariznabarreta, L. (1998). p21WAF1 mutation is not a predominant alteration in pediatric bone tumors. *Pediatric research* **43,** 393-395.

Pavletich, N.P., Chambers, K.A. and Pabo, C.O. (1993). The DNA-binding domain of p53 contains the four conserved regions and the major mutation hot spots. *Genes Dev* **7,** 2556-2564.

Pedersen, C., Dickmeiss, E., Gaub, J., Ryder, L.P., Platz, P., Lindhardt, B.O. and Lundgren, J.D. (1990). T-cell subset alterations and lymphocyte responsiveness to mitogens and antigen during severe primary infection with HIV: a case series of seven consecutive HIV seroconverters. *AIDS* **4,** 523-526.

Pedersen, C., Lindhardt, B.O., Jensen, B.L., Lauritzen, E., Gerstoft, J., Dickmeiss, E.*, et al.* (1989). Clinical course of primary HIV infection: consequences for subsequent course of infection. *BMJ* **299,** 154-157.

Pediconi, N., Guerrieri, F., Vossio, S., Bruno, T., Belloni, L., Schinzari, V.*, et al.* (2009). hSirT1-dependent regulation of the PCAF-E2F1-p73 apoptotic pathway in response to DNA damage. *Mol Cell Biol* **29,** 1989-1998.

Pereyra, F., Jia, X., McLaren, P.J., Telenti, A., de Bakker, P.I., Walker, B.D.*, et al.* (2010). The major genetic determinants of HIV-1 control affect HLA class I peptide presentation. *Science* **330,** 1551-1557.

Peterhans, E. (1997). Oxidants and antioxidants in viral diseases: disease mechanisms and metabolic regulation. *The Journal of nutrition* **127,** 962S-965S.

Peterlin, B.M. and Trono, D. (2003). Hide, shield and strike back: how HIV-infected cells avoid immune eradication. *Nature reviews. Immunology* **3,** 97-107.

Pfeffer, S.R. (2007). Unsolved mysteries in membrane traffic. *Annual review of biochemistry* **76,** 629-645.

Pfluger, P.T., Herranz, D., Velasco-Miguel, S., Serrano, M. and Tschop, M.H. (2008). Sirt1 protects against high-fat diet-induced metabolic damage. *Proc Natl Acad Sci U S A* **105,** 9793-9798.

Philipp, J., Vo, K., Gurley, K.E., Seidel, K. and Kemp, C.J. (1999). Tumor suppression by p27Kip1 and p21Cip1 during chemically induced skin carcinogenesis. *Oncogene* **18,** 4689-4698.

Picard, F., Kurtev, M., Chung, N., Topark-Ngarm, A., Senawong, T., Machado De Oliveira, R.*, et al.* (2004). Sirt1 promotes fat mobilization in white adipocytes by repressing PPAR-gamma. *Nature* **429,** 771-776.

Piguet, V. (2005). Receptor modulation in viral replication: HIV, HSV, HHV-8 and HPV: same goal, different techniques to interfere with MHC-I antigen presentation. *Current topics in microbiology and immunology* **285,** 199-217.

Piguet, V., Gu, F., Foti, M., Demaurex, N., Gruenberg, J., Carpentier, J.L. and Trono, D. (1999). Nef-induced CD4 degradation: a diacidic-based motif in Nef functions as a lysosomal targeting signal through the binding of beta-COP in endosomes. *Cell* **97,** 63-73.

Piguet, V., Wan, L., Borel, C., Mangasarian, A., Demaurex, N., Thomas, G. and Trono, D. (2000). HIV-1 Nef protein binds to the cellular protein PACS-1 to

downregulate class I major histocompatibility complexes. *Nat Cell Biol* **2,** 163-167.

Ple, P.A., Green, T.P., Hennequin, L.F., Curwen, J., Fennell, M., Allen, J.*, et al.* (2004). Discovery of a new class of anilinoquinazoline inhibitors with high affinity and specificity for the tyrosine kinase domain of c-Src. *Journal of medicinal chemistry* **47,** 871-887.

Pluemsampant, S., Safronova, O.S., Nakahama, K. and Morita, I. (2008). Protein kinase CK2 is a key activator of histone deacetylase in hypoxia-associated tumors. *International journal of cancer. Journal international du cancer* **122,** 333-341.

Poe, J.A. and Smithgall, T.E. (2009). HIV-1 Nef dimerization is required for Nef-mediated receptor downregulation and viral replication. *Journal of molecular biology* **394,** 329-342.

Pollard, V.W. and Malim, M.H. (1998). The HIV-1 Rev protein. *Annual review of microbiology* **52,** 491-532.

Polyak, K., Xia, Y., Zweier, J.L., Kinzler, K.W. and Vogelstein, B. (1997). A model for p53-induced apoptosis. *Nature* **389,** 300-305.

Ponugoti, B., Kim, D.H., Xiao, Z., Smith, Z., Miao, J., Zang, M.*, et al.* (2010). SIRT1 deacetylates and inhibits SREBP-1C activity in regulation of hepatic lipid metabolism. *J Biol Chem* **285,** 33959-33970.

Poole, A.J., Heap, D., Carroll, R.E. and Tyner, A.L. (2004). Tumor suppressor functions for the Cdk inhibitor p21 in the mouse colon. *Oncogene* **23,** 8128-8134.

Popovic, M., Sarngadharan, M.G., Read, E. and Gallo, R.C. (1984). Detection, isolation, and continuous production of cytopathic retroviruses (HTLV-III) from patients with AIDS and pre-AIDS. *Science* **224,** 497-500.

Preusser, A., Briese, L., Baur, A.S. and Willbold, D. (2001). Direct in vitro binding of full-length human immunodeficiency virus type 1 Nef protein to CD4 cytoplasmic domain. *Journal of virology* **75,** 3960-3964.

Pulvirenti, T., Giannotta, M., Capestrano, M., Capitani, M., Pisanu, A., Polishchuk, R.S.*, et al.* (2008). A traffic-activated Golgi-based signalling circuit coordinates the secretory pathway. *Nat Cell Biol* **10,** 912-922.

Qiao, X., He, B., Chiu, A., Knowles, D.M., Chadburn, A. and Cerutti, A. (2006). Human immunodeficiency virus 1 Nef suppresses CD40-dependent immunoglobulin class switching in bystander B cells. *Nature immunology* **7,** 302-310.

Radhakrishna, H. and Donaldson, J.G. (1997). ADP-ribosylation factor 6 regulates a novel plasma membrane recycling pathway. *J Cell Biol* **139,** 49-61.

Raver-Shapira, N., Marciano, E., Meiri, E., Spector, Y., Rosenfeld, N., Moskovits, N.*, et al.* (2007). Transcriptional activation of miR-34a contributes to p53-mediated apoptosis. *Mol Cell* **26,** 731-743.

Ravi, R., Mookerjee, B., Bhujwalla, Z.M., Sutter, C.H., Artemov, D., Zeng, Q.*, et al.* (2000). Regulation of tumor angiogenesis by p53-induced degradation of hypoxia-inducible factor 1alpha. *Genes Dev* **14,** 34-44.

Rayne, F., Debaisieux, S., Yezid, H., Lin, Y.L., Mettling, C., Konate, K.*, et al.* (2010). Phosphatidylinositol-(4,5)-bisphosphate enables efficient secretion of HIV-1 Tat by infected T-cells. *EMBO J* **29,** 1348-1362.

Reinhardt, H.C. and Schumacher, B. (2012). The p53 network: cellular and systemic DNA damage responses in aging and cancer. *Trends in genetics : TIG* **28,** 128-136.

Rhee, S.S. and Marsh, J.W. (1994). Human immunodeficiency virus type 1 Nef-induced down-modulation of CD4 is due to rapid internalization and degradation of surface CD4. *Journal of virology* **68,** 5156-5163.

Richardson, C.J., Gao, Q., Mitsopoulous, C., Zvelebil, M., Pearl, L.H. and Pearl, F.M. (2009). MoKCa database--mutations of kinases in cancer. *Nucleic Acids Res* **37,** D824-831.

Richman, D.D. and Bozzette, S.A. (1994). The impact of the syncytium-inducing phenotype of human immunodeficiency virus on disease progression. *The Journal of infectious diseases* **169,** 968-974.

Riley, T., Sontag, E., Chen, P. and Levine, A. (2008). Transcriptional control of human p53-regulated genes. *Nature reviews. Molecular cell biology* **9,** 402-412.

Rine, J. and Herskowitz, I. (1987). Four genes responsible for a position effect on expression from HML and HMR in Saccharomyces cerevisiae. *Genetics* **116,** 9-22.

Rini, B.I. and Atkins, M.B. (2009a). Resistance to targeted therapy in renal-cell carcinoma. *The lancet oncology* **10,** 992-1000.

Rini, B.I., Garcia, J.A., Cooney, M.M., Elson, P., Tyler, A., Beatty, K.*, et al.* (2009b). A phase I study of sunitinib plus bevacizumab in advanced solid tumors. *Clin Cancer Res* **15,** 6277-6283.

Riquelme, E., Carreno, L.J., Gonzalez, P.A. and Kalergis, A.M. (2009). The duration of TCR/pMHC interactions regulates CTL effector function and tumor-killing capacity. *European journal of immunology* **39,** 2259-2269.

Robinson, M.S. and Bonifacino, J.S. (2001). Adaptor-related proteins. *Current opinion in cell biology* **13,** 444-453.

Robinson, M.S., Sahlender, D.A. and Foster, S.D. (2010). Rapid inactivation of proteins by rapamycin-induced rerouting to mitochondria. *Developmental cell* **18,** 324-331.

Rodgers, J.T., Lerin, C., Haas, W., Gygi, S.P., Spiegelman, B.M. and Puigserver, P. (2005). Nutrient control of glucose homeostasis through a complex of PGC-1alpha and SIRT1. *Nature* **434,** 113-118.

Roeth, J.F. and Collins, K.L. (2006). Human immunodeficiency virus type 1 Nef: adapting to intracellular trafficking pathways. *Microbiology and molecular biology reviews : MMBR* **70,** 548-563.

Roeth, J.F., Williams, M., Kasper, M.R., Filzen, T.M. and Collins, K.L. (2004). HIV-1 Nef disrupts MHC-I trafficking by recruiting AP-1 to the MHC-I cytoplasmic tail. *J Cell Biol* **167,** 903-913.

Roninson, I.B. (2002). Oncogenic functions of tumour suppressor p21(Waf1/Cip1/Sdi1): association with cell senescence and tumour-promoting activities of stromal fibroblasts. *Cancer letters* **179,** 1-14.

Ronnen, E.A., Kondagunta, G.V., Ishill, N., Spodek, L., Russo, P., Reuter, V.*, et al.* (2006). Treatment outcome for metastatic papillary renal cell carcinoma patients. *Cancer* **107,** 2617-2621.

Ross, T.M., Oran, A.E. and Cullen, B.R. (1999). Inhibition of HIV-1 progeny virion release by cell-surface CD4 is relieved by expression of the viral Nef protein. *Current biology : CB* **9,** 613-621.

Rousseau, D., Cannella, D., Boulaire, J., Fitzgerald, P., Fotedar, A. and Fotedar, R. (1999). Growth inhibition by CDK-cyclin and PCNA binding domains of p21 occurs by distinct mechanisms and is regulated by ubiquitin-proteasome pathway. *Oncogene* **18,** 4313-4325.

Rowland-Jones, S. (1999). HIV infection: where have all the T cells gone? *Lancet* **354,** 5-7.

Rudnicka, D. and Schwartz, O. (2009). Intrusive HIV-1-infected cells. *Nature immunology* **10,** 933-934.

Ryan, K.M. (2011). p53 and autophagy in cancer: guardian of the genome meets guardian of the proteome. *Eur J Cancer* **47,** 44-50.

Sabeti, P.C., Walsh, E., Schaffner, S.F., Varilly, P., Fry, B., Hutcheson, H.B.*, et al.* (2005). The case for selection at CCR5-Delta32. *PLoS biology* **3,** e378.

Safai, B., Sarngadharan, M.G., Groopman, J.E., Arnett, K., Popovic, M., Sliski, A.*, et al.* (1984). Seroepidemiological studies of human T-lymphotropic retrovirus type III in acquired immunodeficiency syndrome. *Lancet* **1,** 1438-1440.

Sakaguchi, K., Herrera, J.E., Saito, S., Miki, T., Bustin, M., Vassilev, A.*, et al.* (1998). DNA damage activates p53 through a phosphorylation-acetylation cascade. *Genes Dev* **12,** 2831-2841.

Saksela, K., Cheng, G. and Baltimore, D. (1995). Proline-rich (PxxP) motifs in HIV-1 Nef bind to SH3 domains of a subset of Src kinases and are required for the enhanced growth of Nef+ viruses but not for down-regulation of CD4. *EMBO J* **14,** 484-491.

Salazar-Gonzalez, J.F., Salazar, M.G., Keele, B.F., Learn, G.H., Giorgi, E.E., Li, H.*, et al.* (2009). Genetic identity, biological phenotype, and evolutionary pathways of transmitted/founder viruses in acute and early HIV-1 infection. *The Journal of experimental medicine* **206,** 1273-1289.

Salvi, R., Garbuglia, A.R., Di Caro, A., Pulciani, S., Montella, F. and Benedetto, A. (1998). Grossly defective nef gene sequences in a human immunodeficiency virus type 1-seropositive long-term nonprogressor. *Journal of virology* **72,** 3646-3657.

Samson, M., Libert, F., Doranz, B.J., Rucker, J., Liesnard, C., Farber, C.M.*, et al.* (1996). Resistance to HIV-1 infection in caucasian individuals bearing mutant alleles of the CCR-5 chemokine receptor gene. *Nature* **382,** 722-725.

Sanchez, V., Greis, K.D., Sztul, E. and Britt, W.J. (2000). Accumulation of virion tegument and envelope proteins in a stable cytoplasmic compartment during human cytomegalovirus replication: characterization of a potential site of virus assembly. *Journal of virology* **74,** 975-986.

Sanders, B.D., Jackson, B. and Marmorstein, R. (2010). Structural basis for sirtuin function: what we know and what we don't. *Biochim Biophys Acta* **1804,** 1604-1616.

Sarngadharan, M.G., Popovic, M., Bruch, L., Schupbach, J. and Gallo, R.C. (1984). Antibodies reactive with human T-lymphotropic retroviruses (HTLV-III) in the serum of patients with AIDS. *Science* **224,** 506-508.

Sasaki, T. and Kitamura, T. (2010). Roles of FoxO1 and Sirt1 in the central regulation of food intake. *Endocrine journal* **57,** 939-946.

Saunders, L.R. and Verdin, E. (2007). Sirtuins: critical regulators at the crossroads between cancer and aging. *Oncogene* **26,** 5489-5504.

Sax, J.K., Fei, P., Murphy, M.E., Bernhard, E., Korsmeyer, S.J. and El-Deiry, W.S. (2002). BID regulation by p53 contributes to chemosensitivity. *Nat Cell Biol* **4,** 842-849.

Schaefer, M.R., Wonderlich, E.R., Roeth, J.F., Leonard, J.A. and Collins, K.L. (2008). HIV-1 Nef targets MHC-I and CD4 for degradation via a final common beta-COP-dependent pathway in T cells. *PLoS pathogens* **4,** e1000131.

Scheppler, J.A., Nicholson, J.K., Swan, D.C., Ahmed-Ansari, A. and McDougal, J.S. (1989). Down-modulation of MHC-I in a CD4+ T cell line, CEM-E5, after HIV-1 infection. *J Immunol* **143,** 2858-2866.

Schermer, B., Hopker, K., Omran, H., Ghenoiu, C., Fliegauf, M., Fekete, A.*, et al.* (2005). Phosphorylation by casein kinase 2 induces PACS-1 binding of nephrocystin and targeting to cilia. *EMBO J* **24,** 4415-4424.

Schlade-Bartusiak, K., Ardinger, H. and Cox, D.W. (2009). A child with terminal 14q deletion syndrome: consideration of genotype-phenotype correlations. *American journal of medical genetics. Part A* **149A,** 1012-1018.

Schug, T.T., Xu, Q., Gao, H., Peres-da-Silva, A., Draper, D.W., Fessler, M.B.*, et al.* (2010). Myeloid deletion of SIRT1 induces inflammatory signaling in response to environmental stress. *Mol Cell Biol* **30,** 4712-4721.

Schuitemaker, H., Koot, M., Kootstra, N.A., Dercksen, M.W., de Goede, R.E., van Steenwijk, R.P.*, et al.* (1992). Biological phenotype of human immunodeficiency virus type 1 clones at different stages of infection: progression of disease is associated with a shift from monocytotropic to T-cell-tropic virus population. *Journal of virology* **66,** 1354-1360.

Schumacher, B., Hofmann, K., Boulton, S. and Gartner, A. (2001). The C. elegans homolog of the p53 tumor suppressor is required for DNA damage-induced apoptosis. *Current biology : CB* **11,** 1722-1727.

Schupbach, J., Popovic, M., Gilden, R.V., Gonda, M.A., Sarngadharan, M.G. and Gallo, R.C. (1984). Serological analysis of a subgroup of human T-lymphotropic retroviruses (HTLV-III) associated with AIDS. *Science* **224,** 503-505.

Schwartz, O., Marechal, V., Le Gall, S., Lemonnier, F. and Heard, J.M. (1996). Endocytosis of major histocompatibility complex class I molecules is induced by the HIV-1 Nef protein. *Nat Med* **2,** 338-342.

Schweppe, R.E., Kerege, A.A., French, J.D., Sharma, V., Grzywa, R.L. and Haugen, B.R. (2009). Inhibition of Src with AZD0530 reveals the Src-Focal Adhesion kinase complex as a novel therapeutic target in papillary and anaplastic thyroid cancer. *The Journal of clinical endocrinology and metabolism* **94,** 2199-2203.

Scott, G.K., Fei, H., Thomas, L., Medigeshi, G.R. and Thomas, G. (2006). A PACS-1, GGA3 and CK2 complex regulates CI-MPR trafficking. *EMBO J* **25,** 4423-4435.

Scott, G.K., Gu, F., Crump, C.M., Thomas, L., Wan, L., Xiang, Y. and Thomas, G. (2003). The phosphorylation state of an autoregulatory domain controls PACS-1-directed protein traffic. *EMBO J* **22,** 6234-6244.

Seaman, M.N. (2008). Endosome protein sorting: motifs and machinery. *Cell Mol Life Sci* **65,** 2842-2858.

Serrano, M. (2011) In SIRT1 Transgenic and Cancer Models, Proceedings of the 102nd Annual Meeting of the AACR, Orlando, FL, Apr 2–6, 2011; Presentation SY11-03.

Serrano, M., Lee, H., Chin, L., Cordon-Cardo, C., Beach, D. and DePinho, R.A. (1996). Role of the INK4a locus in tumor suppression and cell mortality. *Cell* **85,** 27-37.

Shah, N.P., Kasap, C., Weier, C., Balbas, M., Nicoll, J.M., Bleickardt, E.*, et al.* (2008). Transient potent BCR-ABL inhibition is sufficient to commit chronic myeloid leukemia cells irreversibly to apoptosis. *Cancer cell* **14,** 485-493.

Shankar, S. and Srivastava, R.K. (2004). Enhancement of therapeutic potential of TRAIL by cancer chemotherapy and irradiation: mechanisms and clinical implications. *Drug resistance updates : reviews and commentaries in antimicrobial and anticancer chemotherapy* **7,** 139-156.

Sherr, C.J. (1994). G1 phase progression: cycling on cue. *Cell* **79,** 551-555.

Sherr, C.J. (2006). Divorcing ARF and p53: an unsettled case. *Nature reviews. Cancer* **6,** 663-673.

Sherr, C.J. and Roberts, J.M. (1995). Inhibitors of mammalian G1 cyclin-dependent kinases. *Genes & development* **9,** 1149-1163.

Sherr, C.J. and Roberts, J.M. (1999). CDK inhibitors: positive and negative regulators of G1-phase progression. *Genes & development* **13,** 1501-1512.

Shi, X., Kachirskaia, I., Yamaguchi, H., West, L.E., Wen, H., Wang, E.W.*, et al.* (2007). Modulation of p53 function by SET8-mediated methylation at lysine 382. *Mol Cell* **27,** 636-646.

Shieh, S.Y., Ahn, J., Tamai, K., Taya, Y. and Prives, C. (2000). The human homologs of checkpoint kinases Chk1 and Cds1 (Chk2) phosphorylate p53 at multiple DNA damage-inducible sites. *Genes Dev* **14,** 289-300.

Shieh, S.Y., Ikeda, M., Taya, Y. and Prives, C. (1997). DNA damage-induced phosphorylation of p53 alleviates inhibition by MDM2. *Cell* **91,** 325-334.

Shiohara, M., el-Deiry, W.S., Wada, M., Nakamaki, T., Takeuchi, S., Yang, R.*, et al.* (1994). Absence of WAF1 mutations in a variety of human malignancies. *Blood* **84,** 3781-3784.

Sieburth, D., Ch'ng, Q., Dybbs, M., Tavazoie, M., Kennedy, S., Wang, D.*, et al.* (2005). Systematic analysis of genes required for synapse structure and function. *Nature* **436,** 510-517.

Silva, A., Yunes, J.A., Cardoso, B.A., Martins, L.R., Jotta, P.Y., Abecasis, M.*, et al.* (2008). PTEN posttranslational inactivation and hyperactivation of the PI3K/Akt pathway sustain primary T cell leukemia viability. *J Clin Invest* **118,** 3762-3774.

Simmen, T., Aslan, J.E., Blagoveshchenskaya, A.D., Thomas, L., Wan, L., Xiang, Y.*, et al.* (2005). PACS-2 controls endoplasmic reticulum-mitochondria communication and Bid-mediated apoptosis. *EMBO J* **24,** 717-729.

Simmen, T., Honing, S., Icking, A., Tikkanen, R. and Hunziker, W. (2002). AP-4 binds basolateral signals and participates in basolateral sorting in epithelial MDCK cells. *Nat Cell Biol* **4,** 154-159.

Simmen, T., Lynes, E.M., Gesson, K. and Thomas, G. (2010). Oxidative protein folding in the endoplasmic reticulum: tight links to the mitochondria-associated membrane (MAM). *Biochim Biophys Acta* **1798,** 1465-1473.

Singh, R.K., Lau, D., Noviello, C.M., Ghosh, P. and Guatelli, J.C. (2009). An MHC-I cytoplasmic domain/HIV-1 Nef fusion protein binds directly to the mu subunit of the AP-1 endosomal coat complex. *PloS one* **4,** e8364.

Sluss, H.K., Armata, H., Gallant, J. and Jones, S.N. (2004). Phosphorylation of serine 18 regulates distinct p53 functions in mice. *Mol Cell Biol* **24,** 976-984.

Smith, J.S. and Boeke, J.D. (1997). An unusual form of transcriptional silencing in yeast ribosomal DNA. *Genes Dev* **11,** 241-254.

Smith, M.L., Chen, I.T., Zhan, Q., Bae, I., Chen, C.Y., Gilmer, T.M.*, et al.* (1994). Interaction of the p53-regulated protein Gadd45 with proliferating cell nuclear antigen. *Science* **266,** 1376-1380.

Sol-Foulon, N., Moris, A., Nobile, C., Boccaccio, C., Engering, A., Abastado, J.P.*, et al.* (2002). HIV-1 Nef-induced upregulation of DC-SIGN in dendritic cells promotes lymphocyte clustering and viral spread. *Immunity* **16,** 145-155.

Soria, J.C., Mark, Z., Zatloukal, P., Szima, B., Albert, I., Juhasz, E.*, et al.* (2011). Randomized phase II study of dulanermin in combination with paclitaxel, carboplatin, and bevacizumab in advanced non-small-cell lung cancer.

Journal of clinical oncology : official journal of the American Society of Clinical Oncology **29,** 4442-4451.

Soros, V.B., Yonemoto, W. and Greene, W.C. (2007). Newly synthesized APOBEC3G is incorporated into HIV virions, inhibited by HIV RNA, and subsequently activated by RNase H. *PLoS pathogens* **3,** e15.

Spira, S., Wainberg, M.A., Loemba, H., Turner, D. and Brenner, B.G. (2003). Impact of clade diversity on HIV-1 virulence, antiretroviral drug sensitivity and drug resistance. *The Journal of antimicrobial chemotherapy* **51,** 229-240.

Staras, S.A., Dollard, S.C., Radford, K.W., Flanders, W.D., Pass, R.F. and Cannon, M.J. (2006). Seroprevalence of cytomegalovirus infection in the United States, 1988-1994. *Clinical infectious diseases : an official publication of the Infectious Diseases Society of America* **43,** 1143-1151.

Staras, S.A., Flanders, W.D., Dollard, S.C., Pass, R.F., McGowan, J.E., Jr. and Cannon, M.J. (2008). Cytomegalovirus seroprevalence and childhood sources of infection: A population-based study among pre-adolescents in the United States. *Journal of clinical virology : the official publication of the Pan American Society for Clinical Virology* **43,** 266-271.

Stenmark, H. (2009). Rab GTPases as coordinators of vesicle traffic. *Nature reviews. Molecular cell biology* **10,** 513-525.

Stephens, J.C., Reich, D.E., Goldstein, D.B., Shin, H.D., Smith, M.W., Carrington, M.*, et al.* (1998). Dating the origin of the CCR5-Delta32 AIDS-resistance allele by the coalescence of haplotypes. *American journal of human genetics* **62,** 1507-1515.

Stevenson, L.F., Sparks, A., Allende-Vega, N., Xirodimas, D.P., Lane, D.P. and Saville, M.K. (2007). The deubiquitinating enzyme USP2a regulates the p53 pathway by targeting Mdm2. *EMBO J* **26,** 976-986.

Stevenson, M. (2003). HIV-1 pathogenesis. *Nat Med* **9,** 853-860.

Stewart, N., Hicks, G.G., Paraskevas, F. and Mowat, M. (1995). Evidence for a second cell cycle block at G2/M by p53. *Oncogene* **10,** 109-115.

Stommel, J.M., Kimmelman, A.C., Ying, H., Nabioullin, R., Ponugoti, A.H., Wiedemeyer, R.*, et al.* (2007). Coactivation of receptor tyrosine kinases affects the response of tumor cells to targeted therapies. *Science* **318,** 287-290.

Stove, V., Naessens, E., Stove, C., Swigut, T., Plum, J. and Verhasselt, B. (2003). Signaling but not trafficking function of HIV-1 protein Nef is essential for Nef-induced defects in human intrathymic T-cell development. *Blood* **102,** 2925-2932.

Strahl, B.D. and Allis, C.D. (2000). The language of covalent histone modifications. *Nature* **403,** 41-45.

Stunkel, W. and Campbell, R.M. (2011). Sirtuin 1 (SIRT1): the misunderstood HDAC. *Journal of biomolecular screening* **16,** 1153-1169.

Sui, G., Affar el, B., Shi, Y., Brignone, C., Wall, N.R., Yin, P.*, et al.* (2004). Yin Yang 1 is a negative regulator of p53. *Cell* **117,** 859-872.

Sun, G., Sharma, A.K. and Budde, R.J. (1998). Autophosphorylation of Src and Yes blocks their inactivation by Csk phosphorylation. *Oncogene* **17,** 1587-1595.

Sun, X.X., Challagundla, K.B. and Dai, M.S. (2012). Positive regulation of p53 stability and activity by the deubiquitinating enzyme Otubain 1. *EMBO J* **31,** 576-592.

Sun, C., Zhang, F., Ge, X., Yan, T., Chen, X., Shi, X. and Zhai, Q. (2007). SIRT1 improves insulin sensitivity under insulin-resistant conditions by repressing PTP1B. *Cell metabolism* **6,** 307-319.

Sutters, M. and Germino, G.G. (2003). Autosomal dominant polycystic kidney disease: molecular genetics and pathophysiology. *The Journal of laboratory and clinical medicine* **141,** 91-101.

Suzu, S., Harada, H., Matsumoto, T. and Okada, S. (2005). HIV-1 Nef interferes with M-CSF receptor signaling through Hck activation and inhibits M-CSF bioactivities. *Blood* **105,** 3230-3237.

Swann, S.A., Williams, M., Story, C.M., Bobbitt, K.R., Fleis, R. and Collins, K.L. (2001). HIV-1 Nef blocks transport of MHC class I molecules to the cell surface via a PI 3-kinase-dependent pathway. *Virology* **282,** 267-277.

Swigut, T., Alexander, L., Morgan, J., Lifson, J., Mansfield, K.G., Lang, S.*, et al.* (2004). Impact of Nef-mediated downregulation of major histocompatibility complex class I on immune response to simian immunodeficiency virus. *Journal of virology* **78,** 13335-13344.

Sykes, S.M., Mellert, H.S., Holbert, M.A., Li, K., Marmorstein, R., Lane, W.S. and McMahon, S.B. (2006). Acetylation of the p53 DNA-binding domain regulates apoptosis induction. *Mol Cell* **24,** 841-851.

Swigut, T., Shohdy, N. and Skowronski, J. (2001). Mechanism for down-regulation of CD28 by Nef. *EMBO J* **20,** 1593-1604.

Swingler, S., Brichacek, B., Jacque, J.M., Ulich, C., Zhou, J. and Stevenson, M. (2003). HIV-1 Nef intersects the macrophage CD40L signalling pathway to promote resting-cell infection. *Nature* **424,** 213-219.

Szak, S.T., Mays, D. and Pietenpol, J.A. (2001). Kinetics of p53 binding to promoter sites in vivo. *Mol Cell Biol* **21,** 3375-3386.

Tamalet, C., Pasquier, C., Yahi, N., Colson, P., Poizot-Martin, I., Lepeu, G.*, et al.* (2000). Prevalence of drug resistant mutants and virological response to combination therapy in patients with primary HIV-1 infection. *Journal of medical virology* **61,** 181-186.

Tang, Y., Luo, J., Zhang, W. and Gu, W. (2006). Tip60-dependent acetylation of p53 modulates the decision between cell-cycle arrest and apoptosis. *Mol Cell* **24,** 827-839.

Tang, Y., Zhao, W., Chen, Y., Zhao, Y. and Gu, W. (2008). Acetylation is indispensable for p53 activation. *Cell* **133,** 612-626.

Tanner, K.G., Landry, J., Sternglanz, R. and Denu, J.M. (2000). Silent information regulator 2 family of NAD- dependent histone/protein deacetylases

generates a unique product, 1-O-acetyl-ADP-ribose. *Proc Natl Acad Sci U S A* **97,** 14178-14182.

Tanno, M., Sakamoto, J., Miura, T., Shimamoto, K. and Horio, Y. (2007). Nucleocytoplasmic shuttling of the NAD+-dependent histone deacetylase SIRT1. *J Biol Chem* **282,** 6823-6832.

Tarasov, V., Jung, P., Verdoodt, B., Lodygin, D., Epanchintsev, A., Menssen, A.*, et al.* (2007). Differential regulation of microRNAs by p53 revealed by massively parallel sequencing: miR-34a is a p53 target that induces apoptosis and G1-arrest. *Cell Cycle* **6,** 1586-1593.

Taylor, G.H. (2003). Cytomegalovirus. *American family physician* **67,** 519-524.

Taylor, W.R., Agarwal, M.L., Agarwal, A., Stacey, D.W. and Stark, G.R. (1999). p53 inhibits entry into mitosis when DNA synthesis is blocked. *Oncogene* **18,** 283-295.

Tazawa, H., Tsuchiya, N., Izumiya, M. and Nakagama, H. (2007). Tumor-suppressive miR-34a induces senescence-like growth arrest through modulation of the E2F pathway in human colon cancer cells. *Proc Natl Acad Sci U S A* **104,** 15472-15477.

Thomas, G. (2002). Furin at the cutting edge: from protein traffic to embryogenesis and disease. *Nature reviews. Molecular cell biology* **3,** 753-766.

Thomas, G.V., Tran, C., Mellinghoff, I.K., Welsbie, D.S., Chan, E., Fueger, B.*, et al.* (2006). Hypoxia-inducible factor determines sensitivity to inhibitors of mTOR in kidney cancer. *Nat Med* **12,** 122-127.

Thompson, J.S., Ling, X. and Grunstein, M. (1994). Histone H3 amino terminus is required for telomeric and silent mating locus repression in yeast. *Nature* **369,** 245-247.

Thoulouze, M.I., Sol-Foulon, N., Blanchet, F., Dautry-Varsat, A., Schwartz, O. and Alcover, A. (2006). Human immunodeficiency virus type-1 infection impairs the formation of the immunological synapse. *Immunity* **24,** 547-561.

Thut, C.J., Chen, J.L., Klemm, R. and Tjian, R. (1995). p53 transcriptional activation mediated by coactivators TAFII40 and TAFII60. *Science* **267,** 100-104.

Tissenbaum, H.A. and Guarente, L. (2001). Increased dosage of a sir-2 gene extends lifespan in Caenorhabditis elegans. *Nature* **410,** 227-230.

Tokarev, A. and Guatelli, J. (2011). Misdirection of membrane trafficking by HIV-1 Vpu and Nef: Keys to viral virulence and persistence. *Cellular logistics* **1,** 90-102.

Toledo, F. and Wahl, G.M. (2006). Regulating the p53 pathway: in vitro hypotheses, in vivo veritas. *Nature reviews. Cancer* **6,** 909-923.

Tomas, M.I., Kucic, N., Mahmutefendic, H., Blagojevic, G. and Lucin, P. (2010). Murine cytomegalovirus perturbs endosomal trafficking of major histocompatibility complex class I molecules in the early phase of infection. *Journal of virology* **84,** 11101-11112.

Tomiyama, H., Akari, H., Adachi, A. and Takiguchi, M. (2002). Different effects of Nef-mediated HLA class I down-regulation on human immunodeficiency virus type 1-specific CD8(+) T-cell cytolytic activity and cytokine production. *Journal of virology* **76,** 7535-7543.

Tooze, S.A., Jefferies, H.B., Kalie, E., Longatti, A., McAlpine, F.E., McKnight, N.C.*, et al.* (2010). Trafficking and signaling in mammalian autophagy. *IUBMB life* **62,** 503-508.

Topley, G.I., Okuyama, R., Gonzales, J.G., Conti, C. and Dotto, G.P. (1999). p21(WAF1/Cip1) functions as a suppressor of malignant skin tumor formation and a determinant of keratinocyte stem-cell potential. *Proc Natl Acad Sci U S A* **96,** 9089-9094.

Trible, R.P., Emert-Sedlak, L. and Smithgall, T.E. (2006). HIV-1 Nef selectively activates Src family kinases Hck, Lyn, and c-Src through direct SH3 domain interaction. *J Biol Chem* **281,** 27029-27038.

Turcotte, S., Chan, D.A., Sutphin, P.D., Hay, M.P., Denny, W.A. and Giaccia, A.J. (2008). A molecule targeting VHL-deficient renal cell carcinoma that induces autophagy. *Cancer cell* **14,** 90-102.

UNAIDS (2009) Global report: UNAIDS report on the global AIDS epidemic 2009. In *Joint United Nations Programme on HIV/AIDS (UNAIDS)*, W.L.C.-i.-P. Data (ed.).

UNAIDS (2010) Global report: UNAIDS report on the global AIDS epidemic 2010. In *Joint United Nations Programme on HIV/AIDS (UNAIDS)*, W.L.C.-i.-P. Data (ed.).

van Dam, E.M., Ten Broeke, T., Jansen, K., Spijkers, P. and Stoorvogel, W. (2002). Endocytosed transferrin receptors recycle via distinct dynamin and phosphatidylinositol 3-kinase-dependent pathways. *J Biol Chem* **277,** 48876-48883.

van der Horst, A., Tertoolen, L.G., de Vries-Smits, L.M., Frye, R.A., Medema, R.H. and Burgering, B.M. (2004). FOXO4 is acetylated upon peroxide stress and deacetylated by the longevity protein hSir2(SIRT1). *J Biol Chem* **279,** 28873-28879.

Van Meir, E.G., Polverini, P.J., Chazin, V.R., Su Huang, H.J., de Tribolet, N. and Cavenee, W.K. (1994). Release of an inhibitor of angiogenesis upon induction of wild type p53 expression in glioblastoma cells. *Nat Genet* **8,** 171-176.

van't Wout, A.B., Kootstra, N.A., Mulder-Kampinga, G.A., Albrecht-van Lent, N., Scherpbier, H.J., Veenstra, J.*, et al.* (1994). Macrophage-tropic variants initiate human immunodeficiency virus type 1 infection after sexual, parenteral, and vertical transmission. *J Clin Invest* **94,** 2060-2067.

Vance, J.E. (1990). Phospholipid synthesis in a membrane fraction associated with mitochondria. *J Biol Chem* **265,** 7248-7256.

Vaquero, A., Scher, M., Erdjument-Bromage, H., Tempst, P., Serrano, L. and Reinberg, D. (2007). SIRT1 regulates the histone methyl-transferase SUV39H1 during heterochromatin formation. *Nature* **450,** 440-444.

Vaquero, A., Scher, M., Lee, D., Erdjument-Bromage, H., Tempst, P. and Reinberg, D. (2004). Human SirT1 interacts with histone H1 and promotes formation of facultative heterochromatin. *Mol Cell* **16,** 93-105.

Vaseva, A.V. and Moll, U.M. (2009). The mitochondrial p53 pathway. *Biochimica et biophysica acta* **1787,** 414-420.

Vaziri, H., Dessain, S.K., Ng Eaton, E., Imai, S.I., Frye, R.A., Pandita, T.K.*, et al.* (2001). hSIR2(SIRT1) functions as an NAD-dependent p53 deacetylase. *Cell* **107,** 149-159.

Venot, C., Maratrat, M., Sierra, V., Conseiller, E. and Debussche, L. (1999). Definition of a p53 transactivation function-deficient mutant and characterization of two independent p53 transactivation subdomains. *Oncogene* **18,** 2405-2410.

Vento, S., Di Perri, G., Garofano, T., Concia, E. and Bassetti, D. (1993). Pneumocystis carinii pneumonia during primary HIV-1 infection. *Lancet* **342,** 24-25.

Venzke, S., Michel, N., Allespach, I., Fackler, O.T. and Keppler, O.T. (2006). Expression of Nef downregulates CXCR4, the major coreceptor of human immunodeficiency virus, from the surfaces of target cells and thereby enhances resistance to superinfection. *Journal of virology* **80,** 11141-11152.

Veracini, L., Simon, V., Richard, V., Schraven, B., Horejsi, V., Roche, S. and Benistant, C. (2008). The Csk-binding protein PAG regulates PDGF-induced Src mitogenic signaling via GM1. *J Cell Biol* **182,** 603-614.

Vermeire, J., Vanbillemont, G., Witkowski, W. and Verhasselt, B. (2011). The Nef-infectivity enigma: mechanisms of enhanced lentiviral infection. *Current HIV research* **9,** 474-489.

Vivier, E., Raulet, D.H., Moretta, A., Caligiuri, M.A., Zitvogel, L., Lanier, L.L.*, et al.* (2011). Innate or adaptive immunity? The example of natural killer cells. *Science* **331,** 44-49.

Vogelstein, B., Lane, D. and Levine, A.J. (2000). Surfing the p53 network. *Nature* **408,** 307-310.

Vollenweider, F., Benjannet, S., Decroly, E., Savaria, D., Lazure, C., Thomas, G.*, et al.* (1996). Comparative cellular processing of the human immunodeficiency virus (HIV-1) envelope glycoprotein gp160 by the mammalian subtilisin/kexin-like convertases. *Biochem J* **314 (Pt 2),** 521-532.

Von Pawel J, H.J., Spigel DR, Dediu M, Reck M, Cebotaru CL (2010) A randomized phase II trial of mapatumumab, a TRAIL-R1 agonist monoclonal antibody, in combination with carboplatin and paclitaxel in patients with advanced NSCLC. *J Clin Oncol***28**,Suppl:7s. Abstract LBA7501.

Vousden, K.H. (2000). p53: death star. *Cell* **103,** 691-694.

Vousden, K.H. and Prives, C. (2009). Blinded by the Light: The Growing Complexity of p53. *Cell* **137,** 413-431.

Waga, S., Hannon, G.J., Beach, D. and Stillman, B. (1994). The p21 inhibitor of cyclin-dependent kinases controls DNA replication by interaction with PCNA. *Nature* **369,** 574-578.

Wahl, G.M. (2006). Mouse bites dogma: how mouse models are changing our views of how P53 is regulated in vivo. *Cell Death Differ* **13,** 973-983.

Waldman, T., Kinzler, K.W. and Vogelstein, B. (1995). p21 is necessary for the p53-mediated G1 arrest in human cancer cells. *Cancer Res* **55,** 5187-5190.

Wan, L., Molloy, S.S., Thomas, L., Liu, G., Xiang, Y., Rybak, S.L. and Thomas, G. (1998). PACS-1 defines a novel gene family of cytosolic sorting proteins required for trans-Golgi network localization. *Cell* **94,** 205-216.

Wang, C., Chen, L., Hou, X., Li, Z., Kabra, N., Ma, Y*., et al.* (2006). Interactions between E2F1 and SirT1 regulate apoptotic response to DNA damage. *Nat Cell Biol* **8,** 1025-1031.

Wang, J. and Chen, J. (2010a). SIRT1 regulates autoacetylation and histone acetyltransferase activity of TIP60. *J Biol Chem* **285,** 11458-11464.

Wang, P., Reed, M., Wang, Y., Mayr, G., Stenger, J.E., Anderson, M.E*., et al.* (1994). p53 domains: structure, oligomerization, and transformation. *Mol Cell Biol* **14,** 5182-5191.

Wang, Q., Zhang, Y., Yang, C., Xiong, H., Lin, Y., Yao, J*., et al.* (2010b). Acetylation of metabolic enzymes coordinates carbon source utilization and metabolic flux. *Science* **327,** 1004-1007.

Wang, R.H., Sengupta, K., Li, C., Kim, H.S., Cao, L., Xiao, C*., et al.* (2008a). Impaired DNA damage response, genome instability, and tumorigenesis in SIRT1 mutant mice. *Cancer cell* **14,** 312-323.

Wang, R.H., Zheng, Y., Kim, H.S., Xu, X., Cao, L., Luhasen, T*., et al.* (2008b). Interplay among BRCA1, SIRT1, and Survivin during BRCA1-associated tumorigenesis. *Mol Cell* **32,** 11-20.

Wang, Y., Reed, M., Wang, P., Stenger, J.E., Mayr, G., Anderson, M.E*., et al.* (1993). p53 domains: identification and characterization of two autonomous DNA-binding regions. *Genes Dev* **7,** 2575-2586.

Wang, Y., Schwedes, J.F., Parks, D., Mann, K. and Tegtmeyer, P. (1995). Interaction of p53 with its consensus DNA-binding site. *Mol Cell Biol* **15,** 2157-2165.

Wang, Y.H., Tsay, Y.G., Tan, B.C., Lo, W.Y. and Lee, S.C. (2003). Identification and characterization of a novel p300-mediated p53 acetylation site, lysine 305. *J Biol Chem* **278,** 25568-25576.

Wang, Y.A., Elson, A. and Leder, P. (1997). Loss of p21 increases sensitivity to ionizing radiation and delays the onset of lymphoma in atm-deficient mice. *Proc Natl Acad Sci U S A* **94,** 14590-14595.

Waterman, J.L., Shenk, J.L. and Halazonetis, T.D. (1995). The dihedral symmetry of the p53 tetramerization domain mandates a conformational switch upon DNA binding. *EMBO J* **14,** 512-519.

Wei, M.C., Zong, W.X., Cheng, E.H., Lindsten, T., Panoutsakopoulou, V., Ross, A.J.*, et al.* (2001). Proapoptotic BAX and BAK: a requisite gateway to mitochondrial dysfunction and death. *Science (New York, N.Y.)* **292,** 727-730.

Wei, X., Ghosh, S.K., Taylor, M.E., Johnson, V.A., Emini, E.A., Deutsch, P.*, et al.* (1995). Viral dynamics in human immunodeficiency virus type 1 infection. *Nature* **373,** 117-122.

Weinberg, R.A. (1991). Tumor suppressor genes. *Science* **254,** 1138-1146.

Weinberg, R.L., Veprintsev, D.B., Bycroft, M. and Fersht, A.R. (2005). Comparative binding of p53 to its promoter and DNA recognition elements. *Journal of molecular biology* **348,** 589-596.

Weiss, R.A. (1985) RNA Tumor Viruses. In: Weiss R.A., T. N. M., Varmus H.E., Coffin J. (ed) Cold Spring Harbor, NY, Cold Spring Harbor Laborartory.

Wen, X., Duus, K.M., Friedrich, T.D. and de Noronha, C.M. (2007). The HIV1 protein Vpr acts to promote G2 cell cycle arrest by engaging a DDB1 and Cullin4A-containing ubiquitin ligase complex using VprBP/DCAF1 as an adaptor. *J Biol Chem* **282,** 27046-27057.

Werneburg, N., Guicciardi, M.E., Yin, X.M. and Gores, G.J. (2004). TNF-alpha-mediated lysosomal permeabilization is FAN and caspase 8/Bid dependent. *American journal of physiology. Gastrointestinal and liver physiology* **287,** G436-443.

Werneburg, N.W., Bronk, S.F., Guicciardi, M.E., Thomas, L., Dikeakos, J.D., Thomas, G. and Gores, G.J. (2012). Tumor Necrosis Factor-related Apoptosis-inducing Ligand (TRAIL) Protein-induced Lysosomal Translocation of Proapoptotic Effectors Is Mediated by Phosphofurin Acidic Cluster Sorting Protein-2 (PACS-2). *J Biol Chem* **287,** 24427-24437.

Werneburg, N.W., Guicciardi, M.E., Bronk, S.F. and Gores, G.J. (2002). Tumor necrosis factor-alpha-associated lysosomal permeabilization is cathepsin B dependent. *American journal of physiology. Gastrointestinal and liver physiology* **283,** G947-956.

Werneburg, N.W., Guicciardi, M.E., Bronk, S.F., Kaufmann, S.H. and Gores, G.J. (2007). Tumor necrosis factor-related apoptosis-inducing ligand activates a lysosomal pathway of apoptosis that is regulated by Bcl-2 proteins. *J Biol Chem* **282,** 28960-28970.

Wheeler, D.L., Iida, M. and Dunn, E.F. (2009). The role of Src in solid tumors. *Oncologist* **14,** 667-678.

Wildum, S., Schindler, M., Munch, J. and Kirchhoff, F. (2006). Contribution of Vpu, Env, and Nef to CD4 down-modulation and resistance of human immunodeficiency virus type 1-infected T cells to superinfection. *Journal of virology* **80,** 8047-8059.

Williams, M., Roeth, J.F., Kasper, M.R., Filzen, T.M. and Collins, K.L. (2005). Human immunodeficiency virus type 1 Nef domains required for disruption of major histocompatibility complex class I trafficking are also necessary for coprecipitation of Nef with HLA-A2. *Journal of virology* **79,** 632-636.

Williams, M., Roeth, J.F., Kasper, M.R., Fleis, R.I., Przybycin, C.G. and Collins, K.L. (2002). Direct binding of human immunodeficiency virus type 1 Nef to the major histocompatibility complex class I (MHC-I) cytoplasmic tail disrupts MHC-I trafficking. *Journal of virology* **76,** 12173-12184.

Wright, T.M. and Rathmell, W.K. (2010). Identification of Ror2 as a hypoxia-inducible factor target in von Hippel-Lindau-associated renal cell carcinoma. *J Biol Chem* **285,** 12916-12924.

Wolf, D. and Goff, S.P. (2008). Host restriction factors blocking retroviral replication. *Annual review of genetics* **42,** 143-163.

Wonderlich, E.R., Williams, M. and Collins, K.L. (2008). The tyrosine binding pocket in the adaptor protein 1 (AP-1) mu1 subunit is necessary for Nef to recruit AP-1 to the major histocompatibility complex class I cytoplasmic tail. *J Biol Chem* **283,** 3011-3022.

Wood, J.D., Nucifora, F.C., Jr., Duan, K., Zhang, C., Wang, J., Kim, Y.*, et al.* (2000). Atrophin-1, the dentato-rubral and pallido-luysian atrophy gene product, interacts with ETO/MTG8 in the nuclear matrix and represses transcription. *J Cell Biol* **150,** 939-948.

Wood, J.G., Rogina, B., Lavu, S., Howitz, K., Helfand, S.L., Tatar, M. and Sinclair, D. (2004). Sirtuin activators mimic caloric restriction and delay ageing in metazoans. *Nature* **430,** 686-689.

Wu, G.S., Burns, T.F., McDonald, E.R., 3rd, Jiang, W., Meng, R., Krantz, I.D.*, et al.* (1997). KILLER/DR5 is a DNA damage-inducible p53-regulated death receptor gene. *Nat Genet* **17,** 141-143.

Wu, Z., Earle, J., Saito, S., Anderson, C.W., Appella, E. and Xu, Y. (2002). Mutation of mouse p53 Ser23 and the response to DNA damage. *Mol Cell Biol* **22,** 2441-2449.

Xiao, H., Pearson, A., Coulombe, B., Truant, R., Zhang, S., Regier, J.L.*, et al.* (1994). Binding of basal transcription factor TFIIH to the acidic activation domains of VP16 and p53. *Mol Cell Biol* **14,** 7013-7024.

Xiong, S., Salazar, G., Patrushev, N. and Alexander, R.W. (2011). FoxO1 mediates an autofeedback loop regulating SIRT1 expression. *J Biol Chem* **286,** 5289-5299.

Xiong, Y., Hannon, G.J., Zhang, H., Casso, D., Kobayashi, R. and Beach, D. (1993). P21 is a Universal Inhibitor of Cyclin Kinases. *Nature* **366,** 701-704.

Xirodimas, D.P., Saville, M.K., Bourdon, J.C., Hay, R.T. and Lane, D.P. (2004). Mdm2-mediated NEDD8 conjugation of p53 inhibits its transcriptional activity. *Cell* **118,** 83-97.

Xu, W., Santini, P.A., Sullivan, J.S., He, B., Shan, M., Ball, S.C.*, et al.* (2009). HIV-1 evades virus-specific IgG2 and IgA responses by targeting systemic and intestinal B cells via long-range intercellular conduits. *Nature immunology* **10,** 1008-1017.

Yamakuchi, M., Ferlito, M. and Lowenstein, C.J. (2008). miR-34a repression of SIRT1 regulates apoptosis. *Proc Natl Acad Sci U S A* **105,** 13421-13426.

Yamamori, T., DeRicco, J., Naqvi, A., Hoffman, T.A., Mattagajasingh, I., Kasuno, K.*, et al.* (2010). SIRT1 deacetylates APE1 and regulates cellular base excision repair. *Nucleic Acids Res* **38,** 832-845.

Yamane, K. and Kinsella, T.J. (2005). CK2 inhibits apoptosis and changes its cellular localization following ionizing radiation. *Cancer Res* **65,** 4362-4367.

Yang, T. and Sauve, A.A. (2006). NAD metabolism and sirtuins: metabolic regulation of protein deacetylation in stress and toxicity. *The AAPS journal* **8,** E632-643.

Yang, Y., Fu, W., Chen, J., Olashaw, N., Zhang, X., Nicosia, S.V.*, et al.* (2007). SIRT1 sumoylation regulates its deacetylase activity and cellular response to genotoxic stress. *Nat Cell Biol* **9,** 1253-1262.

Yang, O.O., Nguyen, P.T., Kalams, S.A., Dorfman, T., Gottlinger, H.G., Stewart, S.*, et al.* (2002). Nef-mediated resistance of human immunodeficiency virus type 1 to antiviral cytotoxic T lymphocytes. *Journal of virology* **76,** 1626-1631.

Yeatman, T.J. (2004). A renaissance for SRC. *Nature reviews. Cancer* **4,** 470-480.

Yee, K.S. and Vousden, K.H. (2005). Complicating the complexity of p53. *Carcinogenesis* **26,** 1317-1322.

Yeung, F., Hoberg, J.E., Ramsey, C.S., Keller, M.D., Jones, D.R., Frye, R.A. and Mayo, M.W. (2004). Modulation of NF-kappaB-dependent transcription and cell survival by the SIRT1 deacetylase. *EMBO J* **23,** 2369-2380.

Yewdell, J.W. and Hill, A.B. (2002). Viral interference with antigen presentation. *Nature immunology* **3,** 1019-1025.

Yonish-Rouach, E., Resnitzky, D., Lotem, J., Sachs, L., Kimchi, A. and Oren, M. (1991). Wild-type p53 induces apoptosis of myeloid leukaemic cells that is inhibited by interleukin-6. *Nature* **352,** 345-347.

York, I.A., Roop, C., Andrews, D.W., Riddell, S.R., Graham, F.L. and Johnson, D.C. (1994). A cytosolic herpes simplex virus protein inhibits antigen presentation to CD8+ T lymphocytes. *Cell* **77,** 525-535.

Youker, R.T., Shinde, U., Day, R. and Thomas, G. (2009). At the crossroads of homoeostasis and disease: roles of the PACS proteins in membrane traffic and apoptosis. *The Biochemical journal* **421,** 1-15.

Youle, R.J. and Strasser, A. (2008). The BCL-2 protein family: opposing activities that mediate cell death. *Nature reviews.Molecular cell biology* **9,** 47-59.

Youngs, E.L., Hellings, J.A. and Butler, M.G. (2011). A clinical report and further delineation of the 14q32 deletion syndrome. *Clinical dysmorphology* **20,** 143-147.

Yu, X., Yu, Y., Liu, B., Luo, K., Kong, W., Mao, P. and Yu, X.F. (2003). Induction of APOBEC3G ubiquitination and degradation by an HIV-1 Vif-Cul5-SCF complex. *Science* **302,** 1056-1060.

Yuan, J., Luo, K., Zhang, L., Cheville, J.C. and Lou, Z. (2010). USP10 regulates p53 localization and stability by deubiquitinating p53. *Cell* **140,** 384-396.

Zack, J.A., Arrigo, S.J., Weitsman, S.R., Go, A.S., Haislip, A. and Chen, I.S. (1990). HIV-1 entry into quiescent primary lymphocytes: molecular analysis reveals a labile, latent viral structure. *Cell* **61,** 213-222.

Zanetti, G., Pahuja, K.B., Studer, S., Shim, S. and Schekman, R. (2012). COPII and the regulation of protein sorting in mammals. *Nat Cell Biol* **14,** 20-28.

Zeng, X., Tamai, K., Doble, B., Li, S., Huang, H., Habas, R.*, et al.* (2005). A dual-kinase mechanism for Wnt co-receptor phosphorylation and activation. *Nature* **438,** 873-877.

Zhang, L. and Fang, B. (2005). Mechanisms of resistance to TRAIL-induced apoptosis in cancer. *Cancer gene therapy* **12,** 228-237.

Zhang, X.H., Wang, Q., Gerald, W., Hudis, C.A., Norton, L., Smid, M.*, et al.* (2009). Latent bone metastasis in breast cancer tied to Src-dependent survival signals. *Cancer cell* **16,** 67-78.

Zhang, Y., Wolf, G.W., Bhat, K., Jin, A., Allio, T., Burkhart, W.A. and Xiong, Y. (2003). Ribosomal protein L11 negatively regulates oncoprotein MDM2 and mediates a p53-dependent ribosomal-stress checkpoint pathway. *Mol Cell Biol* **23,** 8902-8912.

Zhang, Y., Fujita, N. and Tsuruo, T. (1999). Caspase-mediated cleavage of p21Waf1/Cip1 converts cancer cells from growth arrest to undergoing apoptosis. *Oncogene* **18,** 1131-1138.

Zhang, Y., Zhang, M., Dong, H., Yong, S., Li, X., Olashaw, N.*, et al.* (2009). Deacetylation of cortactin by SIRT1 promotes cell migration. *Oncogene* **28,** 445-460.

Zhao, S., Xu, W., Jiang, W., Yu, W., Lin, Y., Zhang, T.*, et al.* (2010). Regulation of cellular metabolism by protein lysine acetylation. *Science* **327,** 1000-1004.

Zhao, W., Kruse, J.P., Tang, Y., Jung, S.Y., Qin, J. and Gu, W. (2008). Negative regulation of the deacetylase SIRT1 by DBC1. *Nature* **451,** 587-590.

Zhao, X., Sternsdorf, T., Bolger, T.A., Evans, R.M. and Yao, T.P. (2005). Regulation of MEF2 by histone deacetylase 4- and SIRT1 deacetylase-mediated lysine modifications. *Mol Cell Biol* **25,** 8456-8464.

Zhou, B.P., Deng, J., Xia, W., Xu, J., Li, Y.M., Gunduz, M. and Hung, M.C. (2004). Dual regulation of Snail by GSK-3beta-mediated phosphorylation in control of epithelial-mesenchymal transition. *Nat Cell Biol* **6,** 931-940.

Zhu, T., Mo, H., Wang, N., Nam, D.S., Cao, Y., Koup, R.A. and Ho, D.D. (1993). Genotypic and phenotypic characterization of HIV-1 patients with primary infection. *Science* **261,** 1179-1181.

Zilfou, J.T. and Lowe, S.W. (2009). Tumor suppressive functions of p53. *Cold Spring Harbor perspectives in biology* **1,** a001883.

Zirbes, T.K., Baldus, S.E., Moenig, S.P., Nolden, S., Kunze, D., Shafizadeh, S.T.*, et al.* (2000). Prognostic impact of p21/waf1/cip1 in colorectal cancer. *International journal of cancer. Journal international du cancer* **89,** 14-18.

Zschoernig, B. and Mahlknecht, U. (2008). SIRTUIN 1: regulating the regulator. *Biochem Biophys Res Commun* **376,** 251-255.

Zuo, J., Currin, A., Griffin, B.D., Shannon-Lowe, C., Thomas, W.A., Ressing, M.E.*, et al.* (2009). The Epstein-Barr virus G-protein-coupled receptor contributes to immune evasion by targeting MHC class I molecules for degradation. *PLoS pathogens* **5,** e1000255.

Zuppini, A., Groenendyk, J., Cormack, L.A., Shore, G., Opas, M., Bleackley, R.C. and Michalak, M. (2002). Calnexin deficiency and endoplasmic reticulum stress-induced apoptosis. *Biochemistry* **41,** 2850-2858.